Studies related to spent fuel reprocessing using tri-iso-amyl phosphate as an alternate extractant to tri-n-butyl phosphate

By

BALIJA SREENIVASULU
(Enrollment No: CHEM02201104011)

Indira Gandhi Centre for Atomic Research, Kalpakkam

A thesis submitted to the

Board of Studies in Chemical Sciences

In partial fulfillment of requirements

For the Degree of

DOCTOR OF PHILOSOPHY

of

HOMI BHABHA NATIONAL INSTITUTE

December 2016

Homi Bhabha National Institute

Recommendations of the Viva Voce Committee

As members of the Viva Voce Committee, we certify that we have read the dissertation prepared by **Balija Sreenivasulu** entitled "**Studies related to spent fuel reprocessing using tri-iso-amyl phosphate as an alternate extractant to tri-n-butyl phosphate**" and recommend that it may be accepted as fulfilling the thesis requirement for the award of Degree of Doctor of Philosophy.

Chairman – Dr. S. Anthonysamy	**Date:**
Guide / Convener – Dr. N. Sivaraman	**Date:**
Examiner -	**Date:**
Member 1- Dr. C. Mallika	**Date:**
Member 2- Dr. M. P. Antony	**Date:**

Final approval and acceptance of this thesis is contingent upon the candidate's submission of the final copies of the thesis to HBNI.

I/We hereby certify that I/we have read this thesis prepared under my/our direction and recommend that it may be accepted as fulfilling the thesis requirement.

Date:

Place: **Dr. N. Sivaraman**

Guide

STATEMENT BY AUTHOR

This dissertation has been submitted in partial fulfillment of requirements for an advanced degree at Homi Bhabha National Institute (HBNI) and is deposited in the Library to be made available to borrowers under rules of the HBNI.

Brief quotations from this dissertation are allowable without special permission, provided that accurate acknowledgement of source is made. Requests for permission for extended quotation from or reproduction of this manuscript in whole or in part may be granted by the Competent Authority of HBNI when in his or her judgment the proposed use of the material is in the interests of scholarship. In all other instances, however, permission must be obtained from the author.

Balija Sreenivasulu

DECLARATION

I, hereby declare that the investigation presented in the thesis has been carried out by me. The work is original and has not been submitted earlier as a whole or in part for a degree / diploma at this or any other Institution / University.

Balija Sreenivasulu

List of Publications arising from the thesis

Journals

1. **B. Sreenivasulu**, A. Suresh, S. Subramaniam, K.N. Sabharwal, N. Sivaraman, K. Nagarajan, T.G. Srinivasan, P.R. Vasudeva Rao. "Separation of U(VI) and Pu(IV) from Am(III) and trivalent lanthanides with tri-iso-amyl phosphate (TiAP) as the extractant by using an ejector mixer-settler". *Solvent Extr. Ion Exch*. **2015**, 33(2), 120-133.
2. **B. Sreenivasulu**, A. Suresh, N. Sivaraman, P.R. Vasudeva Rao. "Solvent extraction studies with some fission product elements from nitric acid media employing tri-iso-amyl phosphate and tri-n-butyl phosphate as extractants". *J. Radioanal. Nucl. Chem*. **2015**, 303(3), 2165-2172.
3. **B. Sreenivasulu,** A. Suresh, N. Sivaraman, P.R. Vasudeva Rao. "Co-extraction and co-stripping of U (VI) and Pu (IV) using tri-iso-amyl phosphate and tri-n-butyl phosphate in n-dodecane from nitric acid media under high loading conditions". *Radiochim. Acta*. **2015**, 104(4), 227-237.
4. **B. Sreenivasulu**, K. Chandran, P. C. Clinsha, A. Suresh, N. Sivaraman, S. Anthonysamy. "Effect of gamma irradiation on thermal decomposition of tri-iso-amyl phosphate–nitric acid biphasic systems". *J. Therm. Anal. Calorim*. **2016** 125: 483.
5. **B. Sreenivasulu**, A. Suresh, N. Sivaraman and M Joseph. "Studies Related to Processing of U-Zr and U-Pu-Zr metallic fuels using Tri-iso-amyl Phosphate (TiAP) as extractant". *Solvent Extr.Ion Exch*. **2016**, 34(5), 422-438.
6. **B. Sreenivasulu**, A. Suresh, S. Rajeswari, N. Ramanathan, M.P.Antony, N. Sivaraman and M.Joseph. "Physicochemical Properties and Radiolytic Degradation Studies on Tri-iso-Amyl Phosphate". *Radiochim. Acta*. **2016**, DOI: 10.1515/ract-2016-2674.
7. **B.Sreenivasulu**, A. Suresh, N. Sivaraman and M.Joseph. "Dissolution and characterisation studies with U–Zr and U–Pu–Zr based alloys in nitric acid medium". *J. Radioanal. Nucl. Chem*. **2016**, DOI 10.1007/s10967-016-5109-6.
8. A. Suresh, **B. Sreenivasulu**, S. Jayalakshmi, S. Subramaniam, K.N. Sabharwal, N. Sivaraman, K. Nagarajan, T.G. Srinivasan, R. Natarajan, P.R. Vasudeva Rao. "Mixer-settler runs for the evaluation of tri-iso-amyl phosphate (TiAP) as an alternate extractant to tri-n-butyl phosphate (TBP) for reprocessing applications". *Radiochim. Acta*. **2015**, 103(2), 101-108.

9. K. Chandran, **B. Sreenivasulu**, N. Ramanathan, P.C.Clinsha, A. Suresh, N. Sivaraman and V. Jayaraman. Thermal decomposition behaviour of irradiated tri n-butyl phosphate and mixture of di and mono n-butyl phosphate-nitric acid systems (Manuscript under preparation)

Conferences

1. **B. Sreenivasulu,** A. Suresh, Arpita Datta, N.L. Sreenivasan, C.V.S. Brahmmananda Rao, S. Subramaniam, K.N. Sabharwal, N. Sivaraman, K. Nagarajan, T.G. Srinivasan, R. Natarajan, P.R. Vasudeva Rao. Separation of U(VI) and Pu(IV) from Am(III) and trivalent lanthanides with TiAP as the extractant by using an ejector mixer-settler: NUCAR 2013, Feb 19–23, 2012, Govt. Model Science College, R.D. University, Jabalpur.
2. **B.Sreenivasulu,** A. Suresh, K.N. Sabharwal, N. Sivaraman, P.R. Vasudeva Rao. Studies on the Extraction behaviour of some fission product elements employing Tri-*iso*-Amyl Phosphate and Tri-*n*-butyl phosphate as extractants. Proc. of Emerging Trends in Separation Science and Technology (SESTEC-2014), BARC, Mumbai, Feb.25-28, 2014. P.98.
3. **B. Sreenivasulu,** A. Suresh, K.N. Sabharwal, N. Sivaraman, P.R. Vasudeva Rao. A comparison of the degradation behavior of Tri-iso-amyl Phosphate and Tri-n-butyl Phosphate. Proc. of Emerging Trends in Separation Science and Technology (SESTEC-2014), BARC, Mumbai, Feb.25-28, 2014. P.97.
4. P.Manoravi, **B.Sreenivasulu**, M.Joseph, and N.Sivakumar: Laser Desorption/Ionization Mass Spectrometric studies on Tri-iso-amyl phosphate. Proc. of Indian Society for mass Spectrometry (ISMAS-2014), Parwanoo, Himachal Pradesh, Mar.9-13, 2014.
5. **B.Sreenivasulu,** A. Suresh, N. Sivaraman and P.R. Vasudeva Rao, Macro level extraction of U(VI) and Pu(IV) by Tri-iso-amyl Phosphate and Tri-n-butyl Phosphate from Nitric Acid Media. NUCAR 2015, Feb 9–13, P.142, BARC, Mumbai.
6. **B.Sreenivasulu,** A. Suresh, N. Sivaraman and P.R. Vasudeva Rao, Solvent extraction studies with U-Zr system from nitric acid media Employing Tri-iso-amyl Phosphate (TiAP) and Tri-n-butyl Phosphate (TBP) as extractants. NUCAR 2015, Feb 9–13, P.154, BARC, Mumbai.
7. K.Chandran, **B.Sreenivasulu,** A.Suresh, N.Sivaraman, S.Anthonysamy. Thermal decomposition studies on Tri-iso-amyl Phosphate in n-Dodecane–nitric acid system. ISMC-2014, DEC 9-13, P.437, BARC, Mumbai.

8. **B.Sreenivasulu,** S. Rajeswari, A. Suresh, M.P. Antony, N. Sivaraman. A comparison of the Interfacial Tension of Tri-iso-amyl Phosphate and Tri-n-butyl Phosphate. SESTEC-2016, May 17-20, P.62, IIT-Guwahati, Guwahati.
9. **B.Sreenivasulu,** A. Suresh, K.N. Sabharwal, N. Sivaraman and M.Joseph. Dissolution of zirconium containing metallic alloy fuels and development of analytical method for Spectrophotometric determination of zirconium. SESTEC-2016, May17-20, P.101, IIT-Guwahati, Guwahati.

Other publications

1. G. Gopakumar, **B. Sreenivasulu,** A. Suresh, C. V. S. Brahmmananda Rao, N. Sivaraman, M. Joseph, and A. Anoop. Complexation Behaviour of the Tri-n-butyl Phosphate Ligand with Pu(IV) and Zr(IV): A Computational Study. *J. Phys. Chem. A*, **2016**, 120 (24), 4201–4210.
2. A. Suresh, **B. Sreenivasulu**, N. Sivaraman, P.R. Vasudeva Rao: Empirical Equations for the Prediction of Third Phase Formation Limits in the Extraction of Thorium Nitrate by Tri-iso-amyl Phosphate (TiAP). *J Radioanal Nucl Chem*, **2015**, *306*(2), 489-495.
3. A. Suresh, C.V.S. Brahmmananda Rao, **B. Sreenivasulu**, N.L. Sreenivasan, S. Subramaniam, K.N. Sabharwal, N. Sivaraman T.G. Srinivasan, R. Natarajan, P.R. Vasudeva Rao. Development of alternate extractants for separation of actinides. *Energy Procedia*. 39, **2013**, 120-126

Balija Sreenivasulu

Dedicated To My Beloved

"Parents and Family"

ACKNOWLEDGEMENTS

I express my sincere thanks to my Ph.D supervisor **Dr. N. Sivaraman,** for his guidance, constant support, and valuable suggestions to improve the quality of work throughout my tenure. His innovative ideas, immense knowledge and keen interest made my research work challenging and stimulating. His mentorship and consolidated review have lead to the successful completion of the thesis work.

I take immense pleasure in thanking **Dr. A. Suresh,** for his keen assessment of work, support, guidance, valuable suggestions and constant encouragement.

I am pleased to express my deep sense of gratitude to my doctoral committee chairman, **Dr. S. Anthonysamy** and members **Dr. C. Mallika** and **Dr. M. P. Antony**, for their valuable suggestions.

I wish to express my special thanks to **Dr. K. Chandran** for his constant support, kind help and valuable suggestions during adiabatic calorimetry experiments.

I would like to thank **Dr. T. S. Lakshmi Narasimhan** for the many useful suggestions and corrections in thesis.

I am grateful to my section colleagues **Dr. K.N. Sabharwal, Mr. N.L. Sreenivasan, Mr. S. Subramaniam, Dr. C.V.S.B. Rao, Mrs. Sujatha, Dr. G. Gopakumar, Mr. K. C. Pitchaiah and Mrs. S. Jayalakshmi** for their co-operation in the lab which helped me to plan and execute the experiments meticulously.

I also wish to express my special thanks to **Mrs. N. Navamani, Mrs. R. Ganga Devi and Mr. P. Amarendiran** for their help and support in handling radioactive materials, analysis of various samples, of U and Pu.

I express my sincere thanks to **Dr. M. Joseph, Dr. K. Sankaran, Dr. N. Ramanathan, Mrs. S. Rajeswari, Mrs. P. C. Clinsha, Dr. Arpita Datta, Sri. G. G. S. Subramanian and Mrs. S. Annapoorani** for their help in experimental work.

I would express my sincere thanks to **Dr. K. Benadict Rakesh and Miss. Aditi Chandrasekar** for their timely help in crucial moments. I profoundly thank all the members of H-13 and H-14 labs for their assistance.

I am extremely thankful to my family members for their constant support and encouragement.

Balija Sreenivasulu

December, 2016

CONTENTS

CHAPTER 1

INTRODUCTION

CHAPTER 2

EXPERIMENTAL

CHAPTER 3

EXTRACTION BEHAVIOUR OF U(VI), Pu(IV) AND FISSION PRODUCTS WITH TiAP-BATCH STUDIES

CHAPTER 4

MIXER-SETTLER RUNS WITH TiAP BASED SOLVENT

CHAPTER 5

DISSOLUTION, CHARACTERISATION AND SOLVENT EXTRACTION STUDIES WITH U-Zr AND U-Pu-Zr ALLOY FUELS

CHAPTER 6

THERMAL DECOMPOSITION STUDIES WITH TiAP AND TBP SOLVENTS

CHAPTER 7

RADIOLYTIC DEGRADATION STUDIES WITH TiAP

CHAPTER 8

CONCLUSIONS

SYNOPSIS

Nuclear energy is an important option for satisfying the growing demand for energy, especially in developing countries like India. Presently, the nuclear energy contribution in our country is only ~3% to the total electricity generation and it is mainly derived from the uranium resources using thermal reactors [1]. India has limited uranium resources and vast thorium resources. The isotopic abundance of natural uranium available in the earth crust is ^{235}U ~0.72% and ^{238}U ~99.3%. Among ^{235}U and ^{238}U, the ^{235}U is the fissile material which undergoes fission in a thermal reactor e.g. Pressurised Heavy Water Reactor (PHWR). The unused ^{235}U (which is usually in the range of 0.2 to 0.4 atom% ^{235}U) along with Pu which is produced in PHWR reactors has to be recycled. For the effective utilization of nuclear fuels and for energy production in our country, a three-stage nuclear power programme was envisaged in the sixties as a long-term strategy [2]. The second stage of Indian nuclear program involves fast reactors, which enables effective utilization of plutonium and uranium. The ^{238}U can be effectively converted to ^{239}Pu in a fast reactor and can be employed as a fuel in subsequent reactors. Thus for better utilization of uranium, FBRs with closed fuel cycle facility is an inevitable option. The major advantages of Fast Breeder Reactor (FBRs) include high burn up (atom % fission or burn-up is the number of fissions per 100 initial heavy element atoms), effective uranium utilization, breeds more fissile material than consumed over a period of time and better energy efficiency [3, 4].

The Indian fast breeder reactor programme was initiated with the commissioning of Fast Breeder Test Reactor (FBTR) in 1985. The experience gained in the construction, commissioning and operation of FBTR as well as worldwide FBR operational experience, have provided the necessary confidence to launch a Prototype FBR (PFBR) of 500 MWe capacity with Uranium-Plutonium mixed oxide as the fuel [3]. Metal fuel will be considered as the fuel for future Indian fast reactors. The normally used metal fuel compositions are U-Zr

and U-Pu-Zr alloys where the Pu content varies from 15-19 wt% and Zr from 6-22 wt%. A ternary alloy of U-19wt%Pu-10wt%Zr has been used earlier [5].

The success of FBR programme depends on the reprocessing of irradiated fuels. The PUREX (Plutonium Uranium Extraction) process which has been well understood is likely to remain the work horse of fast reactor fuel reprocessing (FRFR) program [6]. The challenges with fast reactor fuel reprocessing involves higher plutonium content, higher specific activity and decay heat generation, enhanced formation of platinum group metals (Ru, Rh and Pd) and insoluble residues during the fuel dissolution in nitric acid medium [6]. These challenges lead to serious modifications in the PUREX process or substituting PUREX process with alternate non-aqueous process (mainly molten inorganic salts) e.g. for the metallic fuels [7].

Tri-n-butyl phosphate (TBP) in n-alkane diluent medium (typically 1.1M of extractant in diluent) has been utilized as a versatile solvent for various separation processes in nuclear technology [8]. However, the experience gained in the last six decades has brought out a few drawbacks of TBP that are of concern during reprocessing of fast reactor fuels. The major drawbacks of TBP include third phase formation with tetravalent metal ions e.g. Pu(IV), higher aqueous solubility, radiation degradation etc [9-11]. Several symmetrical trialkyl phosphates (TalP) e.g. tri-*n*-amyl phosphate (TAP), a higher homologue of TBP, some of its isomers such as tri-2-methyl butyl phosphate (T2MBP), tri-*iso*-amyl phosphate (TiAP, tri-3-methyl butyl phosphate), tri-*sec*-amyl phosphate (TsAP) etc., have been investigated in our laboratory towards identification of an alternate extractant to TBP for fast reactor fuel reprocessing [12-14]. Studies on physicochemical and extraction properties as well as third phase formation behavior have revealed that TiAP is a potential extractant for fast reactor fuel reprocessing.

Prior to the deployment of a novel solvent, TiAP /n-dodecane (n-DD) in an actual reprocessing plant, it is essential to understand the various aspects of TiAP system. These include extraction and stripping behavior of U and Pu under process conditions, possibility of

third phase formation with Pu(IV), extraction behavior of fission products, decontamination factors achievable, behavior of a solvent in a continuous counter-current solvent extraction, radiolytic stability and thermal decomposition behavior of a solvent in biphasic systems.

In this context, the present study mainly focused on the issues arising from reprocessing of fast reactor fuels. The objective of the present study is to understand extraction behavior of actinides (U, Pu and Am), troublesome fission products (e.g. Zr, Ru, Tc) and some of the lanthanides (La, Pr, Nd, Sm, Eu) as fission product representatives with TiAP and compare with the TBP/n-DD system under identical experimental conditions. Continuous counter-current solvent extraction runs with TiAP based solvent using a mixer-settler have been carried out under various experimental conditions. Preliminary studies have been also carried out to develop an alternate method for the processing of metallic alloy fuels by aqueous route using PUREX process with TiAP based system. Thermal and radiolytic stability of TiAP system have been investigated; the results of TiAP solvent are compared with TBP. The thesis is organized into eight chapters and the details of these are described as follows.

Chapter 1: Introduction

Chapter 1 describes the importance of nuclear energy. The significance of three stage nuclear program adopted by India to effectively utilize the limited uranium reserves and abundant thorium reserves is discussed. The importance of FBRs for effective utilization of uranium in India has been highlighted. The major differences between thermal reactor and fast reactor fuel reprocessing are explained. The chemistry of actinides, lanthanides and troublesome fission products are described. Introduction to different types of solvent extraction processes and the difference between different types of liquid-liquid contactors are provided. Methodologies for the dissolution of metallic fuels are discussed. Methods employed in literature to estimate Zr in the presence of other elements are described. The basis for development of an aqueous route for processing of the metallic fuels has been

discussed. The thermal and radiolytic degradation aspects of a solvent are explained. The effect of degradation products on the extraction of actinides and fission products are briefly explained. The details about TiAP, a potential extractant for fast reactor fuel reprocessing have been discussed. The overview and scope of the present work is also explained in this chapter.

Chapter 2: Experimental

Chapter 2 describes the details of chemicals, instruments and experimental procedures employed in the present study. The details about the preparation of standard solution, indicator solution, buffer solution and extractant solution are discussed. The methods used for the quantitative determination of metal ions such as U(VI), Pu(IV), Ln(III), Zr(IV), $RuNO^{3+}$, TcO^{4-}, Am(III) and free acidity in the presence of other metal ions are provided. The details about the measurements of physicochemical parameters such as density, viscosity and interfacial tension (IFT) are described. The experimental procedures for the extraction of metal ions as a function of equilibrium aqueous phase metal ion as well as concentration of nitric acid are explained. The details about the stage-wise extraction and stripping of metal ions with trialkylphosphates in cross-current mode are discussed. Details about the mixer-settler facility and experimental details of counter-current solvent extraction runs with 1.1M TiAP/HNP (Heavy Normal Paraffin) are discussed. The methodologies for the dissolution of U-Zr and U-Pu-Zr metallic alloy fuels in nitric acid medium are discussed. The procedures for the extraction and stripping of metal ions from the U-Zr and U-Pu-Zr feed solutions are explained. Details about the adiabatic calorimeter and quadruple mass spectrometry (QMS) facility are explained in this chapter.

Chapter 3: Extraction behavior of U(VI), Pu(IV) and fission products with TiAP-Batch studies

Chapter 3 explains the batch extraction of Pu(IV) using 1.1M TiAP/n-DD under high metal loading conditions as a function of equilibrium aqueous phase Pu(IV) concentration and

concentration of nitric acid at 303 K. Co-extraction behavior of U(VI) and Pu(IV) using 1.1 M solutions of TiAP and TBP in n-DD from 4M HNO_3 at 303 K has been investigated and the results are discussed. Batch studies were carried out in the cross-current mode to assess the number of stages required for co-extraction and co-stripping of heavy metal ions using 1.1M TiAP/n-DD system. The percentage efficiencies were calculated for 1.1M TiAP/n-DD and compared with the TBP system.

Batch studies were also carried out to investigate the extraction behavior of fission products such as Zr(IV), RuNO(III), TcO_4^-, La(III), Ce(III) and Nd(III) along with Am(III) with 1.1M solutions of TiAP as well as TBP in *n*-alkane diluent from nitric acid medium. The extraction of Zr(IV) has been evaluated with unirradiated and gamma irradiated solvents as a function of organic phase U(VI) loading. The influence of degradation products of TiAP and TBP on the extraction behavior of fission products has been discussed. The formation of interfacial deposits during the washing of gamma irradiated solvents with alkali solution has been discussed.

Chapter 4: Mixer-settler runs with TiAP based solvent system

Chapter 4 deals with the mixer-settler runs carried out using 1.1M TiAP/HNP as the solvent. Mixer-settler runs were carried out with U(VI) solution to understand the extraction and stripping behavior of U(VI) with TiAP under high solvent loading conditions. Separation of U(VI) and Pu(IV) from Am(III) and lanthanides with 1.1M TiAP/HNP solvent using an ejector mixer-settler has been demonstrated and the results are discussed. Profiles for the extraction and stripping of nitric acid, U(VI) and Pu(IV) were plotted against stage number and the results are discussed. Overall and stage-wise mass balance data for the above runs are also provided in this chapter.

Chapter 5: Dissolution, characterization and solvent extraction studies with U-Zr and U-Pu-Zr alloy fuels

Chapter 5 deals with the dissolution of Zr containing metallic alloy fuels such as U-Zr and U-Pu-Zr in HNO_3 media under various conditions. Electro-oxidative dissolution technique using cerium as the oxidizing agent has been examined for the dissolution of Zr containing alloys. Explosive nature of metallic alloy fuels during the dissolution in concentrated nitric acid medium (16M) has been investigated. A method has been developed for the determination of microgram quantities of Zr in the presence of U and Pu matrix. This chapter also deals with the possible use of aqueous reprocessing based method as an alternate to pyro-processing of metallic fuels. Solvent extraction studies in the batch mode were carried out with U-Zr and U-Pu-Zr metallic alloy systems. Batch studies were carried out for the co-extraction and co-stripping of heavy metal ions with 1.1M TiAP and 1.1M TBP in n-DD medium from U-Zr as well as U-Pu-Zr feed solutions in stage–wise mode. Percentage extraction and stripping of metal ions were computed in each stage and the results are discussed in this chapter.

Chapter 6: Thermal decomposition studies with TiAP and TBP based solvents

Chapter 6 deals with the thermal decomposition behavior of TiAP-nitric acid biphasic systems using an adiabatic calorimeter. Experiments were conducted in a closed air ambience under heat-wait-search (H-W-S) mode. Thermal decompostion of TiAP has been investiagated by varying the parameters such as concentration of nitric acid, HNO_3/TiAP volume ratio, gamma irradiation and influence of diluent. Thermochemical and kinetic parameters have been derived from the calorimetric data and results are presented. The results of unirradiated TiAP-HNO_3 system have been compared with the irradiated system. The gaseous end products generated during thermal decomposition were characterised by employing techniques such as FT-IR and QMS. Similarly, thermal decomposition studies

were also carried out with TBP based solvent under identical conditions and the results are compared with TiAP based system.

Chapter 7: Radiolytic degradation studies with TiAP

Chapter 7 deals with the radiolytic degradation of TiAP based solvent system. Physicochemical properties such as density, viscosity and interfacial tension (IFT) were measured for unirradiated and irradiated TiAP solutions. The extent of degradation was determined by measuring the variation in the extraction behavior of U(VI) and Pu(IV) with irradiated solvent systems. U and Pu retention by the irradiated solvents were also measured. Effect of alpha degradation was studied by Pu retention as a function of time using 1.1M TiAP/n-DD. Laser desorption/ionization mass spectrometric technique was employed to identify the possible radiolytic degradation products. Similar studies were also carried out with TBP based solvent under identical conditions.

Chapter 8: Conclusions

The conclusions drawn from the present investigations are summarized in Chapter 8. Some of the highlights of studies carried out towards the thesis are listed below.

- TiAP based solvent does not form third phase during the extraction of Pu(IV) from a wide range of concentration of nitric acid , unlike TBP based system.
- Co-extraction studies with U(VI) and Pu(IV) by TiAP indicate that it is possible to achieve maximum loading of heavy metal ions into the organic phase without phase splitting.
- The studies on distribution ratio of fission product elements indicate that the decontamination factors that can be achieved for U and Pu against the fission product elements with TiAP are nearly similar to TBP.
- Investigations also indicate an enhancement in the extraction of Zr in the presence of degradation products of TiAP or TBP.

- Mixer-settler experiments demonstrated that TiAP can be employed as an extractant for reprocessing of spent fast reactor fuels with negligible loss of heavy metals into the raffinate and lean organic streams.
- Preliminary studies were carried out to develop an alternate method for reprocessing of metallic alloy fuels using aqueous route; complete dissolution of U, Pu and partial dissolution of Zr (~70%) was obtained with HNO_3 medium. Complete dissolution of Zr was achieved in the presence of HF medium.
- A modified spectrophotometric method was developed for the determination of Zr in the presence of U and Pu matrix (U: Pu: Zr= 1000:400:1).
- Batch studies with U-Zr and U-Pu-Zr feed solutions indicate that TBP based solvent forms third phase with Zr under certain experimental conditions.
- The thermal decomposition studies of irradiated and unirradiated TiAP and TBP in the presence and absence of nitric acid have been studied in detail using an adiabatic calorimeter and the results indicate that thermal stability of TiAP is on par with TBP.
- The lower aqueous phase solubility of TiAP (80µg/mL) compared to TBP (400µg/mL) has a great advantage in minimizing red oil related issues e.g. runaway reactions.
- The present study indicated that the radiolytic degradation behavior of TiAP system is on par with TBP based system
- The lower third phase formation tendency, lower aqueous solubility, stability against thermal and radiation degradation makes TiAP based solvent system, a potential extractant for fast reactor spent fuel reprocessing program.

References:

1. Grover R, Chandra S (2006) Scenario for growth of electricity in India. Energy Policy 34:2834-2847
2. Chidambaram R, Ganguly C (1996) Plutonium and thorium in the Indian nuclear programme. Current Science 70:21-35
3. Chetal S, Chellapandi P, Puthiyavinayagam P (2011) Current status of fast reactors and future plans in India. *Energy Procedia* 7:64-73
4. Raj B, Kamath H, Natarajan R (2005) A perspective on fast reactor fuel cycle in India. Progress in Nuclear Energy 47:369-379
5. Carmack W, Porter D, Chang Y (2009) Metallic fuels for advanced reactors. *J. Nucl. Mater*.392:139-150
6. Natarajan R, Raj B (2007) Fast reactor fuel reprocessing technology in India. *J. Nucl. Sci. Technol.* 44:393-397
7. Ackerman JP (1991) Chemical basis for pyrochemical reprocessing of nuclear fuel. *Ind. Eng. Chem. Res.*30:141-145
8. Sood DD, Patil SK (1996) Chemistry of nuclear fuel reprocessing: Current status. *J. Radioanal. Nucl. Chem. Art.* 203:547-573
9. Mincher B, Modolo G, Mezyk S (2009) Review Article: The Effects of Radiation Chemistry on Solvent Extraction: 1. Conditions in Acidic Solution and a Review of TBP Radiolysis. *Solvent Extr. Ion Exch*. 27:1-25
10. Rao PRV, Kolarik Z (1996) A review of third phase formation in extraction of actinides by neutral organophosphorus extractants. *Solvent Extr. Ion Exch*.14:955-993
11. Wright A, Paviet-Hartmann P (2010) Review of Physical and Chemical Properties of Tributyl Phosphate/Diluent/Nitric Acid Systems. *Sep. Sci. Technol.*45:1753-1762

12. Suresh A, Srinivasan TG, Rao PRV (2009) Parameters Influencing Third-Phase Formation in the Extraction of Th $(NO_3)_4$ by some Trialkyl Phosphates. *Solvent Extr. Ion Exch.*27:132-158

13. Suresh A, Srinivasan TG, Rao PRV (2009) The Effect of the Structure of Trialkyl Phosphates on their Physicochemical Properties and Extraction Behavior. *Solvent Extr. Ion Exch.*27:258-294

14. Suresh A, Srinivasan TG, Rao PRV (1994) Extraction of U(VI), Pu(IV) and Th(IV) by some trialkyl phosphates. *Solvent Extr. Ion Exch*.12:727-744.

LIST OF FIGURES

LIST OF TABLES

ABBREVIATIONS

ABBREVIATION	FULL NAME
AA	Ascorbic acid
Aq	Aqueous
BDL	Below detection limit
C_P	Heat capacity
CE	Centrifugal extractors
CEPOD	Catalysed Electro-Chemical Plutonium Oxide Dissolution
CyDTA	Trans-1, 2-Cyclohexanediamine-N, N, N', N'-tetraacetic acid
CORAL	Compact reprocessing of advanced fuels in lead mini cells
DAAP	Diamylamyl phosphonate
DiAP	Di-iso-amyl phosphate
DBP	Dibutyl phosphate
DFs	Decontamination factors
DHOA	N,N-Dihexyl octanamide
DTBP	Di-tert-butyl peroxide
D	Distrubution ratio
D_A, D_B, D_M, $D_{U(VI)}$, $D_{Pu(IV)}$, $D_{Zr(IV)}$, D_{HNO3}	Distribution ratio of solute A, solute B, metal ion, U(VI), Pu(IV), Zr(IV) and HNO_3, respectively
MiAP	Mono-iso-amyl phosphate
n-DD	n-Dodecane
EODT	Electrooxidative dissolution
EDTA	Ethylenediaminetetraacetic acid
FBTR	Fast breeder test reactor
FRFR	Fast reactor fuel reprocessing
$[HNO_3]_{aq,eq}$	Equilibrium aqueous phase concentration of nitric acid
$[U(VI)]_{aq,eq}$	Equilibrium aqueous phase U(VI) concentration
$[Pu(IV)]_{aq,eq}$	Equilibrium aqueous phase Pu(IV) concentration
$[Zr(IV)]_{aq,eq}$	Equilibrium aqueous phase Zr(IV) concentration
K_{eq}	Equilibrium constant
$[Pu(IV)]_{org,eq}$	Equilibrium organic phase Pu(IV) concentration

$[U(VI)]_{org,eq}$	Equilibrium organic phase U(VI) concentration
$[Zr(IV)]_{org,eq}$	Equilibrium organic phase Zr(IV) concentration
IFT	Interfacial tension
FBR	Fast breeder reactors
HNP	Heavy normal paraffins
HLLW	High level liquid waste
HPLC	High Performance Liquid Chromatography
IR	Infra red
ICP-OES	Inductively Coupled Plasma-Optical Emission Spectrometry
Ln	Lanthanides
LET	Linear energy transfer
LIMS	Laser ionization mass spectrometer
LPC	Liquid pulsed columns
LOC	Limiting organic concentration
LSC	Liquid scintialltion counting
LWR	Light water reactors
MBP	Monobutyl phosphate
NMR	Nuclear magnetic resonance
NPH	Normal paraffin hydrocarbon
CMPO	Octyl(phenyl)-N,N-diisobutyl carbamoylmethylphosphine oxide
OK	Odourless kerosene
Org	Organic
KHP	Potassium hydrogen phthalate
PHWR	Pressurized heavy water reactor
PUREX	Putonium uranium extraction
QMS	Qudropole mass spectrometer
RSD	Realtive standard deviation
n-TD	n-Tetradecane
TRFR	Thermal reactor fuel reprocessing
TTA	Thenoyl trifluoroacetone
TalP	Trialkyl phosphate
TalPs	Trialkyl phosphates
TiAP	Tri-iso-amyl phosphate

TsAP	Tri-sec-amyl phosphate
TAP	Tri-n-amyl phosphate
TEA	Triethanol amine
THP	Trihexyl phosphate
TBP	Tri-n-butyl phosphate
T2MBP	Tri-2-methyl butyl phosphate
XO	Xylenol orange
Br-PADAP	2-(5-Bromo-2-pyridylazo)-5-(diethylamino) phenol

Chapter 1

INTRODUCTION

1

1.1 Nuclear energy scenario in India

Nuclear energy is an important option for satisfying the growing demand for energy, especially in developing countries like India [1-3]. At present the nuclear energy contribution in India is only about 3% to the total electricity generation and it is mainly derived from the uranium resources using thermal reactors. In thermal reactors, fission is caused by thermalized neutrons (0.025eV) [4]. India has limited uranium resources and vast thorium resources. The isotopic abundance of natural uranium available in the earth crust is ^{235}U (~ 0.72%) and ^{238}U (~ 99.3%). Among ^{235}U and ^{238}U, ^{235}U is the fissile material, which undergoes fission in a thermal reactor e.g. Pressurised Heavy Water Reactor (PHWR) [5, 6]. The spent fuel from PHWR comprises of uranium (~ 0.2 to 0.4 atom % ^{235}U of the total uranium) along with Pu (^{239}Pu: 73% and ^{240}Pu: 23%, with small amounts of ^{241}Pu and ^{242}Pu). The fertile ^{238}U can also be utilised effectively in a fast reactor / fast breeder reactor (FBR) [7, 8]. In India, for maximum utilization of nuclear fuel resources and for energy production, a three-stage nuclear programme was envisaged in the sixties as a long-term strategy [9]. The first stage comprises of PHWR fuelled with natural uranium; the second stage consists of fast reactors fuelled with U and Pu mixed oxide/carbide and thorium as the blanket material. The third stage reactors (thermal breeders) are expected to be fuelled with ^{233}U, which will be produced in fast reactors [10-13]. In this manner, natural uranium can be utilised upto ~ 60-70% using thermal and fast reactors. The major advantages of FBRs are as follows [14].

1. High burn up can be achieved which minimises the fuel fabrication and reprocessing costs
2. Uranium utilisation can be increased with the conversion of uranium to plutonium
3. Fast reactors can be used as plutonium and minor actinide burning machines; they also can be employed for transmuting other long lived radionuclides
4. Fast reactors breeds more fissile material than consumed over a period of time

5. Higher operating temperature compared to thermal reactors, leading to better energy efficiency

The annual requirement of fuel for 1000MWe FBR is compared in Table 1.1 with equivalent capacity of thermal reactors as well as with other power production plants. In FBRs, the uranium (fissile equivalent) requirement is only 1.3 tonnes compared to 200 tonnes of natural uranium needed for PHWRs.

Table 1.1: The annual requirement of fuel for 1000MWe power plant

Fuel	Amount/Area	Energy potential (kWh)/kg
Coal	2600000 tonnes	3
Oil	2000000 tonnes	4
Solar thermal/photovoltaic parks	20-50 km^2	-
Wind power	50-150 km^2	-
Biomass plantations	4000-6000 km^2	-
Natural uranium in PHWRs	200 tonnes	50,000
FBRs	1.3 tonnes of uranium(fissile equivalent)	3, 500,000

1.2 FBR Programme in India

FBRs with closed fuel cycle facility are an inevitable option in view of its better uranium utilization. FBRs are also crucial for converting ^{232}Th to ^{233}U for third stage Indian nuclear programme. In India, the power potential of PHWRs is ~10GWe, whereas with FBRs, power potential can be increased to ~ 530GWe and with the implementation of third stage nuclear programme, it could further be enhanced to ~ 1,55,000GWe [15-17]. Several countries such as UK, France, Germany, Japan and China generate power through fast reactors. In India, the fast reactor programme was initiated in 1975 and the Fast Breeder Test Reactor (FBTR) with uranium and plutonium mixed carbide as the fuel was commissioned in 1985 [18]. The experience gained from the construction, commissioning and operation of FBTR as well as worldwide FBR operational experience have provided the necessary

confidence to launch a Prototype FBR of 500MWe capacity (PFBR) [15]. In addition, it is proposed to construct six more units of 500MWe reactors based on MOX fuel and twin unit design with improved economy and enhanced safety. Metallic fuel reactors of 1000MWe capacity, with emphasis on breeding will be deployed in future fast reactors [19, 20]. The success of FBR programme depends on the reprocessing of irradiated spent fuels [16].

1.3 Open and closed nuclear fuel cycles

Economic considerations as well as possible proliferation of nuclear materials lead to adopting once through fuel cycle by many countries. In once through fuel cycle, the spent nuclear fuels are not reprocessed, but cooled and stored in a repository [21-24]. The total uranium utilization in this process is only about 3%. This programme is not useful for countries like India, where uranium resources are limited and hence it is mandatory to reprocess the spent nuclear fuels. Countries such as France, Japan, Russian Federation and the United Kingdom also reprocess the spent nuclear fuels. The utilisation of uranium can be increased with the use of fast reactors by adopting closed fuel cycle. In the case of fast reactors, multiple recycling of fissile material is absolutely essential, since the fissile content after irradiation is generally higher. In the case of thermal reactors, either once through or closed fuel cycle can be adopted; however, fast reactors will not be sustainable without a closed fuel cycle. The experience gained from thermal reactor fuel reprocessing (TRFR) will be useful for fast reactor fuel reprocessing (FRFR) program. However, there are major differences in reprocessing spent fuels of fast reactors compared to thermal reactors due to higher burn up and higher plutonium content encountered with the fast reactor fuels [24-26].

1.4 General considerations in fast reactor fuel reprocessing

Fast reactor fuel reprocessing differs from thermal reactor reprocessing in many aspects [27, 28]. The differences arise mainly from the following characteristics of spent fast reactor fuels:

- High specific activity and high decay heat generation due to high burnup (e.g. 10 atom% fission)
- Presence of sodium on subassemblies in the case of sodium cooled fast reactors resulting in additional steps to completely remove sodium
- Enhanced formation of platinum group metals during the course of fission in a fast reactor; dissolution of fast reactor spent fuel in nitric acid medium generally results in insoluble residues, mainly from platinoids
- Inert atmosphere to be maintained while dismantling and decladding fast reactor fuel pins due to the pyrophoric nature of carbide, nitride and metallic fuels
- The fissile material content in a fast reactor fuel can be as high as 30% compared to 0.7 to 4% in thermal reactors, thus making criticality an issue during reprocessing of spent fuels.
- Higher plutonium content in the spent fuel can lead to "third phase formation" during solvent extraction process; plutonium hydrolysis will be a concern during the stripping cycle of solvent extraction process.
- The quantity of fission products and radioactivity will be much higher in the spent fast reactor fuels, leading to higher solvent degradation

Hence modifications in the Plutonium Uranium Extraction (PUREX) process are required to meet the above challenges. Table 1.2 shows the major differences between thermal and fast reactor fuels. Table 1.3 represents the elemental composition and metal ion concentration in a dissolver solution obtained from thermal and fast reactor fuels. The plutonium contents are found to be about ten times higher in a fast reactor fuel compared to a thermal reactor fuel. The mixed uranium, plutonium carbide fuel discharged from FBTR (2.5 years cooled, 100 GWd/t burnup MC fuel with 70% Pu) has been successfully reprocessed in the Compact Reprocessing of Advanced fuels in Lead mini cells (CORAL), which was commissioned in late 2003 at IGCAR, Kalpakkam. The PUREX process has gained

significance due to the very high Pu content and high specific activity of the spent fuel discharged from FBTR [29-31].

Table 1.2 Differences between TRFR and FRFR

Properties	LWR-UOX	FBR-MOX
Cooling time/years	4	7
Burnup (GWd/t HM[#])	50	185
Total decay heat (W/t HM[#])	3.48	21.77
Dose emitted by aqueous phase (Wh/L)	0.57	6.72
Dose received by solvent (Wh/L)	0.20	2.40
Pu/(U+Pu)	0.004	0.15 to 0.7
Specific β, γ activity	~200 Ci/L	~1000 Ci/L
Third phase with plutonium	-	Expected under certain conditions

(# heavy metal)

1.5 Solution Chemistry of actinides, lanthanides and troublesome fission products

1.5.1 Uranium (U)

Four oxidation states such as tri, tetra, penta and hexavalent states are identified for uranium ions in solution and are represented as U(III), U(IV), UO_2^+ and UO_2^{2+}, respectively [33]. Each oxidation state has a characteristic colour in solution [Fig.1.1] and it depends on the type and number of ligands. Of these, only U(IV) and U(VI) are important ions in solution. In aqueous solutions, U(IV) is more prone to undergo hydrolysis similar to Pu(IV) and the free U(IV) ion is only observed at fairly high acidity [34]. The hydrolysis reaction of U(IV) is as follows;

$$U(IV) + xH_2O \leftrightarrow U(OH)_x^{(4-x)} + xH^+ \ (x = 1 \text{ to } 5) \quad \text{.....(1.1)}$$

Table 1.3 Elemental compositions and metal ion concentrations in dissolver solution for thermal and fast ractor fuel reprocessing (concentrations are obtained by dissolving 1000 kg of spent fuel in 3500 L of nitric acid) [32]

Metal ion	PWR-UO_2, 60 GWd/t, 5 wt% ^{235}U, 5 years cooling		FBR-MOX, 90 GWd/t, 20 wt% initial Pu, 4 years cooling	
	Weight (kg)/t	Concentration (g/L)	Weight (kg)/t	Concentration (g/L)
U	942	264	776	222
Pu	12.8	3.66	128	36.6
Np	0.93	0.265	0.466	0.133
Am	0.78	0.223	4.60	1.31
Cm	0.13	0.037	1.36	0.389
Sr	1.45	0.41	1.06	0.303
Zr	6.44	1.84	6.21	1.77
Mo	6.02	1.72	7.57	2.16
Tc	1.36	0.39	1.86	0.531
Cs	4.71	1.35	8.73	2.49
Ln(La-Gd)	17.8	5.08	29.0	8.29
Toatal FPs[#]	51.2	14.6	78.0	22.3

#FPs does not include contributions from Kr, Xe and I

In PUREX process, spent fuel is usually dissolved in nitric acid. The dissolution of uranium and uranium oxide in boiling nitric acid medium (11.7M) under reflux condition is shown in equations 1.2 and 1.3, respectively [35].

$$4\ U + 18\ HNO_3 \leftrightarrow 4\ UO_2(NO_3)_2 + 3NO_2 + 7NO + 9H_2O \quad \text{.....(1.2)}$$

$$UO_2 + 4\ HNO_3 \leftrightarrow UO_2\ (NO_3)_2 + 2NO_2 + 2H_2O \quad \text{..... (1.3)}$$

Fumeless dissolution can be achieved by sparging oxygen gas as reactant without any net evolution of gaseous products except the gaseous fission products. In the dissolver solution, uranium exists mainly in the form of uranyl nitrate ($UO_2(NO_3)_2$). In PUREX process, 30% Tri n-Butyl Phospahte (TBP) in n-alkane diluents has been employed as the solvent for the separation of uranium and plutonium from fission products in nitric acid medium. TBP extracts metal ion through coordinate covalent bond and in the case of acids

and water by hydrogen bonding. The extraction mechanism of U(VI) by TBP is presented in the following equation (1.4) [26].

$$UO_2^{2+} + 2NO_3^- + 2TBP \leftrightarrow UO_2(NO_3)_2.2TBP \text{ ..... } (1.4)$$

The Distribution ratio (*D*) of U(VI) is directly proportional to the square of free TBP concentration and nitrate ion concentration. The $D_{U(VI)}$ initially increases with concentration of nitric acid; however, at higher acidities, the *D* value decrease due to competition between nitric acid and metal ion for free TBP [36].

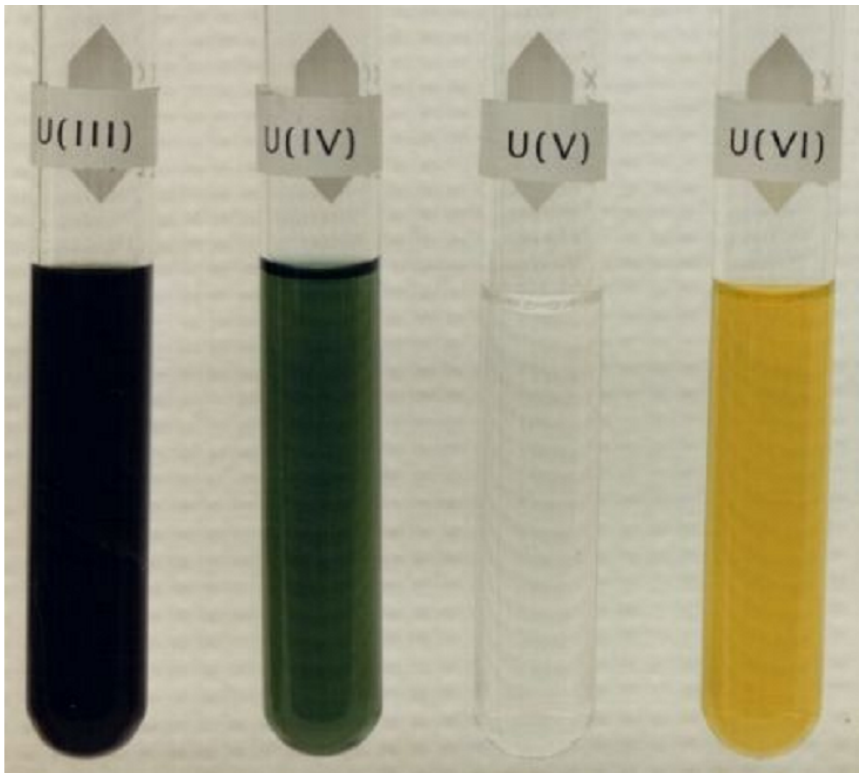

Fig.1.1: The colour of uranium ions in solution (Courtesy: Image taken from Dr. Andreas Kronenberg, Los Alamos National Laboratory, USA; http://www.chemie-master.de/FrameHandler.php?loc=http://www.chemie-master.de/pse/pse.php?modul=U, accessed on 23/09/2016)

1.5.2 Plutonium (Pu)

The chemistry of plutonium is important for several reasons, including the processing and purification of plutonium for preparation of pure metal, for managing nuclear waste, for predicting its behaviour in the environment, aging effects and the safety of nuclear weapons. Because of its electropositive nature, plutonium in aqueous solution will readily lose three to

seven of its outer electrons to form positively charged cations in five formal oxidation states, namely, Pu(III), Pu(IV), Pu(V), Pu(VI) and Pu(VII) and these ions in solution are represented as Pu^{3+}, Pu^{4+}, PuO_2^{+} and PuO_2^{2+} and PuO_5^{3-} respectively [37, 38].

Because of unique relationship between equilibria and the kinetics of converting from one oxidation state to another, it is possible for all four oxidation states (Pu(III), Pu(IV), Pu(V), Pu(VI)) to coexist in an appreciable concentrations in a given medium. Stabilization of a single ionic species is possible under controlled conditions. Tetravalent plutonium is the most stable oxidation state in nitric acid medium. Aqueous solutions of plutonium are frequently employed in reprocessing spent nuclear fuels. Plutonium nitrate solutions, were prepared by dissolving its metal or oxide in nitric acid medium (> 8M HNO_3). Dissolution rates are enhanced by the addition of hydrofluoric acid (~ 0.05M) or using oxidizing species such as Ag(II) and Ce(IV) [39].

Fig. 1.2: The colour of plutonium ions in solution (Courtesy: Image taken from Clark, D.L., 2000. The chemical complexities of plutonium. Los Alamos Science, 26, pp.364-381)

Solution chemistry of plutonium depends on the nature of its oxidation state and it has a characteristic colour in solution. The colours are specific and depends on the type and

number of ligands [40]. Fig.1.2 shows the aquo ions in 1M perchlorate ($HClO_4$) solution. (Pu(V) is in $NaClO_4$ at pH = 7, Pu(VII) is in 2.5M NaOH.).

Plutonium is unique among all the elements and the redox potentials of the couple in acid solution (III, IV, V and VI) are all remarkably similar and approximately equal to ~ 1.0 V. The plutonium cations have marked tendency to undergo disproportionate reaction, in which two interacting ions in the same oxidation state are simultaneously oxidized and reduced to higher and lower states [41-43] (Eq 1.5 and 1.6).

$$3Pu^{4+} + 2H_2O \leftrightarrow 2Pu^{3+} + PuO_2^{2+} + 4H^+ \text{ .....(1.5)}$$

$$2PuO_2^{+} + 4H^+ \leftrightarrow Pu^{4+} + PuO_2^{2+} + 2H_2O \text{ .....(1.6)}$$

Plutonium forms very stable complexes with strong Lewis bases such as CO_3^{2-}, F^- and PO_4^{3-}. The complex forming ability for plutonium ions are Pu(IV) > Pu(VI) ~ Pu(III) > Pu(V). Generally, Pu in any given valence is more strongly complexed than the corresponding uranium and neptunium ions.

The hydrolysis of tetravalent plutonium in an aqueous solution produces a complex hydroxide polymer [44-46]. The extent of polymer formation depends on the Pu(IV) concentration, pH, presence of other metal ions and temperature. With ageing, bright green polymeric product may settle or precipitate with loss of solution homogeneity and enhancement of the criticality risk. The net hydrolysis process, which is described by the following reaction, has an equilibrium constant, K_{eq}, 3.1×10^{-10}:

$$Pu(IV) + xH_2O \leftrightarrow Pu(OH)_x^{(4-x)} + xH^+ \text{ (x = 1 to 5).....(1.7)}$$

Plutonium dissolves slowly in HNO_3 and an oxide film is formed on the metal that inhibits the dissolution [37]. Pu metal dissolution in HNO_3 medium has been enhanced by the addition of HF, which destroys the passive layer by forming strong Pu(IV) fluoride complexes. It is important to keep the HNO_3 concentration below 5M to minimize the oxidation of the metal surface, while dissolving the metal. An optimum concentration is about 3M HNO_3 with 0.13M HF [39].

In PUREX process at the end of dissolution, plutonium will be present mainly in the tetravalent state (80-85%) and hexavalent state (15-20%). For complete extraction of plutonium by TBP during solvent extraction, tetravalent state has to be ensured by the addition of $NaNO_2$ followed by digestion at 50°C or by purging with NO_2 gas. The dual function of nitrite (i.e. it reduces Pu(VI) to Pu(IV) and oxidizes Pu(III) to Pu(IV)) makes it an ideal feed conditioning agent in PUREX process. NO_2 gas is generally preferred over $NaNO_2$ since it precludes the introduction of sodium ion as an impurity, thereby reducing the salt load to High Level Liquid Waste (HLLW) [26].

$$PuO_2^{2+} + NO_2^- + 2H^+ \leftrightarrow Pu^{4+} + NO_3^- + H_2O \text{.....(1.8)}$$

$$Pu^{3+} + NO_2^- + 2H^+ \leftrightarrow Pu^{4+}\,NO + H_2O \text{.....(1.9)}$$

$$6Pu^{3+} + 2NO_2^- + 8H^+ \leftrightarrow 6Pu^{4+} + N_2 + 4H_2O \text{.....(1.10)}$$

The extraction mechanism of Pu(IV) by TBP is represented in the following equation 1.11.

$$Pu^{4+} + 4NO_3^- + 2TBP \leftrightarrow Pu(NO_3)_4.2TBP \text{.....(1.11)}$$

The Distribution ratio (*D*) of Pu(IV) is directly proportional to the square of free TBP concentration and fourth power of nitrate ion concentration [47-49].

1.5.3 Zirconium (Zr)

Zr is one of the troublesome fission products along with Ru, Tc etc [50]. Zr exists as ZrO_2 in irradiated U-Pu oxide fuels. It dissolves as non-polymeric nitrato complexes in nitric acid medium and is also identified as $ZrMo_2O_8.nH_2O$ under low acidity conditions in the dissolver solution or if the solution is left to age or heated for a period of time [51-53]. It mainly exists as Zr(IV) in solutions of nitric acid and its chemistry is largely complicated by its tendency to hydrolyse and polymerise. In general, hydrolysis and polymerisation increase with increasing temperature and decreasing acidity [54]. Several authors reported the existence of various Zr complexes with the general formula $[Zr(OH)_x(NO_3)_y(H_2O)_z]^{4-x-y}$ in nitric acid medium. The amount of Zr produced in LWR (60 GWd/t, 4.5% ^{235}U, 5 year cooling) and FBRs (120 Gwd/t, 30% Pu, 5 year cooling) is about 6.3 and 9.36 kg/t, respectively.

Zr exists mainly in tetravalent oxidation state as Zr(IV) in nitric acid media; however, it exists in different chemical forms, depending upon the concentration of the acid, concentration of Zr and temperature [55]. For e.g. in the concentration range of 1-3M, $[Zr(OH)_x(H_2O)_y]^{4-x}$ was the species observed and hydroxo-bridged polymers were reported if concentration is reduced further. These polymers undergo an irreversible dehydration to form oxo-bridged species with time. For most of the elements, the distribution ratio increase with concentration of nitric acid (up to 6M HNO_3) and then decrease with further rise in concentration of nitric acid; this is due to the competition for the free extractant by HNO_3. However, the continuous increase in the case of D_{Zr} with increase in concentration of nitric acid is unusual extraction behaviour of Zr; i.e. the D_{Zr} depends only on the total nitrate concentration. Solovkin reported the extraction of three complexes of zirconium, namely, $Zr(NO_3)_4$. 2TBP, $Zr(OH)_2(NO_3)_2$. 2TBP , $Zr(OH)(NO_3)_3$. 2TBP, when the concentration is < 6M [55]. Increase in temperature and concentration of nitric acid increases the extraction of Zr. The extraction mechanism of Zr species by TBP is given in the following equations (1.12, 1.13).

$$Zr^{4+} + 4NO_3^- + 2\ TBP \leftrightarrow Zr(NO_3)_4\ .\ 2TBP\ (org) \quad \ldots\ldots\ldots\ldots\ldots\ldots\ (1.12)$$

$$ZrOH^{3+} + 3NO_3^- + 2TBP \leftrightarrow Zr(OH)(NO_3^-)_3.\ 2TBP \quad \ldots\ldots\ldots\ldots\ldots\ldots\ (1.13)$$

Zr is strongly retained by the PUREX solvent due to the presence of degradation products such as dibutyl phosphate (DBP) and monobutyl phosphate (MBP). Several studies were reported for the extraction of Zr by these degradation products and diluent degradation products such as nitroparaffins, hydroxamic acids, carbonyl compounds and long-chain carboxylic acids. The presence of small fraction of DBP and MBP in TBP organic phase increases D_{Zr}. Non-scrubbable Zr species was observed when TBP-DBP mixtures were allowed to age [56, 57].

1.5.4 Ruthenium (Ru)

Ruthenium is found to be the most troublesome fission product in the PUREX dissolver solution [26, 58]. In nuclear reactor, mainly two isotopes of ruthenium are produced, namely, ^{103}Ru ($t_{1/2}$ = 40 d) and ^{106}Ru ($t_{1/2}$ = 374 d). These two isotopes are high energy beta-gamma emitters, contributing significantly to the total radioactivity of dissolver solution. Ru also contributes to residual activity in U and Pu products and also in recycled solvent. During the dissolution, Ru exists in solid, liquid as well as in gas phase. It has been reported that Ru also exists in small inclusions of noble metals, which are alloyed with other fission products and actinides. Cumulative mass yield of ruthenium is about two times higher with fast neutrons compared to thermal neutrons. The amount of Ru produced in LWR (60 GWd/t, 4.5% ^{235}U, 5 year cooling) and FBRs (120 Gwd/t, 30% Pu, 5 year cooling) is about 4.13 and 10.9 kg/t, respectively. Ruthenium chemistry is very complex due to its multiple oxidation states and presence of variety of ruthenium complexes in nitric acid medium. In fast reactor fuel reprocessing, the intricate chemistry of Ru is further complicated by higher concentration of ruthenium in dissolver solution. Ruthenium mainly exists as RuNO(III) with the general formula of the type, $[Ru(NO)(NO_3)_x(H_2O)_{5-x}]^{3-x}$ in nitric acid medium [59, 60]. The most extractable species of ruthenium nitrosyl ion are tri and tetra nitrato complexes. The extraction mechanism of ruthenium nitrosyl ion by TBP is given below:

$$RuNO^{3+} + xNO_3^- + yH_2O + 2TBP \leftrightarrow RuNO(NO_3)_x(H_2O)_y.\ 2TBP \quad .....(1.14).$$

Careful choice of operation parameters for the removal of ruthenium in fast reactor fuel reprocessing should be made. Decontamination factor of $>10^3$ for Ru can be obtained by dual scrubbing of loaded organic phase using 3M and 6M nitric acid with 60–70% uranium loading in organic phase using a mixer-settler [61].

1.5.5 Technetium (Tc)

Among the long-lived fission products, ^{99}Tc is an important beta emitting nuclide of concern ($t_{1/2}$ = 2.11x10^5 year). It has significant fission yield of ~ 6% and it is of concern in

long-term nuclear waste management [62]. The amount of Tc produced in LWR (60 GWd/t, 5% ^{235}U, 5 year cooling) and FBRs (90 Gwd/t, 20% Pu, 4 year cooling) is about 1.36 and 1.86 kg/t, respectively. Tc also catalyzes the oxidation of hydrazine, which is used as a nitrite scavenger in the reductive separation of plutonium from uranium. Tc exists as pertechnetate ions (TcO_4^-) in dissolver solution. A small amount of Tc (2-5wt%), remains as an insoluble residue [63]. The extraction mechanism of TcO_4^- by TBP is shown below.

$$H^+ + TcO_4^- + 3TBP \leftrightarrow HTcO_4.\ 3TBP \quad \text{..... (1.15)}$$

TcO_4^- co-extract with actinide elements and with some of the fission products (e.g. Zr), thereby drastically reducing the decontamination factors for U and Pu. Generally high solvent loading is preferred to achieve better decontamination factors for U and Pu with respect to other fission product elements (Zr, Ru etc.). However in the case Tc, DFs decrease with high solvent loading due to the co-extraction of Tc with U and Pu. The co-extraction of TcO_4^- with U, Pu and Zr is shown in equations. TcO_4^- replaces one nitrate ion in the coordination sphere of the extracted metal complex [64, 65].

$$UO_2^{2+} + TcO_4^- + NO_3^- + 2TBP \leftrightarrow UO_2(TcO_4^-)(NO_3^-).\ 2TBP \quad \text{.....(1.16)}$$

$$Pu^{4+} + TcO_4^- + 3NO_3^- + 2TBP \leftrightarrow Pu(TcO_4^-)(NO_3^-)_3.\ 2TBP \quad \text{.....(1.17)}$$

$$Zr^{4+} + TcO_4^- + 3NO_3^- + 2TBP \leftrightarrow Zr(TcO_4^-)(NO_3^-)_3.\ 2TBP \quad \text{.....(1.18)}$$

1.5.6 Lanthanide elements

The amount of lanthanides produced in nuclear fission of ^{235}U and ^{239}Pu is one fourth of the total fission products. Some of the isotopes of lanthanides such as Sm, Eu, Gd and Dy have very high neutron absorption cross-section [66]. The quantities of Lns (La-Gd) produced in LWR (60 GWd/t, 5% ^{235}U, 5 year cooling) and FBRs (90 Gwd/t, 20% Pu, 4 year cooling) are about 17.8 and 29.0 kg/t, respectively. Lanthanides dissolve completely in nitric medium and exist as trivalent ions. The reported *D* values for lanthanides are significantly lower compared to U and Pu; therefore high concentrations of extractant and salting-out agents are required to enhance the extraction of lanthanides [67]. Lanthanides do not affect the DFs for

U and Pu. The chemistry of trivalent lanthanides is similar to the chemistry of later trivalent actinides (Am onwards), making it difficult to separate mutually. The extraction mechanism of Lns with TBP is shown below.

$$Ln^{3+} + 3NO_3^- + 3TBP \leftrightarrow Ln(NO_3)_3.\ 3TBP \quad \text{.....(1.19)}$$

1.6 Third Phase formation with Pu(IV)

Third phase formation is an important phenomenon in solvent extraction process during the reprocessing of spent nuclear fuels. This is particularly a serious concern during the extraction of tetravalent metal ions such as Pu(IV), Th(IV), U(IV) and Zr(IV) using TBP [68, 69]. Third phase formation can lead to phase inversion (organic phase with higher densities) and can result in criticality related issues with plutonium. Third phase formation can also lead to flooding in organic/aqueous phase separators such as mixer-settler, centrifugal extractor etc. Due to flooding, the organics comprising metal nitrates could carry over to locations where aqueous solutions are collected e.g. evaporator. Evaporation of aqueous products containing nitrates of uranium, plutonium and thorium generated from a solvent extraction process can lead to "red oil formation", which can result in explosion [70].

Usually feed solutions with U(VI) and Pu(IV) concentrations of about 360 and 1 g/L respectively in 3-4M HNO_3 medium are employed in PUREX process for thermal reactor fuel reprocessing [71]. Therefore, third phase formation is not expected to occur with lower concentrations of plutonium using 1.1M TBP/n-DD. Third phase formation is particularly important with respect to fast rector fuel reprocessing, where the plutonium concentrations are expected to be higher [25]. It also restricts the plutonium loading in the organic phase and affects the throughput of the process. The maximum loading (U+Pu) in TRFR is about 70-80 g/L, whereas in FRFR, it is difficult to achieve a loading of above 80 g (U+Pu)/L with a Pu(IV) loading of 25 g/L during the extraction from nitric acid medium (3–4M) due to third phase formation at 303 K. Hence for fast reactor fuel reprocessing, the extractant should have higher capacity to load Pu without third phase formation.

The Limiting Organic Concentration (LOC) of Pu initially decreases and after passing through a minimum at about 2M HNO_3, it increases with increase of concentration of nitric acid. It has been reported that the LOC values for Pu(IV) decreases with increase of uranium loading in the organic phase and also under the conditions that decreases the free TBP concentration [72, 73]. The LOC for third phase formation in the extraction of Pu(IV) from 4M HNO_3 by 1.1M TBP/n-DD is about 50 g/L [74]. In general, co-extraction of U(VI) decreases the LOC of Pu(IV) in the concentration range, from 2 to 5M HNO_3. The effect is more pronounced at higher acidities (4-5M) than at lower acidities (2- 4M).

1.7 Classification of Extraction Processes

1.7.1 Single-stage extraction

In a single stage extraction, distribution ratio of a solute (X) between the aqueous and organic phase is defined by $D_x = [X]_{org}/[X]_{aq}$ and the fraction extracted in a single stage is defined by $E_x = D_x.\Phi/ (D_x.\Phi+1)$ where Φ is the phase ratio = $V_{org}/V_{aq.}$ The fraction extracted in a single stage is function of both D_x and Φ. In a single-stage extraction, it is not possible to achieve both high recovery and high degree of separation [75]. The general rule in solvent extraction process is to saturate the solvent with a metal ion loading to reduce the free ligand concentration. Single-stage extraction is rarely adopted due to the limitations on the recovery and product purity.

1.7.2 Cross-current extraction

Degree of extraction could be improved if the raffinate is subjected to solvent extraction with a fresh solvent. The first and second extracts could then be combined to give a better overall recovery than that could be achieved in a single stage. In order to recover residual solute from the raffinate stream, the stream could be sent to one or several subsequent stages for further extraction. Fresh extracting solvent is generally fed into each stage and a corresponding extract is obtained. All extract streams are combined together to obtain the bulk extract while the raffinate is obtained from the last stage. Cross-current extraction gives a

significant improvement in the product purity relative to single-stage, but it will result in mixed extract solution and "too dilute" to be processed without further treatment. Cross-current extraction has some application in industries since they result in high recoveries and product purities compared to single-stage extraction [76].

1.7.3 Counter-current extraction

The extract from the last stage in cross-current extraction is not saturated. Therefore it could be the solvent to the next stage where the aqueous concentration is higher. These types of systems are called counter-current extraction [77, 78]. The drawback of diminishing concentration driving force observed in cross-current extraction can be eliminated by counter-current extraction. The feed stream enters the n^{th} stage and the extracting solvent stream enters the 1^{st} stage. The raffinate phase is collected from the 1^{st} stage while the extract phase is collected from the n^{th} stage. Using this scheme, the concentration driving force is maintained more or less uniform in all the stages comprising the cascade. Equipment used for counter-current extraction varies widely. Counter-current extraction provides a greater overall recovery in a fewer stages with minimum phase ratio for a given degree of extraction and can yield both high recoveries and concentrated extracts. However scrubbing has to be performed in two component systems to get better product purity. Similarly in the case of stripping, phase ratios have to be chosen in such a way to get higher concentration of the desired species in the strip solution. McCabe-Theile diagram is used to evaluate the number of stages required for a solvent to extract a metal ion. It is the graphical construction of an extraction isotherm, an operating line and stepwise evaluation of number of stages [75]. The volume of solvent required for processing of an aqueous feed depends on the type of extraction process, i.e. a single stage extraction requires more solvent than a cross-current extraction, which in turn needs more than a counter current extraction.

1.8 Liquid-Liquid contactors in nuclear fuel reprocessing

Liquid-liquid extraction also known as solvent extraction is the most important step in spent fuel reprocessing. In this operation, solute of interest is transferred from one phase to another phase when two immiscible liquids are brought into contact. This was carried out by several types of equipment known as "liquid-liquid extractors". The design of the equipment mainly depends on the rate of solute transfer. The rate of mass transfer is a function of interfacial area, concentration difference, diffusional resistances residing within the dispersed and continuous phases and any resistance that may be found at the interface. Interfacial area can be increased by dispersing one of the phases into small droplets in the other continuous phase by supplying energy to surmount the interfacial tension of the liquid pair [79]. Interfacial area per unit volume depends on mean drop size; smaller the drop size, larger is the interfacial area; hence higher the dispersed phase holdup. Functional requirements of liquid-liquid extractors are to develop a sufficient interfacial area, turbulence to promote mass transfer and to facilitate counter-current flow of two phases without excessive entrainment. Industrial extractors are mainly classified into two types of extractors, namely, stage-wise (both phases attain equilibrium) and differential extractors (equilibrium is never achieved between the phases in any part of the stage) [75, 80, 81]. All extractors are operated in counter-current mode to get better product purity, recovery and lower solvent inventory. Mixer-settler and centrifugal extractors are stage-wise extractors whereas columns are differential type extractors. In reprocessing plants, three types of extractors such as mixer-settlers, centrifugal extractors and liquid pulsed columns could be used because of special requirements. The differences, advantages and limitations of the above three extractors are briefly detailed below.

1.8.1 Mixer-settlers

Mixer-settlers are mostly individual stage units, simple to construct and operate and also cost effective. Phase dispersion can be achieved by impellers or by air pulsing. Good

contact of phases can be achieved by mixer-settlers; can handle wide range of flow ratios and liquids with high viscosity. Mixer-settlers have the advantages of low headroom, high efficiency, many stages, reliable scale-up, low maintenance etc. Dispersion and liquid transfer is achieved by ejector in mixer-settlers developed by Koganti et al. [82]. The disadvantages are the problems associated with large holdup volume, large floor area, high solvent inventory, inter-stage pumping which is required in some designs, large residence time etc.

1.8.2 Liquid Pulsed Columns (LPC)

Liquid pulsed columns are largely used in nuclear fuel reprocessing. These are differential in nature (equilibrium is never achieved between the phases in any part of the stage), simple to construct and operate. LPC provides high interfacial area and high degree of turbulence. LPC has a contact time of about 1/3 to 1/2 that of mixer-settler resulting in lesser solvent damage. LPC has low solvent inventory, short residence time, high efficiency and low maintenance. Contact time of LPC lies between that of mixer-settler and centrifugal extractors. LPC has limited throughput and cannot handle wide flow ratios.

1.8.3 Centrifugal extractors (CE)

Centrifugal extractors are small in size, with lesser holdup volume for a given throughput, low inventory of a solvent etc. CE have shorter contact time (5-10 sec) compared to mixer-settlers and liquid pulsed columns, making it useful for spent fuel reprocessing, where radiation doses are expected to be higher, especially for fast reactor fuel reprocessing. CE can handle systems that have smaller density difference between organic and aqueous phases. However, CEs have higher initial cost, higher operating cost, higher maintenance cost etc. Koganti et al. [82] developed remotely maintainable centrifugal contactors of capacities varying from 5 to 1000 L/h, employing a unique liquid seal.

1.9 Aqueous reprocessing of metallic fuels

1.9.1 History

Metal fuel was the original choice in early fast reactors mainly because of its better thermal and nuclear properties. Clementine was the first fast reactor in the world at Los Alamos, USA with ^{239}Pu as the fuel in the form of metal. Later, several fast reactors (EBR-I, EBR-II, Fermi-1 and Dounreay Fast Reactor), were commissioned in the world with different fuels in the form of oxide, carbide, nitride etc. Metal fuel was also employed in EBR-II as U-5% Fissium (Fs) alloy (5% Fs = 0.2% Zr, 2.5% Mo, 1.5% Ru, 0.3% Rh and 0.5% Pd); metal fuel was the foundation for IFR (Integrated Fast Reactor) concept [83-85].

The use of metallic (U-Zr and U-Pu-Zr) fuels in FBRs, development of different alloy compositions, compatibility with clad and irradiation studies were carried out at Argonne National Laboratory (ANL). Metallic fuels have higher thermal conductivity, higher fissile atom density and better breeding ratio. Metal fuel is a key to achieve inherent passive safety characteristics and the closed fuel cycle based on electrorefining and injection-casting refabrication makes it compact and economical. However, metallic fuel could not be irradiated to higher burn up because of its higher swelling. Several irradiation campaigns were carried out using both U-Zr and U-Pu-Zr fuels [86]. The normally used fuel compositions are U-Zr and U-Pu-Zr alloys where the Pu content varies from 15-19% and Zr from 6-22%. A ternary alloy of U-19 wt% Pu-10 wt% Zr has been widely used. For future Indian FBRs, U-Pu-Zr alloy is considered as a candidate fuel material. Fabrication of metallic fuels will be mainly carried out using injection casting method [86, 87].

1.9.2 Reprocessing of metallic fuels

The reprocessing of metallic fuels could be carried out using pyrochemical process. A number of non-aqueous processes have been investigated for the processing of spent nuclear fuels. Among the non-aqueous processes, some are primarily based on gas-solid reactions and others on the use of non-aqueous media such as molten salts and alloys for chemical

separations [88, 89]. Pyrochemical processes are suitable for high radioactive targets, short cooled fuels using compact equipment. Unlike aqueous based reprocessing, the pyrochemical process generates waste which is mainly solid in nature. However, pyrochemical processes also poses a number of challenges such as low decontamination factors compared to aqueous process, aggressive nature of process media (molten salts and liquid metals) towards process equipment, difficulties associated with the development of continuous operations. Also, these processes have not yet been demonstrated in large scale plants. In this context, development of an alternate method to pyrochemical reprocessing of metallic fuels using aqueous based reprocessing method by well-established PUREX process will be of importance. In PUREX process, dissolution of metallic fuels in nitric acid medium is an important step. The feed solutions generated after the dissolution could be directly employed for the subsequent solvent extraction cycles in PUREX process.

1.9.3 Dissolution aspects of metallic fuels

Studies have been reported to dissolve uranium and its alloys in various reagents [90]. Laue et al. [35] investigated that for effective dissolution of uranium and its alloys, dissolvent should contain an oxidizing and a complexing agent. Electrochemical methods were also reported for the dissolution of uranium and its alloys. Use of sulphuric, nitric and tartaric acids have resulted in good dissolution rates of uranium metal [35]. Kinetics of the anodic dissolution of metallic uranium in 1 to 4M HNO_3 solutions at 30^oC has been reported by Rodrigues et al. [91]. Electrochemical dissolution of U-5 wt% Zr alloy in solutions of nitric acid has been investigated by Nikitin et al. [92].

Ryan and Bray have reported a Catalysed Electro-Chemical Plutonium Oxide Dissolution (CEPOD) in nitric acid medium using intermediate redox reagents Ce(IV)/Ce(III) and Ag(II)/Ag(I) and demonstrated that dissolution rates were ~ 2 to 5 times faster than the rates obtained using the normal dissolution process involving fluoride ions (12M HNO_3-0.18M HF at 90^oC) [39]. The advantage of the electrochemical process is that fluoride ions

were not employed in dissolution. Harmon [93] has studied the dissolution of PuO_2 with cerium(IV) and fluoride promoters and concluded that Ce(IV) in lower concentration is an effective promoter for PuO_2 dissolution in nitric acid medium. Palamalai et al. [94] also studied the electrooxidative dissolution technique (EODT) for dissolution of PuO_2 solids. Dissolution mechanism proceeds with the oxidation of Pu(IV) to Pu(VI) with a corresponding reduction of Ce(IV) to Ce(III). However no studies have been reported in literature for the dissolution of Zr containing alloy fuels using electrochemical methods.

The metal fuel, U-Pu-Zr comprising of 20 wt% Pu, 10 wt% Zr and 70 wt% U, requires consideration of the dissolution chemistry of the above three metals in order to develop a process flowsheet. A chop-leach process, in which the fuel rods are sheared into short segment and the acid dissolvent attacks the metal fuel constituents from the open ends. Since the metal fuels are pyrophoric in nature, chopping has to be carried out in an inert atmosphere. Cladding hulls can be compacted and disposed as radioactive waste. Mixture of nitric acid and hydrofluoric acid is recommended for the complete dissolution of zirconium containing alloys and to prevent any violent and explosive reactions during dissolution. Dissolution of zirconium containing alloys in large scale (industrial scale) is a challenging task and has not yet been demonstrated. Corrosion of dissolver materials is expected to be higher during the dissolution process with use of fluoride medium. The excess fluoride would be complexed with aluminium nitrate and could be employed as feed solution in PUREX process.

1.9.4 Explosive reactions during dissolution of metallic fuels

Aqueous processing of U-Pu-Zr metal fuels with stainless-steel-clad has been reviewed by Christian [95]. Dissolution processes for the individual metal constituents and the chemistry required to dissolve the combination of metals including vessel materials that will enable utilization of solvent extraction processes were also discussed. It has been reported that selective leaching of uranium from U-Zr fuel can result in the formation of epsilon phase, which reacts explosively with nitric acid [95]. It has been examined that 2 wt%

Zr alloy did not dissolve completely in nitric acid and that dangerous explosions did occur during the dissolution of zirconium metallic alloys in nitric acid medium. The formation of finely divided residue during the dissolution may react explosively with nitric acid; it may set off explosion spontaneously or in the presence of nitric acid [96-99]. Addition of a small amount of fluoride could prevent the formation of explosive residues.

Larsen et al. [96] have investigated that alloy composition and thermal history appear to have the most prominent effect on the severity of the explosion and even five gram alloy sample containing 2 to 20 wt% Zr can undergo explosion when treated with nitric acid. H.P. Roth [98] has observed explosions during chemical etching or pickling of uranium-zirconium alloys. Explosion during the dissolution of one gram sample are violent enough to shatter the glass vessel in which they are contained. Samples containing as low as 1wt% zirconium have exploded violently during direct dissolution in nitric acid medium. Thus the dissolution of zirconium containing alloy fuels in nitric acid medium in large scale is a challenging task and it necessitates addition of small quantities of hydrofluoric acid to prevent explosion related issues.

Zircex and modified Zirflex processes were developed for the dissolution of spent reactor fuels to recover uranium in chloride and fluoride medium, respectively [100]. Corrosion of dissolver materials is expected during the dissolution process with use of chloride and fluoride medium. To decrease the corrosion rate of stainless steel equipment, chloride is distilled off from the Zircex product and aluminium nitrate was added to the modified Zirflex product. Dissolution and corrosion rates were reported during the dissolution of zirconium reactor fuels in titanium equipment [101].

1.9.5 Characterisation of metallic fuels

In the fuel cycle of metallic alloys, estimation of zirconium in the presence of other elements is mandatory for controlling the processes at various stages such as fabrication, reprocessing etc. Several methods were reported for the estimation of zirconium either by

spectrophotmetry or by gravimetry [102-105]. Most of the spectrophotometric methods use alizarin sulfonate as the chromogenic reagent and gravimetric methods use mandelic acid and its derivatives as precipitating agents. In the alizarin sulfonate method, it has been reported that uranium does not interfere in the estimation of zirconium [106] whereas other elements especially fissium elements (Nb, Mo, Tc, Ru, Rh and Pd) interfere. Buchanan et al. [107] estimated zirconium in Pu-U-Fissium alloys by alizarin red-S lake method. In all the spectrophotometric methods, interference from other elements will be a major issue. Hence it becomes essential to separate the interfering elements prior to the estimation. This is a challenging task as it increases the number of steps in the estimation of zirconium by spectrophotometry.

K.L. Cheng [108, 109] developed a method for the estimation of zirconium by spectrophometry using xylenol orange as the chromogenic agent and studied the interference of various elements. It was also reported that most of the elements does not interfere in the estimation of zirconium except niobium, molybdenum and hafnium and these elements can be masked by suitable masking agents [108, 109]. However the interference of plutonium in the estimation of zirconium has not been reported, as this is important in the context of use of U-Pu-Zr alloys. Hence, there is a need to develop a method for the estimation of zirconium in the presence of U and Pu which is useful at various stages of U-Pu-Zr metal fuel cycle and also to estimate zirconium in raffinate streams.

1.9.6 Solvent extraction studies with metallic fuels

Gercke et al. [110] have reported the dissolution of zirconium-clad uranium target elements in nitric acid and fluoride medium to form feed solutions suitable to PUREX process. Fluoride concentration in these feed solutions is about 2.5 to 5 times higher than zirconium concentration. The U, Zr and concentration of nitric acids were reported to be 1.1M, 0.33M and ~2M, respectively. It is reported that the extraction of uranium is not affected by the presence of zirconium and fluoride; the extraction of zirconium in the

presence of fluoride is found to be negligible with a solution of 1.1M TBP in carbon tetrachloride. It was also reported that the concentration of U in aqueous phase is less than 10^{-4}M after four successive contacts with 1.1M TBP/CCl_4 and these results were found to be similar where no fluoride ions are present. However the presence of fluoride ions affects the extraction of Pu and Zr [111]. The *D* values for Pu with TBP decreases in the presence of fluoride ions. TBP is inefficient for the extraction of Zr when fluoride ions are present in the system [111].

1.10 Thermal decomposition of a solvent

The experience gained in the past several decades reveals that TBP has some limitations. The limitations of TBP include higher aqueous solubility (0.4 g/L), third phase formation and radiation degradation [68, 112, 113]. Solubility of TBP in aqueous streams as well as inadvertent entrainments to the aqueous streams can lead to "red oil" formation during evaporation of aqueous streams containing nitric acid and heavy metal nitrates. Red oil formation leads to violent runaway reactions causing several accidents in various plants [70].

Red oil is a dense organic material consisting of metal solvate and nitric acid with density ranging from 1.1 to 1.5 g/cm^3. The red oil undergoes exothermic decomposition at lower temperatures than that of metal solvate. Explosions have been reported due to red oil formation in reprocessing plants, fuel fabrication plants, waste management plant etc [114, 115]. Red oil was synthesized resembling those produced during the actual incidents and energetics were investigated [114]. The typical energy content of the red oil has been found to be ~ 200 Jg^{-1} allowing it to be classified as an energetic material. Several accidents attributed to the formation of red oil and its violent decomposition has been widely discussed in literature [116-119].

In this context, several authors reported the thermal decomposition behaviour of TBP based solvent. Paddleford et al. [120, 121] reported the decomposition of TBP and nitric acid systems. The energetics of a runaway reaction strongly depends on the pressure and

temperature. The enthalpy of exothermic reaction increases in the presence of concentration of nitric acid and decreases in the presence of diluents. Hyder et al. [122] have reported that runaway reactions could be controlled by properly ventilating the vessels.

TBP undergoes degradation in several ways such as hydrolysis, radiolysis, pyrolysis, nitrolysis and oxidation. The main degradation products of TBP by the above reactions are DBP and butanol. DBP further undergoes degradation and produces MBP and H_3PO_4. It is reported that thermal decomposition of TBP can produce ~1.2% of DBP at 451 K after 70 hr and ~8.4% at 513 K after 2 hr [123]. The production rate of DBP increases with increase in temperature. Butanol can undergo nitration and oxidation in the presence of nitric acid and produces butyl nitrate and carboxylic acids. Pyrolysis of TBP and its degradation products at higher temperature leads to formation of non-condensable gases such as H_2, N_2, N_2O, NO, NO_2, CO_2, CO and lower hydrocarbons (< C_4) [112]. It has been reported that 2-butene is the major flammable decomposition product and butyl nitrate is another major volatile decomposition product, which causes explosion [124]. The aqueous solubility of TBP decreases with increase in concentration of nitric acid [125]; the aqueous solubility of DBP is higher than that of TBP. It is well known that DBP form complexes with heavy metal ions such as U(VI), Pu(IV), Th(IV) and a few fission products e.g. Zr(IV). These metal complexes with DBP can undergo oxidative thermal decomposition with nitric acid, which may also cause runaway reactions in evaporators.

1.11 Radiolysis of solvent in a reprocessing plant

The important limitation of TBP based solvent is its radiolytic degradation. During the extraction of metal ions, nitric acid also gets extracted into the organic phase. The solvent is expected to undergo degradation by various pathways such as hydrolysis, radiolysis, nitrolysis and oxidation at various stages of processing. Degradation products can alter the fission product decontamination factors. Degradation products can also affect the physicochemical

properties such as density, viscosity, phase separation time, interfacial tension and changes the extraction and stripping behaviour of U, Pu and fission products [126-129].

The major degradation products of TBP are DBP, MBP, H_3PO_4 and butanol, whereas the degradation of diluent (n-DD) leads to the formation several products such as hydrocarbons, nitroalkanes, which are produced by the nitration of n-paraffin hydrocarbon diluents and derivatives of nitroalkanes such as carboxylic acids, hydroxamic acids etc [130-132]. The extent of degradation of TBP and n-DD depends on several factors such as concentration of nitric acid, absorbed dose, temperature etc. In general, degradation rate increases with increase in the above parameters and the presence of heavy metal ions (U or Pu) enhances the degradation [133-136]. Degradation also leads to the formation of interfacial deposits in the first extraction cycle of PUREX process due to the formation of Zr-DBP complex [58, 137-139].

Diluent improves the physicochemical properties of TBP by reducing density and viscosity of organic phase, thereby reducing the phase separation time. Density of the organic phase decreases from ~ 0.98 to ~ 0.82 g/mL whereas viscosity decreases from ~ 3.5 to < 1.8 cP from neat TBP to 1.1M TBP/n-DD. It has been reported that density marginally increases for chemically degraded samples and also for the samples irradiated in the presence of nitric acid due to extraction of nitric acid by TBP, whereas viscosity of organic phase increases significantly with increase of absorbed dose [126, 127]. The interfacial tension (IFT) of 1.1M TBP/n-DD-HNO_3-H_2O-$UO_2(NO_3)_2$ system has been reported [140]. The IFT initially increases with aqueous phase acidity and then decrease. An empirical equation was also derived for IFT, which involves concentrations of TBP, U(VI) and nitric acid in the aqueous phase.

Nitration of n-paraffin hydrocarbon diluent produces nitro and nitrite compounds of alkanes, alcohols, unsaturated alcohols, nitro alkenes and carboxylic acids, hydroxamic acids. The above degradation products are mainly responsible for the retention of heavy metal ions

(U or Pu) during the stripping with dilute nitric acid solution [133, 141]. Diluent degradation products produced in the presence of nitric acid and radiation are responsible for the formation interfacial deposits during the alkaline solvent wash. It was reported that due to the precipitation of salts of carboxylic acids and agglomerates of surface-active diluent degradation products, interfacial deposits were formed [142]. TBP, DBP and MBP can also undergo degradation producing butyl nitrate, alcohols, carboxylic acids and light hydrocarbons [143]. The degradation mechanism of TBP has been explained by several authors. Blake et al. [136] reported the degradation of 1M TBP/Amsco 125-82, when treated with boiling nitric acid or with gamma irradiation. The nitroparaffins (RNO_2) were reported to be the major degradation products. Tallent et al. [143] reported the chemical degradation of normal paraffin hydrocarbon (NPH) diluents and extractant systems in NPH.

Chemical degradation of TBP/diluent solvent system was reported by Sze et al.[144] Reaction mechanisms were proposed for the formation of species which are responsible for Zr metal retention. It has been reported that the species formed by chemical degradation is identical to those formed by radiolytic degradation. Tandem mass spectrometry (MS/MS) was employed for the identification of degradation products obtained during the radiolysis of TBP solvent [145]. It has been investigated that fraction of TBP-dimer is found to be < 0.03% of the total mixture obtained during the radiolysis of a solvent. Lesage et al. [146] reported the identification of minor products obtained during radiolysis of 1.1M TBP/n-DD in the presence of nitric acid; TBP-TBP and TBP-DBP dimers were identified which are bonded through an octane chain. They also identified the nitro and nitroso-substituted TBP and dimers, hydroxybutyl dibutyl phosphates and their oxidation products.

1.12 TiAP-A potential alternate extractant for spent fuel reprocessing

A solution of TBP diluted with n-alkane diluents (1.1M) has been utilized as a versatile solvent for the reprocessing of thermal and fast reactor fuels (PUREX process) for the past several decades [25, 26, 147-149]. TBP has also been employed in various separation

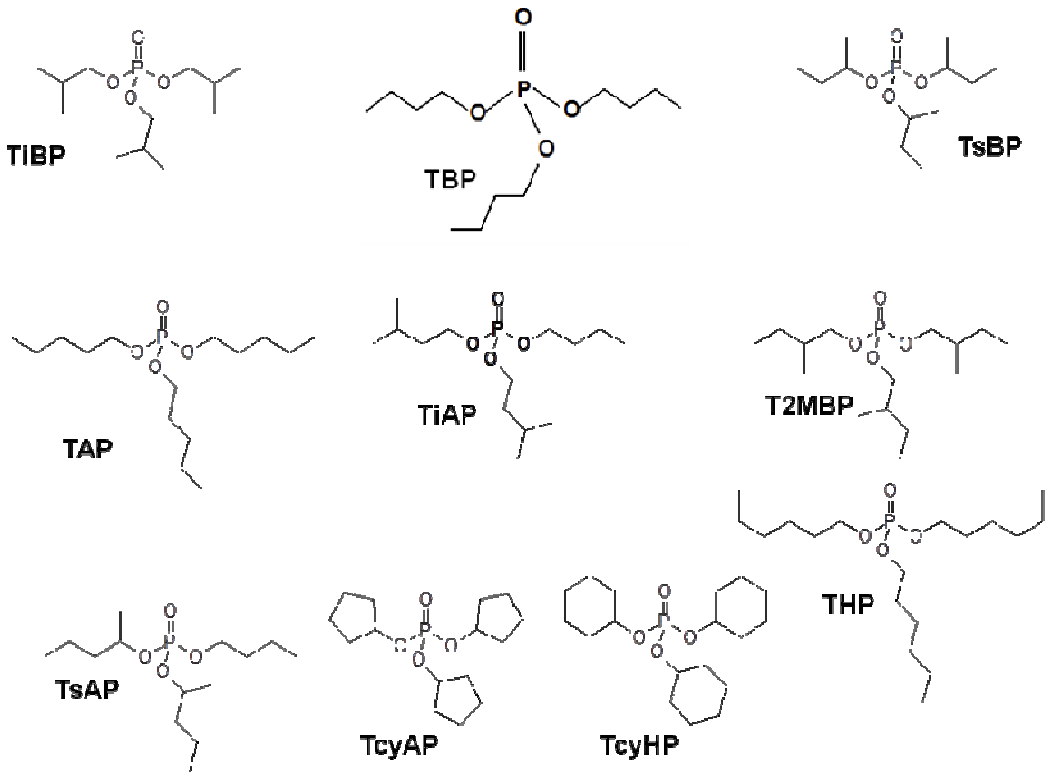

Fig.1.3: Chemical structures of various trialkyl phosphates

processes such as separation of ^{233}U from irradiated thorium by THOREX/Interim-23 process, monazite processing, Zr/Hf separation, Nb/Ta separation etc. The experience gained in the spent nuclear fuel reprocessing revealed that TBP has some limitations such as third phase formation with tetravalent metal ions and higher aqueous solubility which can lead to "red oil formation". Several symmetrical trialkyl phosphates such as tri-n-amyl phosphate (TAP), a higher homologue of TBP, some of its isomers such as tri-2-methyl butyl phosphate (T2MBP), tri-iso-amyl Phosphate (TiAP, tri-3-methyl butyl phosphate) and tri-sec-amyl phosphate (TsAP) have been investigated towards the identification of an alternate extractant to TBP for spent fuel reprocessing, especially for fast reactor fuel reprocessing [150-155]. The structures of some of these extractants are shown in Fig.1.3. Hasan and Shukla investigated the feasibility of using TiAP as an alternate extractant for spent fuel reprocessing [154]. Their studies demonstrated the fact that the chemical degradation of TiAP is lower compared to TBP. Several studies such as thermodynamics of extraction of U and Pu,

physico-chemical properties, extraction behaviour of actinides, third phase formation studies with Th(IV), thermal decomposition behaviour of TiAP were carried out to explore the possible use of TiAP for spent fuel reprocessing [150, 156-161].

1.13 Scope of the present work

In literature, most of the work dedicated towards the batch studies to investigate the extraction behaviour of actinides with TiAP based solvent. No reports exist to understand the extraction behaviour of fission products and actinides under process conditions with TiAP based solvent. Prior to the deployment of a novel solvent (TiAP) in actual reprocessing plant, it is essential to understand the various properties of a solvent under actual process conditions. The present study mainly focuses on the issues arising from reprocessing of fast reactor fuels. The objective of the present study is to demonstrate the feasibility of using TiAP for spent fuel reprocessing. Highlights of the studies with TiAP based solvent are as follows:

- Extraction behaviour of actinides (U and Pu) under high loading conditions, extraction behaviour of fission products (Zr, Ru, Tc and some lanthanides) as fission product representatives.
- Continuous counter-current solvent extraction runs with mixer-settler facility under various experimental conditions.
- Development of an alternate method for the processing of metallic alloy fuels by aqueous route using PUREX process.
- Investigations on thermal and radiolytic stability of the solvent. The results of these studies with TiAP are compared with the TBP based solvent under identical conditions.

Chapter 2

EXPERIMENTAL 2

This chapter describes the experimental procedures employed in the present work and about the chemicals, reagents, materials and instruments used for carrying out various experiments. Preparation of feed solutions, indicator solutions, buffer solutions, stock solutions, standard solutions and organic solutions are elaborated. The analytical methods used for determination of various metal ions are also discussed.

2.1 Chemicals

Acids

Acids such as nitric, hydrofluoric, phosphoric, sulphamic, sulphuric acids (AR grade) were obtained from M/S. Merck, India. Acetic and formic acids (AR grade) were supplied by M/S. Ranbaxy Fine Chemicals, India was used as such without any further purification.

Ammonium molybdate

Ammonium molybdate (AR grade) obtained from M/S. Fischer Inorganics and Aromatics, India was used.

Arsenazo-I

Arsenazo-I indicator (AR grade) procured from M/S. Merck, India was used as received.

Barium diphenylamine sulphonate

Barium diphenylamine sulphonate (AR grade) supplied by M/S. Merck, India was used as an indicator in the Davies-Gray method.

Borax

Borax (AR grade) obtained from M/S. Sarabhai Chemicals, India was used as such without further purification for preparation of buffer solution.

Disodium hydrogen phosphate

Disodium hydrogen phosphate (AR grade) was received from M/S. Sarabhai Chemicals, India and used as received.

Disodium salt of ethylenediaminetetraacetic acid (EDTA)

EDTA (AR grade) purchased from M/S. Ranbaxy Fine Chemicals, India was used for the complexometric titration of metal ions.

Ethanol

Ethanol (AR grade) procured from M/S. Shymlakhs International, UK was used as such without further purification.

Ferrous ammonium sulphate

Ferrous ammonium sulphate (AR grade) received from M/S. Merck, India was used as such without further purification.

Heavy Normal Paraffins (HNP)

HNP was obtained from Tamil Nadu Petroproducts Ltd. Chennai, India. It is a mixture of n-decane (18.4%), n-undecane (33.1%), n-dodecane (28.8%) and n-tridecane (19.7%). The composition was established using Gas Chromatographic (GC) technique.

Hydrocarbon diluents

Linear chain alkane diluents such as n-dodecane and n-tetradecane each with 99% purity procured from M/S. Lancaster Synthesis Ltd. (England) were used for the preparation of organic solutions.

Metallic alloy samples

U-Zr and U-Pu-Zr alloy samples were received from BARC, Mumbai, India.

Nitrates of Lanthanides (Ln)

Nitrate salts of lanthanides (La, Pr, Nd, Sm and Eu) supplied by Indian Rare Earths Ltd, Mumbai, India were used without any further treatment.

Phenolphthalein

Phenolphthalein (AR grade), supplied by M/S. Merck Specialities Pvt. Ltd., India was used as received.

Potassium dichromate

Potassium dichromate (AR grade) supplied by M/S. Ranbaxy Fine Chemicals, India was used as received.

Potassium dihydrogen phosphate

Potassium dihydrogen phosphate (AR grade) was purchased from M/S. Sarabhai Chemicals, India and used for the preparation of buffer solution.

Potassium hydrogen phthalate (KHP)

KHP (AR grade) was procured from M/S. Glaxo Laboratories, India and used as received.

Potassium oxalate

Potassium oxalate (AR grade) obtained from M/S. Loba Chemie, India was used for the determination of free acidity of solutions containing hydrolyzable metal ions.

Pyridine

Pyridine (AR grade) procured from M/S. Ranbaxy Fine Chemicals, India was used.

Ruthenium nitrosyl nitrate solution

Ruthenium nitrosyl nitrate solution as RuNO(III) [M/S. Aurora Matthey Limited, India] was used as received.

Sodium acetate

Sodium acetate (AR grade) obtained from M/S. Merck, India was used for the preparation of buffer solution.

Sodium fluoride

Sodium fluoride (AR grade) obtained from M/S. Merck, India was used as received.

Sodium hydroxide (NaOH)

NaOH (AR grade) procured from M/S. Ranbaxy Fine Chemicals, India was used for acid-base titration and also for washing organic solutions to remove the acidic impurities.

Sodium nitrate

Sodium nitrate (AR grade) procured from M/S. SD Fine-Chem Ltd., India was used as received.

Technitium-99

^{99}Tc [M/S. Cerca-lea, France] was supplied in the form of ammonium pertechnetate.

Trans-1,2-diaminocyclo-hexane-N,N,N',N'-tetraacetic acid (CyDTA)

CyDTA (98% pure) purchased from M/S. Acros Chemicals, USA was used for the preparation of complexing solution in the estimation of U(VI) by spectrophotometric technique.

Tri-n-butyl phosphate (TBP)

TBP provided by M/S. Fluka Chemicals, Switzerland was used for the extraction studies.

Triethanolamine (TEA)

TEA (AR grade) received from M/S. Merck, India was used for the preparation of buffer solution.

Uranyl nitrate

Uranyl nitrate (Nuclear Fuel Complex, Hyderabad) was used without further purification.

Vanadyl sulphate

Vanadyl sulphate (AR grade) was procured from M/S. BDH Chemicals Ltd., England.

Xylenol Orange

Xylenol orange indicator (AR grade) provided by M/S. TCI Chemicals, Japan was used as received.

Zirconium

Nuclear grade zirconium metal with < 150 ppm of hafnium (Nuclear Fuel Complex, Hyderabad) was used to prepare zirconium nitrate solutions.

2-(5-Bromo-2-pyridylazo)-5-(diethylamino) phenol (Br-PADAP)

Br-PADAP (AR grade) obtained from M/S. Merck, India was used for the spectrophotometric determination of U(VI).

2,6-Pyridinedicarboxylic acid (PDCA)

PDCA (98% Pure) procured from M/S. Lancaster, England was used as titrant for the complexometric determination of U(VI).

Synthesis and characterisation of Tri-iso-amyl phosphate

Tri-iso-amyl phosphate (TiAP) was synthesized by the condensation reaction between phosphoryl chloride and isoamyl alcohol in the presence of pyridine in n-heptane medium. Approximately 3.3 moles of alcohol, 3 moles of pyridine and 2 litres of n-heptane were taken in a five litre three necked round bottom flask kept in an ice bath maintained at 0^{o}C. Excess of alcohol is necessary to avoid the formation of di and mono amyl phosphates and pyridine is used as a scavenger to remove HCl from the medium.

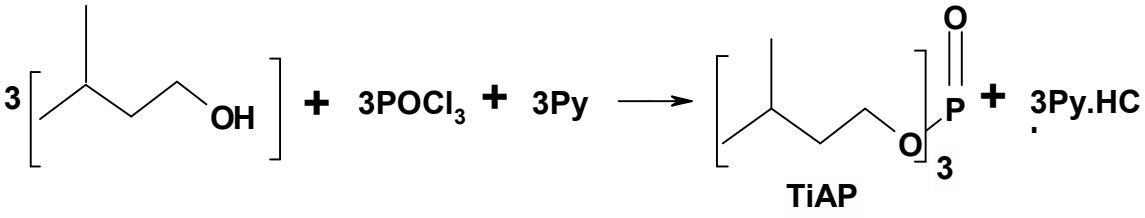

1 mole of $POCl_3$ was taken in a pressure equalizing funnel attached to one of the side necks and added to the contents in the flask drop by drop. An overhead mechanical stirrer was used to stir the contents of the flask. After completing the addition of $POCl_3$, stirring of slurry was continued for an additional 24 hours for completion of the reaction. The slurry containing TiAP was washed with distilled water repeatedly to remove pyridinium hydrochloride. It was further washed with sodium carbonate solution to remove acidic impurities. Heptane was removed using a rotary evaporator. Finally the crude TiAP was purified by vacuum distillation at a temperature of 105°C and 0.04 mbar pressure and characterised by GC, NMR and IR techniques. The purity of TiAP (99.9%) was confirmed by GC technique. TiAP or its

solutions in diluent were washed with alkali solution followed by water wash prior to the experimental work.

2.2 Instrument/facility

Electronic single pan balance

A calibrated electronic balance (AUW220D SHIMADZU make) with a sensitivity of ± 0.01 mg was used for weighing various chemicals (both solids and liquids).

Gamma chamber

Neat and 1.1M solutions of TiAP and TBP in n-alkane diluents were irradiated using ^{60}Co gamma chamber facility that gives a dose rate of 0.5M Rad/hr and was calibrated by Fricke dosimetry.

NaI(Tl) detector

Gamma counting using a NaI(Tl) detector based counting system at 60 kev was used for the estimation of ^{241}Am.

Inductively Coupled Plasma-Atomic Emission Spectrometry (ICP-AES)

Inductively Coupled Plasma-Atomic Emission Spectrometry (ICP-AES) using sequential spectrometer of ULTIMA-C spectroanalyser system (John Yvon, France) was employed for the analysis of ruthenium samples.

pH meter

A Cyberscan pH meter procured from M/S. Eutech Instruments, Singapore calibrated using standard pH buffers of 4.00, 6.86 and 9.18 was used for the measurement of pH of various solutions.

UV-VIS spectrophotometer

A SHIMADZU model UV-3600 spectrophotometer with wavelength range of 200-800 nm and a cuvette with a path length of 1 cm were used for the measurement of absorbance of various metal ion complexes.

Viscometer

An Ostwald viscometer was used for the determination of viscosity of the organic solutions.

Adiabatic calorimeter

An adiabatic calorimeter (PHI-TEC 1 of HEL, UK) was used in the present study. The calorimeter consists of stainless steel cylindrical containment vessel lined with cylindrical copper block and a stainless steel lid. The lid of the containment vessel has several leak tight ports to connect test cell, thermocouple and pressure transducer and feed line with ball valve, etc. The sample heater with wire coiled helically over the spherical test cell heats the sample, while three guard heaters at bottom, top and surrounding were used to maintain the adiabatic environment in the calorimeter by maintaining the surrounding temperature equal to that of the sample. These heaters are independently controlled using a PID control algorithm and can track temperature ramps up to 100 K min^{-1} and heat the vessel to 773 K, the limiting temperature of the calorimeter. Stainless steel sheathed K-type thermocouples are provided at bottom, top and side of the vessel for temperature measurement. The calorimeter has a detachable spherical sample cell, made of Hastelloy®, of capacity 10 cm^3 with Swagelok fitting. A thermocouple (Hastelloy sheathed) placed inside the test cell, in direct contact with the sample measures the sample temperature. The calorimeter has a pressure transducer, to measure the pressure build-up in the range of 0–120 bar with an accuracy of ± 0.15%, during the course of reaction. Electronics housed in a rack provides all the necessary signal conditioning for the transducers such as those for temperature and pressure and power for heaters. It has facilities such as (i) PCG2 interface module which communicates the signals between computer and the electronic rack, (ii) A watchdog module which checks for software malfunctions to switch the rack to a safe preset state if the controlling software fails, (iii) thermocouple module, (iv) pressure module (v) heater control module and (vi) actuator module. WinISO software supplied by M/S HEL, UK, was used for the acquisition of

temperature, pressure data as a function of time and controlling the heating pattern. IQ software supplied by M/S. HEL, UK, was used to derive enthalpy and kinetics parameters.

Gas cell

To characterize the gaseous products generated during the thermal decomposition of TiAP and TBP based solvents, gaseous products were collected in a specially designed cell for IR studies. This gas cell consisted of a glass cylinder with KBr windows on both sides, with an inlet port and an outlet port fitted with valves.

IR Spectrometer

An BOMEM FT-IR spectrometer with a range of 4000-400 cm^{-1} and with a resolution of 4 cm^{-1} (ABB FTLA 2000) was used to perform the IR characterization of the trialkyl phosphates(irradiated and unirradiated) and gaseous products obtained during thermal decomposition of TalPs.

Liquid scintillation counter

The α-radioactivity of various radioisotopes was estimated using α-β discriminating liquid scintillation counter (300SL TDCR liquid scintillation analyzer, Hidex, Finland). Known amount of samples from both organic and aqueous phases were taken in ultima gold AB cocktail (Perkin Elmer) for liquid scintillation counting.

Mercury-mercurous sulphate electrode

Mercury-mercurous sulphate standard electrode (ER-78, pH Products Company, India) was used for the potentiometric estimation of uranium and plutonium.

Platinum electrode

A platinum wire of 2 mm thickness was used as indicator electrode in the potentiometric experiments for plutonium analysis and Davies and Gray method for uranium analysis. The electrode was activated before starting the experiment, by heating the wire in a Bunsen flame to red hot condition followed by dipping it in a concentrated nitric acid medium, followed by rinsing in distilled water and repeating this procedure several times.

Mixer-Settler facility

The facility consists of an ejector mixer-settler unit and valve-less metering pumps housed in a double-module glove box which have been interconnected by means of a transfer port for the transfer of materials from one glove box to the other. The transfer port was kept closed to isolate the boxes from each other during the mixer-settler operations. In addition, a separate feed through connection has also been provided for the transfer of organic and aqueous solutions through narrow flexelene tubings across the boxes. Metering pumps kept in Glove box-1 have been used to pump solutions to mixer-settler kept in Glove box 2. The mixer-settler is a 16 stage equipment and is fabricated from a monolithic polypropylene block with a hold up volume of ~ 640 mL [82]. A photograph of the facility is shown in Fig. 2.1.

Engineering drawing of entire mixer-settler facility is shown in Fig.2.2. Several safety features have been incorporated in the system. Separate air inlets through ball valves were provided in both the boxes and the individual exhaust lines through separate ball valves from both the boxes were given to the glove box exhaust system through a common stainless steel pipe. A ball valve has been provided beyond the common pipeline junction. Additional stainless steel pipe-line routes were also provided before the common junction to connect the boxes to a common vacuum pump through an electrically operated solenoid valve and the exhaust from the vacuum pump was directed to a fume hood. A ball valve was also connected in parallel to the solenoid valve for the manual operation of the system in case of failure of the solenoid valves. These solenoid valves are electrically connected to a photohelic pressure gauge, which was mounted on the boxes to sense the glove box pressure. When the glove box pressure goes above -15 mm water column, the pressure gauge gets actuated and the solenoid valves open and the boxes get evacuated till it reaches -15 mm water column. As an additional safety precaution, an electrically operated butterfly valve which was connected to the photohelic pressure gauge has been also incorporated in the inlet line, which feeds air to the header.

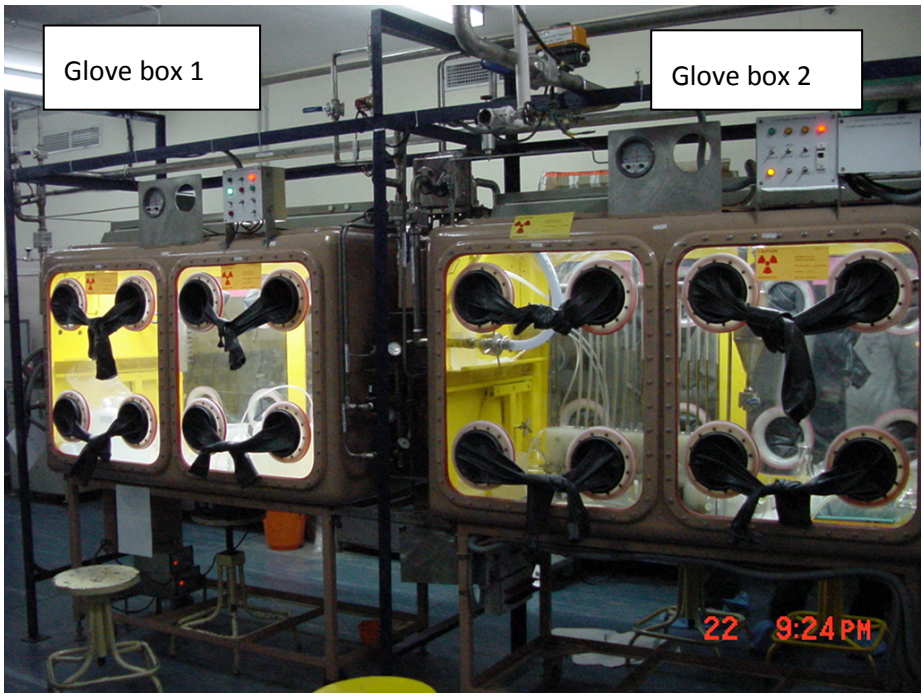

Fig. 2.1: Double-module glove box facility consists of mixer-settler and metering pumps for flowsheet development studies

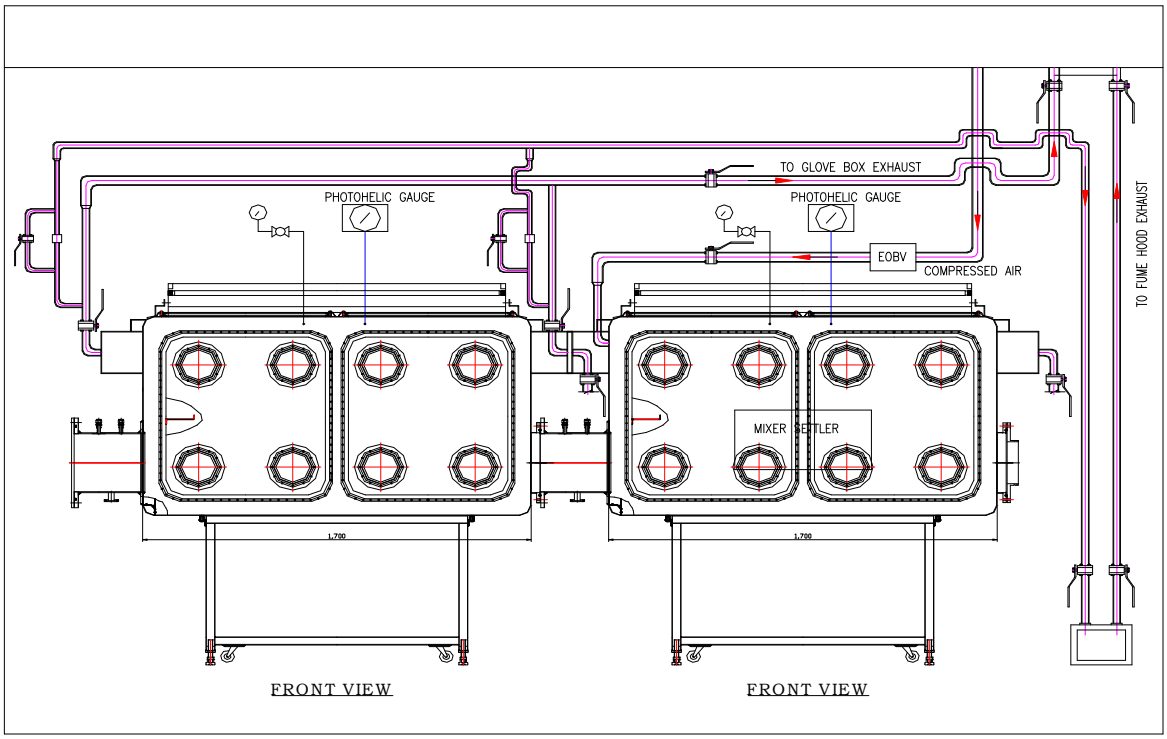

Fig 2.2: Detailed engineering drawing of the entire mixer settler facility

Laser ionization mass spectrometer (LIMS)

Mass spectrometric studies were carried out using a laser ionization mass spectrometer (LIMS). This facility contains a home-made reflectron time-of-flight mass spectrometer (RTOF-MS) having a resolution of about 1000 for gas samples [162]. The laser used is a picosecond (100 ps), custom made to user specification (M/S. Geola Digital Lab, Lithuania). The above laser has a Q-switched master oscillator (pulse width is about 3 ns), which is pumped by a diode laser. Subsequently, the laser beam pulse is compressed by stimulated Brillouin scattering (SBS) in CCl_4 and then amplified using three successive Nd-YAG based, flash lamp pumped amplifiers. The transverse beam profile is a TEM mode. A quartz lens with a focal length of 50 cm has been used for focusing the laser beam on the sample and the sample was positioned after the focus. The focal area used was large (2 mm dia). The pulse energy used was about 1 mJ/pulse and the corresponding laser fluence for the focused beam was of the order of ~ 0.03 J/cm^2.

A secondary electron multiplier (SEM) with a sensitive area of ~ 10 x 25 mm, rise time of ~ 2.0 ns and recovery time of < 5 ns was used as the detector. The typical gain of the detector was ~ 1x10^6 at 2.8kV, the operating voltage used in these experiments. The bare SEM detector provided by the supplier was mounted on a 6" OD CF flange with the required electrical connectors for high voltage and signal leads. Signal from the SEM was pre-amplified and then recorded using a fast digital storage oscilloscope (DSO), interfaced to a PC through a GPIB (general purpose interface bus) for data collection. The DSO was triggered externally by a fast photodiode, illuminated by a diffuse reflection of the laser beam. Each laser pulse yields one sweep; each spectrum obtained was a sum average of about 100 sweeps, providing improved signal to noise ratio. Schematic of the experimental facility is shown in Fig. 2.3. The acceleration voltage used in the RTOF-MS is typically 4 kV.

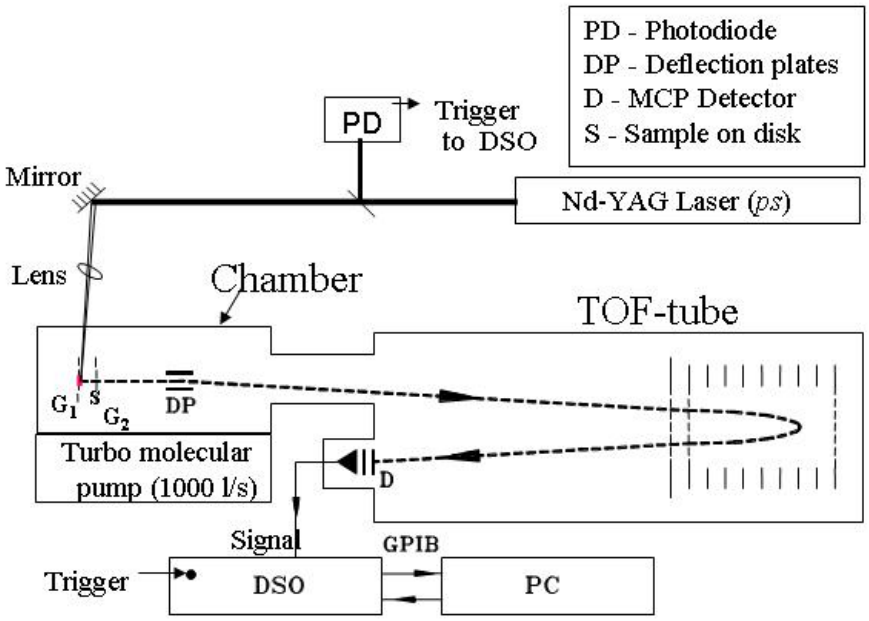

Fig.2.3: Schematic of in-house developed laser mass spectrometric facility

2.3 Preparation of solutions

2.3.1 Indicator solutions

Arsenazo-I solution

Arsenazo-I indicator solution was prepared by dissolving ~ 0.1 g of arsenazo-I in 50 mL of distilled water.

Br-PADAP solution

A 0.05% Br-PADAP solution was prepared by dissolving 0.05 g of Br-PADAP in 100 mL of ethanol.

Phenolphthalein solution

About 0.25 g of phenolphthalein was dissolved in 50 mL of 1:1 mixture (volume ratio) of distilled water and ethanol to prepare the indicator solution.

Xylenol orange solution

This solution was prepared by dissolving 0.05 g of xylenol orange in 100 mL of distilled water.

2.3.2 Complexing solutions

CyDTA complexing solution

CyDTA complexing solution was prepared by dissolving 5 g of CyDTA, 1 g of sodium fluoride and 13 g of sulphosalicylic acid in 40 mL of distilled water. The pH of this solution was adjusted to 7.8 with NaOH and the solution was made up to 100 mL with distilled water.

Neutral saturated potassium oxalate solution

Potassium oxalate was dissolved in distilled water to saturation and adjusted to pH 7. About 5 mL of this solution was used to complex metal ions prior to acid-base titration for the estimation of free acidity. A 10% potassium oxalate solution was also prepared by dissolving 10 g of potassium oxalate in 100 mL of distilled water.

Sodium fluoride solution

Sodium fluoride solution (1 M) was prepared by dissolving 4.2 g of sodium fluoride in 100 mL of distilled water.

2.3.3 Buffer solutions

Acetic acid – Sodium acetate buffer

About 90 mL of 0.2 M acetic acid solution and 10 mL of 0.2 M sodium acetate solution were mixed and adjusted to pH 3.7 using small volume of acetic acid or sodium acetate solution. This freshly prepared buffer solution (10 mL) was used to maintain a pH of 3.7 during the estimation of U(VI) with PDCA.

Borax buffer

A solution of 0.05 M borax ($Na_2B_4O_7.10H_2O$) was prepared by dissolving requisite quantity of borax in distilled water (pH : 9.18, at 298 K).

Potassium Hydrogen Phthalate (KHP) buffer

Required amount of KHP dried at 383 K was dissolved in distilled water to prepare 0.05M KHP buffer solutions (pH 4.01 at 298 K).

Potassium dihydrogen phosphate – Disodium hydrogen phosphate buffer

Potassium dihydrogen phosphate (0.0680 g) and disodium hydrogen phosphate (0.0891g) were added in to a 50 mL volumetric flask and made up to the mark with distilled water to prepare a buffer solution with pH 6.86 at 298 K.

Triethanolamine (TEA) buffer

About 14 g of TEA was dissolved in 80 mL of distilled water, adjusted to pH 7.8 with conc. $HClO_4$ and allowed to stand overnight. The pH of this solution was then re-adjusted to 7.8 with perchloric acid and diluted to 100 mL with water to prepare TEA buffer solution.

2.3.4 Actinide tracers

Americium-241

Americium oxide ($^{241}Am_2O_3$) was received from Bhabha Atomic Research Centre (BARC), Mumbai, India. The sample was dissolved in conc. nitric acid (16 M) and diluted with dilute nitric acid for the preparation of americium tracer solution.

Plutonium tracer

Plutonium purified by an anion exchange technique was used. In this procedure, the plutonium sample was dissolved in 1:1 HNO_3 (8M) and it was passed through a DOWEX anion exchange resin (1x8, 200-400 mesh). The column was washed with 3 column volumes of 8M HNO_3 to remove americium impurity. Subsequently, Pu was eluted using 0.5M HNO_3 medium. The isotopic composition of plutonium was determined using thermal ionisation mass spectrometer (TIMS) and was found to be (in atom %): ^{238}Pu: 0.017, ^{239}Pu: 93.60, ^{240}Pu:6.24, ^{241}Pu:0.12, ^{242}Pu:0.023. The oxidation state of Pu was maintained as Pu(IV) by the addition of 0.1 mL of 2.5 M $NaNO_2$ and Pu(IV) was extracted with 0.5M TTA/xylene. The organic phase containing Pu(IV) was scrubbed with 1M nitric acid and stripped with 8M nitric acid. The aqueous phase (strip solution) was washed twice with equal volume of n-hexane to remove the entrained organic phase. The solution was used for preparing aqueous

Pu(IV) solutions for extraction experiments. All experiments were carried out using 0.002 M ammonium metavanadate as holding agent.

Uranium-233

The ^{233}U separated from irradiated ThO_2 was obtained from Reprocessing Development Laboratory, Kalpakkam, India. The purification of ^{233}U was carried out by repeated solvent extraction using 4M nitric acid with 5% TBP/n-dodecane. This was followed by scrubbing the organic phase with 4M nitric acid and stripping with 0.01M nitric acid.

2.3.5 Stock solutions

Acid Mixture

Ammonium molybdate (0.4 g) was dissolved in 30 mL of distilled water; about 60 mL of conc. HNO_3 (16M) was subsequently added to this solution; it was mixed for 5 minutes to allow the heat produced to dissipate and 10 mL of saturated sulphamic acid was added to the solution to prepare the acid mixture, which was used for the estimation of U(VI) by Davies-Gray method.

H_2SO_4 solution

H_2SO_4 solution with different concentrations e.g. 1M and 0.1M were prepared by diluting concentrated sulphuric acid (17.8 M) with distilled water.

NaOH solution

NaOH solution was prepared by dissolving requisite quantity of NaOH pellets in distilled water in a volumetric flask. This solution was standardized by acid-base titration with KHP using phenolphthalein indicator.

Solutions of nitric acid

Nitric acid stock solution (e.g. 10M) was prepared from the commercially available conc.HNO_3 (16M) and standardized by acid-base titration with standard NaOH solution using phenolphthalein as the indicator. This standardized nitric acid stock solution was used for the preparation of various concentrations of solutions of nitric acid.

PDCA solution

About 2.5 g of PDCA and 1.2 g of NaOH were dissolved in 500 mL of distilled water to prepare 0.03 M PDCA solution. This solution was standardized using standard uranyl nitrate solution with arsenazo-I as the indicator. Similarly, 0.01 M PDCA solution was prepared by dissolving 0.83 g of PDCA and 0.4 g of NaOH in 500 mL of distilled water and standardized using dilute standard uranyl nitrate solution.

Phosphoric acid treated with potassium dichromate solution

About 2.5 g of 0.05 N potassium dichromate solution was mixed with 500 mL of phosphoric acid to prepare phosphoric acid treated with potassium dichromate.

Uranyl nitrate solution in nitric acid media

A nearly saturated solution of uranyl nitrate in 1M HNO_3 was prepared in a volumetric flask by dissolving urnayl nitrate crystals in distilled water with the required quantity of nitric acid. The free acidity of the solution was estimated by acid-base titration using mixed oxalate-fluoride solution as the complexing agent [159, 163].

Zirconium nitrate solution in nitric acid media

The stock solutions of Zr(IV) containing 1 g/L in nitric acid media (0.5-6M) with and without uranium (10-300 g/L) were prepared from zirconium nitrate solution. Nuclear grade zirconium metal was used to prepare zirconium nitrate solutions [164]

Zirconium nitrate standard solution for spectrophotmetric studies

A standard solution of zirconium (~ 89 μg/mL) was prepared from zirconium nitrate stock solution. The stock solution was standardised by complexometric titration using EDTA as the titrant.

Ruthenium nitrosyl nitrate solution

Stock solutions of ruthenium nitrosyl nitrate containing 1 g/L were prepared by taking suitable amount with the required concentration of nitric acid.

^{99}Tc-pertechnetate solution

Technetium supplied as ammonium pertechnetate was heated to dryness and redissolved in 8M HNO_3 and refluxed for several hours and finally redissolved in 1M HNO_3. This procedure was adopted to ensure that the entire technetium was in the pertechnetate form [65]. A stock solution containing 1 g/L of Zr(IV) and ^{99}Tc tracer in concentration of nitric acid (0.1-6M) was prepared by taking suitable amount of nitric acid and zirconium.

Nitrates of lanthanides

Individual stock solutions of La(III), Ce(III) and Nd(III) containing about 1 g/L were prepared by dissolving the corresponding oxides in 16M HNO_3 followed by suitable dilution.

U-Zr and U-Pu-Zr samples

U-Zr and U-Pu-Zr samples were received from BARC, Mumbai. These alloy samples were prepared by injection casting route which involves heating of melt to ~ 1700 K under vacuum, then open ends of quartz moulds were immersed in the melt. De-moulding set-up was employed for removing the fuel slugs from the quartz moulds. Typical diameter of the alloy slugs was about 5 mm [87].

2.3.6 Feed solutions

Plutonium nitrate solution

The plutonium nitrate solution was purified by an anion exchange technique to remove ^{241}Am. The oxidation state of plutonium in the stock solution was adjusted to Pu(IV) by purging with NO_2 gas and the oxidation state was confirmed by UV-Vis Spectrophotmetric technique. A concentrated stock solution of plutonium (75-300 g/L) was used in the experiments.

U(VI)-Pu(IV) feed solutions for batch studies

Aqueous feed solutions containing plutonium and uranium in 4M HNO_3 were prepared by mixing plutonium nitrate solution with appropriate quantities of uranyl nitrate and nitric acid.

U(VI)-Pu(IV) feed solution for mixer-settler runs

An aqueous feed solution containing ~ 30 g/L of plutonium, ~ 70 g/L of uranium, ~ 0.53 g/L of Am(III) and ~ 1.6 g/L of lanthanides in 4M HNO_3 was prepared by dissolving requisite quantity of PuO_2 in 16M HNO_3, followed by mixing plutonium nitrate solution with desired quantities of the nitrate salts of uranium and lanthanides and nitric acid. Plutonium in the solution was maintained in tetravalent oxidation state with the addition of required amount of sodium nitrite. The concentrations of lanthanide in the feed solution were chosen according to their fission yields based on PFBR fuel, with 10 atom% burnup. The fission yields of La, Pr, Nd, Sm and Eu have been reported to be about 5, 6, 20, 4 and 1.5% atom% [165] and accordingly their concentrations in the feed solution were fixed as 317, 286, 804, 159 and 36 μg/mL, respectively. The entire amount of Am present in the feed solution has come from plutonium stock, in which it has been produced by the beta decay of ^{241}Pu.

Uranyl nitrate feed solution for mixer-settler runs

A feed solution containing 241 mg U(VI)/mL in 4M HNO_3 was prepared by mixing requisite quantities of saturated solutions of uranyl nitrate and 16M HNO_3.

U-Zr and U-Pu-Zr feed solutions

Aqueous feed solutions containing higher concentration (g/L) of U and Zr with various concentrations of nitric acids were prepared by taking requisite quantities of uranyl nitrate and zirconium nitrate from their stock solutions. The feed solution containing U, Pu and Zr in nitric acid was prepared by dissolving U-Pu-Zr alloy in 16M HNO_3 under reflux conditions at ~130^{o}C. The resultant solution which contained completely dissolved U and Pu along with ~70% dissolved Zr was centrifuged and the residue (~ 30% Zr) was filtered. The acidity of the feed solution and oxidation state of Pu was adjusted to ~4M and Pu(IV), respectively.

2.4 Experimental procedure

2.4.1 Measurement of *D* values for various metal ions

- The aqueous phase containing either plutonium nitrate solution in nitric acid medium (0.5–6 M) or uranium-plutonium nitrate solutions in 4M nitric acid was contacted with equal volume (2 mL) of 1.1M solutions of TiAP and TBP in n-dodecane (with or without pre-equilibration).
- The aqueous phase containing 1 g/L of Zr(IV), RuNO(III) and Ln(III) in nitric acid medium (0.5–6M), was contacted with equal volume of the pre-equilibrated 1.1M TiAP solution in *n*-alkane (irradiated and unirradiated).
- The pre-equilibrated 1.1M solutions of TiAP and TBP in n-DD were contacted with equal volume of aqueous phase containing either U-Zr or Pu-Zr solutions in nitric acid media (0.5–6 M).
- The pre-equilibrated 1.1M solutions of TiAP and TBP in n-DD (irradiated or unirradiated) were contacted with equal volume of aqueous solution containing either U or Pu tracers in 4M nitric acid.

The two phases were mixed in a flat-bottom equilibration tube kept in a thermostatted vessel. Mixing was performed using a PTFE coated magnetic stirring bar with magnetic stirrer at 303 K for 15 min. After the equilibration, the phases were allowed to settle by gravity. Suitable aliquots of both the phases (aqueous and organic) were pipetted for the estimation of metal ion concentration. The distribution ratio (*D*) of a metal ion is defined as ratio of the concentration of metal ion in the organic phase to the concentration of metal ion in the aqueous phase at equilibrium. All the *D* values were measured in duplicate. Experimental values of the distribution data were within ± 3%. In order to compare the results obtained with TiAP, similar experiments were carried out with TBP under identical conditions.

2.4.2 Extraction and stripping of U(VI) and Pu(IV) in cross-current mode

Prior to the cross current experiments, the organic phase (1.1M TiAP/n-DD and 1.1M TBP/n-DD) was pre-equilibrated with 4M HNO_3. The acidity of the aqueous phase was maintained close to 4M in all the stages using the appropriate volume of organic phase, which was pre-equilibrated with 4M HNO_3. In cross-current experiments, co-extraction was performed by equilibrating equal volumes (2 mL) of aqueous feed solution and organic phase (1.1M TiAP/n-DD and 1.1M TBP/n-DD) for 15 mins at 303 K. After the phase separation, the organic phase was completely removed; fresh solvent was added to the above aqueous solution and this procedure was repeated for 4 times (4 stages). Stripping was also carried out in a similar manner by equilibrating loaded organic phase with equal volume of the strippant (0.35M HNO_3).

2.4.3 Extraction and stripping of metal ions from U-Zr and U-Pu-Zr feed solutions in cross-current mode

In cross-current mode of experiments, extraction of metal ions was carried out by mixing aqueous feed solution (3 mL) with equal volume of organic phase (1.1M TiAP/n-DD and 1.1M TBP/n-DD) for 15 min at 303 K. After the phase separation, organic phase was completely removed; fresh solvent was added to the above aqueous solution and this procedure was repeated four times (4 stages). Stripping was also carried out in a similar manner by equilibrating loaded organic phase with equal volume of the strippant. The extraction (%) and stripping (%) of metal ions in each stage was calculated by summing up the organic concentrations and the total % extraction and stripping (in the final stage) was calculated by using the following procedure.

$$\textbf{\% extraction or stripping} = \frac{\textbf{[Initial Concentration]-[Final concentration]}}{\textbf{[Initial concentration]}} \textbf{ x100}$$

All the experiments were carried out in duplicate and the distribution ratios were measured to a precision of ± 3%. Similar experiments were also carried out with TBP based solvent under identical conditions.

2.4.4 Radiolytic degradation experiments

TiAP and TBP samples were irradiated using a ^{60}Co gamma chamber facility with a dose rate of 0.5M Rad/hr and it was calibrated by Fricke dosimetry. Radiolytic degradation experiments involved irradiation of 100% as well as 1.1M solutions of extractant in n-DD / n-TD with and without pre-equilibration with 4M HNO_3 to the required dose levels. Irradiated samples were taken to carry out various experiments such as measurement of (a) physicochemical properties, (b) distribution ratios of U, Pu and fission products and (c) identification of degradation products and (d) to study the effect of radiolytic degradation on thermal decomposition of solvents.

2.4.5 Mixer-Settler experiments

All the mixers and settlers of the unit were initially filled with sufficient volume of the respective organic and aqueous solutions and pulsing was initiated to agitate the organic and aqueous phases during the mixer-settler runs. Simultaneously, organic and aqueous solutions were fed into respective mixer inlet ports of the mixer-settler at the predetermined rates using calibrated metering pumps. A pulse amplitude of 100 – 150 mm in the pulse probe (id = 6 mm) and an optimum pulse frequency of 30 cycles/min were maintained in all mixer-settler runs. Outlet organic and aqueous streams were collected from 1^{st} and 16^{th} settlers, respectively. In all the runs, organic and aqueous stage samples (~ 5 - 10 mL) were collected from all the settlers after the attainment of steady state. All the stage samples were taken out of the glove box and analysed. After completing each run, organic and aqueous solutions were removed from the equipment and washed with 1M HNO_3.

2.4.6 Dissolution of U-Zr metallic alloys in nitric acid medium

U-Zr alloy samples were taken in a round bottom (RB) flask containing nitric acid and were placed either in water bath or silicon oil bath. Constant volume of nitric acid was maintained throughout the experiment by cooling the vapours using a condenser. Dark brown fumes (NO_x) were initiated during dissolution and they were terminated after ~ 4 hr. Heating

was continued for an additional 4 hr; U and Zr were subsequently analysed by suitable analytical methods.

2.4.7 Dissolution of U-Pu-Zr alloy in HNO_3-HF medium

Alloy samples (U-Pu-Zr) prepared by injection casting were taken in a glass beaker containing 5mL of HNO_3 (16 M)-HF (0.05 M) solution and the contents were heated on a hot plate for about 5 hours till complete dissolution of sample, which was indicated by the absence of black residue. Constant volume of the solution was maintained throughout the dissolution process by the addition of nitric acid at regular intervals of time (every half an hour). Finally the sample was heated to near dryness and made up with 1M HNO_3 (6 mL). The solutes were analysed by suitable analytical methods.

2.4.8 Electrolytic dissolver for metallic alloy samples

A laboratory scale (75 mL) electrolytic dissolver was employed for the dissolution of metallic alloy samples inside a glove-box. The electrolytic cell was heated to the desired temperature using a furnace by placing the electrolytic cell in it. The solution was mixed by thermal agitation. Platinum electrodes, a cylindrical platinum gauze anode of 20 cm height and 4 cm in diameter and a platinum foil cathode of 20 cm height and 0.2 cm in diameter were used. The cathode was enclosed in a glass tube and the voltage required to sustain the passage of one ampere current through the cell was applied from 4 to 5 V. A condenser was used to condense the vapours evolved.

2.4.9 Estimation of zirconium by spectrophotometry

A suitable aliquot of zirconium solution (either pure or in the presence of other elements) was taken in a 10 mL standard flask. In all the experiments, a known quantity of zirconium (8.9 μg) from standard zirconium solution was pipetted into 10 mL volumetric flask. To the above, 0.8 mL of xylenol orange solution was added and flask was made up using 0.2N sulphuric acid. The solution was allowed to stand for one hour and the absorbance

was measured at 535 ± 2 nm. By this method Zr could be analysed to a precision of ± 2 % Relative Standard Deviation (RSD).

2.4.10. Adiabatic calorimetric measurement

The thermal decomposition behaviour of solvents was studied using heat-wait-search mode by heating the sample initially to 313 K and allowing it to stay at this temperature for 40 min to attain thermal equilibrium with the surrounding and then searching for any possible exothermic event. In the absence of any such event, the sample was further heated in steps of 10 K until an exothermic event occurred. This was continued up to 773 K, the upper limit of the calorimeter. A closed spherical Hastelloy® test cell of 10 mL capacity, assembled in the containment vessel of calorimeter was employed for conducting the experiments at air ambience. A thermocouple was placed in a direct contact with the sample. To study the decomposition behaviour in the presence of nitric acid, organic samples and HNO_3 (4 M or 8 M solutions) with different volume ratios (1:3, 1:1 and 3:1) were taken together in the test cell. A sample volume of 2 mL was maintained throughout the study. All the experiments were conducted in duplicates / triplicates. The uncertainty in the temperature and pressure measurement was ± 0.1 K and ± 0.1 bar, respectively.

2.4.11 Infrared spectral measurements

The infrared spectra of organic samples (irradiated or unirradiated) were recorded in the range of 4,000–400 cm^{-1} using a Fourier Transform Infrared Spectrometer at a resolution of 4 cm^{-1}. Initially a reference spectrum was obtained by scanning the two KBr pellets kept pressed together without sample. Subsequently a thin liquid film of sample made by sandwiching it between two KBr pellets was scanned for recording the spectrum in all the cases.

The gaseous products formed during the decomposition of TiAP and TBP were collected in a gas cell of 10 cm path length fitted with KBr windows at both ends. One of the stopcocks in gas cell was connected to the calorimeter feed line and the other was connected

to a rotary pump using suitable fittings. The cell was initially evacuated (~ 1.0 x 10^{-3} torr) and subsequently isolated from the vacuum system. The gaseous products formed during the decomposition of samples were transferred into the gas cell by opening feed valve of the calorimeter for recording the infrared spectrum. The residue obtained from the decomposition reaction was collected from the test cell at end of the experiment, thoroughly mixed and ground with KBr powder, pelletized and employed for recording IR spectrum.

2.4.12 Quadruple mass spectrometric studies

The gases generated during the thermal decomposition of TiAP-HNO_3 systems in the adiabatic calorimeter were collected in a leak tight SS chamber. Initially, one end of the gas sampler was connected to the calorimeter feed line while the other was connected to a rotary vacuum pump. The gas cell was then evacuated to 1.0 x 10^{-3} torr and isolated from the vacuum system. The gaseous products formed during the decomposition of the respective systems were transferred into the gas cell by opening the feed valve of the calorimeter. The SS chamber was then connected to QMS inlet and the mass spectrum was recorded covering a mass range of 1 to 100 amu. Vacuum of the QMS chamber was maintained at 1×10^{-6} torr.

2.4.13 Measurement of density and viscosity

The density of organic phases was measured at room temperature by taking the weight of a known volume of sample in a previously weighed micropipette (500 μL). Ostwald viscometer which was standardised with water has been employed for the measurement of organic phase viscosity. The viscosity of organic samples was estimated with water as the reference liquid, whose density (ρ_w) and viscosity (η_w) were known for a particular temperature. The viscometer was kept in a double walled glass container through which water from a constant temperature water bath was circulated to maintain a temperature of 303 ± 0.1 K. Initially, the viscometer was filled with a known volume (~15 mL) of the sample and the time taken for the sample to cross the marked region of the viscometer (t_s) was determined. Subsequently, the procedure was repeated to obtain the time taken for the same volume of

water to cross the marked region (t_w). The viscosity of the sample solution (η_s) was calculated from the following expression where, ρ_s represents the density of the sample.

$$\eta_s = \frac{\eta_w \rho_s t_s}{\rho_w t_w} \quad \text{.....(2.1)}$$

2.4.14 Interfacial tension

Prior to the measurements of interfacial tension, 5 mL of each of organic and aqueous phases (4M HNO_3) were equilibrated at 303 K for 30 mins, centrifuged and separated. The pre-equilibrated organic phases along with aqueous phase were placed in a constant temperature bath to achieve thermal equilibrium. The organic phase was transferred to a glass vial and placed in the thermostated vessel maintained at the desired temperature. The aqueous phase was taken in Agla syringe. Drops of aqueous phase formed at the end of the capillary tip and dispensed extremely slowly into the organic phase. Several such drops were dispensed and increase in weight was measured with an analytical balance of 0.01 mg sensitivity. The mass of one drop was then calculated from the differences in mass of glass vial before and after aqueous phase addition. The densities of organic and aqueous phases were measured by weighing a known volume of respective phase, using a class "A" pre-calibrated microliter glass pipette at ambient temperature, in an analytical balance. The interfacial tension measurements were carried out by drop weight technique in which the interfacial tension, Γ is given by [166-168].

$$\Gamma = [\, V \times (\rho_{aq} - \rho_{org}) \times g \,] / (2 \times \pi \times r \times f_s) \text{.....(2.2)}$$

Where fs is the Smith's correction factor and is given by

$$f_s = (1 - r / R) \text{.....(2.3)}$$

V is the volume of the drop at the moment of separation, ρ_{aq}, ρ_{org} are the densities of aqueous and the organic phases, respectively, r is the radius of the capillary tip, R is the drop radius at the moment of separation and g is the acceleration due to gravity.

The instrument used for IFT measurement employs an Agla(R) (M/S. Burroughs Wellcome) micrometric syringe, coupled to a glass capillary tube and a micrometer capable of

delivering volumes as low as 0.2 microlitres. The diameter of the capillary tip was measured using an optical microscope. The values are the average of ten replicate measurements. The results are found to agree well with the literature values in the range of ±0.1 mN/m.

2.4.15 Metal retention test

Initially the metal ions (^{233}U or Pu) were extracted into the organic phase (1.1M TiAP/n-DD or 1.1M TBP/n-DD) which was equilibrated with equal volume of (2 mL) 4M HNO_3 for 30 min. The aqueous phase was removed and stripping of the metal ions was carried out. Stripping of U(VI) was carried out by equilibrating the organic phase with equal volume of 0.01M HNO_3 for 30 min. The amount of ^{233}U in the organic phase was measured by LSC technique by taking suitable aliquots after three successive stripping contacts. Similarly stripping of Pu(IV) was carried out with 0.5M HNO_3 and the amount of Pu(IV) retained in the organic phase was measured after three successive stripping contacts.

2.4.16 Alpha degradation studies by Pu(IV)

Plutonium sample with an isotopic composition (atom%), ^{238}Pu – 0.017%, ^{239}Pu – 93.33%, ^{240}Pu – 6.24%, ^{241}Pu - 0.12%, ^{242}Pu – 0.023% and with an α-specific activity of 1.65 x 10^5 dpm/μg was used. The absorbed dose corresponding to the plutonium loading and ageing was computed by taking into account the individual contributions from the isotopes and α energies assuming entire α energy is dissipated into the medium. Initially Pu(IV) was extracted with 1.1M solutions of trialkyl phosphate (TalP) in n-DD at 4M HNO_3. After the extraction of Pu(IV) by TalP (TBP and TiAP), organic phase was allowed to stand for typically about 400 hr to study the effect of alpha (α) degradation. Organic phase was removed at regular time intervals and plutonium was stripped by equilibrating the organic and aqueous phases (1 mL each), with an O/A ratio of 1 : 1, from stoppered glass tubes. The phases were centrifuged, separated and analysed for plutonium by liquid scintillation counting after appropriate dilution. Stripping was carried out three times with 0.05M and further three times with 0.01M nitric acid successively, without any valency adjustment.

2.5 Analytical methods

2.5.1 Determination of Uranium and Plutonium

In the present study U and Pu were estimated by different analytical procedures depending on the aliquot. Uranium in macro quantities was estimated by potentiometry using Davies & Gray method [169]. In this method an aliquot containing 3-5 mg/mL of uranium was analysed by redox procedure using mercury-mercurous sulphate as reference electrode and platinum as indicator electrode for end point detection. Plutonium in macro quantities was analysed by potentiometry using Drummond & Grant method [169] which involves the analysis of samples containing 3-5 mg/mL of plutonium. In both the methods, metal ions can be analysed to a precision of ± 0.5 % RSD.

Uranium and plutonium in micro quantities were determined using spectrophotometric technique; uranium was analysed using Br-PADAP as the chromogenic agent by measuring the absorbance of metal complex at 577 ± 1 nm [170]; plutonium was analysed using thoron as the chromogenic agent by measuring absorbance of the complex at 540 ± 1 nm [171]. In the spectrophotometric analysis, the lowest measurable concentrations of uranium and plutonium were found to be 1 and 2 μg/mL respectively, with a precision of ± 2%.

Uranium (macro quantities) was estimated by complexometry using Pyridine-2,6-dicarboxylic acid (PDCA) as the titrant and Arsenazo I as the indicator at pH 3.7 [172]. Solutions of 0.03M / 0.01M PDCA were used for the analysis of concentrated and dilute uranium solutions, respectively. In this method, the concentrations of uranium were estimated to a precision of ± 2% RSD.

In some cases, uranium and plutonium (micro quantities) were also estimated by High Performance Liquid Chromatographic (HPLC) technique. A reversed phase chromatographic technique was employed for the separation of U(VI) from Pu(IV). A reversed phase C18 monolithic chromatographic column (10 cm length) was employed with 0.1M α-hydroxy

isobutyric acid (α-HIBA) as the mobile phase (pH:4) for the separation and determination of U and Pu. The samples containing uranium and plutonium in HNO_3 medium were dissolved in the mobile phase with appropriate dilution and injected into the HPLC system. Arsenazo(III) was used as the post-column reagent and U and Pu – arsenazo complexes were detected at 655 nm. Lanthanides and Am were separated from each other and determined using dynamic ion-exchange HPLC technique [173]. A solution of 0.03M camphor sulphonic acid (CSA) + 0.1M α-HIBA (pH: 3.6) was used as the mobile phase with reversed phase monolithic column as the stationary phase support; arsenazo (III) was used as the post-column reagent and the metal complexes were detected at 655 nm. In the above-mentioned HPLC methods, the concentrations of uranium, plutonium, lanthanides and americium were determined to a precision of ± 2% RSD. The minimum concentrations that could be estimated for all these elements using HPLC were found to be about 1 μg/mL.

2.5.2 Determination of concentration of nitric acid in aqueous and organic Phases

Concentration of nitric acid in the aqueous and organic samples was determined by acid-base titration after complexing the metal ions with potassium oxalate-sodium fluoride solution and the solution were titrated with standard NaOH solution. By this method, nitric acid can be analyzed to a precision of ± 1% [163].

2.5.3 Determination of Zirconium

Macro and micro quantities of zirconium were estimated by complexometry and spectrophometry respectively, with a precision of ± 2% [48, 22]. The macro level concentration of Zr(IV) in the organic and aqueous samples was determined by the addition of excess EDTA solution followed by the back titration of excess EDTA with standard $Th(NO_3)_4$ solution using xylenol orange as the indicator [164]. Zr was analysed spectrophotometrically using xylenol orange as the chromogenic agent. The absorbance of Zr(IV)-Xylenol orange complex was measured at 535 nm using Zr solutions with a concentration range of 0.5–3.5 μg/mL.

2.5.4 Determination of Ruthenium

Ruthenium was analysed by Inductively Coupled Plasma-Atomic Emission Spectrometry (ICP-AES) using sequential spectrometer of ULTIMA-C spectroanalyser system (John Yvon, France) with a precision of ± 4%.

2.5.5 Determination of Lanthanides

Lanthanides such as Nd, Ce and La were also estimated by using arsenazo-I as the chromogenic reagent. The absorbance of Ln(III) - arsenazo I complex was estimated at 575 nm using lanthanide solutions in the concentration range of 0.5–3.5 μg/mL with a precision of ± 3%.

2.5.6 Determination of Am-241

^{241}Am was estimated by gamma counting using a NaI(Tl) detector based counting system at 60 keV with a precision of ± 4%.

2.5.7 Determination of Tc-99

^{99}Tc was assayed by beta counting with LSC using dioxane based solvents. In this method, ruthenium can be analyzed to a precision of ± 4%.

2.5.8 Measurement of enthalpy of decomposition

The enthalpy of decomposition was derived using the data generated from calorimetric experiments, employing the following expression.

$$\Delta H_r = C_p \times \Delta T_{ad} = C_p \times \Delta T_{\exp} \times \Phi \qquad (2.4)$$

where ΔH_r is the enthalpy change of a reaction, C_p is the heat capacity of reactants, ΔT_{exp} is the experimentally observed temperature rise, ΔT_{ad} is the true temperature rise and the Φ-factor [174] is defined by the following expression,

$$\Phi = 1 + \frac{(mC_P)_C}{(mC_P)_S} \qquad (2.5)$$

where $(mC_p)c$ and $(mC_p)s$ are the thermal mass of the sample container and sample respectively. The heat capacity (C_P) of the sample mixture was assumed to be 2 $Jg^{-1}K^{-1}$, as it

could not be measured for the wide variety of organic phase compositions studied and organic phase-nitric acid volume ratios employed. The above assumption was based on the fact that the heat capacities of TBP, TiAP, diamylamyl phosphonate (DAAP), octyl(phenyl)-*N,N*-diisobutylcarbamoylmethylphosphine oxide (CMPO) and their acid solvates are about 2 $Jg^{-1}K^{-1}$ in the temperature range (350–390 K) [156, 175-177]; similarly, concentration of nitric acids employed in the present study have a C_p value of approximately 2 $Jg^{-1}K^{-1}$. The calorimeter was standardised using di-tert-butyl peroxide (DTBP) [178]. It undergoes thermal decomposition to produce acetone and ethane as shown below [179].

$$(CH_3)_3C\text{-}O\text{-}O\text{-}C(CH_3)_3 \rightarrow 2(CH_3)_2CO + C_2H_6 \qquad (2.6)$$

The thermal hazard and thermokinetic properties of DTBP are reported elsewhere [180]. The enthalpy change for the above reaction was derived and found to be -207.5 kJ mol^{-1} (for a Φ-factor of 1.76), which agrees with the value reported in the literature for a Φ-factor range of 1.3–1.8 [181]. The onset temperature for the decomposition, activation energy and pre-exponential factor are 396.5 K, 156.7 kJ mol^{-1} and 6.1 x 10^{15} s^{-1}, respectively, which are in good agreement with the values reported in literature [181], indicating reliability of the calorimetric measurements.

2.5.9 Kinetic parameters for thermal decomposition

The rate constant (k) for an exothermic reaction is given by

$$k^* = \frac{\frac{dT}{dt}}{(T_f - T_i)\left(\frac{T_f - T}{T_f - T_i}\right)^n} \qquad (2.7)$$

i.e.

$$\ln k^* = \ln\left(\frac{\mathrm{dT}}{\mathrm{dt}}\right) - \ln(T_f - T_i) - n\ln\left[\frac{T_f - T}{T_f - T_i}\right] \qquad (2.8)$$

Where n is order of the reaction, dT/dt is rate of temperature rise. T_i, T_f and T are the temperatures in the initial, final and at any time t of the exothermic process. The Arrhenius equation is given by

$$k = A\exp\left(\frac{-E_a}{RT}\right) \tag{2.9}$$

i.e.

$$\ln k = \ln A - \frac{E_a}{RT} \tag{2.10}$$

Where A is the frequency factor and E_a is the activation of the reaction. By equating equations 2.8 and 2.10 rearranging, Eqn.(2.11) can be obtained.

$$\ln\left(\frac{\mathrm{dT}}{\mathrm{dt}}\right) = \ln\left(A.\left(T_f - T_i\right)\right) + \left(\frac{-E_a}{R}\right)\left(\frac{1}{T}\right) + n\ln\left[\frac{T_f - T}{T_f - T_i}\right] \tag{2.11}$$

Eqn. (2.11) was solved by employing the multiple linear regression method and the kinetic parameters (E_a, A and n) were obtained; ln(dT/dt) is a dependant variable, ln(A.(T_f-T_i)) is a constant, $1/T$ and ln(T_f -T/T_f-T_i) are the independent variables.

Chapter 3

EXTRACTION BEHAVIOUR OF U(VI), Pu(IV) AND FISSION PRODUCTS WITH TiAP-BATCH STUDIES

3

3.1 Introduction

The extraction behaviour of U(VI) and Pu(IV) (quantities in tracers, ~10^{-5}M) with TBP as well as TiAP based solvents has been investigated by Suresh et al. [151]. The extraction of U(VI) and HNO_3 into 1.1M TBP/n-DD and 1.1 M TiAP/n-DD from nitric acid media has been investigated as a function of equilibrium aqueous phase acidity and U(VI) concentration [150, 159]. Similarly extraction behaviour of Pu(IV) under high loading conditions was studied by Srinivasan et al. [74] using 1.1M TBP in n-DD and Shellsol-T. It was reported that TBP based solvent forms third phase with Pu(IV) at higher concentration in nitric acid medium. Macro-level extraction of U(VI) and Pu(IV) using TBP based solvent was investigated [72, 73]. It has been observed that Pu(IV) forms third phase in the presence of U(VI) and the LOC values for Pu(IV) decreased with increase of U(VI) in the organic phase. However similar studies with Pu(IV) and in the presence of U(VI) were not investigated with TiAP based solvent.

Decontamination factors (10^6 to 10^7) were obtained for U(VI) and Pu(IV) against fission products in the PUREX process. The experience gained from spent nuclear fuel reprocessing revealed that some fission products such as Zr, Ru and Tc etc. are troublesome in their nature as their complete removal from U(VI) and Pu(IV) is rather difficult. The complex chemistry of these fission products has been studied and reported [50]. In addition, the quantities of fission products produced in the fast reactors are higher compared to thermal reactors. Hence it is difficult to achieve higher decontamination factors in fast reactor fuel reprocessing compared to thermal reactor reactor fuel reprocessing. However the extraction behaviour of fission products with TiAP based solvent has not been studied.

The extraction of Pu(IV) from nitric acid media was carried out and the results are discussed in this chapter. The co-extraction of U(VI) and Pu(IV) as a function of metal ion

concentration was investigated with 1.1M TiAP/n-DD. The co-extraction and co-stripping of U(VI) and Pu(IV) using 1.1M TiAP/n-DD and 1.1M TBP/n-DD in cross current mode were also carried out and the results are discussed in this chapter. This chapter also deals with the extraction behaviour of fission products (Zr, Ru, Tc, Lns) with TiAP as a function of nitric acid concentration. The effects of uranium loading and diluent chain length on the extraction of Zr, the effect of radiolytic degradation on the extraction of fission products have been investigated. This chapter also describes some aspects of the formation of interfacial deposits during the alkali wash of degraded solvent.

3.2 Extraction behaviour of U(VI) and Pu(IV) using TiAP

3.2.1 Extraction of Pu(IV) by 1.1M TiAP/n-DD under high metal loading conditions

Distribution ratios for the extraction of Pu(IV) by 1.1M TiAP/n-DD from plutonium nitrate solution have been measured as a function of equilibrium aqueous phase Pu(IV) and nitric acid concentration. The variation of $D_{Pu(IV)}$ with $[Pu(IV)]_{aq,eq}$ for various concentrations of nitric acid is shown in Fig.3.1. These studies indicated that $D_{Pu(IV)}$ initially decrease steeply and then flatten with increase in $[Pu(IV)]_{aq,eq}$ at concentrations of 2M, 4M and 6M nitric acid. However, in the case of 0.5M HNO_3, $D_{Pu(IV)}$ initially showed an increase and then decrease (Fig.3.2).

The extraction and stripping behaviour of U(VI) using TBP and TiAP in nitric acid media have been studied in our laboratory and a correlation between $D_{U(VI)}$, $[NO_3^-]$ and [TiAP] was established [159]. In a similar manner, Eq.3.1 which represents the extraction mechanism of Pu(IV) with TiAP could be used to deduce the correlation between $D_{Pu(IV)}$, $[NO_3^-]$ and [TiAP] as represented in Eq.3.2. Extraction of nitric acid by TiAP is shown in Eq.3.3.

$$Pu^{4+}_{(aq)} + 4\ NO_3^-{}_{(aq)} + 2\ TiAP_{(org)} \leftrightarrow Pu(NO_3)_4 \,.\, 2TiAP_{(org)} \quad \text{.....(3.1)}$$

$$D_{Pu(IV)} = K[NO^-_3]^4_{(aq)}[TiAP]^2_{(org)} \quad \text{.....(3.2)}$$

$$H^+_{(aq)} + NO_3^-{}_{(aq)} + TiAP_{(org)} \leftrightarrow HNO_3\,.TiAP_{(org)} \quad \text{.....(3.3)}$$

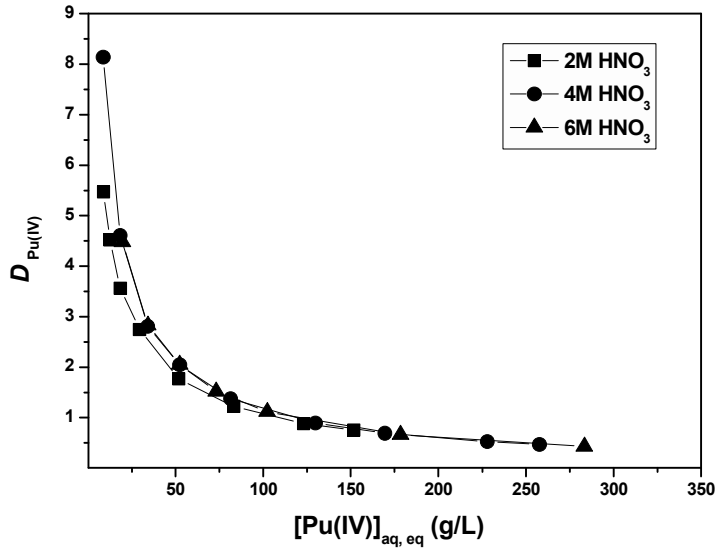

Fig.3.1: Variation of $D_{Pu(IV)}$ with $[Pu(IV)]_{aq,eq}$ for the extraction of Pu(IV) by 1.1M TiAP/n-DD from plutonium nitrate solutions in nitric acid media at 303 K

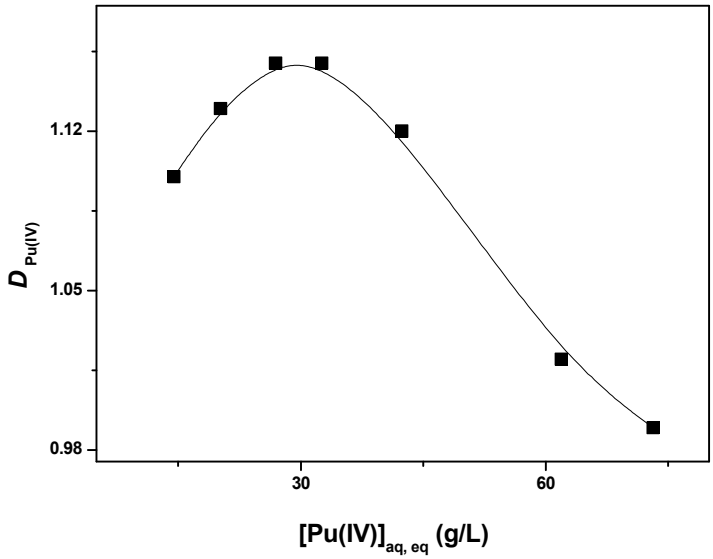

Fig.3.2: Variation of $D_{Pu(IV)}$ with $[Pu(IV)]_{aq,eq}$ for the extraction of Pu(IV) by 1.1M TiAP/n-DD from plutonium nitrate solution in 0.5M nitric acid media at 303 K

The profile shown in Fig.3.1 can be explained based on Eq.3.1; with the increase of $[Pu(IV)]_{aq,eq}$, free extractant concentration in the organic phase showed a decrease; therefore $D_{Pu(IV)}$, which is directly proportional to the square of the free extractant concentration ($[TiAP]^2_{(org)}$), also decreases. It can also be seen from Fig.3.1 that with the increase in concentration of nitric acid in the aqueous phase, there is a marginal increase in $D_{Pu(IV)}$. The

effect of concentration of nitric acid was found to be insignificant on $D_{Pu(IV)}$ under higher metal loading conditions; the influence of acidity on $D_{Pu(IV)}$ was observed only during tracer (~ 10^{-4}M) extraction of Pu(IV). In the case of 0.5M HNO_3, the initial increase of $D_{Pu(IV)}$ with increase in $[Pu(IV)]_{aq,eq}$ is attributed to the self-salting effect. Beyond certain loading, the effect due to decrease in free extractant concentration begins to dominate, resulting in decrease of $D_{Pu(IV)}$.

The concentration of Pu(IV) in the organic phase increases with the increase of $[Pu(IV)]_{aq,\ eq}$ and reaches up to a near saturation limit (theoretical loading) except in the case of 0.5M HNO_3 (Fig.3.3). At a particular $[Pu(IV)]_{aq,\ eq}$, the loading in the organic phase increases with the increase in concentration of nitric acid in the aqueous phase. As shown in Fig. 3.4, $[HNO_3]_{org,\ eq}$ decreases with increase in $[Pu(IV)]_{org,\ eq}$. This is attributed to the fact that the metal ion and nitric acid in the aqueous phase are competing to get extracted by the free extractant in the organic phase as shown in Eq.3.1 and 3.3. The $[HNO_3]_{org,\ eq}$ decreases linearly with $[Pu(IV)]_{org,eq}$ for various concentrations of nitric acid the aqueous phase. Therefore, $[HNO_3]_{org,\ eq}$ can be expressed as a function of $[Pu(IV)]_{org,\ eq}$ as shown in Eq. 3.4.

$$[HNO_3]_{org,\ eq} = m[Pu(IV)]_{org,eq} + c \quad \text{.....(3.4)}$$

where '*m*' is the slope and '*c*' is the y-intercept of the "line segment" representing the linear fit for the variation of $[HNO_3]_{org,\ eq}$ with $[Pu(IV)]_{org,eq}$. The y-intercept (c) also represents the $[HNO_3]_{org,\ eq}$ for the extraction from nitric acid media in the absence of metal ions. The results also indicate that the slope (-*m*) and y intercept decrease as $[HNO_3]_{aq,\ eq}$ decreases. The variation of slope '*m*' and y-intercept '*c*' as a function of $[HNO_3]_{aq,\ eq}$ is linear and hence both "*m*" and "*c*" can be correlated to $[HNO_3]_{aq,\ eq}$ as shown by Eq. 3.5 and 3.6.

$$m = -0.001[HNO_3]_{aq,\ eq} \text{.....(3.5)}$$

$$c = 0.19[HNO_3]_{aq,\ eq} \text{.....(3.6)}$$

Therefore, the terms 'm' and 'c' in equation (3.4) can be replaced with the expressions in terms of $[HNO_3]_{aq,\ eq}$. Hence $[HNO_3]_{org,\ eq}$ can be expressed in terms of $[HNO_3]_{aq,\ eq}$ and $[Pu(IV)]_{org,eq}$ and is shown by Eq.3.7.

$$[HNO_3]_{org,\ eq} = \{-0.001[Pu(IV)]_{org,eq}+0.19\}[HNO_3]_{aq,\ eq} \text{……..(3.7)}$$

This equation could be used for predicting the $[HNO_3]_{org,\ eq}$ for the extraction of Pu(IV) by 1.1M TiAP/n-DD as the solvent from nitric acid media at 303 K, if $[Pu(IV)]_{org,eq}$ and $[HNO_3]_{aq,\ eq}$ are known.

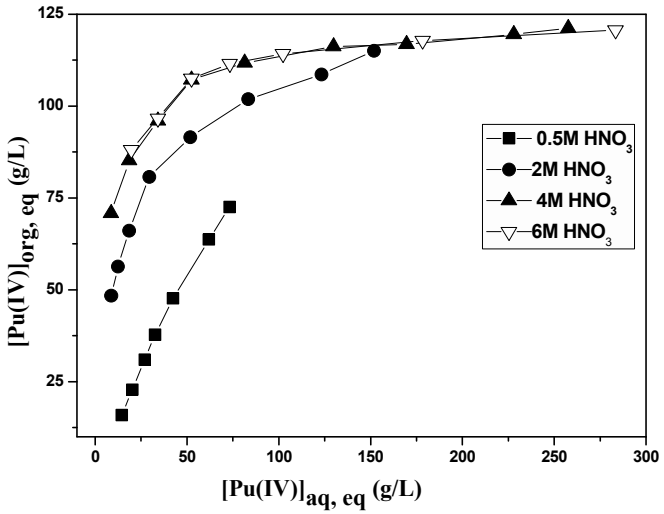

Fig. 3.3: Variation of $[Pu(IV)]_{org,\ eq}$ with $[Pu(IV)]_{aq,eq}$ for the extraction by 1.1MTiAP/ n-DD from plutonium nitrate solutions in nitric acid media at 303 K

The theoretical loading of Pu(IV) in the organic phase can be computed using Eq. 3.1 and is about 130 g/L, which corresponds to 0.55M. In the present study, about 120 g/L (0.502M) of Pu(IV) was loaded from nitric acid media without third phase formation. However, the maximum organic loading of Pu(IV) from 0.5M HNO_3 is only about 73 g/L (0.31M); this is due to the difficulties associated with the preparation of concentrated Pu(IV) feed solution in 0.5M HNO_3. The aqueous and organic phase Pu(IV) concentrations in various solutions of nitric acid is shown in Table 3.1. It was reported that in the case of Pu(IV)-1.1M TBP/n-DD-HNO_3 system, tendency for third phase formation was higher at 2M HNO_3, whereas in the case of TiAP system, phase splitting was not observed even at this acidity. These studies indicated that TiAP can be employed for the processing of plutonium rich fuels.

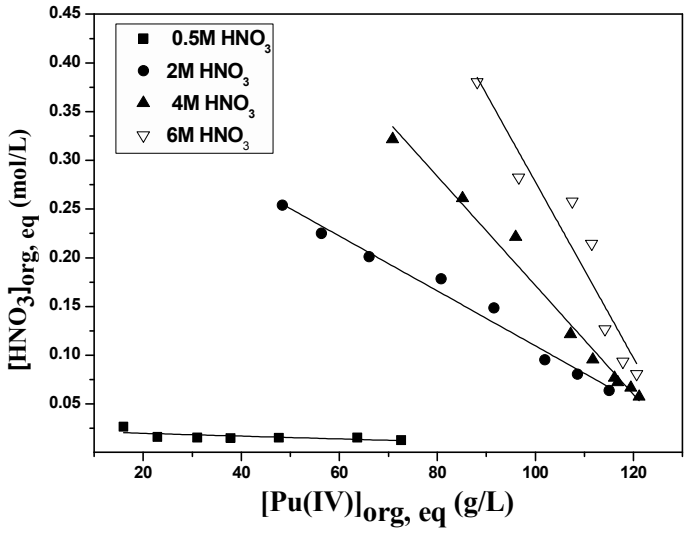

Fig. 3.4: Variation of $[HNO_3]_{org,\ eq}$ as a function of $[Pu(IV)]_{org,\ eq}$ for the extraction by 1.1MTiAP/n-DD from plutonium nitrate solutions in nitric acid media at 303 K

The results obtained reveal that Pu(IV) does not form third phase with 1.1M TiAP/ n-DD. An increase in the chain length of the extractant increases the LOC values in the extraction of Th(IV) [152]. The LOC values for the extraction of Th(IV) are higher for TiAP than TBP system, whereas in the case of Pu(IV), third phase was not observed with TiAP system. For example, the LOC for third phase formation in the extraction of Th(IV) by 1.1M TiAP/n-DD and 1.1M TBP/n-DD from 4M HNO_3 at 303K is about 75 g/L and 36 g/L, respectively. Organic phase splitting occurs due to the non-compatibility of polar metal-solvate with non-polar hydrocarbon diluent. The presence of additional methyl groups makes TiAP more hydrophobic compared to TBP and hence TiAP has lower affinity towards organic phase splitting. The same can be explained based on reverse micelle concept. Formation of reverse micelles during the third phase formation phenomenon was reported by Borkowski et al. [182]. The average distance between the polar metal-solvate molecules increase with the increase in the alkyl chain length of the extractant and hence the attractive interactions become difficult. The aggregation of "reverse micelle" becomes difficult, therefore the tendency for third phase formation is less likely with TiAP based system.

Table 3.1: Extraction of Pu(IV) by 1.1M TiAP/n-DD from plutonium nitrate solutions in nitric acid at 303 K

0.5M HNO_3		2M HNO_3		4M HNO_3		6M HNO_3	
$[Pu(IV)]_{aq}$ (g/L)	$[Pu(IV)]_{org}$ (g/L)	$[Pu(IV)]_{aq}$ (g/L)	$[Pu(IV)]_{org}$ (g/L)	$[Pu(IV)]_{aq}$ (g/L)	$[Pu(IV)]_{org}$ (g/L)	$[Pu(IV)]_{aq}$ (g/L)	$[Pu(IV)]_{org}$ (g/L)
73.14	72.56	151.74	115.04	257.64	121.18	283.35	120.66
61.88	63.67	123.11	108.57	227.94	119.49	178.42	117.85
42.35	47.65	83.27	101.89	169.49	116.82	102.32	114.18
32.59	37.77	51.83	91.56	129.79	116.18	73.27	111.49
26.92	31.02	29.39	80.78	81.52	111.73	52.43	107.52
20.16	22.88	18.53	66.08	52.41	107.17	34.20	96.62
14.45	15.97	12.47	56.36	34.22	96.00	19.68	88.12
		8.85	48.37	18.50	85.18		

3.2.2 Co-extraction of U(VI) and Pu(IV) by 1.1M TiAP/n-DD and 1.1M TBP/n-DD

Third phase formation with Pu(IV) in the presence of U(VI) is a major concern in fast reactor fuel reprocessing. Srinivasan et al. [72] observed that the presence of U(VI) in the organic phase decreased the LOC of Pu(IV) in U(VI)-Pu(IV)-HNO_3-TBP system. TiAP solvent has been examined for U(VI)-Pu(IV)-HNO_3 system under high metal loading conditions. The concentrations of U(VI) and Pu(IV) in the feed solution were chosen to simulate the dissolver solution of PFBR MOX fuel (21% initial Pu) with 10 atom% burnup. A feed solution with U(VI) and Pu(IV) concentrations of ~ 243 and ~ 38 g/L (1.02 and 0.16 M), respectively, in 4M HNO_3 was prepared and employed for the extraction experiments. Co-extraction behavior of U(VI) and Pu(IV) was investigated and the *D* values for the co-extraction of U(VI) and Pu(IV) were measured as a function of their equilibrium aqueous phase metal concentrations using 1.1 M solutions of TiAP and TBP in n-DD from 4M HNO_3 at 303 K.

The *D* values for the extraction of U(VI) and Pu(IV) initially decreased steeply and flatten with the increase in metal ion concentration in the aqueous phase (Fig. 3.5 and 3.6). The maximum concentrations of U(VI) and Pu(IV) in the organic phase obtained under the

present experimental conditions are 107 and 15 g/L (0.45 and 0.06 M), respectively, with 1.1M TiAP/n-DD system. The data on the variation of $[Pu(IV)]_{org,eq}$ with $[Pu(IV)]_{aq,eq}$ at 4M HNO_3 is shown in Table 3.2. The sum of the maximum concentrations of U(VI) and Pu(IV) in the organic phase was found to be about 120 g/L. Hence it is possible to achieve theoretical loading (~120 g/L) in the organic phase without third phase formation under the present experimental conditions. The results also indicated that the distribution data of U(VI) and Pu(IV) with 1.1M TiAP/n-DD are comparable to 1.1M TBP/n-DD system. The *D* values for uranium are marginally higher than that of plutonium over a wide range of equilibrium aqueous phase metal ion concentration in the case of both TiAP and TBP systems (Fig.3.5 and Fig.3.6).

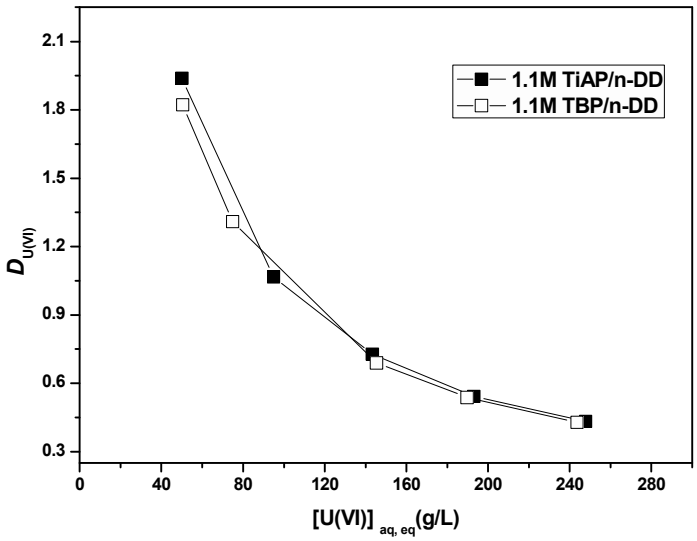

Fig.3.5: Variation of $D_{U(VI)}$ with $[U(VI)]_{aq,\ eq}$ for the extraction of U(VI) by TalP from a solution of U(VI) and Pu(IV) in 4M nitric acid at 303 K

3.2.3 Co-processing of U(VI) and Pu(IV) in cross-current mode

Co-processing of U(VI) and Pu(IV) which involves the recovery of Pu along with U results in resistance to nuclear proliferation and reduces the cost of the process by avoiding Pu partitioning cycle and Pu purification cycle. Prior to continuous counter-current solvent extraction runs with high metal loading conditions using a mixer-settler facility, batch studies were carried out in the cross-current mode to assess the number of stages required for the co-

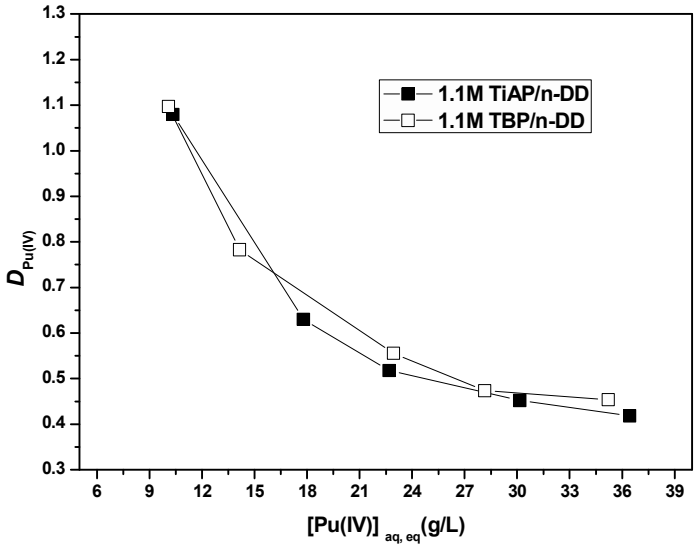

Fig.3.6: Variation of $D_{Pu(IV)}$ with $[Pu(IV)]_{aq, eq}$ for the extraction of Pu(IV) by TalP from a solution of U(VI) and Pu(IV) in 4M nitric acid at 303 K

Table 3.2: Co-extraction of U(VI) and Pu(IV) by 1.1M TiAP/n-DD and 1.1M TBP/n-DD from a mixture of U(VI) and Pu(IV) in 4M nitric acid at 303 K

1.1M TiAP/n-DD				1.1M TBP/n-DD			
$[Pu(IV)]_{aq}$ (g/L)	$[Pu(IV)]_{org}$ (g/L)	$[U(VI)]_{aq}$ (g/L)	$[U(VI)]_{org}$ (g/L)	$[Pu(IV)]_{aq}$ (g/L)	$[Pu(IV)]_{org}$ (g/L)	$[U(VI)]_{aq}$ (g/L)	$[U(VI)]_{org}$ (g/L)
36.42	15.25	247.68	107.25	35.20	15.99	243.40	104.33
30.14	13.63	192.92	104.48	28.14	13.33	189.66	101.98
22.69	11.75	143.25	104.16	22.93	12.75	145.28	100.22
17.78	11.20	94.90	101.21	14.14	11.07	74.85	98.03
10.34	11.16	50.03	96.99	10.08	11.05	50.40	91.81

extraction and co-stripping of heavy metal ions using 1.1M TiAP/n-DD system. The concentrations of feed solution are chosen to simulate the dissolver solution of PFBR MOX fuel (28% initial Pu) with a burnup of 10 atom%. The concentrations of U(VI) and Pu(IV) in the feed solution were 254 and 64 g/L (1.07 and 0.27 M), respectively in 4M HNO_3. The Pu(IV) concentration in the feed solution was higher than the feed solution described in the previous section (3.2.2).

The flowsheet for the co-extraction of U(VI) and Pu(IV) by 1.1M TiAP/n-DD in cross-current mode is shown in Fig.3.7. The maximum loading of U(VI) and Pu(IV) in the organic phase was found to be 106 and 20.9 g/L (0.46 and 0.088 M), respectively, in the 1st stage of cross-current extraction and the loadings in the organic phase decreases from stage 1 to 4. The total concentration of U(VI) and Pu(IV) in the organic phase without phase splitting was found to be about 120 g/L, which is close to the theoretical loading. The acidity of the aqueous phase was maintained close to 4M in all these stages. The concentration of Pu(IV) in aqueous phase (raffinate) in 4th stage was found to be below detection limit (BDL = 2 µg/mL), whereas U(VI) concentration was about 0.14 g/L. Subsequently, stripping of metal ions from the organic phase was carried out using 0.35M HNO_3 (minimum acidity required to prevent the hydrolysis and polymerisation of Pu(IV)) [31]. The flowsheet for the stripping of heavy metal ions is shown in Fig.3.8. The first three loaded organic solutions (LO 1, LO 2 and LO 3) except LO 4 were mixed to get a concentrated loaded organic phase (~ 80%), which is the approximate loading in actual reprocessing plants. The concentrations of U(VI) and Pu(IV) in the mixed loaded organic phase were about 85 and 18 g/L, respectively. Most of the Pu(IV) was stripped within the two stages whereas stripping of U(VI) was observed in all the four stages (Fig.3.8). The concentrations of U(VI) and Pu(IV) in the organic phase (lean organic) after four stages of stripping were about 15.4 and 3.26 g/L, respectively.

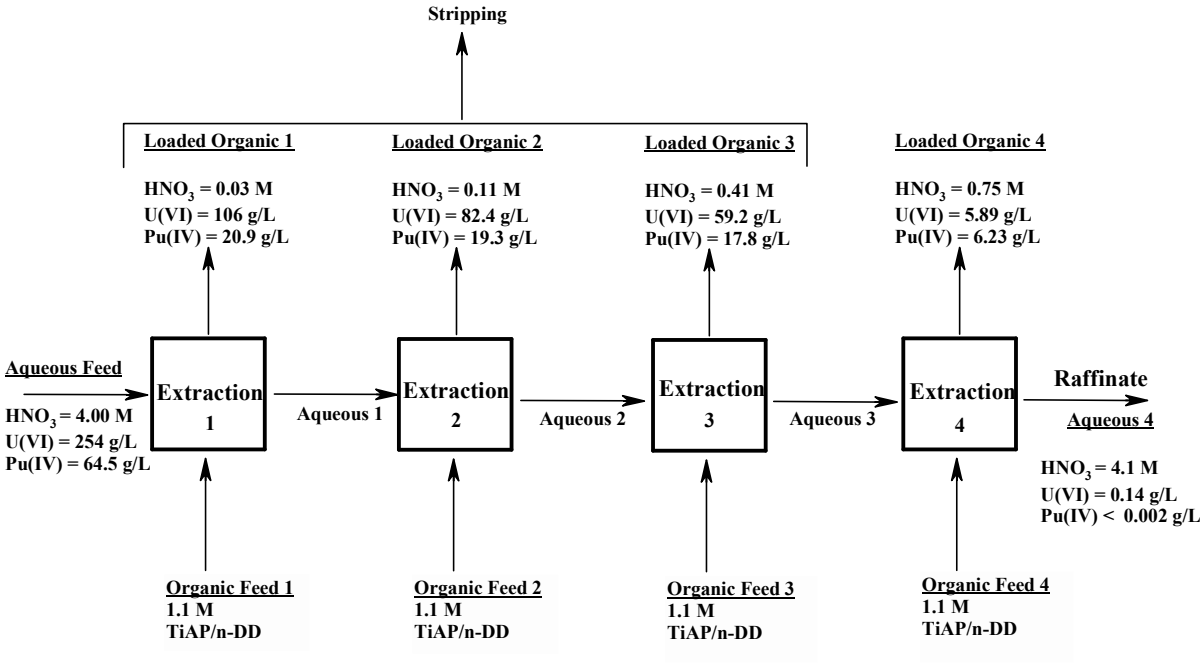

Fig. 3.7: Co-extraction of U(VI) and Pu(IV) from 4M HNO_3 by 1.1M TiAP/n-DD in cross-current mode at 303 K

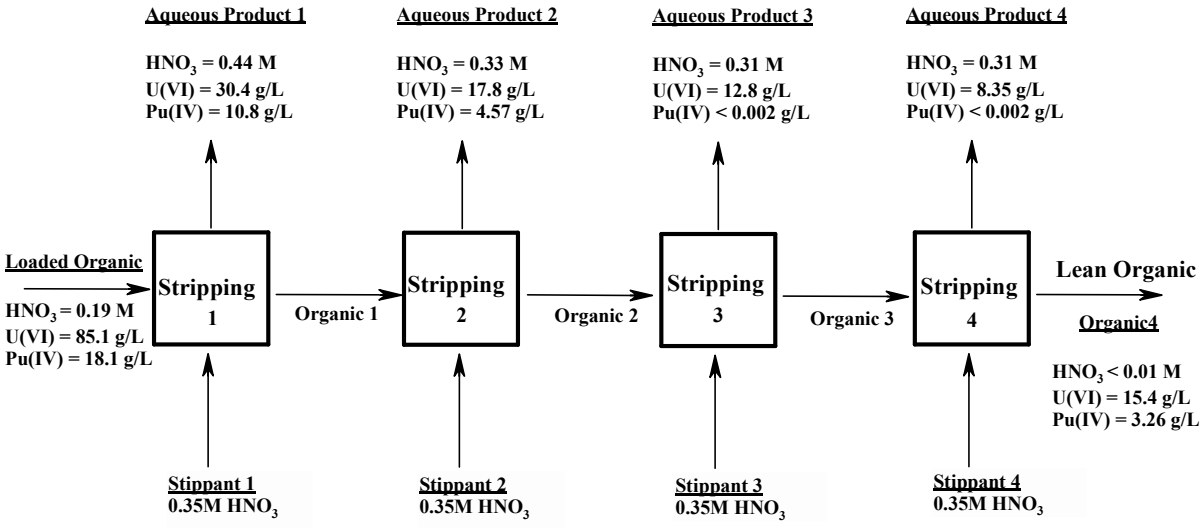

Fig. 3.8: Co-stripping of U(VI) and Pu(IV) from loaded 1.1M TiAP/n-DD with 0.35M HNO_3 in cross-current mode at 303 K

Similar experiments were performed with 1.1M TBP/n-DD under identical conditions. The results indicated that the extraction and stripping behaviour of U(VI) and Pu(IV) were found to be comparable with both the extractant systems. However, the U(VI) concentration (Fig.3.9) in the raffinate was marginally higher for TBP system compared to TiAP system indicating that loss of heavy metal ions into the raffinate stream is marginally lower with TiAP system. In the case of stripping, most of the Pu(IV) was stripped within two stages and

the concentrations of U(VI) and Pu(IV) in the organic phase (lean organic) was marginally lower with the TBP system compared to TiAP system (Fig.3.10).

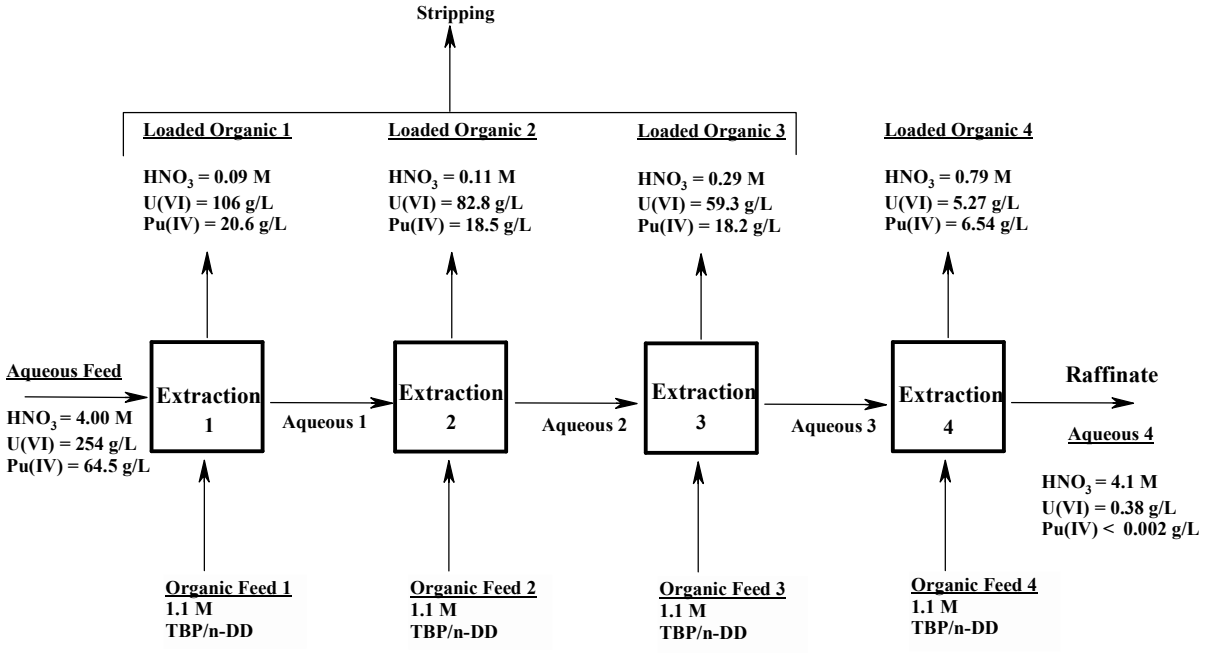

Fig. 3.9: Co-extraction of U(VI) and Pu(IV) from 4M HNO_3 by 1.1M TBP/n-DD in cross-current mode at 303 K

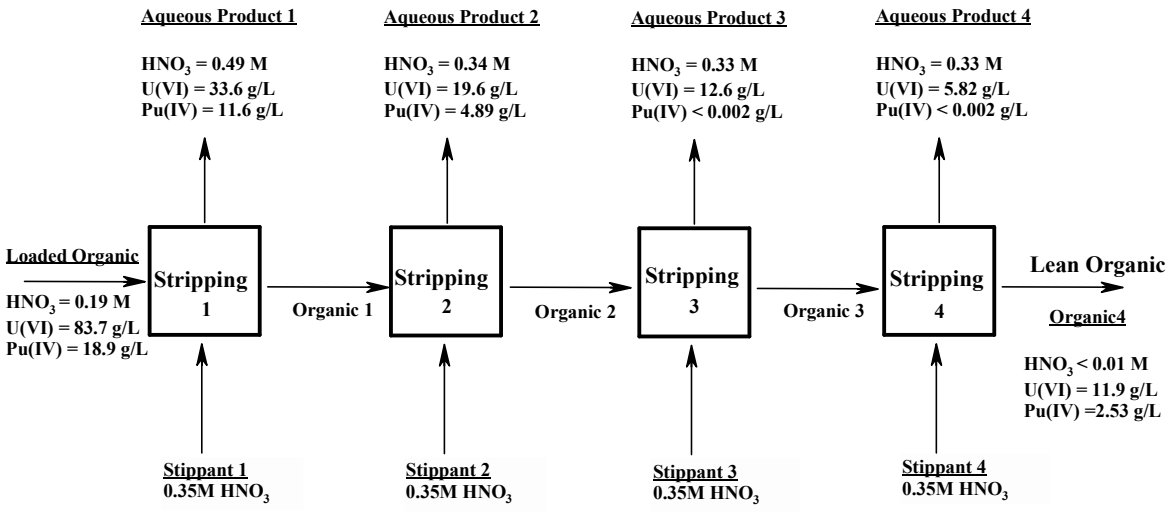

Fig. 3.10: Co-stripping of U(VI) and Pu(IV) from loaded 1.1M TBP/n-DD phase with 0.35 M HNO_3 in cross-current mode at 303 K

The co-extraction and co-stripping (%) of U(VI) and Pu(IV) in cross current mode were calculated from the flowsheet data for both 1.1M TiAP/n-DD and 1.1M TBP/n-DD systems (Table 3.3). Results indicated that the extraction of Pu(IV) was found to be 99.98 %

in both the systems, whereas the extraction of U(VI) was 99.94 % and 99.85 %, respectively for TiAP and TBP based solvents. The stripping of U(VI) and Pu(IV) was about 82 % with 1.1M TiAP/n-DD and in the case of 1.1M TBP/n-DD system, it was found to be ~ 86 %. These studies have established that additional stages are required for the complete stripping of U(VI) and Pu(IV). The stripping of U(VI) and Pu(IV) with TiAP is marginally lower compared to TBP and is attributed to higher *D* values of U(VI) and Pu(IV) with TiAP for a given concentration of nitric acid [151].

Table 3.3: Comparison of co-extraction and co-stripping of U(VI) and Pu(IV) by 1.1M TiAP/n-DD and 1.1M TBP/n-DD in cross current mode

Solvent	Extraction (%)		Stripping (%)	
	U(VI)	Pu(IV)	U(VI)	Pu(IV)
1.1M TiAP/n-DD	99.9	99.9	81.9	81.9
1.1M TBP/n-DD	99.8	99.9	85.8	86.6

3.3 Extraction behaviour of fission products with TiAP based solvent

3.3.1 Extraction of Zr(IV) and RuNO(III)

The extraction behaviour of Zr(IV) and RuNO(III) with 1.1M solutions of TiAP in n-DD from nitric acid (0.5–6M) media has been investigated. Results indicated that the $D_{Zr(IV)}$ increase with increase in concentration of nitric acid (Fig.3.11), whereas the $D_{RuNO(III)}$ initially showed an increase up to 1.5M HNO_3 and then decreases with the increase in concentration of nitric acid (Fig.3.12). The *D* values for the extraction of Zr(IV) and RuNO(III) with TiAP are marginally lower than that of TBP, indicating a possibility of achieving better decontamination factor with TiAP based solvent ($D_{Zr(IV)}$ at 6M HNO_3 is 1.27 and 1.71 with TiAP and TBP, respectively).

In general, for the extraction of a metal ion by a neutral extractant, initially the *D* increase and after passing through a maximum, it decreases. Unlike other elements, the $D_{Zr(IV)}$ increase continuously as a function of [HNO_3]. This could be attributed to the fact that $D_{Zr(IV)}$ depends only on the total nitrate ion concentration. On the other hand, the effect of

concentration of nitric acid on $D_{RuNO(III)}$ has two effects; (i) intially, ruthenium nitrosyl complex forms more extractable species such as tri and tetra nitrato species thereby increasing $D_{RuNO(III)}$; (ii) the formation of non-extractable ruthenium nitrosyl complexes or competition from nitric acid for free extractant could be possible reasons for decrease in $D_{RuNO(III)}$.

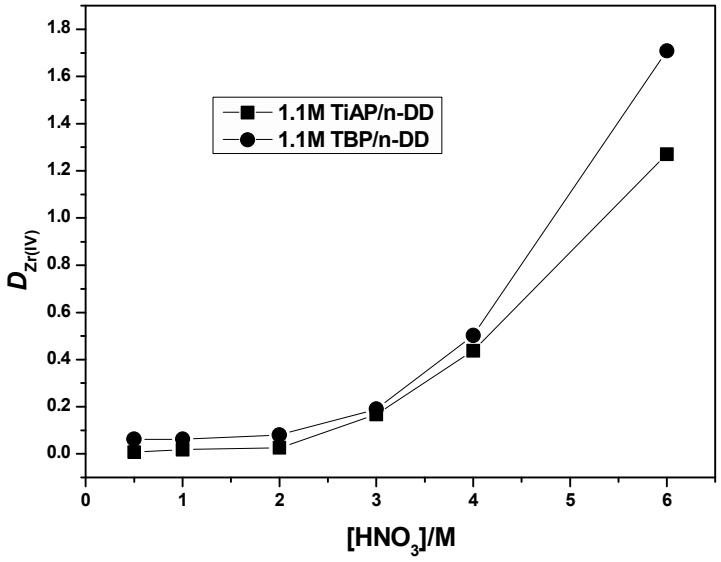

Fig.3.11: Variation of $D_{Zr(IV)}$ as a function of concentration of nitric acid

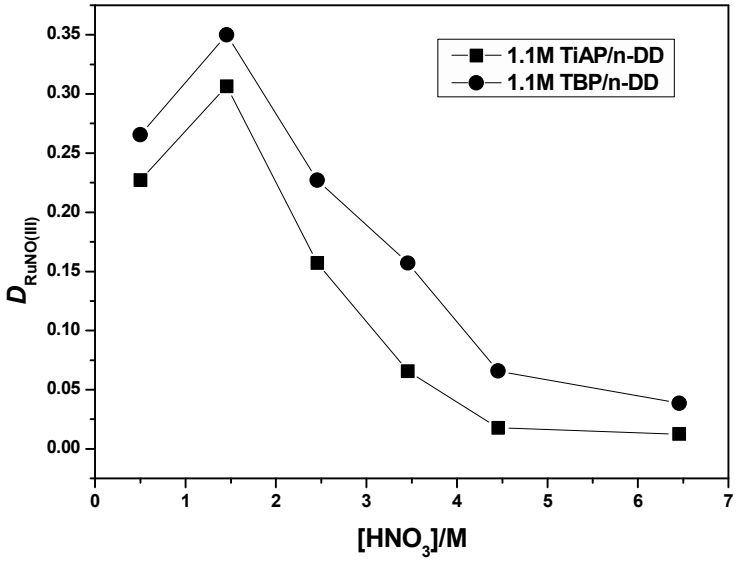

Fig.3.12: Variation of $D_{RuNO(III)}$ as a function of concentration of nitric acid

3.3.2 Extraction of TcO_4^-

The extraction behaviour of Tc (exists in the form of TcO_4^- in nitric acid media) by 1.1M TiAP/n-DD has been investigated as a function of nitric acid concentration (0.1-6M). Like ruthenium, the D_{Tc} first increases up to 0.5M HNO_3 and then decreases with [HNO_3] (Fig.3.13). The initial increase in D_{Tc} can be attributed to the formation and extraction of $HTcO_4$ as the extractable species with increase in concentration of nitric acid as represented in Eq.(3.8).

$$H^+ + TcO_4^- + 3TBP \leftrightarrow HTcO_4.3TBP \quad \text{..... (3.8)}$$

The competition from nitric acid for the free extractant could be responsible for the subsequent decrease in D_{Tc} beyond 0.5M HNO_3. Similar extraction behaviour was also observed for the extraction of TcO_4^- with TBP [64]. The D_{Tc} by TiAP are marginally lower than that of TBP over a wide range of acidity.

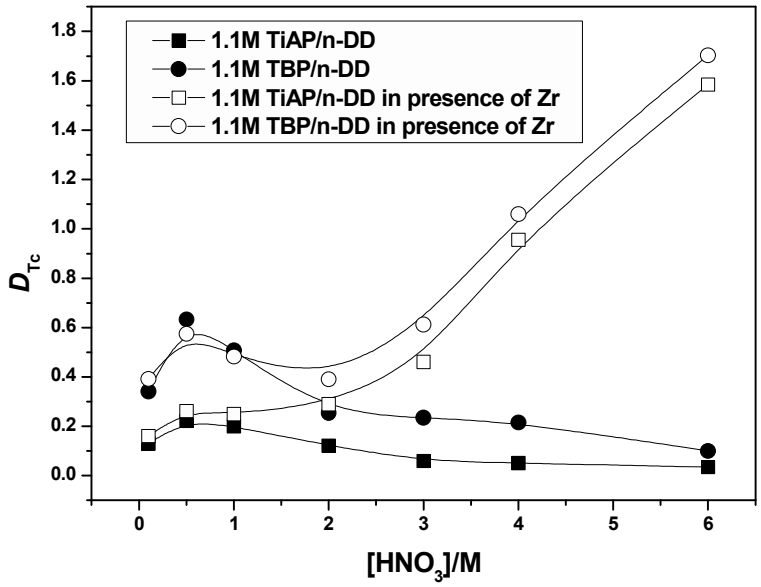

Fig.3.13: Variation of D_{Tc} as a function of concentration of nitric acid

Earlier studies carried out in our laboratory indicated that TiAP has higher *D* values for actinide elements (U(VI), Pu(IV) and Th(IV)) compared to TBP [151]. Similarly, the present study indicated that *D* values for troublesome fission products (Zr, Ru and Tc) with TiAP are marginally lower than that of TBP. An ideal extractant should have higher *D* values

for the metal ions (U, Pu) to be extracted over the fission products. In this context, TiAP meets these requirements, marginally better as compared to TBP.

3.3.3 Extraction behaviour of TcO_4^- in the presence of Zr(IV)

The extraction behaviour of TcO_4^- in the presence of Zr(IV) has been investigated with TiAP and compared with TBP under identical conditions. Results indicated that the extraction behaviour of TcO_4^- in the presence of Zr was found to be similar as in the case of pure TcO_4^- at lower concentration of nitric acids (0.1-1M). This may be due to the negligible extraction of Zr(IV) by trialkyl phosphates from aqueous solutions at lower concentration of nitric acid. However, the extraction of TcO_4^- increases with increase in concentration of nitric acid beyond 2M HNO_3 (Fig.3.13). The co-extraction of TcO_4^- with Zr(IV) by TBP explains the above-mentioned trends in the extraction. The extraction mechanism of TcO_4^- along with Zr(IV) is shown in Eq.(3.9).

$$Zr(IV) + 3NO_3^- + 2TBP + TcO_4^- \leftrightarrow Zr(NO_3)_3.(TcO_4).2TBP \quad \ldots\ldots\ldots \quad (3.9)$$

The extraction data (Fig.3.13) clearly indicated that even in the presence of Zr(IV), *D* values for the extraction of TcO_4^- by TiAP system are marginally lower than that observed with TBP system. Garraway et al. [65] also reported a similar extraction behaviour of TcO_4^- in the presence of Zr(IV) with a concentration of about 0.8 g/L with 1.1M TBP in odourless kerosene (OK) and the extracted complex contains only one TBP molecule.

3.3.4 Extraction behaviour of Nd(III), Ce(III), La(III) and Am(III)

Extraction behaviour of lanthanides [Nd(III), Ce(III) and La(III)] and Am(III) with 1.1M solution of TiAP in n-DD from nitric acid (0.5–6 M) media has been examined. Results indicated that the *D* values for the lanthanides and Am(III) increase marginally up to 3M HNO_3 and then decrease thereafter (Fig.3.14 and Fig.3.15). The *D* values for the lanthanides and Am(III) by TiAP is comparable to that of TBP throughout the acidity range. The DFs with respect to Ln(III) and Am(III) that can be obtained with the employment of TiAP/n-DD

as solvent would be comparable to the analogous TBP/n-DD system. Kulkarni et al. [183] also observed similar extraction behaviour for the lanthanides with TBP/n-DD system.

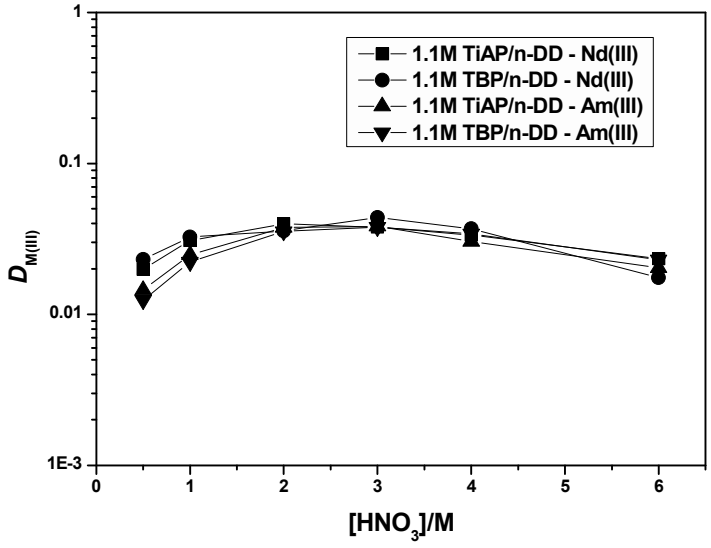

Fig.3.14: Variation of $D_{M(III)}$ as a function of concentration of nitric acid

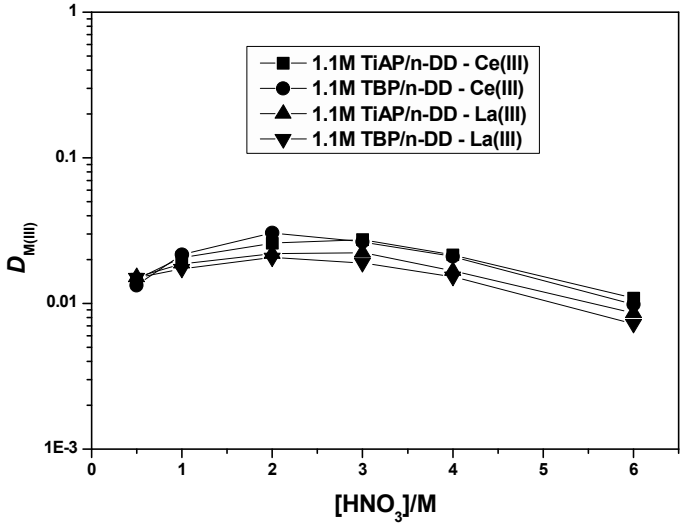

Fig.3.15: Variation of $D_{M(III)}$ as a function of concentration of nitric acid

3.3.5 Effect of radiolytic degradation on the extraction of fission products (Zr, Ru, Tc, Lns) and Am(III)

The effects of gamma irradiation on the extraction behaviour of fission products such as Zr(IV), RuNO(III), TcO_4^-, Nd(III) and Am(III) with 1.1M TiAP/n-DD and 1.1M TBP/n-DD systems have been studied. The 1.1M solutions of TiAP in n-DD pre-equilibrated with

4M HNO_3 were irradiated to different dose levels and *D* values were measured. The $D_{Zr(IV)}$ for the TiAP and TBP solvents irradiated up to 10M Rad were found to be 5.17 and 4.78, respectively. It was observed that the *D* values are significantly higher compared to the unirradiated samples. This is attributed to the fact that the degradation products such as dialkyl and monoalkyl phosphates have higher affinity for Zr(IV). The *D* values could not be measured for samples irradiated up to 50 and 100M Rad due to the accumulation of interfacial deposits at the aqueous-organic interface during the extraction of Zr(IV) from 4M HNO_3. However, interfacial deposits were not observed with the samples irradiated to 10M Rad. The complexes of Zr(IV) and dialkyl phosphates are usually anticipated as one of the causes for the formation of interfacial deposit.

Gamma irradiation has negligible effect on the extraction of RuNO(III), TcO_4^-, Nd(III) and Am(III) with TiAP and TBP based solvents. The similar extraction behaviour was reported by Pai et al. [57] with TBP based solvents; the extraction of Zr(IV) increases sharply with absorbed dose, whereas in the case of ruthenium, the extraction remains unaffected by the absorbed dose.

3.3.6 Effect of diluent chain length on the extraction of FPs

Heavy Normal Paraffin (HNP) is being used as a diluent in some of the reprocessing plants in India. It mainly consists of n-decane, n-undecane, n-DD, n-tridecane and n-tetradecane. In order to investigate the effect of diluent chain length on the extraction of fission products, 1.1M solutions of TiAP in n-tetradecane (n-TD) was prepared. The extraction behaviour of Zr(IV), RuNO(III) and Lns with 1.1M solutions of TiAP in *n*-tetradecane from nitric acid (0.5–6 M) media has been investigated. These results indicate that the extraction behaviour for the above FPs by 1.1M TiAP/*n*-TD was found to be similar to that of 1.1M TiAP/n-DD.

Solutions of 1.1M TiAP in n-DD as well as 1.1M TiAP in n-tetradecane pre-equilibrated with 4M HNO_3, were irradiated to different dose levels to understand the effect

of diluent degradation products on the extraction of Zr(IV). The $D_{Zr(IV)}$ values with TiAP were found to be comparable in both the diluents (10M Rad). Results indicated the extraction of Zr(IV) remains unaffected by diluent degradation products. For example, the *D* values for the extraction of Zr(IV) by TiAP/n-DD and TiAP/*n*-TD were found to be 5.17 and 4.97, respectively (Table 3.4). For comparison, similar experiments were also performed with 1.1M TBP in both n-DD and n-TD.

Table 3.4: $D_{Zr(IV)}$ values for 1.1M TiAP and 1.1M TBP in n-DD and n-TD

Sample	$D_{Zr(IV)}$			
	Unirradiated	10MRad (without washing)	10 M Rad (with washing)	50 M Rad (with washing)
1.1M TBP/n-DD	0.50	4.19	0.56	1.61
1.1M TiAP/n-DD	0.44	6.83	0.45	2.60
1.1M TBP/n-TD	0.55	4.58	0.53	1.69
1.1M TiAP/n-TD	0.46	4.97	0.59	2.56

3.3.7 Effect of alkali wash on the extraction of Zr(IV)

Samples irradiated to different dose levels were washed with 5M NaOH followed by several times with water to remove the degradation products. Subsequently, the samples were pre-equilibrated with 4M HNO_3 and $D_{Zr(IV)}$ was measured at 303K. Results indicated the $D_{Zr(IV)}$ for irradiated samples (10M Rad) followed by alkali and water wash were comparable to that of unnirradiated samples. It can be concluded that solvents irradiated up to 10M Rad can be recycled by one alkali wash, whereas in the case of samples irradiated up to 50M Rad followed by alkali wash, the $D_{Zr(IV)}$ values were found to be marginally higher compared to unirradiated samples, indicating that one alkali wash is not adequate to recycle the solvent. For example, the $D_{Zr(IV)}$ values measured for 1.1M TiAP/n-DD were found to be 0.45 and 2.6, respectively, for samples irradiated up to 10 and 50M Rad followed by alkali wash. These results are presented in Table 3.4. The $D_{Zr(IV)}$ data with TiAP were found to be marginally higher compared to TBP in both the diluents. The reddish brown interfacial deposit has been observed at the aqueous-organic interphase during the solvent wash of 1.1M solutions of

TiAP in n-DD and n-TD (irradiated up to 100M Rad) with 5M NaOH; hence the *D* values have not been reported for 100 M Rad samples after alkali wash. However, such deposits have not been observed during the alkali wash of samples irradiated up to 10 and 50M Rad. Similar kind of results have also been observed in the case of TBP system.

3.3.8 Formation of interfacial deposits during the alkaline solvent wash

In order to examine the species responsible for the formation of interfacial deposit during the solvent wash, different combinations of both fresh and gamma irradiated (100M Rad) organic phase components (extractant and diluents) were thoroughly mixed with equal volume of 5M NaOH for an hour; results indicate that interfacial deposits were observed only in the case of 1.1M solution of TiAP in n-DD pre-equilibrated with 4M HNO_3 and irradiated up to 100M Rad (Table 3.5). Similar results have been observed with 1.1M TiAP/n-TD system. Interfacial deposits were also investigated with 1.1M TBP in n-DD and n-TD and the results were found to be comparable with TiAP based system. Interfacial deposits were not observed in most of the cases such as fresh and gamma irradiated extractants, diluents and their different combinations. Thus the interfacial deposits with extractant/diluent were observed only when the same is irradiated in the presence of nitric acid, above 100MRad. Smith et al. [142] reported the formation of interfacial deposits during the alkaline solvent wash of chemically degraded solvents with sodium carbonate. It was noticed that interfacial deposits have been observed with chemically degraded diluents, odourless kerosene or n-DD and combination of TBP/n-DD or TBP/OK. Smith et al. [142] have identified the possible potential crud forming species and proposed various mechanisms for the formation of interfacial deposits during the alkaline solvent wash.

3.3.9 Effect of uranium loading in the organic phase on the extraction of Zr(IV)

The spent fuel dissolver solutions mainly contain uranium and plutonium with smaller quantities of fission products. Most of the studies to understand the effect of uranium loading in the extraction of Zr(IV) were carried out with unirradiated solvents. In general, the solvent

(30% TBP/diluent) undergoes degradation mainly during the first extraction cycle of PUREX process. Therefore it is of great significance to understand the loading effect of uranium on the extraction behaviour of fission products with degraded and unirradiated solvents.

The *D* values for Zr(IV) by 1.1M TiAP/n-DD and 1.1M TBP/n-DD decrease steadily with uranium loading in the organic phase for both the solvents (Fig.3.16 and Fig.3.17). This is due to decrease in the free extractant (TiAP or TBP) concentration in the organic phase with increase in the uranium loading. It is important to note that the extraction of Zr(IV) with TiAP is marginally lower compared to TBP in the case of unirradiated samples, indicating that TiAP based solvent can yield marginally better decontamination factors over TBP. For example at 70% uranium loading, the $D_{Zr(IV)}$ by TiAP (0.066) is lower than that of TBP (0.073), whereas in case of irradiated (10M Rad) samples, the reverse trend has been observed, the decontamination factors achievable with TiAP based system can be marginally lower than that of TBP system (Fig.3.17).

Table 3.5: Formation of interfacial deposits during alkaline solvent wash of gamma irradiated samples (100M Rad)

Organic phase	Observation
TiAP*	No interfacial deposit
TiAP*+pre-equilibrated with 4M HNO_3	No interfacial deposit (only brown coloration was observed in both the phases)
DD*	No interfacial deposit
TiAP*/n-DD	No interfacial deposit
1.1M TiAP*/n-DD*	No interfacial deposit
(1.1M TiAP/n-DD)*	No interfacial deposit
(1.1M TiAP/n-DD+ pre-equilibrated with 4M HNO_3)*	Interfacial deposit

* Irradiation of samples up to 100M Rad.

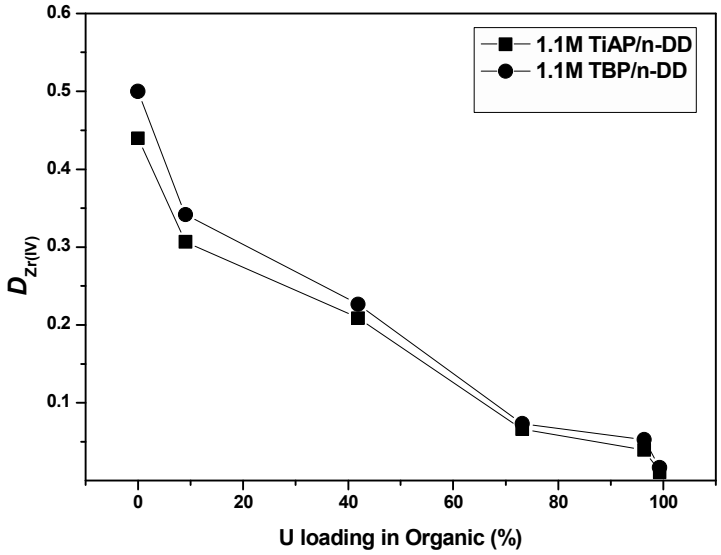

Fig.3.16: $D_{Zr(IV)}$ as a function of uranium loading [HNO_3] = 4M

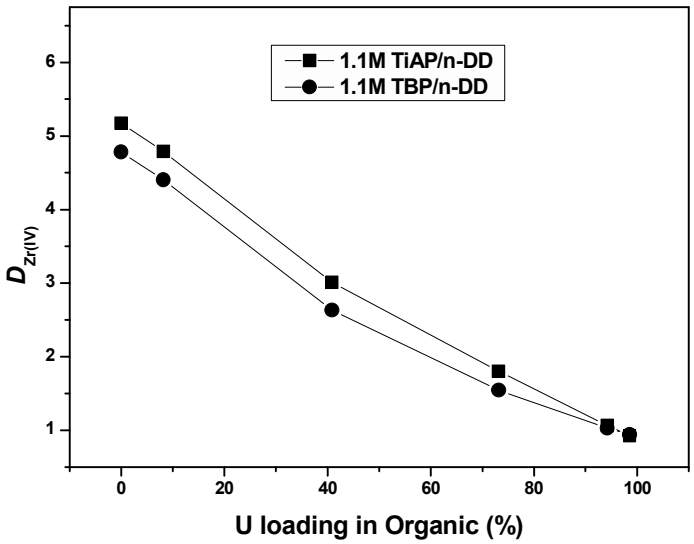

Fig.3.17: $D_{Zr(IV)}$ as a function of uranium loading [HNO_3] = 4M for irradiated samples (10 M Rad)

3.4 Conclusions

The present study established that the TiAP based solvent does not form third phase during extraction of Pu(IV) from aqueous solutions over a wide concentration range of nitric acid. Co-extraction studies of U(VI) and Pu(IV) with TiAP demonstrated that it is possible to achieve maximum metal ion loading in the organic phase without phase splitting. Though TBP based solvent does not form third phase during the co-extraction of U(VI) and Pu(IV)

under the present feed conditions, it forms third phase in the presence of higher plutonium feed solution. The studies on the distribution ratio of fission product elements revealed that the decontamination factors achieved for uranium and plutonium with respect to the fission product elements with TiAP are more or less similar to TBP. Investigations also revealed an enhancement in the extraction of Zr(IV) in the presence of degradation products of both TiAP as well TBP. These studies will be useful in designing flowsheet for the processing of dissolver solution of a fast reactor spent fuel.

Chapter 4

MIXER-SETTLER RUNS WITH TiAP BASED SOLVENT

4

4.1 Introduction

The flowsheet adopted for processing the fast reactor fuels could be different from thermal reactor fuels. For example, the spent fuel discharged from the Fast Breeder Test Reactor (FBTR) is being processed in the Compact Reprocessing of Advanced fuels in Lead mini cells (CORAL) facility by employing a modified PUREX process with 30% TBP in n-dodecane as the solvent for the recovery of uranium and plutonium from fission products. After extraction, heavy metals are stripped from the loaded organic phase using 0.01M and 4M HNO_3 as dual strippants. Natarajan et al. [25] have reported that third phase is likely to form under certain conditions in fast reactor fuel reprocessing. Therefore, it is beneficial to explore the feasibility of using extractant, with lesser third phase formation tendency for fast reactor fuel reprocessing.

Chuanbo et al. [184] studied the possibility of co-stripping of U(VI) and Pu(IV) based on a simplified PUREX process with 30%TBP/kerosene solution containing U(VI), Pu(IV) and HNO_3. Nakahara et al. [185] developed a process flowsheet for Pu(IV) partitioning, based on acid split method without reductant. Co-processing of U(VI) and Pu(IV) enhances resistance to nuclear proliferation, avoiding Pu(IV) polymerization and third phase formation. Similar studies were not carried out with TiAP based solvent, which doesn't form third phase during the co-extraction of U(VI) and Pu(IV) as mentioned in the chapter 3.

This chapter deals with the feasibility studies of using TiAP as an alternate extractant to TBP for fast reactor fuel reprocessing in a continuous counter-current liquid-liquid extraction using a mixer-settler facility. In this context, mixer-settler facility was set-up for flowsheet development studies with radioactive materials. Continuous counter-current solvent extraction runs with 1.1M TiAP/HNP have been carried out for the extraction and stripping of U(VI) under high metal loading conditions. In order to investigate the decontamination factors

achievable with TiAP system, the solvent used in an earlier runs has been regenerated and employed to perform mixer-settler runs for the demonstration of bulk separation of U(VI) and Pu(IV) from Ln(III) and Am(III). Stage profile data generated for the above separation studies are reported in this Chapter. Overall and stage-wise mass balance data for the above runs are also discussed.

4.2 Counter-current extraction and stripping of 1.1M TiAP/HNP–U(VI)-HNO_3 system

Mixer-settler runs were carried out with U(VI) solution containing about 241 g/L to understand the extraction and stripping behavior with TiAP in nitric acid media for a continuous solvent extraction process under high solvent loading conditions. Counter-current extraction of U(VI) was carried out by passing uranyl nitrate solution with a concentration of about 241 g/L in 4.3M HNO_3 as the aqueous feed from the 7^{th} stage, 3.3M HNO_3 solution as the scrub from the 1^{st} stage and 1.1M TiAP/HNP solution as the solvent from the 16^{th} stage with flow rates of 2.8 mL/min, 1.4 mL/min and 7.5 mL/min, respectively (Fig. 4.1). Though fission product elements were not present in the feed solution, organic phase was scrubbed to generate an extraction profile for 1.1M TiAP/HNP-U(VI)-HNO_3 system under extraction-scrub conditions.

These studies indicate that concentration of nitric acid in the aqueous phase of the scrub section (1 to 4 stages) is about 3.2 M and after 4^{th} stage, it increases and after passing through a maximum of ~ 5.4 M at the 10^{th} stage, it decreases (Fig. 4.2). Similar trend was also observed in the case of HNO_3 loading in organic phase in extraction section and it was found to be ~ 1M. These HNO_3 loadings with negligible U(VI) in the organic phase also match with the batch extraction data reported earlier [150].

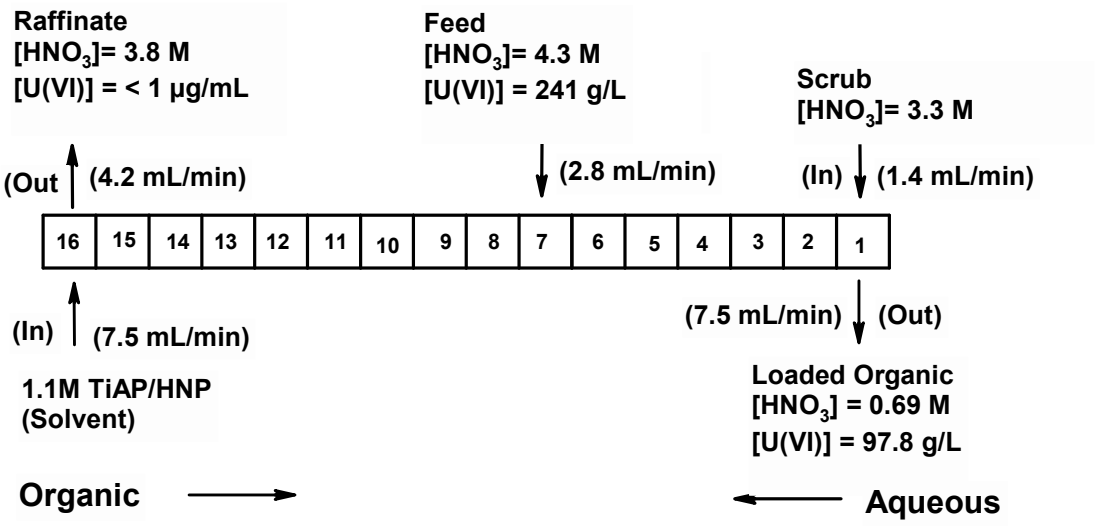

Fig. 4.1: Flowsheet for the extraction run-U(VI)-HNO_3-1.1M TiAP/HNP system

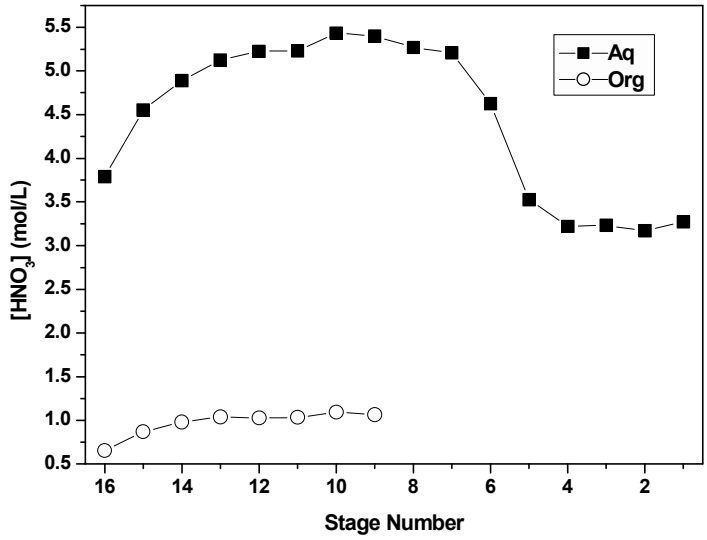

Fig. 4.2: Organic and aqueous stage profiles for extraction of HNO_3 in the extraction run-U(VI)-HNO_3-1.1M TiAP/HNP system

The profile for U(VI) extraction (Fig. 4.3) indicates that major portion of it has been extracted into the organic phase in the 7th stage itself (where the feed enters the extractor bank). The study indicated that concentrations of U(VI) and HNO_3 in the loaded organic are about 97 g/L and 0.7M respectively. The profile for the uranium extraction also indicated that its concentration decreased towards the 16th stage and found to be below detectable limit (< 1 µg/mL) in the 16th stage.

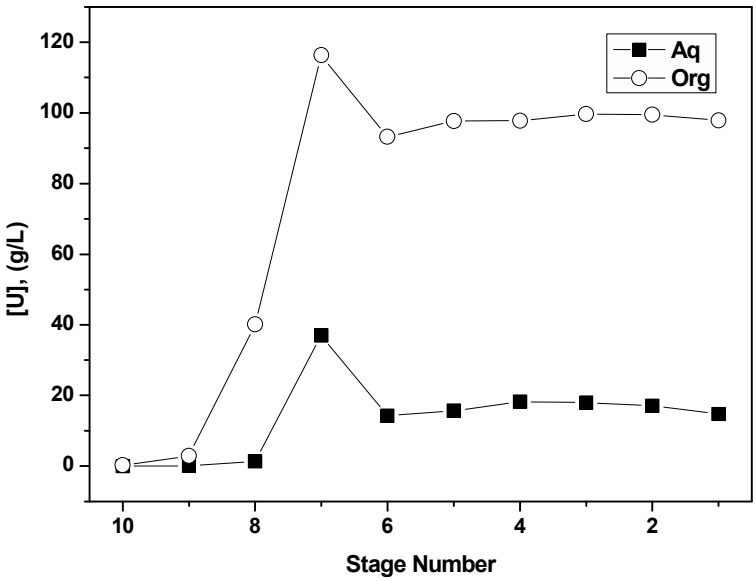

Fig. 4.3: Organic and aqueous stage profiles for the extraction of U(VI) in the extraction run-U(VI)-HNO_3-1.1M TiAP/HNP system

Subsequent stripping of U(VI) from the loaded organic phase was carried out by passing loaded organic from 16th to 1st stage and 0.01M HNO_3 from 1st stage to 16th stage with a flow rate of 6 mL/min for both streams in a counter-current mode (Fig. 4.4). The study (Figs. 4.5 and 4.6) indicated that both concentrations of HNO_3 and uranium decreased towards the 1st stage, where the strippant enters the mixer-settler bank. The decreasing trend of HNO_3 and uranium concentrations towards 1st stage is an indication that both are getting stripped from the loaded organic phase. However, uranium concentration in the lean organic was found to be significant (~8.8 g/L). The stripping of uranium was found to be about 89.7%, indicating that more number of stages are required for its complete stripping.

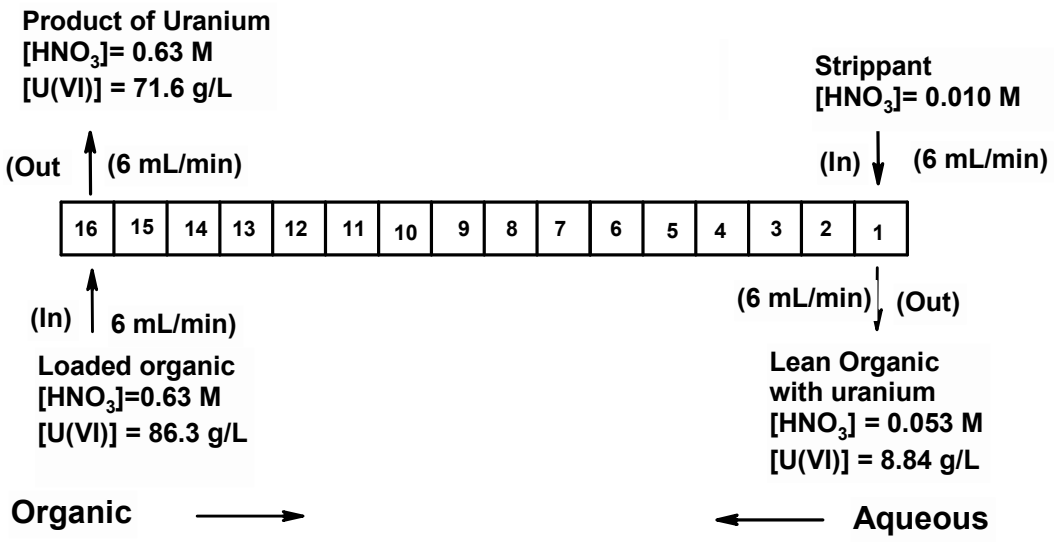

Fig. 4.4: Flowsheet for the strip run-U(VI)-HNO_3-1.1M TiAP/HNP system

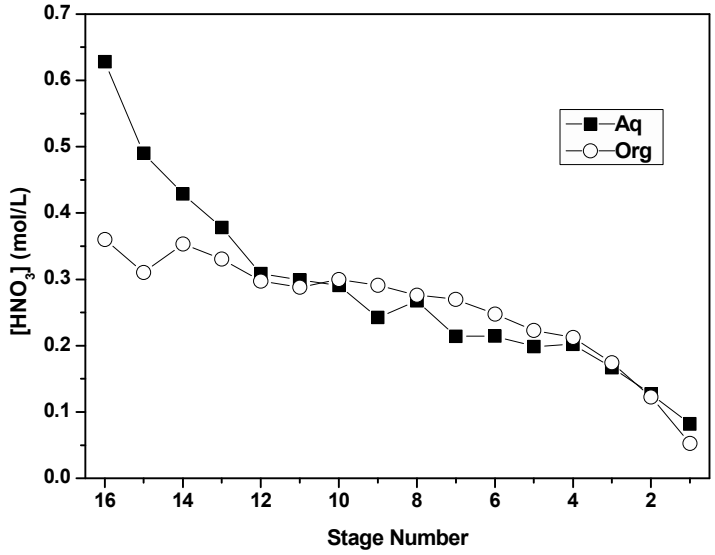

Fig. 4.5: Organic and aqueous stage profiles for HNO_3 in the strip run for U(VI)-HNO_3-1.1M TiAP/HNP system

4.3 Separation of U(VI) and Pu(IV) from Am(III) and trivalent lanthanides with TiAP as the extractant using an ejector mixer-settler

Gonda et al. [186] have reported that third phase formation was observed during mixer-settler runs for the extraction of heavy metal ions by 1.1M TBP/n-DD from a feed solution containing ~ 15.5 g/L Pu(IV) and ~ 0.33 g/L U(VI) in 3.2M HNO_3. The mixer-settler used in their studies was made of Plexiglas and is completely transparent with a mixer capacity of 5.6 mL and a settler capacity of 16.7 mL. They have reported that after 2 hr of operation, the plutonium began to accumulate in the scrub section and both the phases became

increasingly dark brown and plutonium third phase formation was observed in the settling chambers, 17th to 19th stages. Third phase formation with Pu(IV) is a major concern for fast reactor fuel reprocessing because of high plutonium content [25]. It was reported that the dissolver solution of a MOX fuel (90 Gwd/T, 20% initial Pu) from a FBR contains about 222 g/L U(VI) and 37 g/L Pu(IV) in 3-4M HNO_3 [187]. Under these conditions, TBP is likely to form third phase with Pu(IV) under certain experimental conditions.

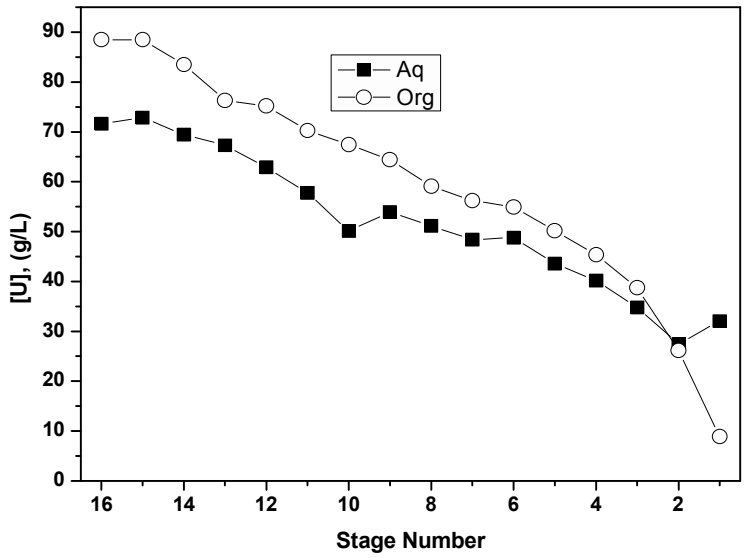

Fig. 4.6: Organic and aqueous stage profiles for U(VI) in the strip run for U(VI)-HNO_3-1.1 M TiAP/HNP system

Separation of U(VI) and Pu(IV) from trivalent lanthanides and Am(III) by 1.1M TiAP/HNP comprises of three runs (Fig. 4.7). The first run involving 10 stages for the extraction and 6 stages for the scrubbing was performed for extraction of U(VI) and Pu(IV) from an aqueous feed solution. Second run involves stripping of Pu(IV) with a fraction of U(VI) by feeding loaded organic at the 16th stage, 4M HNO_3 at the 7th stage and 0.01M HNO_3 at the 1st stage with flow rates of 6.3 mL/min, 0.55 mL/min and 6 mL/min, respectively. The purpose of using dual strip solutions is to maintain minimum acidity (~ 0.35M) in the stages 7 to 16 to avoid the plutonium hydrolysis. In the second strip run (third run), remaining fraction of U(VI) was stripped by passing the outlet organic stream from the first strip run from 16th to

1st stage and 0.01M HNO_3 from 1st to 16th stage with flow rates of 6.3 mL/min and 6.0 mL/min, respectively in a counter-current manner.

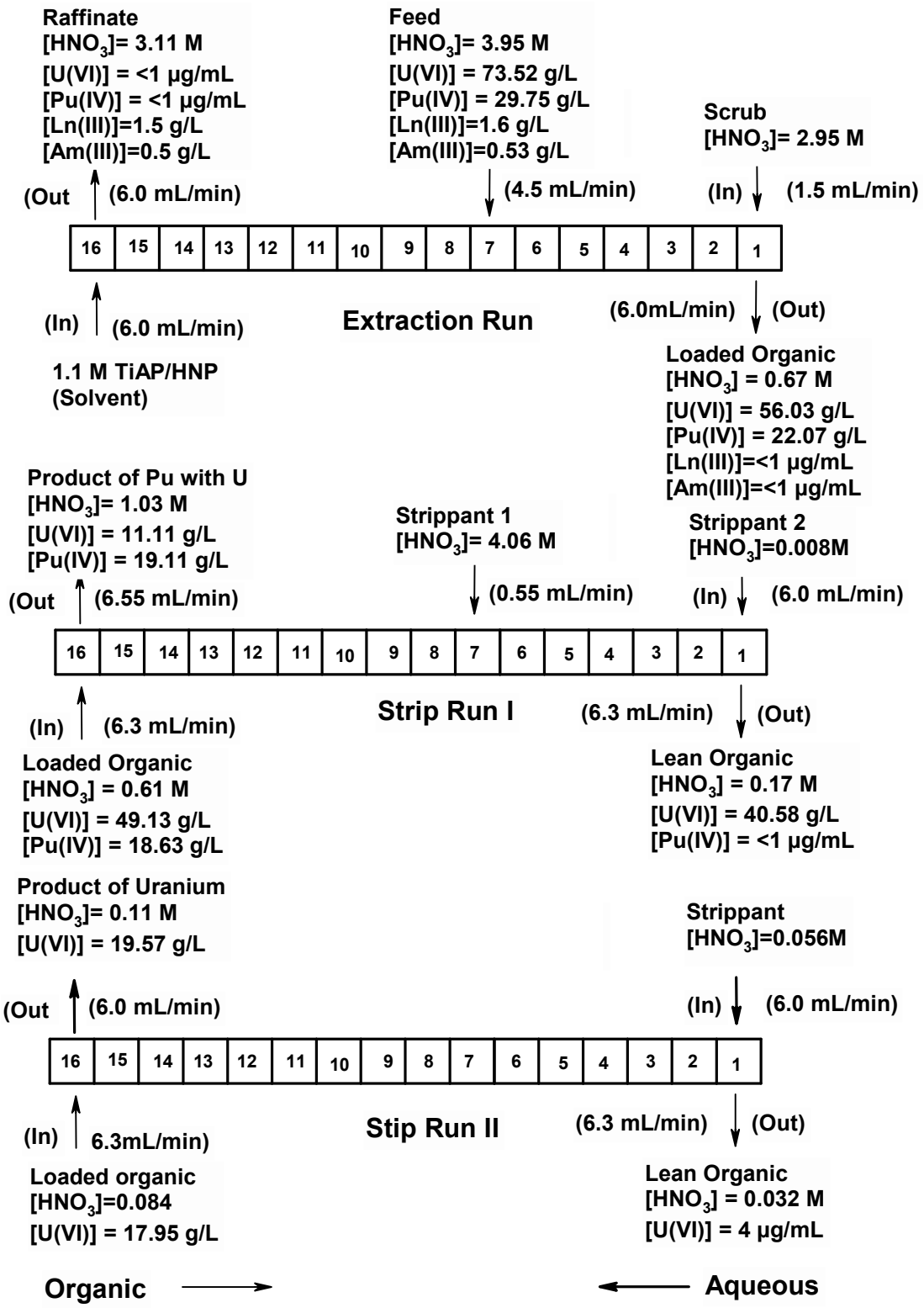

Fig. 4.7: Flowsheet for separation of U(VI) and Pu(IV) from Am(III) and Ln(III) by 1.1M TiAP/HNP (Outlet samples represent the samples collected after attainment of steady state; Inlet loaded organic streams in the strip runs are outlet organic solutions collected from beginning to end of the respective previous run)

Present studies indicated that concentration of nitric acid in the aqueous phase at the 1st stage in the scrub section was about 3.2 M and concentration of nitric acid was increased from stage 1 to 6 (Fig. 4.8.). When the loaded organic phase which in equilibrium with an aqueous phase with higher concentration of nitric acid leaves the 7th stage and enters the scrub section at the 6th stage, stripping of the HNO_3 from the loaded organic phase can increase the aqueous phase acidity in the scrub section, stages away from the scrub feeding point. In the extraction section, concentration of nitric acid in the aqueous phase was about 4.5 M between the 7th and 13th stages. However, there is a steep decrease in concentration of nitric acid beyond 13th stage and its concentration in raffinate solution leaving the 16th stage was about 3.1M. Further a similar trend in variation of nitric acid in organic phase with stage number has been observed.

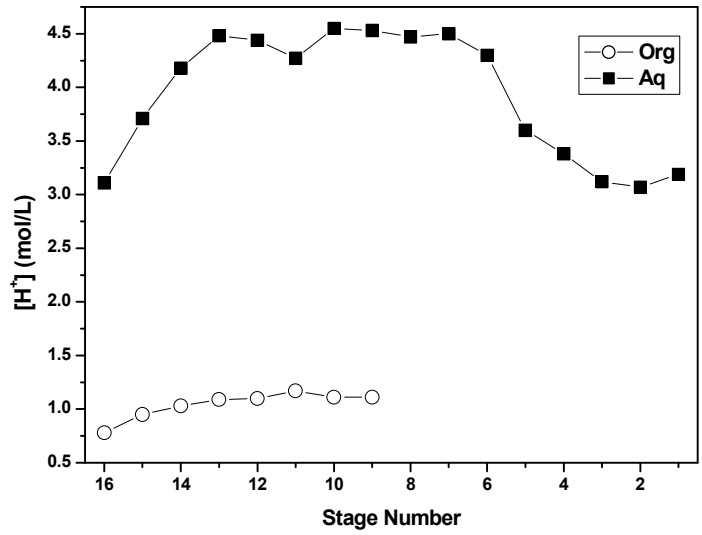

Fig. 4.8: Organic and aqueous stage profiles for the extraction of HNO_3 in the extraction run - U(VI)–Pu(IV)–Lns(III)–Am(III)–HNO_3–1.1 M TiAP/HNP system

The data indicate that only 3 to 4 stages are required for the extraction of U(VI) and Pu(IV) (Figs.4.9 and 4.10). Also, it can be seen that in the scrub section, there is no significant difference in heavy metal loadings between the stages. Analysis indicated that concentrations of U(VI), Pu(IV) and HNO_3 in the loaded organic phase are about 56 g/L, 22 g/L and 0.67 M, respectively with negligible amount (< 1 µg/mL) of lanthanides and

Am(III). The profiles also indicate that concentrations of heavy metal decrease towards the 16th stage where the raffinate comprising of lanthanides and Am(III) in nitric acid solution (3.1M HNO_3) leaves the extractor bank and goes below detectable limit in the 16th stage.

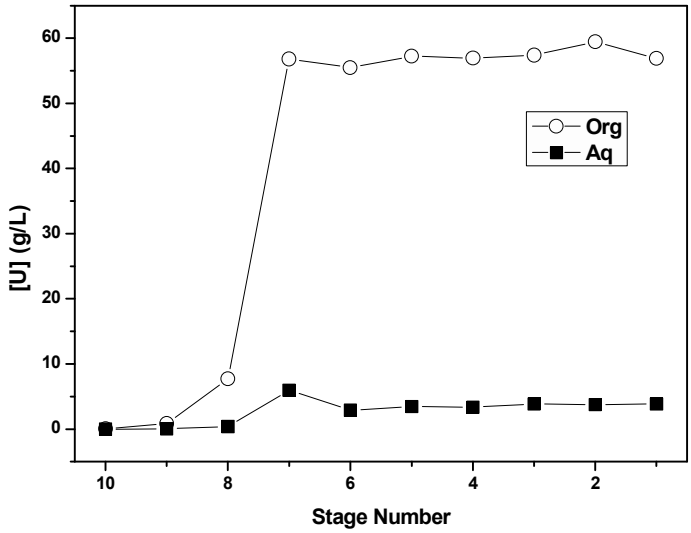

Fig. 4.9: Organic and aqueous stage profiles for the extraction of U(VI) in the extraction run - U(VI)–Pu(IV)–Lns(III)–Am(III)–HNO_3–1.1 M TiAP/HNP system

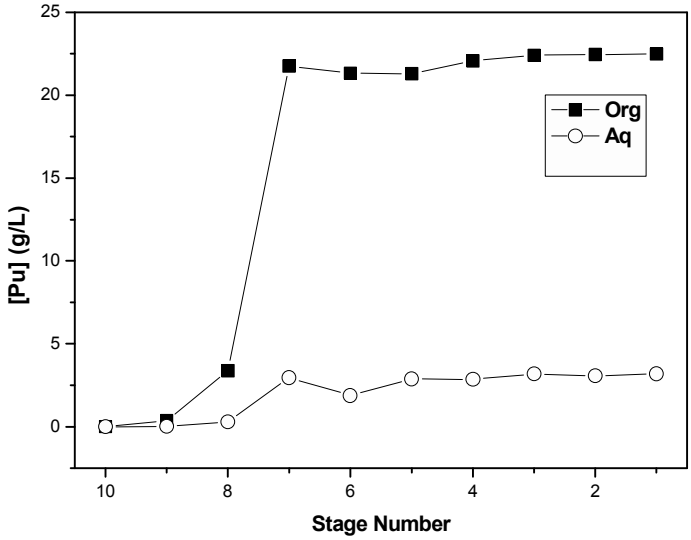

Fig. 4.10: Organic and aqueous stage profiles for the extraction of Pu(IV) in the extraction run - U(VI)–Pu(IV)–Lns(III)–Am(III)–HNO_3–1.1 M TiAP/HNP system

The stage profiles for Ln(III) and Am(III) in the aqueous phase are shown in Fig.4.11. Results indicate that concentration of Ln(III) and Am(III) in the aqueous phase at various

stages of the extraction section is comparable. Analysis of the stage samples of scrub section indicates that Ln(III) and Am(III) were present in the 6th stage aqueous phase and it was found to be below detection limit in other stages of scrub section. The loaded organic was also analysed for Ln(III) and Am(III) and the concentration was found to be below detection limit. These results indicate that Ln(III) and Am(III) are not extracted by TiAP.

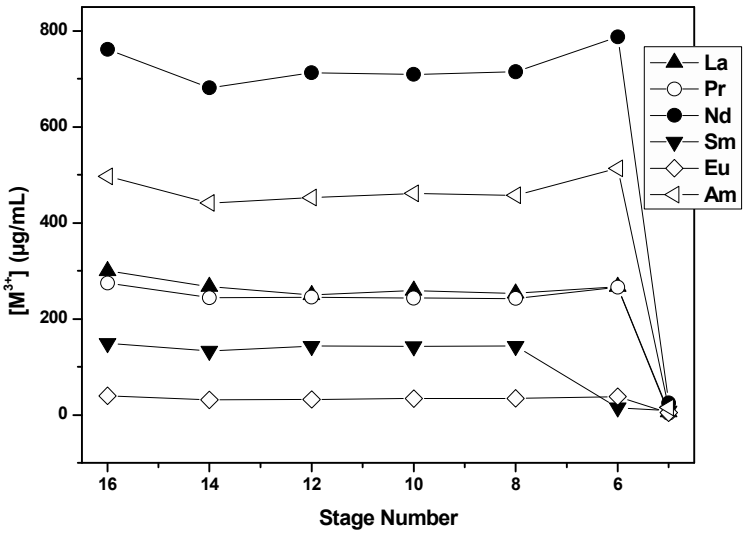

Fig. 4.11: Stage profiles for Lns and Am in aqueous phase in the extraction run

The stage profile data for nitric acid, U(VI) and Pu(IV) in the strip run – I are shown in Fig. 4.12, Fig. 4.13 and Fig. 4.14, respectively. The concentration of nitric acid in the aqueous phase decreases from 16th stage to 14th stage and almost remains constant from 13th to 7th stage, then it starts decreasing from 6th to 1st stage. A similar trend is observed for the nitric acid in the organic phase. It is seen from Figs.4.13 and 4.14 that loaded organic with ~ 49.1 g/L U(VI) and ~ 18.6 g/L Pu(IV) enters the 16th stage and leaves the 1st stage with a concentration of ~ 40.6 g/L U(VI) and < 1 µg/mL Pu(IV). This illustrates that complete stripping of Pu(IV) along with a small fraction of U(VI) from the loaded organic phase has taken place.

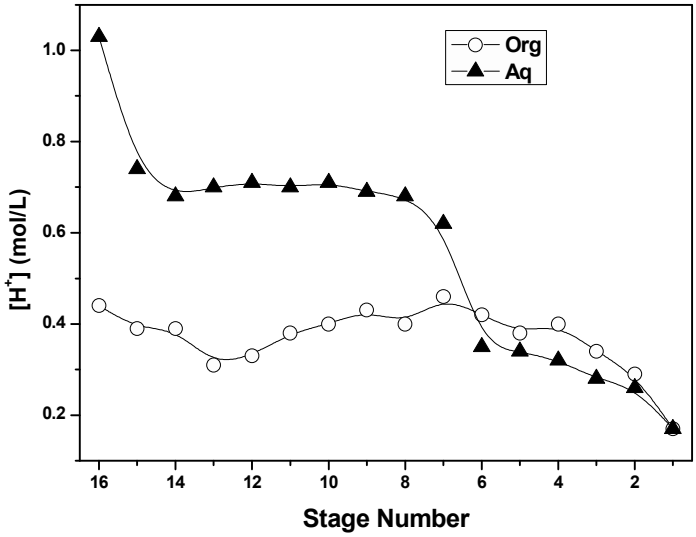

Fig. 4.12: Organic and aqueous stage profiles for HNO_3 in strip run I

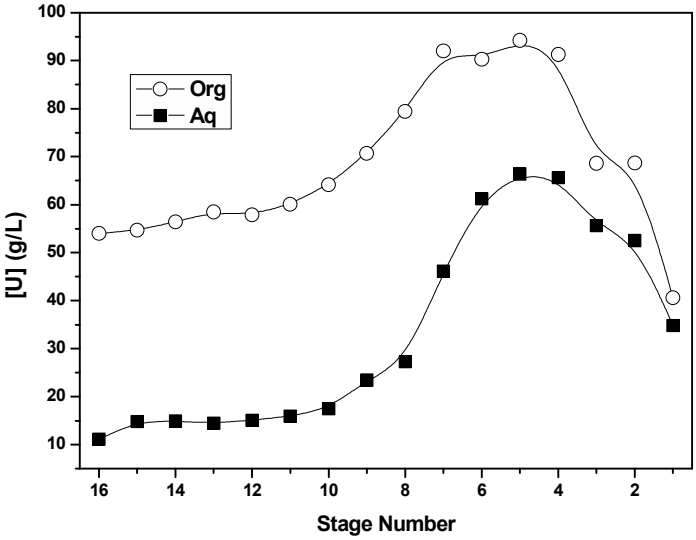

Fig.4.13: Organic and aqueous stage profiles for U(VI) in strip run I

The stage profiles for U(VI) and Pu(IV) indicate that Pu(IV) preferentially gets stripped from the organic phase in the section from 16th stage to 6th stage, whereas the stripping of U(VI) starts from 6th stage where the Pu(IV) concentration is very small. Earlier studies on the batch extraction of U(VI) and Pu(IV) by TiAP from nitric acid media have revealed that *D* values for the extraction of U(VI) by TiAP under similar conditions are higher than that of Pu(IV) between 0.5M – 4M HNO_3 [151]. Similar trend can be expected for the extractions from very dilute solutions of nitric acid.

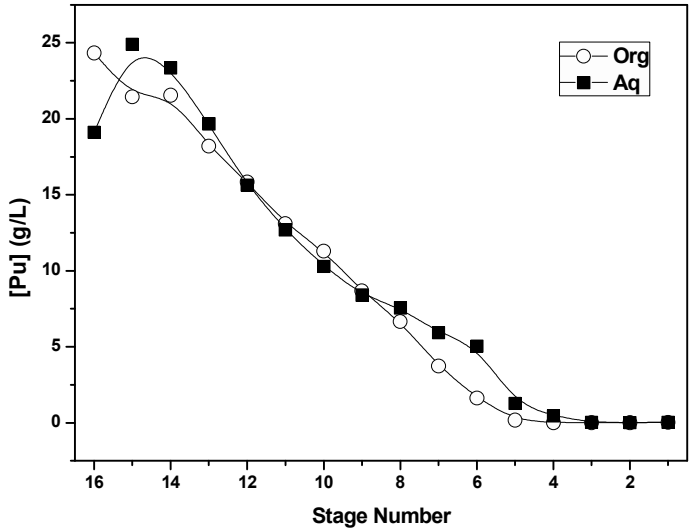

Fig.4.14: Organic and aqueous stage profiles for Pu(IV) in strip run I

The stage profile data for U(VI) is shown in Fig. 4.15. It reveals that the fraction of U(VI) retained in the organic outlet stream of the Strip Run – I was stripped using 0.06 M HNO_3 as the strippant in Strip Run – II, and the loss of U(VI) in the lean organic stream was found to negligible (~ 4 µg/mL). Results indicate that the major fraction of U(VI) was stripped within 6 stages from 16 to 10 and in the remaining stages, it was found to be very less; the recovery of uranium was about 99.97%.

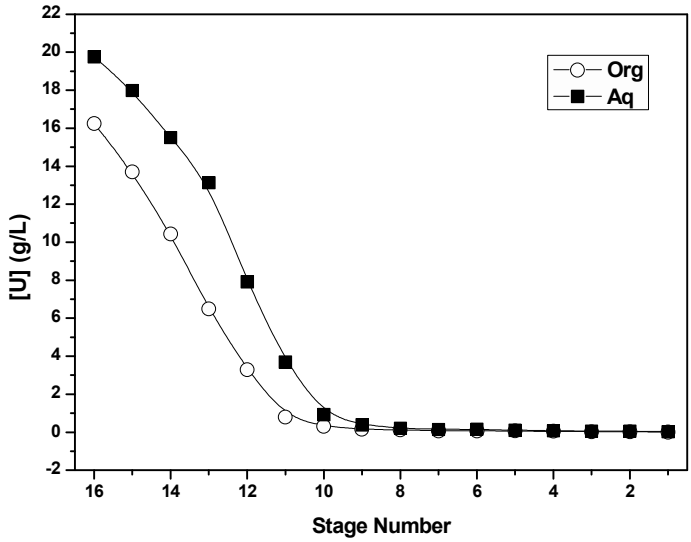

Fig. 4.15: Organic and aqueous stage profiles for U(VI) in strip run II

Aqueous products of strip run I and run II were analysed for lanthanides to calculate the decontamination factors (DF) achievable for the present system. Analytical results revealed that lanthanide concentrations in both the aqueous products are less than 1 μg/mL. The DF which represents the extent of separation in a solvent extraction cycle has been calculated for Nd(III) in the present mixer-settler runs. It is the ratio of total Nd(III) per gram of heavy metals in the feed to the total Nd(III) per gram of heavy metals in the product. The decontamination factor for Nd(III) was > 10^4.

In PUREX process, complete recovery of uranium and plutonium with fission product decontamination factors in the range of 10^6 is possible after 2 cycles of extraction. As described in chapter 3, *D* values for the extraction of lanthanides by TBP and TiAP systems are comparable, whereas *D* values for the extraction of certain troublesome fission products such as Zr, Ru and TcO_4^- by 1.1M TiAP/n-DD are marginally lower than 1.1M TBP/n-DD. This in turn indicates that better DFs could be achieved with TiAP compared to TBP based system which is employed in PUREX process.

4.4 Mass balance of solutes in mixer-settler runs

4.4.1 Stage-wise mass balance

Each mixer (M_n) of the equipment used for the present study is connected to three settlers ($S_{(n-1)}$, S_n and $S_{(n+1)}$) and each settler (S_n) is connected to three mixers ($M_{(n-1)}$, M_n and $M_{(n+1)}$) in such a way that the n^{th} stage mixer receives organic and aqueous phases from $(n+1)^{th}$ and $(n-1)^{th}$ settlers, respectively and the mixed phase from n^{th} stage mixer enters the n^{th} stage settler, where separation of organic and aqueous phases takes place. The organic and aqueous phases from the n^{th} stage settler flow in opposite directions to $(n-1)^{th}$ mixer and $(n+1)^{th}$ mixer respectively, to maintain a counter-current flow. A representation of the flow of organic and aqueous streams through the mixers and settlers within three neighbouring stages in the equipment is shown in Fig. 4.16. Therefore, stage-wise mass balance can be calculated by using the equation (4.1) given below

$$A\,X_{(n-1)} + O\,Y_{(n+1)} = A\,X_n + O\,Y_n \quad \text{.....(4.1)}$$

Where *A* and *O* stand for the flow-rates of aqueous and organic streams, respectively. *X* and *Y* refer to the concentrations of aqueous and organic phases respectively and the corresponding subscripts refer to the respective stages. Stage-wise mass balance data of HNO_3 and U(VI) for U(VI)-HNO_3-1.1M TiAP/HNP system are provided in Table 4.1. Stage-wise mass balance data of HNO_3, U(VI) and Pu(IV) for the extraction and strip runs in U(VI)–Pu(IV)–Lns(III)–Am(III)–HNO_3–1.1M TiAP/HNP system are presented in Table 4.2 and 4.3, respectively. These results obtained indicate that the stage-wise mass balance in all the stages for all runs are in good agreement, indicating the excellent stage-wise performance of the equipment.

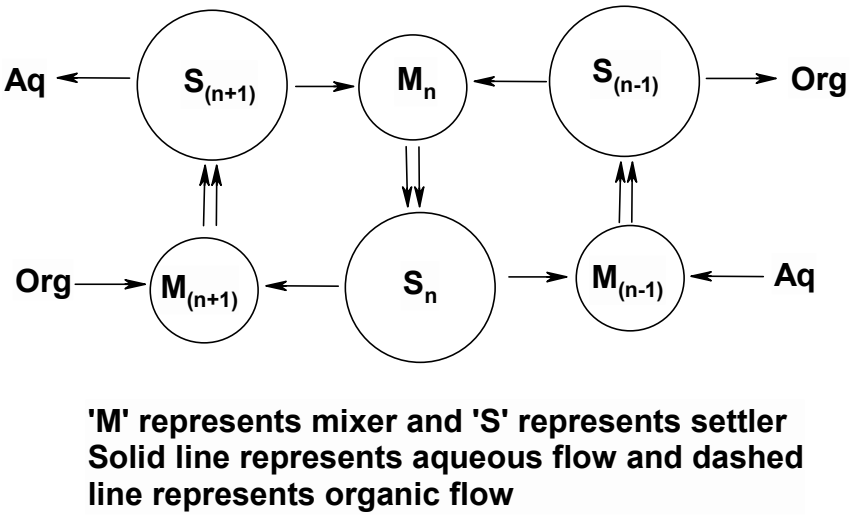

Fig. 4.16: Counter-current flow of organic and aqueous streams within three neighbouring stages in the mixer-settler

Table 4.1: Stage-wise mass balance data for U(VI)-HNO_3-1.1M TiAP/HNP system

Stage No	Extraction Run				Strip Run			
	Acid (mmole/min)		Uranium (mg/min)		Acid (mmole/min)		Uranium (mg/min)	
	In	Out	In	Out	In	Out	In	Out
1	9.3	9.8	747	754	0.8	0.8	157	246
2	9.3	9.1	768	771	1.5	1.5	425	322
3	9.3	9.2	757	773	2.0	2.0	437	441
4	9.6	9.3	758	759	2.3	2.5	510	513
5	9.3	10.0	725	754	2.7	2.5	571	563
6	9.7	11.2	895	719	2.8	2.8	599	623
7	26.9	26.6	993	1028	2.9	2.9	648	628
8	29.9	29.1	-	-	3.0	3.3	677	662
9	30.3	30.7	-	-	3.4	3.2	711	710
10	30.4	31.0	-	-	3.2	3.5	746	706
11	30.5	29.7	-	-	3.5	3.5	752	768
12	29.8	29.6	-	-	3.8	3.6	805	828
13	29.3	29.3	-	-	4.0	4.3	878	862
14	28.0	27.9	-	-	4.1	4.7	935	918
15	25.4	25.6	-	-	4.7	4.8	948	968
16	19.1	20.9	-	-	6.7	5.9	955	960

Table 4.2: Stage wise mass balance of solutes for the extraction run-U(VI)–Pu(IV)–Lns(III)–Am(III)–HNO_3–1.1M TiAP/HNP system

Stage No	HNO_3 (mmol/min)		Uranium (mg/min)		Plutonium (mg/min)	
	In	Out	In	Out	In	Out
1	8.1	8.8	357	347	135	140
2	8.8	8.3	350	362	139	139
3	8.3	8.6	347	350	137	139
4	8.3	8.8	349	347	133	137
5	9.2	9.0	338	349	132	132
6	9.7	10.6	346	337	135	131
7	30.6	31.3	357	347	135	140
8	33.7	33.2	41	48	20	22
9	33.5	33.8	-	-	-	-
10	34.2	33.9	-	-	-	-
11	33.9	32.6	-		-	-
12	32.2	33.2	-	-	-	-
13	32.8	33.4	-	-	-	-
14	32.6	31.3	-	-	-	-
15	29.8	27.9	-	-	-	-
16	22.3	23.3	-	-	-	-

Table 4.3: Stage wise mass balance of solutes for strip runs in U(VI)–Pu(IV)–Lns(III)–Am(III)–HNO_3–1.1M TiAP/HNP system

Stage No	Strip I Run						Strip II Run	
	HNO_3 (mmol/min)		Uranium (mg/min)		Plutonium (mg/min)		Uranium (mg/min)	
	In	Out	In	Out	In	Out	In	Out
1	1.9	2.1	433	465	0.1	0.4	0.1	0.2
2	3.2	3.4	642	748	0.3	0.2	0.3	0.5
3	4.1	3.8	891	766	0.2	0.3	0.7	0.5
4	4.1	4.4	927	969	1.3	2.7	0.7	0.7
5	4.6	4.4	963	992	12.9	8.7	0.9	1.0
6	4.9	4.8	978	936	31.1	40.5	1.1	1.5
7	6.8	7.0	868	882	72.1	62.3	1.7	1.4
8	6.8	7.0	747	679	94	91	1.8	2.0
9	7.0	7.2	583	599	121	110	3.2	3.3
10	6.9	7.2	532	518	138	139	7.3	7.5
11	6.7	7.0	479	483	167	166	35.9	27.1
12	6.5	6.7	473	463	198	202	63.1	68.2
13	7.1	6.5	454	464	238	244	113	120
14	7.0	6.9	439	453	264	289	165	159
15	7.2	7.3	438	441	306	298	195	194
16	8.7	9.5	407	413	281	279	221	221

4.4.2 Overall mass balance

Overall mass balance for the nitric acid extraction and strip runs was calculated using the equations (4.2) and (4.3), respectively. Similarly, equation (4.4) was used to calculate the overall mass balance for the extraction run in both the systems i.e. U(VI)-HNO_3-1.1M TiAP/HNP and U(VI)–Pu(IV)–Lns(III)–Am(III)–HNO_3–1.1M TiAP/HNP.

Overall mass balance for the strip run in U(VI)-HNO_3-1.1M TiAP/HNP system was calculated by using equation (4.3). The terms *S*, *F*, *R, St* and *P* represent the flow-rates of scrub, feed, raffinate, strippant and product streams respectively. Subscripts '*i'* and '*o*' refer to the solvent 'in' and 'out' of the extractor bank.

$$F\ X_F + O\ Y_i = R\ X_R + O\ Y_O \quad (4.2)$$

$$St\ X_{St} + O\ Y_i = P\ X_P + O\ Y_O \quad (4.3)$$

$$S\ Xs + F\ X_F + O\ Y_i = R\ X_R + O\ Y_O \quad (4.4)$$

Mass balance for the strip I run was calculated using the equation (4.5), where St_1 and St_2 of Eq (4.5) stand for the flow-rates of strippant 1 and strippant 2 respectively. Equation (4.3) was used to the calculate the overall mass balance for the strip II run in U(VI)–Pu(IV)–Lns(III)–Am(III)–HNO_3–1.1M TiAP/HNP.

$$St_1 \times X_{St1} + St_2 \times X_{st2} + O \times Y_i = P \times X_P + O \times Y_O \quad (4.5)$$

Overall mass balance data of solutes for both the systems i.e. U(VI)-HNO_3-1.1M TiAP/HNP and U(VI)–Pu(IV)–Lns(III)–Am(III)–HNO_3–1.1M TiAP/HNP are shown in Table 4.4 and 4.5 respectively. Results indicated good overall mass balance for all mixer-settler runs.

Table 4.4: Overall mass balance data for U(VI)-HNO_3-1.1M TiAP/HNP system

Run	Mass Balance			
	HNO_3 (mmole/min)		U(VI) (mg/min)	
	In	Out	In	Out
Extraction run	16.7	15.9	672	734
Strip run	3.9	4.1	518	483

Table 4.5: Overall mass balance data of all solutes for U(VI)–Pu(IV)–Lns(III)–Am(III)–HNO_3–1.1M TiAP/HNP system

Run	Solute					
	HNO_3 (mmol/min)		Uranium (mg/min)		Plutonium (mg/min)	
	In	Out	In	Out	In	Out
Extraction Run	22.2	22.7	331	336	134	132
Strip Run-I	6.1	7.8	310	329	117	125
Strip Run-II	0.9	0.9	113	117	-	-

4.5 Conclusions

Present study revealed that the mixer-settler facility commissioned in our laboratory can be used for flowsheet development studies with radioactive feed solutions. Mixer-settler experiments revealed that TiAP can be used as an extractant for reprocessing applications. Considering the lesser third phase formation tendency of TiAP compared to TBP, it can be used as an alternate extractant to TBP in the fast reactor fuel reprocessing. Present study also demonstrates the separation of U and Pu from fission products by employing TiAP as an extractant for fast reactor fuel reprocessing. Separation of U and Pu from fission products using mixer-settler facility comprising of 16 stages for extraction-scrubbing and 2 × 16 stages for heavy metal stripping also indicates that loss of heavy metals into the raffinate and lean organic streams has been negligible.

Chapter 5

DISSOLUTION, CHARACTERISATION AND SOLVENT EXTRACTION STUDIES WITH U-Zr AND U-Pu-Zr ALLOY FUELS

5

5.1 Introduction

For future Indian FBRs, U-Pu-Zr alloy is considered as a candidate fuel. The metal fuel could be reprocessed using aqueous route by well established PUREX process apart from the pyrochemical reprocessing. Therefore it is necessary to investigate the dissolution behavior of metallic fuels in nitric acid medium and solvent extraction of U-Zr and U-Pu-Zr feed solutions. The objective of the present study is to develop a method for the processing of metallic alloy fuels by aqueous route using PUREX process. In this study, dissolution aspects of metallic alloys in nitric acid medium were studied. Dissolution behavior using electrochemical method has been investigated. Explosive nature of U-Zr alloys during dissolution in nitric acid was studied. A spectrophotometric method has been developed for the determination of zirconium in the presence of large amounts of uranium and plutonium using xylenol orange as the chromogenic agent. Further, solvent extraction studies were carried out with U-Zr and U-Pu-Zr feed solutions. The co-extraction of U and Zr as a function of equilibrium aqueous phase metal ion and concentration of nitric acid was carried out using 1.1M TiAP/n-DD and the results are compared with 1.1M TBP/n-DD at 303K. The co-extraction and co-stripping of U, Pu and Zr using 1.1M TiAP/n-DD and 1.1M TBP/n-DD as solvents in cross-current mode were also examined and the results are discussed in this chapter.

5.2 Dissolution aspects of zirconium containing metallic alloys

5.2.1 Dissolution of U-Pu-Zr alloy in HNO_3-HF medium

The U-Pu-Zr alloy samples (~ 50 mg each during each experiment) were dissolved in HNO_3-HF medium. Complete dissolution of U and Pu was observed in 16M HNO_3-0.05M HF medium corresponding to ~ 76 and ~ 18 wt% respectively. Zirconium was estimated by

spectrophotometric method and it was found to be lower (~ 3.2 wt%) compared to expected Zr content in the matrix (~ 6 wt%) indicating that fluoride ion interferes in the estimation of Zr. Further, Zr was estimated by ICP-AES method and it was found to be 6 wt% in the matrix. Dissolution in HNO_3-HF medium was employed only for characterisation (for analytical applications) of materials and it is not advisable to use fluoride ions for actual dissolution applications in reprocessing plants due to corrosion of dissolver equipments. Therefore in further studies, dissolution was carried out in neat nitric acid medium only (without use of fluoride ions).

5.2.2 Dissolution of U-Zr metallic alloys in nitric acid medium (~75^{o}C)

Dissolution of U-Zr alloy samples was carried out in nitric acid medium at a temperature of ~ 75^{o}C for ~ 8 hr. More than 98% of U was dissolved in all the cases and about 30% of Zr dissolution was observed (Table 5.1). Results also indicated that even in 8M HNO_3, complete dissolution of U was possible whereas dissolution of Zr was found to be ~ 33% (Batch 4 of Table 5.1), similar to the one observed with 12M HNO_3 (Batch No.2). Black residue got settled over night at the bottom of the round-bottom flask and it was separated by centrifugation (Batch 1). The residue was subjected for further dissolution in 12M HNO_3 (25mL) for about 5 hr under similar conditions to check for any U presence and it was found to be ~ 5 mg (0.8% of initial U in the matrix), indicating that most of the U was dissolved in the first 5 hr period itself.

Table.5.1: Dissolution of U-Zr metallic alloys in nitric acid medium (~ 75^{o}C)

Batch No	Alloy	Sample weight/g	[HNO_3]/M Volume =25 mL	Zr dissolution (%)	U dissolution (%)
1	U-6 wt% Zr	0.673	12	32.2	98.7
2	U-6 wt% Zr	0.864	12	34.2	98.1
3	U-6 wt% Zr	1.493	8	32.7	99.9

* Samples prepared by Injection casting

5.2.3 Dissolution of metallic alloys in nitric acid media under reflux conditions (~130^{o}C)

Dissolution of metallic alloys was carried out in nitric acid media (4, 8 and 12M) under reflux conditions (~130^{o}C) as well as at room temperature. Dissolution kinetics was studied for the individual metal ions U, Pu and Zr. Results indicated that dissolution rates of U, Pu and Zr increase with time under reflux conditions as well as at room temperature (Fig.5.1-5.3). Uranium dissolves more or less completely (>98%) under reflux conditions in 4, 8, 12M HNO_3, whereas at room temperature the dissolution of U was found to be ~ 92% both in the case of U-Zr and U-Pu-Zr alloys (Table 5.2). The dissolution of Zr was found to be ~ 52% in 4 and 8M HNO_3 and it was 74% with 12M HNO_3 under reflux conditions. The dissolution of Zr was found to be ~ 17 and 24% at room temperature in the case of U-Zr and U-Pu-Zr, respectively. The dissolution of Pu was found to be ~ 70% at room temperature (Batch 5 of Table 5.2).

Table 5.2: Dissolution of metallic alloys in nitric acid medium under reflux conditions (~ 130^{o}C) and at room temperature (RT = ~ 25^{o}C)

Batch No	Alloy	Sample weight/g	Condition/[HNO_3]	Dissolution (%)		
				U	Zr	Pu
1	U-6 wt% Zr	1.544	Reflux/4M	98.5	52.1	-
2	U-6 wt% Zr	1.487	Reflux/8M	98.2	51.4	-
3	U-6 wt% Zr	1.492	Reflux/12M	98.5	73.7	-
4	U-6 wt% Zr	1.321	RT/12M	91.3	16.7	-
5	U-19 wt% Pu-6 wt% Zr	0.133	RT/12M	92.7	23.7	70.2

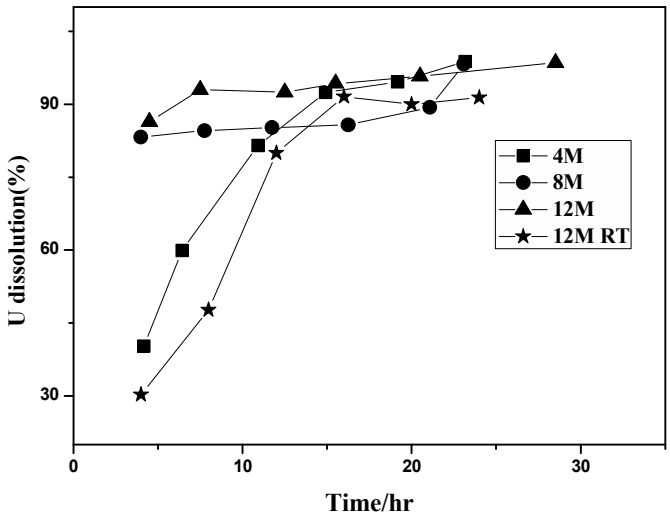

Fig.5.1: Dissolution of U in U-Zr metallic alloys in nitric acid media

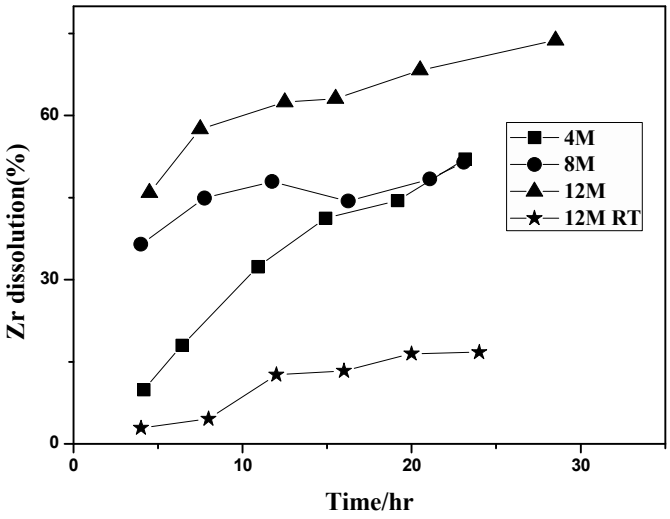

Fig.5.2: Dissolution of Zr in U-Zr metallic alloys in nitric acid media

5.2.4 Electrochemical dissolution of metallic alloys

U-Zr metallic alloy samples were taken in an electrolytic cell containing nitric acid (50 mL) and cerium (III) nitrate (0.05M). The contents in the electrolytic cell were heated to boiling condition (~ 130^{o}C) except in Batch 3 (~ 90^{o}C). Evolution of dark brown fumes (NOx) indicated initiation of dissolution and brown fumes were terminated after ~ 4 hr. The dissolution of uranium was found to be > 99% in 11.5M HNO_3 whereas dissolution of zirconium was found to be about 73% indicating that complete dissolution of Zr is not possible in 11.5M HNO_3 (Batch 1). Hence in the next set of experiments, the concentration of

nitric acid was increased to 15.7M and in this case the dissolution of uranium was found to be > 99%. The dissolution of zirconium only marginally increased to about 75% (Batch 2) indicating that complete dissolution of Zr was not possible even with 15.7M HNO_3 medium (Table 5.3).

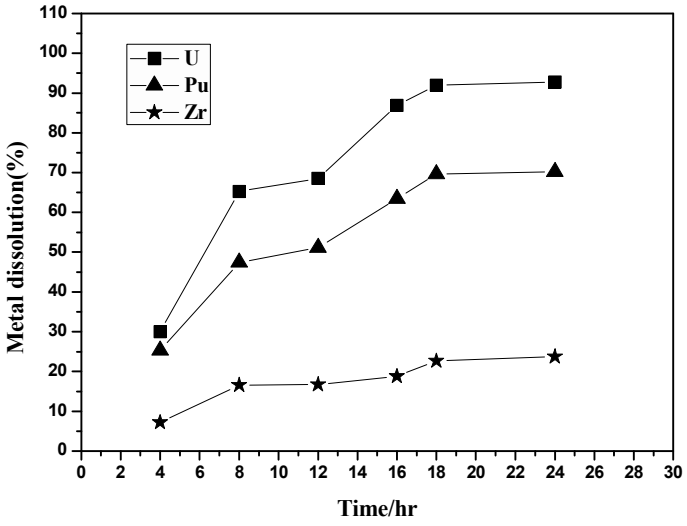

Fig.5.3: Dissolution of U, Pu and Zr in U-Pu-Zr metallic alloys in 12M nitric acid medium at room temperature

Dissolution of U-Pu-Zr metallic alloys was also carried out using a similar electrolytic dissolver cell. In the case of U-Pu-Zr alloy samples, Zr dissolution kinetics was studied and results indicated that dissolution of Zr increases with time and reaches saturation limit after 12-13 hr (Fig.5.4). The maximum Zr dissolution was found to be ~ 53% and ~ 72%, respectively (batch 3 and 4 of Table 5.3). The difference in Zr dissolution between these two batches was due to the difference in temperature employed indicating that it plays an important role in the dissolution of metallic alloys. In batch 5, the Zr dissolution was found to be about 68%. The dissolution of U and Pu was found to be > 99% in all these cases. These results indicate that there is no enhancement in the dissolution of Zr by EODT compared to dissolution under reflux conditions.

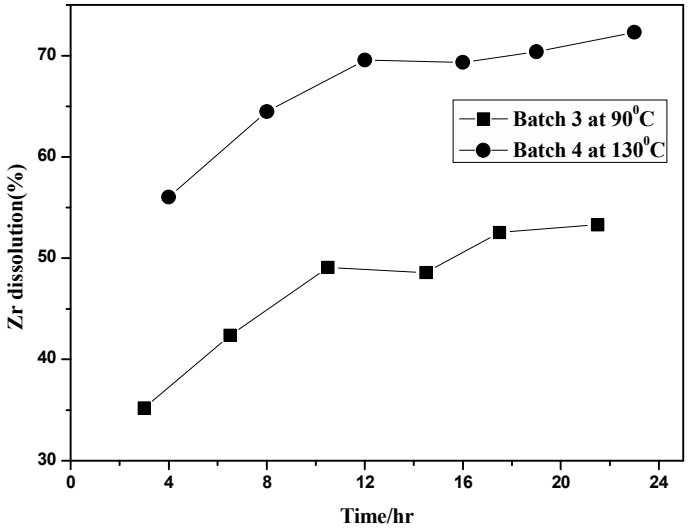

Fig.5.4: Dissolution kinetics of Zr in U-Pu-Zr metallic alloys by EODT

Table 5.3: Dissolution of metallic alloys using EODT method

Batch No	Alloy	Sample weight/g	$[HNO_3]$/M	Time (hr)	Zr dissolution (%)
1	U-6 wt% Zr*	1.627	11.5	17	72.6
2	U-6 wt% Zr*	1.580	15.7	17	74.9
3	U-19 wt% Pu-6 wt% Zr**	0.464	15.7	22	53.1
4	U-19 wt% Pu-6 wt% Zr*	0.544	15.7	24	72.2
5	U-19 wt% Pu-6 wt% Zr*	0.288	15.7	24	68.4

*Dissolution carried out under nitric acid reflux conditions at ~130^{o}C
**Dissolution carried out at ~90^{o}C

5.2.5 Comparison studies of U-6 wt% Zr dissolution by EODT and reflux methods under identical conditions

In order to compare the dissolution behavior of metallic alloys under reflux conditions and by EODT method, experiments were carried out under identical conditions such as temperature (~130^{o}C), sample weight and dissolution period (Table 5.4). Dissolution kinetics (Batch 1) was studied for both the metal ions, U and Zr. It was observed that dissolution of U increased with time and dissolution was nearly complete (>97%) by reflux and EODT

methods (Fig.5.5). Similarly the dissolution of Zr also increased with time and it was found to be approximately 80 and 70 wt% by reflux and EODT methods, respectively (Fig.5.6). Results also indicated that even in 12 M HNO_3, the dissolution of U and Zr was found to be similar to the one observed with 15.7M HNO_3 (Table 5.4). Electrooxidative dissolution does not help in the complete dissolution of Zr in metallic alloys. This may possibly due to the existence of mainly single oxidation state (Zr(IV)) in aqueous solutions.

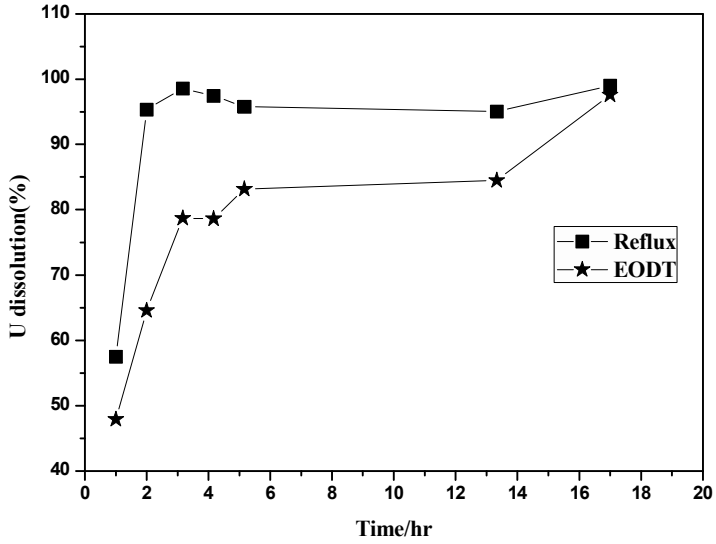

Fig.5.5: Dissolution of U in U-Zr metallic alloys by both methods (Batch 1)

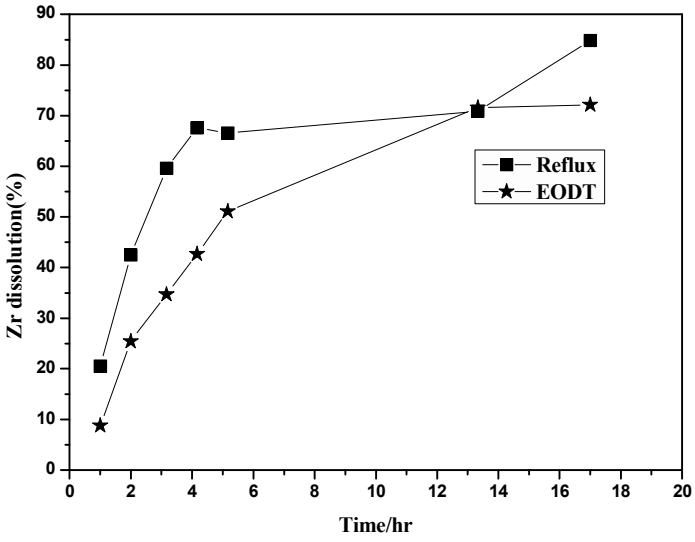

Fig.5.6: Dissolution of Zr in U-Zr metallic alloys by both methods (Batch 1)

Table 5.4: Results of nitric acid reflux method against EODT under identical conditions

Batch No	Sample weight/g		Time/hr	$[HNO_3]$/M	Zr dissolution (%)		U dissolution (%)	
	Reflux	EODT			Reflux	EODT	Reflux	EODT
1	1.269	1.431	17	15.7	81.4	72.1	98.9	97.6
2	1.287	1.225	15	15.7	82.4	70.3	98.6	97.8
3	1.332	1.176	13	12.0	82.8	68.2	96.4	97.5

To confirm the role of intermediate redox reagent Ce(IV)/Ce(III) in EODT, dissolution of neat Zr metal in the form of wire was carried out by taking a wire (0.275 g) in 50mL of nitric acid (15.7 M) containing cerium(III) nitrate (0.05M) in an electrolytic cell. Heating was carried out for about 17 hr and the solution was checked for Zr content and was found to be insignificant i.e. < 0.2 μg/mL. It was also observed that there was no weight loss in the Zr wire after 17 hr, indicating that EODT does not play any role in the dissolution of Zr. However, the dissolution of zirconium observed with U-Zr or U-Pu-Zr alloy samples indicates that preferential dissolution of heavy metals (U or Pu) aids the leaching of Zr due to the collapse of the alloy matrix, whereas the same is not possible with neat Zr metal.

The present study indicates that Zr dissolution was found to be about 70% and the remaining 30% settled as black residue (fine particles). This solution could also be employed as a feed in PUREX process with appropriate steps to filter insoluble Zr residue. In a way, incomplete dissolution of Zr from the metallic alloys using HNO_3 process can reduce the Zr load in the organic phase, leading to better decontamination factors for U and Pu.

5.2.6 Studies carried out to examine the explosive properties of U-Zr alloy samples

To examine the explosive nature of Zr (2-10 wt%) containing U-Zr metallic alloys during dissolution processes, different compositions of U-Zr samples were prepared by injection casting method and the following dissolution experiments were carried out as a function of acid treatment period, concentration of acid, temperature etc.

Test 1: About 10 gram alloy (U-6 wt% Zr) was placed in a round bottom flask containing 50 mL of nitric acid (15.7 M) at room temperature with stirring for about one hour and later it was heated to the boiling condition (~120^{o}C) for about 2 hr. To this solution, an additional 10 gram alloy and ~ 80 mL of nitric acid (15.7M) was added followed by heating under boiling condition. After 4 hr, the solution was filtered and the residue was again taken-up for dissolution under reflux conditions for 6 hr. Under these experimental conditions, no explosion was observed with 20 gram, sample when it was treated with 15.7M HNO_3. The dissolution of U and Zr were found to be about 99% and 62%, respectively.

Test 2: 10 gram alloy (U-6 wt% Zr) sample was placed in a RB flask containing 50 mL of nitric acid (15.7 M) for 5 days at room temperature and later an additional 50 mL HNO_3 was added and refluxed for about 6 hr. Under these experimental conditions, no abnormal event was observed (no shattering of the acid/glass beaker). The dissolution of U and Zr were found to be about 99% and 64%, respectively.

Test 3: 10 gram alloy sample (U-10 wt% Zr) was placed in a RB flask containing 200 mL of 15.7M HNO_3 for about 3 hr with stirring at room temperature followed by refluxing at ~130^{o}C for about 3 hr. No explosion was observed under these conditions. The dissolution of U and Zr were found to be about 99% and 38 %, respectively.

Test 4: 10 gram alloy sample (U-10 wt% Zr) was placed in a RB flask containing 100 mL of 15.7M HNO_3 for about 2.5 hr at room temperature; the sample was removed, washed with water followed by acetone and dried. Subsequently this solid sample was sparked with tesla coil in air and no explosion was observed under these conditions.

Test 5: 10 gram alloy sample (U-10 wt% Zr) was placed in a RB flask containing 100mL of 15.7M HNO_3 and heated for about 20 min at 100^{o}C. The sample was removed, washed with water followed by acetone and dried; solid sample was sparked with tesla coil in air. A bright flash was observed. The residue left over after the complete dissolution of uranium (mainly

consisting of zirconium) was collected from all the above tests, washed with water and dried with acetone. Sample was sparked with tesla coil in air; no violent reaction was observed.

5.3 Determination of Zr by spectrophotometry

5.3.1 Effect of HNO_3 in the presence of H_2SO_4

Cheng [108] developed a method for the estimation of zirconium in H_2SO_4 medium using xylenol orange as the chromogenic agent; since nitric acid is the commonly used reagent for the dissolution of U-Zr and U-Pu-Zr alloys in reprocessing applications, in the present study its role has been investigated. In order to estimate the tolerance limit of nitric acid in sulfuric acid medium, the absorbance of the zirconium-xylenol orange complex was measured as a function of nitric acid concentration. Results indicate that the absorbance decreases with increase in nitric acid content (Fig.5.7). The study also indicated that the absorbance of zirconium-xylenol orange (Zr-XO) complex in 0.2N H_2SO_4 is maximum at 0.3 mmoles of HNO_3 (0.3 mmoles in 10mL volumetric flask). Therefore it is recommended that the concentration of nitric acid should not exceed 0.03M. In all further experiments, Zr was estimated in sulphuric acid medium (0.2N) with concentration of nitric acid not exceeding 0.03M.

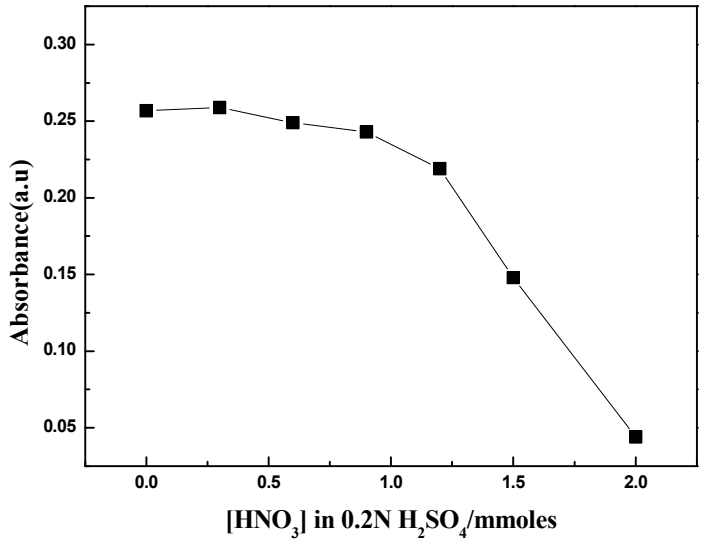

Fig.5.7: Variation of absorbance of Zr-XO complex with HNO_3 in 0.2N H_2SO_4 (Zr: 0.89 µg/mL)

5.3.2 Effect of uranium in the analysis of zirconium

In general, U-Zr metallic alloys contain a large excess of U (about 90 wt%) with a Zr content of about 6-10 wt%. A systematic study has been carried out for the determination of zirconium in a large excess of uranium (U : Zr = 1000 : 1). The absorbance of Zr-XO complex was nearly constant with increase in U concentration indicating that uranium does not interfere in the analysis of zirconium (U:Zr=1000:1) and the uncertainty associated with the estimation of Zr is presented in Table 5.5.

Table 5.5: Effect of uranium content on the absorbance of zirconium-xylenol orange complex (Zr = 0.89 µg/mL)

[U](µg/mL)	Absorbance	Error (%)	[U] (µg/mL)	Absorbance	Error (%)
0	0.257	-	400	0.255	-0.8
1	0.261	1.6	500	0.258	0.4
7.1	0.256	-0.4	600	0.258	0.4
100	0.25	-2.7	700	0.262	1.9
200	0.252	-1.9	1000	0.256	-0.4
300	0.251	-2.3			

5.3.3 Effect of Pu (IV) in the analysis of Zirconium

The absorbance was found to increase with increase in Pu(IV) concentration (Fig.5.8) indicating interference of Pu(IV) in the estimation of zirconium. A spectrum was recorded for Pu-xylenol orange complex from 700-400 nm (Fig.5.9) in the presence and absence of Zr. These studies indicated that Pu-xylenol orange complex absorbs at λ_{max} similar to that of zirconium-xylenol orange complex (535 ± 2 nm).

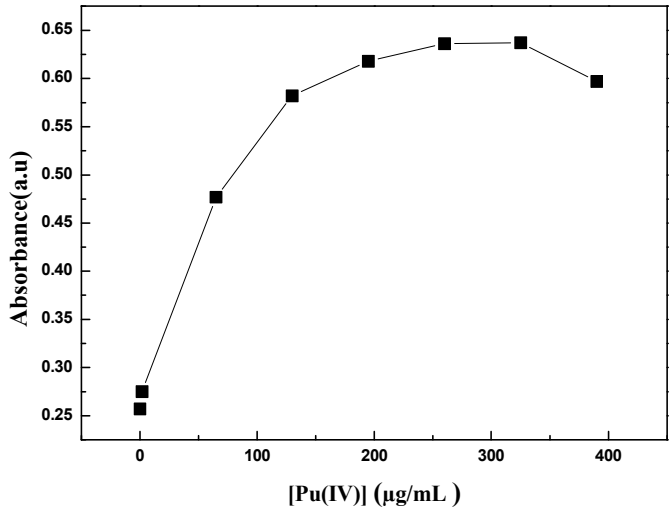

Fig.5.8: Variation of absorbance of (Zr, Pu(IV))-XO complex as a function of Pu(IV) concentration (Zr: 0.89 µg/mL)

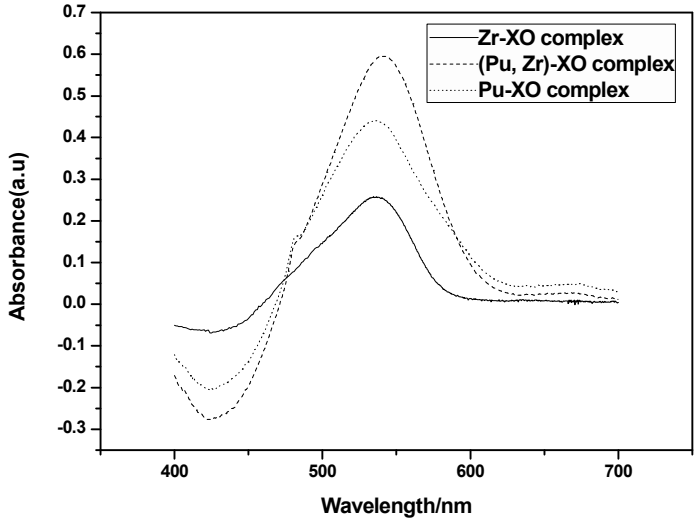

Fig.5.9: Absorption spectra of Zr-XO, Pu-XO and (Pu, Zr)-XO complexes

The reagents such as trans-1, 2-Cyclohexanediamine-N, N, N', N'-tetraacetic acid (CyDTA) and acetohydroxamic acid have been employed as masking agents for the determination of Zr in the presence of plutonium. It was observed that the above masking agents are not selective for Pu(IV) and also form complexes with zirconium. Pu(IV) interferes in the estimation of zirconium (Fig.5.9), but it may be possible to determine zirconium in presence of Pu(III) or Pu(VI). In this context, several reducing agents such as hydrazine hydrate and hydroxylamine hydrochloride have been investigated in the present work for the reduction of Pu(IV) to Pu(III). However, it was observed that none of the above reducing

agents could be employed for the reduction of Pu(IV) due to the reaction between xylenol orange with these reagents (hydrazine hydrate and hydroxylamine hydrate). Ferrous ammonium sulphate was also examined for the reduction of Pu(IV); during this reaction, Fe(II) was converted to Fe(III); however, it has been reported that Fe(III) interferes in the estimation of zirconium [108].

Studies on the identification of suitable masking/reducing agents for Pu(IV), revealed that ascorbic acid is a suitable reducing agent. A spectrum of Pu(IV) in 0.2N H_2SO_4 was recorded against sulfuric acid as blank reagent. To the Pu(IV) solution, ascorbic acid was added and the spectrum was recorded from 700-400 nm. Results indicate that ascorbic acid reduces Pu(IV) to Pu(III) (Fig.5.10). To this, xylenol orange was added and spectrum was recorded against reagent blank. A base line was observed (Fig.5.11) indicating that Pu(III) does not interfere in the estimation of zirconium. Therefore, ascorbic acid can be employed for the estimation of zirconium in the presence of plutonium.

5.3.4 Effect of quantity of ascorbic acid

Studies were taken-up to identify the quantity of ascorbic acid required for the reduction of Pu(IV) to Pu(III). In the absence of ascorbic acid, absorbance of the complex was found to be higher for (Pu, Zr)-xylenol orange complex (A= 0.477) and with the addition of ascorbic acid, the absorbance was found to reduce and remain constant (A=0.257). Therefore, it is recommended that a quantity of ~10 mg of ascorbic acid is sufficient for the reduction of Pu(IV) to Pu(III).

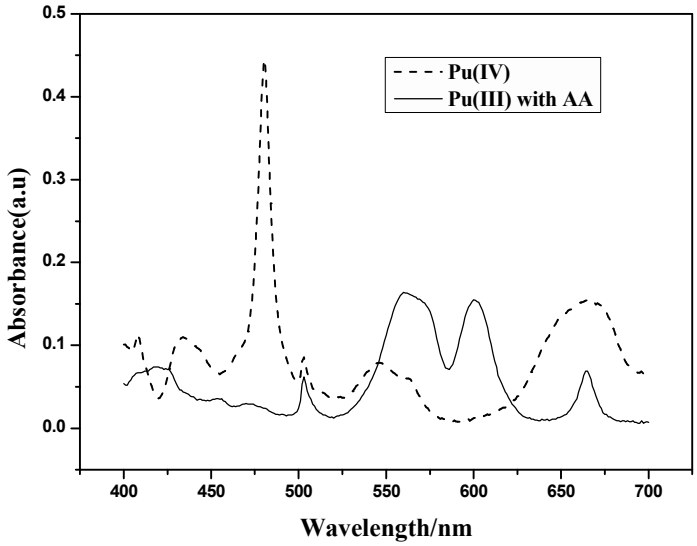

Fig.5.10: Absorption spectrum of Pu(IV) and Pu(III) in the presence of ascorbic acid (Zr: 0.89 µg/mL)

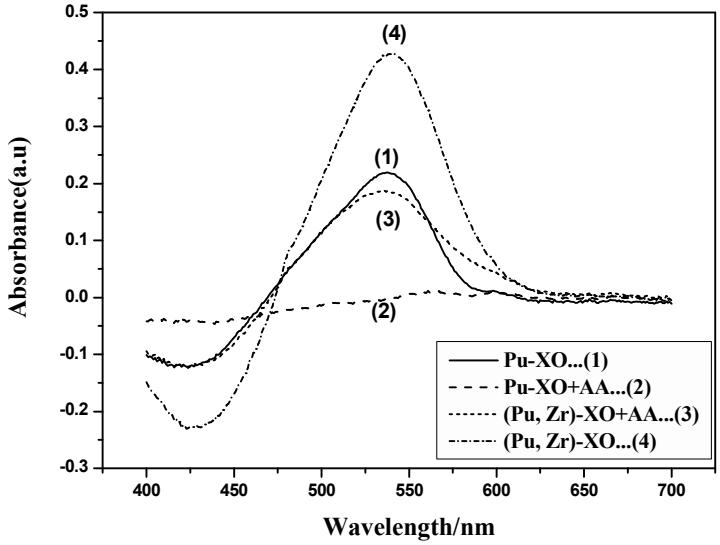

Fig.5.11: Absorption spectra of Zr and Pu with xylenol orange with and without ascorbic acid (Zr: 0.89 µg/mL)

5.3.5 Estimation of Zr in the presence of Pu and ascorbic acid

Zirconium was estimated in the presence of plutonium ranging from 0 to 400 µg/mL and in the presence of ascorbic aicd (10 mg). The absorbance of Zr-XO complex remains constant with increase of plutonium concentration (Table 5.6). These studies demonstrated that Zr can be determined in the presence of Pu matrix (Pu: Zr = 400:1).

Zr was also estimated in the presence of Pu (0-400 µg/mL), U(1000 µg/mL) and ascorbic acid (10 mg). Results indicate that the absorbance remains constant over a wide range of Pu concentration with fixed concentration of U (1000 µg/mL) (Table 5.6). In addition, Zr was also estimated in varying amounts of U and Pu with a constant U/Pu ratio (U/Pu = 3.74) as in the case of 71wt% U-19 wt% Pu-10 wt% Zr. It was found that the absorbance was almost constant in all the cases indicating that Zr can be determined in varying amounts of U and Pu (Table.5.7).

Table 5.6: Influence of plutonium and uranium/plutonium content on the absorbance of zirconium-xylenol orange complex in sulphuric acid medium (0.2N) (Zr: 0.89 µg/mL, Ascorbic acid: 10 mg)

[Pu] (µg/mL)	Absorbance	Error (%)	[Pu] (µg/mL) with 1000 µg/mL of U	Absorbance	Error (%)
0	0.259	-	0	0.256	0.0
2	0.262	1.2	2	0.257	0.4
50	0.258	-0.4	50	0.253	-1.2
75	0.254	-1.9	75	0.263	2.7
100	0.260	0.4	100	0.252	-1.6
150	0.252	-2.7	150	0.250	-2.3
200	0.257	-0.8	300	0.259	1.2
300	0.256	-1.2	400	0.254	-0.8
400	0.253	-2.3			

5.3.6 Calibration plot for Zr in the presence of U and Pu

Calibration plots for (i) neat zirconium, (ii) zirconium in the presence of uranium (700 µg/mL), (iii) zirconium in the presence of uranium (700 µg/mL) and plutonium (190 µg/mL) were obtained. Results obtained indicated that Zr-XO complex exhibits molar absorptivity (Ɛ) of ~ 26295 ± 175 L mol^{-1} cm^{-1} for neat Zr as well as for Zr in the presence of U and Pu (Fig.5.12).

Table 5.7: Variation of absorbance of zirconium-xylenol orange complex with different concentrations of U and Pu with a constant ratio of [U]/[Pu]=3.74. (Zr: 0.89 µg/mL, ascorbic acid: 10 mg, medium: 0.2N sulphuric acid)

U (µg/mL)	Pu (µg/mL)	Absorbance	E_r(%)
-	-	0.260	0.0
7.1	1.9	0.257	-1.2
186.8	50	0.255	-1.9
280.2	75	0.262	0.8
373.6	100	0.256	-1.5
560.4	150	0.254	-2.3
747.4	200	0.258	-0.7

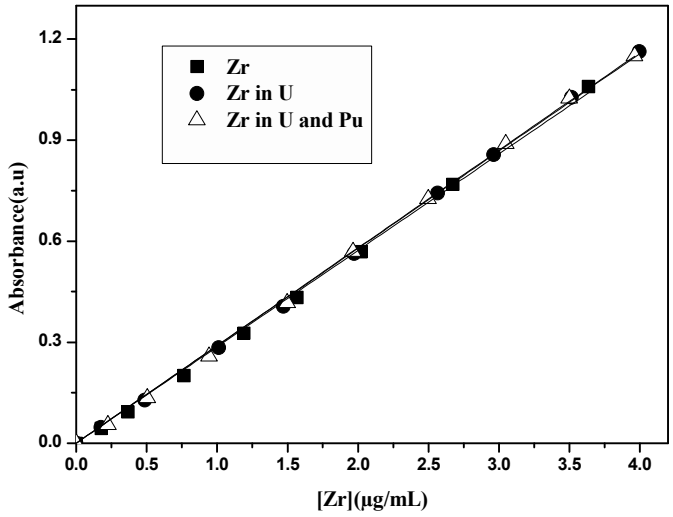

Fig.5.12: Calibration plot for (i) zirconium, (ii) zirconium in the presence of uranium, (iii) zirconium in the presence of uranium (700µg/mL) and plutonium (190µg/mL)

5.3.7 Analysis of Zr in U-19 wt% Pu-6 wt% Zr alloy sample

The above method was applied to estimate Zr in actual U-Pu-Zr alloy sample. Initially the sample was dissolved in HNO_3-HF medium. U and Pu were analysed by potentiometry, which corresponds to about 76 wt% and 18 wt%, respectively. Subsequently, Zr was estimated by the above procedure and it was found to be 3.2 wt%. However, the expected composition of Zr in the alloy sample was 6 wt%, which was confirmed with ICP-AES. The decrease in the absorbance of Zr-XO complex is due to the interference of fluoride

ions added during the dissolution. It was reported that fluoride ions can mask Zr and hence reduce the absorbance of Zr-XO complex [108]. It has been investigated that interference of fluoride ions could be masked by the addition of aluminium nitrate since aluminium forms a strong complex with fluoride ions. However, zirconium forms much stronger complexes with fluoride ion than that of aluminium. The stability constants of zirconium fluoride complexes (log β_1=8.27 and log β_2=9.09) are higher than that of aluminium fluoride complexes (β_1=6.69 and log β_2=5.35) indicating that aluminium nitrate cannot be used to mask fluoride ions in the presence of zirconium[188]. It was reported that fluoride ions can be removed by repeated fuming with concentrated sulphuric acid [106]. Therefore, the above method was adopted in the present study to remove hydrofluoric acid by repeated fuming in a teflon beaker. However, reproducible results were not obtained by adopting this procedure for the removal of fluoride ions and the uncertainty was ~ ± 10 %. Thus the estimation of Zr in the presence of fluoride ions is a challenging task, necessitating the use of ICP-AES method.

5.4 Solvent extraction studies with U-Zr and U-Pu-Zr metallic alloys

5.4.1. Extraction of ^{233}U, ^{239}Pu and natural Zr as a function of concentration of nitric acid

The *D* values were measured for the extraction of U and Zr by 1.1M TiAP/n-DD and 1.1M TBP/n-DD as a function of concentration of nitric acid (0.5-6M) from a solution containing ~10^{-4} M U and 10^{-2} M Zr at 303K. It was observed that the *D* values for the extraction of U and Zr increase with increase in concentration of nitric acid from a solution containing U and Zr (Fig.5.13). Similarly the *D* values were also measured for the extraction of Pu and Zr from a solution containing ~10^{-4} M Pu and 10^{-2} M Zr at 303K. The D_{Pu} and D_{Zr} also increase with concentration of nitric acid (Fig.5.14). For most of the metal ions, including U and Pu, the *D* values passes through a maximum with increase in concentration of nitric acid (trend not shown in Figs) whereas D_{Zr} increases continuously with increase in concentration of nitric acid. The unusual behaviour of Zr extraction is reflected in the

continuous increase in D_{Zr} with concentration of nitric acid. Alcock et al. [189] reported the D_{Zr} for a wide range of concentration of nitric acid and the D_{Zr} was found to be maximum (D_{Zr}=134) at 13M HNO_3.

It is important to note that D_U and D_{Pu} are marginally higher for TiAP based system compared to TBP over a wide range of concentration of nitric acid. However reverse trend was observed in the case of Zr i.e. D_{Zr} was relatively lower with TiAP than that of TBP at all acidities. This is an important aspect with respect to decontamination factors for U and Pu against Zr in PUREX process. Another important observation is that the extraction behavior of Zr by both the extractants is found to be similar in the presence of U or Pu.

For a given extractant concentration (1.1M in this study), D_U depends on the square of nitrate ion concentration, whereas D_{Pu} and D_{Zr} depends on the fourth power of nitrate ion concentration. At a given concentration of nitric acid, the D values for the extraction of U, Pu and Zr were found to be in the order $D_U > D_{Pu} >> D_{Zr}$. In the case of Pu and Zr, even though both form disolvate with TiAP, the D_{Pu} is significantly higher than that of D_{Zr}. This highlights the influence of the nature of metal ion on extraction behavior. Similar extraction behavior is also exhibited by TBP based system.

5.4.2 Extraction of U and Zr under high organic loading conditions

Co-extraction of U and Zr from 4.5M HNO_3 medium was carried out using 1.1M solutions of TiAP and TBP in n-dodecane. Third phase was observed when a feed solution containing U and Zr ~ 247 and 29 g/L, respectively in 4.5M HNO_3 were equilibrated with 1.1M TBP/n-DD. However, 1.1M TiAP/n-DD does not form third phase under these conditions and hence solvent extraction studies were carried out with 1.1M TiAP/n-DD using the above feed solution. Distribution ratios for the co-extraction of U and Zr by 1.1M TiAP/ n-DD from U-Zr feed solution have been measured as a function of their equilibrium aqueous phase metal ion concentration and the results are shown in Fig.5.15 and Fig.5.16.

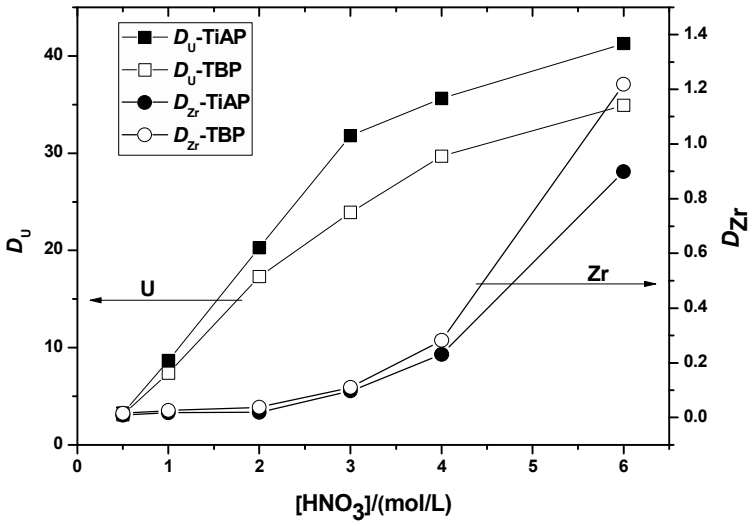

Fig.5.13: Variation of D_U and D_{Zr} with concentration of nitric acid for the extraction of U and Zr by 1.1M TalP/n-DD from U-Zr solutions at 303K (U: 10^{-4}M and Zr: 10^{-2}M)

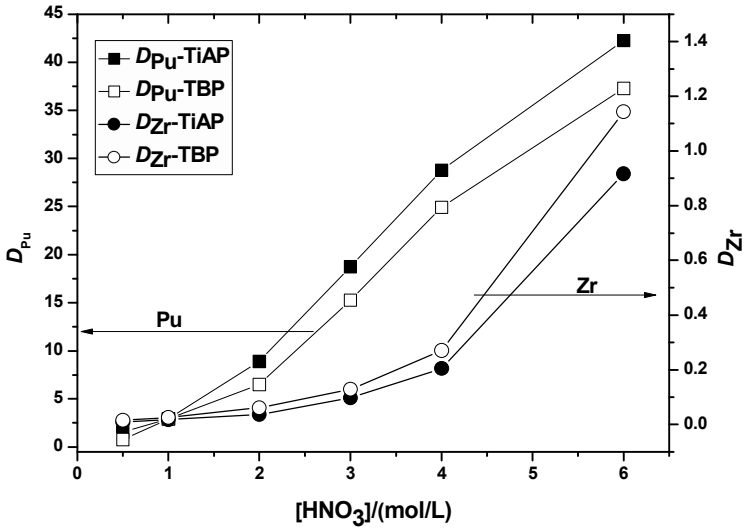

Fig.5.14: Variation of D_{Pu} and D_{Zr} with concentration of nitric acid for the extraction of Pu and Zr by 1.1M TalP/n-DD from Pu-Zr solutions at 303K (Pu: 10^{-4}M and Zr: 10^{-2}M)

These studies revealed that D_U and D_{Zr} initially decrease steeply and flatten with increase in concentration of U and Zr in aqueous phase at 4.5M concentration of nitric acid. The trends shown in Fig.5.15 and Fig.5.16 can be explained as follows;

- With increase of equilibrium metal ion concentration in the aqueous phase, loading in the organic phase increase; thus free extractant concentration in the organic phase decrease;

therefore D_U and D_{Zr} which are directly proportional to the square of the free extractant concentration ($[TiAP]^2_{(org)}$), decrease.

- The concentration of U in the organic phase increases with increase of $[U]_{aq,eq}$ and reaches up to near saturation limit (theoretical loading ~ 130 g/L) (Fig.5.15).
- The concentration of Zr in the organic phase also increases with increase in $[Zr]_{aq,eq}$ but the maximum loading of Zr in the organic phase was found to be about 0.23 g/L though the solvent has the capacity to load Zr up to ~50 g/L (theoretical loading) as shown in Fig.5.16.

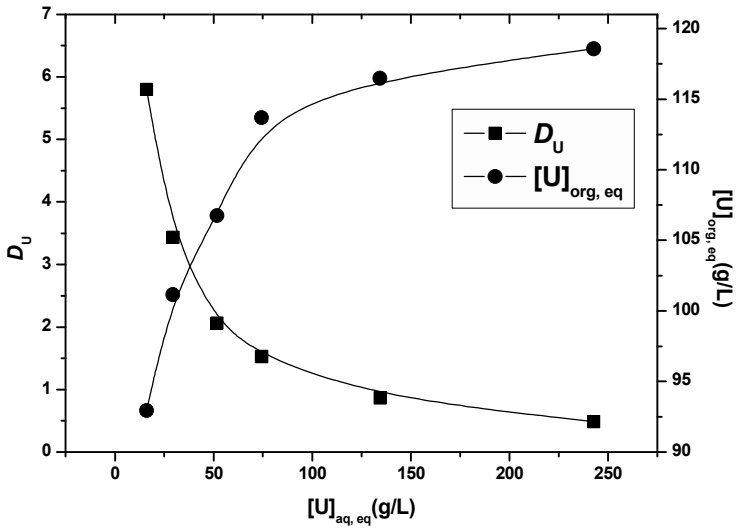

Fig.5.15: Variation of D_U and $[U]_{org, eq}$ with $[U]_{aq, eq}$ for the extraction of U from U-Zr solution in 4.5 M nitric acid by 1.1M TiAP/n-DD at 303 K

As third phase formation was observed during the extraction of Zr in the presence of U by 1.1M TBP/n-DD under the above feed conditions, the concentrations of the feed solution were reduced to ~ 90 g/L and ~ 10 g/L of U and Zr, respectively and studies were carried out using 1.1M TiAP/n-DD and 1.1M TBP/n-DD. Results indicate that TBP does not form third phase under these conditions in various concentration of nitric acid (2-6M). The variation of D_U and D_{Zr} with concentration of nitric acid for the co-extraction of U and Zr by 1.1M TiAP and 1.1M TBP in n-dodecane is shown in Fig.5.17 and Fig.5.18, respectively. The D_U decreases marginally as a function of aqueous phase acidity, whereas D_{Zr} increases with

increase in aqueous phase concentration of nitric acid. Results obtained also confirm that D_U is higher for TiAP than that of TBP and in the case of Zr, *D* values are almost comparable for both the solvents. The marginal decrease in D_U with HNO_3 concentration is due to the competition from acid for the extractant at higher acidities. However in the case of Zr, the *D* values increase with increase in concentration of nitric acid. The reason for this behavior is not known clearly. However it was mentioned [190] that "for most of the elements *D* passes through a maximum as a function of equilibrium HNO_3 concentration due to competition for the extractant by HNO_3. In contrast, D_{Zr} depends only on the total nitrate concentration when extracted from mixtures of HNO_3 and inextractable nitrate salts".

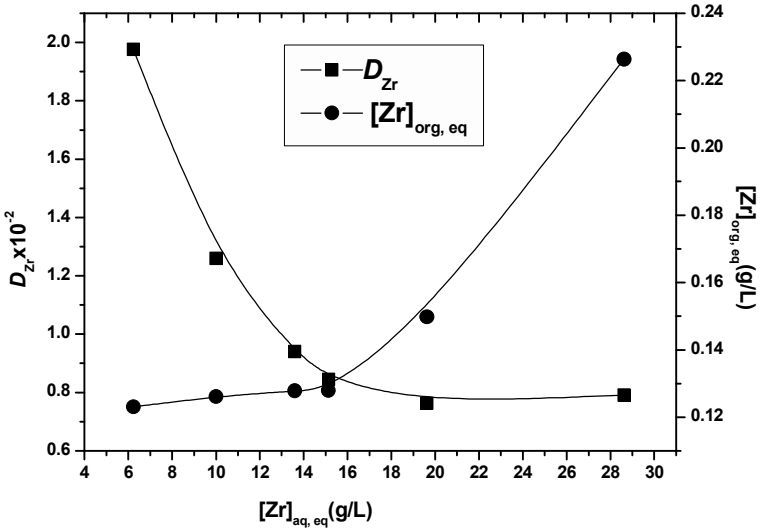

Fig.5.16: Variation of D_{Zr} and $[Zr]_{org, eq}$ with $[Zr]_{aq, eq}$ for the extraction of Zr from U-Zr solution in 4.5 M nitric acid by 1.1M TiAP/n-DD at 303 K

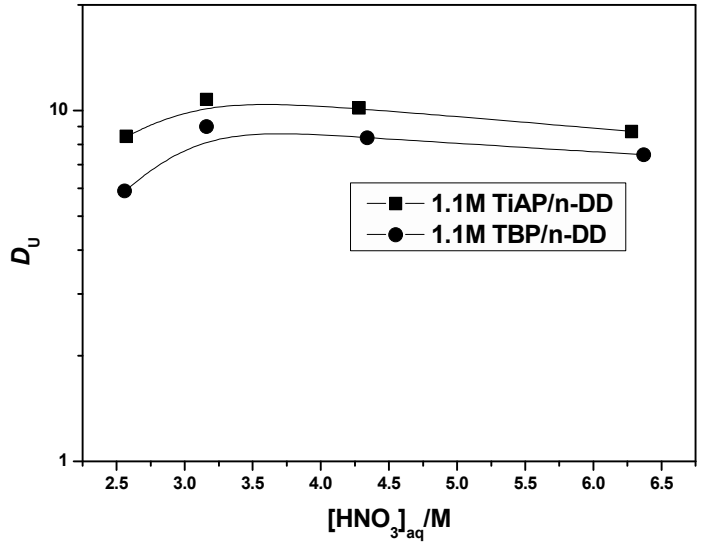

Fig.5.17: Variation of D_U with $[HNO_3]_{aq, eq}$ for extraction of U by 1.1 M TalP/n-DD from U-Zr feed at 303K (U: ~ 90 g/L and Zr: ~ 10 g/L)

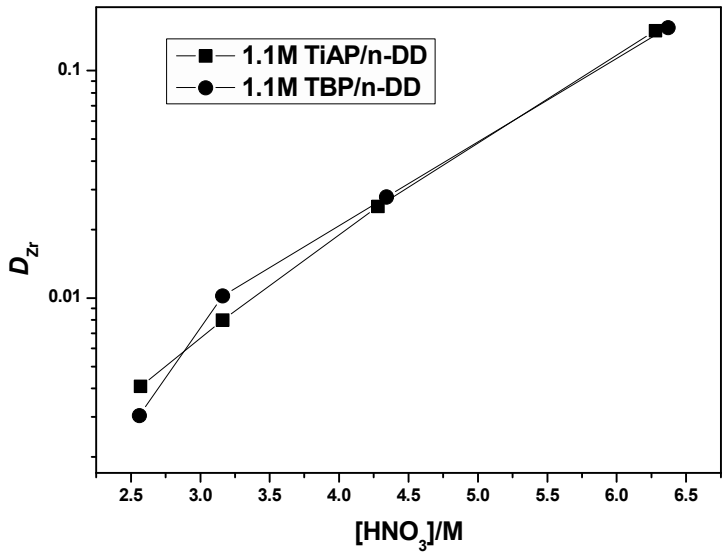

Fig.5.18: Variation of D_{Zr} with $[HNO_3]_{aq, eq}$ for extraction of Zr by 1.1 M TalP/n-DD from U-Zr feed at 303 K (U: ~ 90 g/L and Zr: ~ 10 g/L)

5.4.3: Co-processing of U-Zr feed solutions in cross-current mode

Batch studies were carried out in cross-current mode to evaluate the number of stages required for the extraction and stripping of U and Zr using 1.1M TiAP/n-DD and 1.1M TBP/n-DD system. The concentrations of U, Zr and nitric acid in the feed solution were about

328 and 31.3 g/L, respectively, in 4M HNO_3. The flowsheet for the extraction of these metal ions from the above feed solution using 1.1M TalP/n-DD is shown in Fig.5.19.

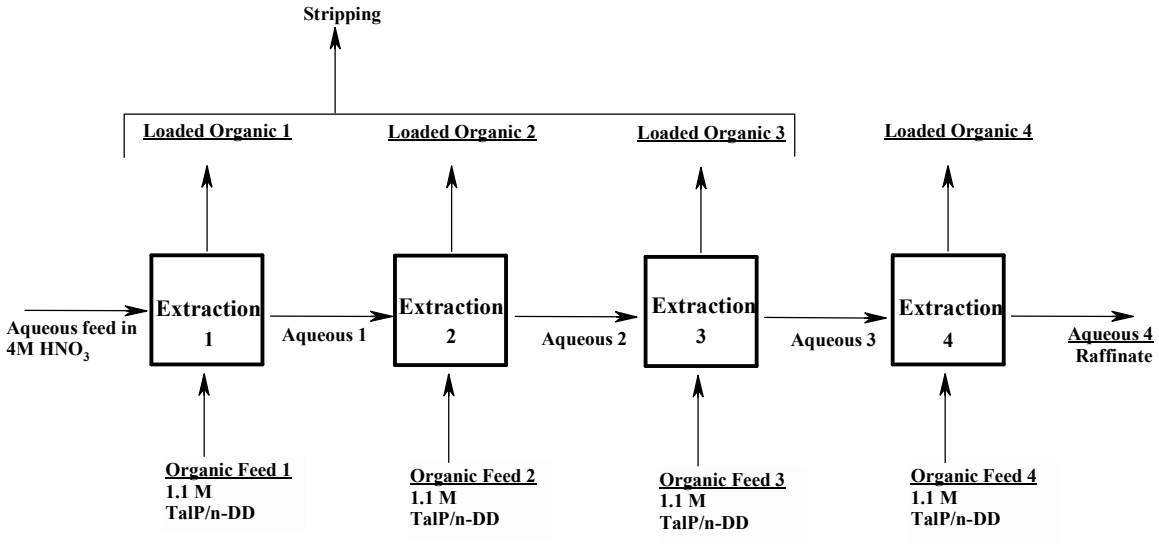

Fig.5.19: Flowsheet for extraction of metal ions from U-Zr and U-Pu-Zr feed solution in 4M HNO_3 by 1.1M TalP/n-DD in cross-current mode at 303 K

The concentrations of U and Zr in the 1st loaded organic phase (LO1) were 131 and 0.27 g/L, respectively and the concentration of U in the loaded organic phase decreased from stage 1 to 4 in the case of TiAP based solvent (Table 5.8). The concentration of U in raffinate was found to be 0.28 g/L after four successive contacts. The quantitative extraction of U (99.9%) was observed within four stages and the extraction of U increased from stage 1 to 4. The acidity of the aqueous phase was maintained close to 4M in all stages using appropriate volume of organic phase comprising of (i) pre-equilibrated organic phase with 4M HNO_3 and (ii) "without pre-equilibrated" organic phase. In the case of Zr, the extraction and concentration of Zr increased from stage 1 to 4, the maximum extraction of Zr was about 15.6% and the raffinate concentration was about 26.4 g/L. The concentration of nitric acid in the loaded organic phase increased from 0.11 to 0.83M from stage 1 to 4 (Table 5.8). Similar experiments were also carried out with 1.1M TBP/n-DD under identical conditions. The extraction behavior of U and Zr by TiAP and TBP systems were found to be similar except

the concentration of U in raffinate was about 0.45 g/L in the case of TBP system against 0.28 g/L of TiAP system (Table 5.8).

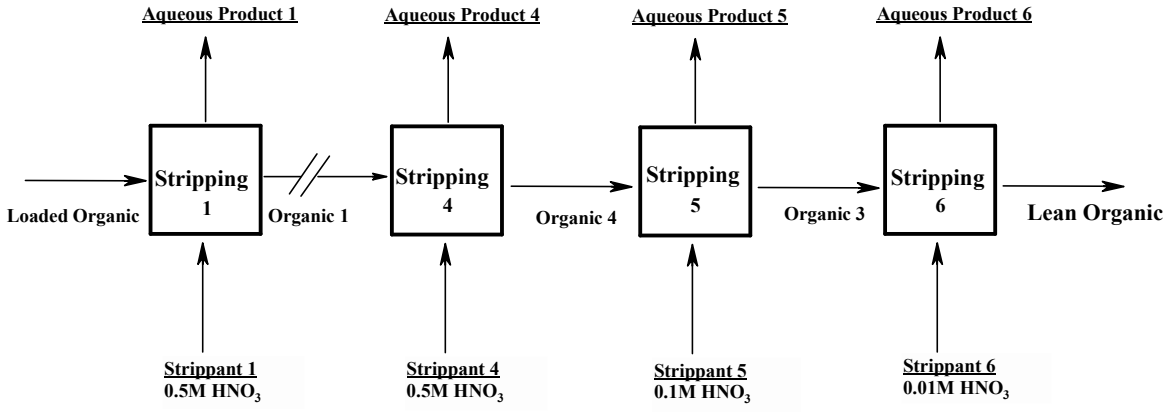

Fig.5.20: Flowsheet for stripping of metal ions from loaded 1.1M TalP/n-DD phase with solutions of nitric acid in cross-current mode at 303 K

Subsequently, stripping of metal ions from loaded organic phase was carried out using different strippants in cross-current mode and the flowsheet is presented in Fig.5.20. In the case of U-Zr system, first three loaded organic samples (LO 1, LO 2 and LO 3) were mixed to prevail the conditions of the PUREX process i.e. to get ~ 80% of the theoretical loading (~130 g/L U by 1.1M TalP/n-DD). Three different strippants such as 0.5M, 0.1M and 0.01M HNO_3 were employed in the first four stages (1 to 4) and in stages 5 and 6, respectively. The concentrations of U and Zr in the feed to the stripping cycle (mixed loaded organic) was found to be 108 and 0.78 g/L, respectively in 0.29M HNO_3. The concentration of Zr in the aqueous phase was found to be below detection limit (<0.2 μg/mL) from stage 3 onwards, indicating complete stripping (> 99.99%) of Zr within the first two stages. The stage profiles for stripping U from loaded 1.1M TiAP/n-DD and 1.1M TBP/n-DD are shown in Fig.5.21. The concentration of U decreases from stage 1 to 6 and the concentration of U in the lean organic were found to be 2.72 g/L after six successive stripping contacts. The concentration and stripping of U (S_U(%)) across various stages are shown in Fig.5.21. The stripping of U was found to be 97.5% and it increased from stage 1 to 6 (Fig.5.21). The significant increase

in the concentration of U in stage 5 was due to stripping using 0.1M HNO_3 rather than 0.5M which was employed in the previous stages (1 to 4). The acidity of the aqueous samples (aqueous product) was also measured (Table 5.9). Similar stage profiles were also observed with 1.1M TBP/n-DD system and the only difference was the concentration of U in lean organic which was 1.85 g/L compared to 2.72 g/L in the case of TiAP. The stripping of U was found to be 98.2%. The higher stripping of U in the case of TBP (98.2%) compared to TiAP (~ 97.5%) is due to lower D_U with TBP at a given concentration of nitric acid [150].

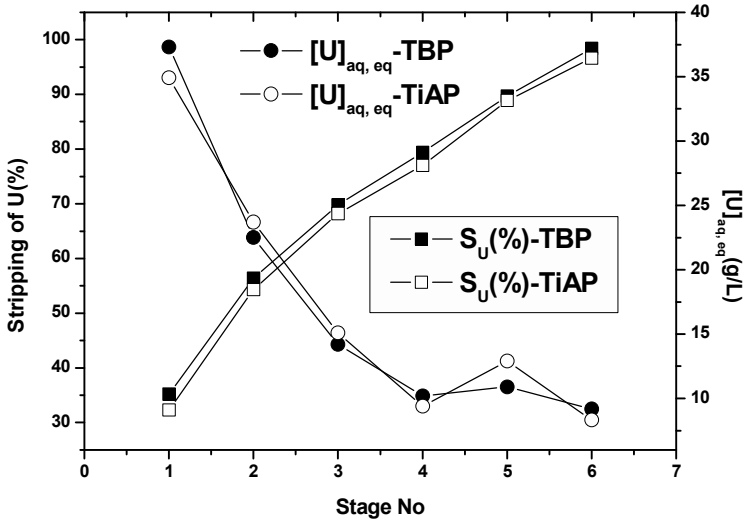

Fig.5.21: Stage profiles for concentrations and stripping of U for co-stripping of U and Zr from 1.1M TalP/n-DD by solutions of nitric acid in cross-current mode at 303K

5.4.4: Co-processing of U-Pu-Zr feed solutions in cross-current mode

Solutions of U, Pu and Zr with concentrations of 156, 19.9 and 6.69 g/L, respectively, in 4M HNO_3 were examined for the co-processing of metal ions in the cross-current mode. The flowsheet employed for the co-processing of U-Zr feed solution was also employed for the co-processing of U-Pu-Zr feed solution (Fig.5.19 and 5.20) and the results are presented in Table 5.10. Co-extraction of U, Pu and Zr from 4M HNO_3 was performed in four stages using 1.1 M TiAP/n-DD systems. The concentrations of U, Pu and Zr in 1st loaded organic were about 103, 14.1 and 0.82 g/L, respectively; the concentrations of U and Zr in the raffinate were about 0.17 and 1.39 g/L whereas the concentration of Pu was found to be BDL (<0.2

μg/mL) indicating that complete extraction of Pu (>99.99%) is possible within three stages. The extraction of U was found to be 99.9% after four successive contacts. The extraction of Zr was about 79.2% after four successive contacts of U-Pu-Zr feed with 1.1M TiAP/n-DD. Similarly, the extraction of U, Pu and Zr was ~99.8%, >99.99% and 83.2%, respectively, in the case of 1.1M TBP/n-DD system; the concentration of U and Zr were 0.27 and 1.12 g/L in raffinate stream and the concentration of Pu was found to be BDL. The extraction of Zr (79.2%) in the case of U-Pu-Zr system by 1.1M TiAP/n-DD was higher compared to its extraction (15.6%) with U-Zr system. This is because, the concentration of U in the U-Zr feed was much higher; therefore the loading of U in the organic phase was found to be higher in the case of U-Zr system leading to lower extraction of Zr (~15.6%). Similar trend was observed in the case of TBP system.

Metal ions were stripped from loaded organic phase (1.1M TiAP/n-DD) using three strippants in cross-current mode. In the case of U-Pu-Zr system, only first two loaded organic samples were mixed to get maximum feed concentration (loaded organic) to the stripping cycle. The concentrations of U, Pu and Zr in the loaded organic were 74.8, 9.78 and 1.61 g/L (Table 5.11). The concentration and stripping of U (S_U(%)) across various stages are shown in Fig.5.22. The concentration of U in the aqueous product decreased, whereas % stripping of U (S_U) increased from stage 1 to 6. The observed stripping percentages of U, Pu and Zr were ~ 96.9%, > 99.99% and > 99.99% in six, three and two stages, respectively. The exit sample (lean organic) contained about 2.33 g/L of U with BDL (<0.2 μg/mL) of Pu and Zr. TBP based solvent also exhibited similar stripping behavior apart from the higher stripping of U (98.5%) and the lower concentration of U (1.12 g/L) in the exit sample compared to that of TiAP based solvent system.

Results from both the flowsheets i.e. U-Zr as well as U-Pu-Zr systems indicated that quantitative extraction (> 99%) of U and Pu occur within 3 to 4 stages, whereas stripping of U (> 96%) in six stages and Pu (> 99%) in four stages can be achieved with both TBP and TiAP

based solvent systems in cross-current mode. However, the extraction of Zr mainly depends on the loading of U and Pu in the organic phase. The extraction of Zr into the organic phase can be minimized by saturating the organic phase with U and Pu when the decontamination factors are matter of concern during the PUREX process. The extraction of U and Pu by 1.1M TiAP/n-DD is marginally higher and stripping of metal ions is marginally lower compared to 1.1M TBP/n-DD system.

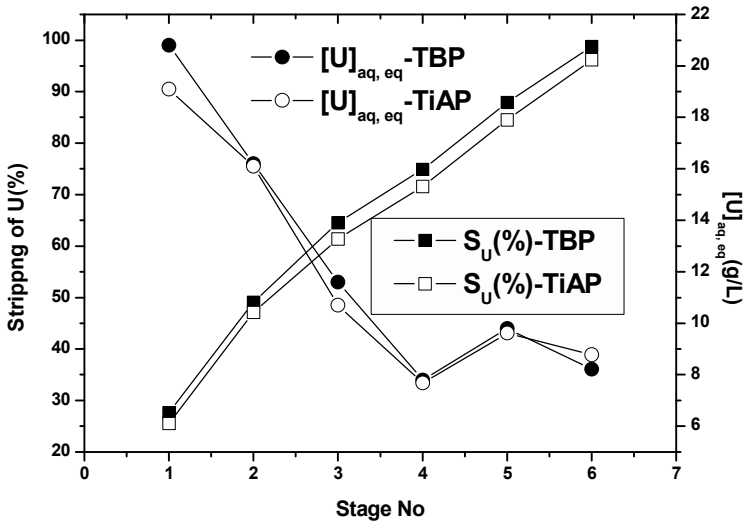

Fig.5.22: Stage profiles for concentrations and stripping of U for co-stripping of U, Pu and Zr from 1.1M TalP/n-DD loaded with nitric acid in cross-current mode at 303K

Table 5.8: Concentrations and extraction (%) for the co-extraction of U and Zr from 4M HNO_3 by 1.1M TalP/n-DD in cross-current mode at 303K

Stream	1.1M TiAP/n-DD					1.1M TBP/n-DD				
	[U] (g/L)	Extraction of U (%)	[Zr] (g/L)	Extraction of Zr (%)	[HNO_3] (M)	[U] (g/L)	Extraction of U (%)	[Zr] (g/L)	Extraction of Zr (%)	[HNO_3] (M)
Aq.										
Feed	328	-	31.3	-	4.1	328	-	31.3	-	4.1
LO1	131	39.9	0.27	0.86	0.11	127	38.7	0.27	0.86	0.12
LO2	114	74.7	0.34	1.95	0.14	114	73.5	0.33	1.92	0.14
LO3	75.8	97.8	1.72	7.44	0.53	77.4	97.1	1.44	6.52	0.49
LO4	6.62	99.9	2.47	15.6	0.83	8.88	99.9	2.76	16.3	0.81
Raffinate	0.28	-	26.4	-	3.98	0.45	-	26.2	-	4.1

Table 5.9: Concentrations and stripping (%) for the co-stripping of U and Zr from nitric acid media by 1.1M TalP/n-DD in cross-current mode at 303K

Stream	1.1M TiAP/n-DD					1.1M TBP/n-DD				
	[U] (g/L)	Stripping of U (%)	[Zr] (g/L)	Stripping of Zr (%)	$[HNO_3]$ (M)	[U] (g/L)	Stripping of U (%)	[Zr] (g/L)	Stripping of Zr (%)	$[HNO_3]$ (M)
Loaded Organic	108	-	0.78	-	0.29	106	-	0.73	-	0.27
AP1	34.9	32.3	0.76	97.4	0.8	37.3	35.2	0.59	80.8	0.81
AP2	23.7	54.3	0.03	>99.99	0.56	22.5	56.4	0.12	>99.99	0.57
AP3	15.1	68.2	-	-	0.55	14.2	69.8	-	-	0.54
AP4	9.41	77.0	-	-	0.54	10.2	79.4	-	-	0.53
AP5	12.9	88.9	-	-	0.11	10.9	89.7	-	-	0.1
AP6	8.32	97.5	-		0.01	9.18	98.2	-	-	0.01
Lean Organic	2.72	-	-	-	<0.01	1.85	-	-	-	<0.01

Table 5.10: Concentrations and extraction (%) for the co-extraction of U, Pu and Zr from 4M HNO_3 by 1.1M TalP/n-DD in cross-current mode at 303K

Stream	1.1M TiAP/n-DD						1.1M TBP/n-DD					
	[U] (g/L)	Extraction of U (%)	[Pu] (g/L)	Extraction of Pu (%)	[Zr] (g/L)	Extraction of Zr (%)	[U] (g/L)	Extraction of U (%)	[Pu] (g/L)	Extraction of Pu (%)	[Zr] (g/L)	Extraction of Zr (%)
Aq.												
Feed	156	-	19.9	-	6.69	-	156		19.9	-	6.69	-
LO1	103	66.0	14.1	70.9	0.82	12.3	103	66.0	13.7	68.8	0.58	8.67
LO2	46.1	95.6	5.58	98.9	2.41	48.3	45.3	95.1	6.1	99.5	2.46	45.4
LO3	5.54	99.1	0.19	>99.99	1.45	70.0	5.59	98.6	0.25	>99.99	1.88	73.5
LO4	1.03	99.9	-	-	0.59	79.2	1.12	99.8	-	-	0.71	83.2
Raffinate	0.17	-	-	-	1.39	-	0.27	-	-	-	1.12	-

Table 5.11: Concentrations and stripping (%) for the co-stripping of U, Pu and Zr from nitric acid media by 1.1M TalP/n-DD in cross-current mode at 303K

Stream	1.1M TiAP/n-DD						1.1M TBP/n-DD					
	[U] (g/L)	Stripping of U (%)	[Pu] (g/L)	Stripping of Pu (%)	[Zr] (g/L)	Stripping of Zr (%)	[U] (g/L)	Stripping of U (%)	[Pu] (g/L)	Stripping of Pu (%)	[Zr] (g/L)	Stripping of Zr (%)
Loaded Organic	74.8	-	9.78	-	1.61	-	75.3	-	9.72	-	1.77	-
AP1	19.1	25.5	4.96	50.7	1.52	94.4	20.8	27.6	4.93	50.7	1.65	93.2
AP2	16.1	47.1	2.69	78.2	0.05	>99.99	16.2	49.1	2.98	81.4	0.08	>99.99
AP3	10.7	61.4	1.59	94.5	-	-	11.6	64.5	1.53	97.1	-	
AP4	7.68	71.6	0.27	>99.99	-	-	7.8	74.9	0.07	>99.99	-	-
AP5	9.62	84.5	-	-	-	-	9.79	87.9	-	-	-	-
AP6	8.78	96.9	-	-	-	-	8.21	98.5	-	-	-	-
Lean Organic	2.33	-	-	-	-	-	1.12		-	-	-	-

5.5 Conclusions

In the present work, dissolution, characterisation and solvent extraction studies with metallic alloys were carried out with an objective to develop an alternate method to pyrochemical reprocessing of metallic alloy fuels. Dissolution studies with U-Zr as well as U-Pu-Zr based metal alloy samples indicated that complete dissolution of uranium/plutonium and partial dissolution of Zr. The present study demonstrates that there is no enhancement in the dissolution of Zr by EODT. A modified spectrophotometric method has been developed for the determination of zirconium in a large excess of uranium and plutonium (U: Pu: Zr = 1000:400:1).

Batch extraction studies indicated third phase formation of Zr in the presence of uranium with TBP based solvent. However, TiAP based solvent system does not form third phase under identical conditions. Batch studies were carried out for the co-processing of U-Zr and U-Pu-Zr alloy fuels with TiAP and TBP extractant systems in a cross-current mode. These studies indicated that loss of U and Pu into the raffinate and lean organic streams has been negligible. The preliminary studies on aqueous processing of metallic fuels demonstrate that TiAP based solvent can be employed for the processing of metallic alloy based fuels. These studies may pave way for the development of alternate route of metal fuel reprocessing using PUREX process.

Chapter 6

THERMAL DECOMPOSITION STUDIES WITH TiAP AND TBP SOLVENTS

6

6.1 Introduction

In addition to having lower tendency for the formation of third phase, TiAP also has lower aqueous solubility (~ 80 mg/L) which minimizes the solubilised extractant getting into the aqueous stream during the evaporation process, where extractant comes into contact with nitric acid of higher concentration and metal nitrates. Hence, with the employment of TiAP based solvent system, the thermal runaway reactions can be minimized in evaporators and de-nitrators, where rapid exothermic reactions are likely to occur between extractant, nitric acid and heavy metal nitrates. TiAP also undergoes radiolytic degradation and generates degradation products similar to that of TBP. The effect of radiolysis on thermal decomposition of TiAP-HNO_3 system has not been studied in detail. Prior to the deployment of TiAP in reprocessing plants, it is important to study the thermal decomposition behaviour of irradiated and unirradiated TiAP-HNO_3 biphasic systems comprising of organic and aqueous phases under the simulated plant conditions.

In this context, the thermal decomposition of TiAP-HNO_3 systems has been examined under various experimental condtitions. The studies were carried out by varying the parameters such as concentration of nitric acid, HNO_3/TiAP volume ratio, gamma irradiation and presence of diluent. Thermo kinetic parameters have been derived from the experimental data. The results of unirradiated TiAP-HNO_3 system have been compared with the irradiated system. The effect of radiolytic degradation products on decomposition enthalpies has been studied in detail. The gaseous end products generated during thermal decomposition were characterized by employing techniques such as FT-IR and QMS. Similarly studies were also carried out with TBP based solvent under identical conditions and results obtained are compared with TiAP-HNO_3 systems.

6.2 Thermal decomposition studies of TBP-HNO_3 and TiAP-HNO_3 systems

6.2.1 Thermal decomposition of neat TiAP and TBP

Fig. 6.1 and 6.2 shows that neat TiAP and TBP are stable up to 540 and 527 K, respectively; both exhibit a small endothermic peak, which is possibly due to boiling of these extractants. Subsequently exothermic reactions due to decomposition of solvents were observed. As soon as the temperature reaches 773 K (calorimeter limit), the instrument terminates heating / searching pattern, thereby allowing the contents of the vessel to reach ambient temperature by natural cooling. The variation of pressure with time is shown in Fig. 6.1 and 6.2. The sharp rise in pressure confirms boiling of TiAP and TBP followed by decomposition. A steady rise in pressure seen in curve 1a (Fig. 6.1) indicates formation of gaseous products by the decomposition of TiAP and TBP. The pressure stabilizes at ~ 6 bar even after temperature reaches ambient, confirming formation of non-condensable gases. The enthalpy of decomposition of neat TiAP and TBP could not be derived due to incomplete reaction.

6.2.2 Effect of HNO_3 concentration

Curves 2 and 2a (Fig. 6.1) are the plots of temperature and pressure profiles versus time for the decomposition of TiAP-4M HNO_3 (1:3) mixture. The decomposition of TiAP in the presence of 4M nitric acid commences at 404 K and stabilizes at 499 K (Table 6.1); the resulting increase in temperature was about 96 K, which indicates enhancement of the decomposition reaction and lowering of onset temperature due to the presence of HNO_3 compared to that of neat TiAP.

As seen in curve 3 of Fig. 6.1, the decomposition of TiAP-8M HNO_3 (1:3) begins at 393 K with a temperature rise of about 173 K. It shows a spike due to the inability of the instrument in maintaining adiabatic conditions under high heat rise rates of ~ $300^oC\ min^{-1}$ which far exceeds the $100^oC\ min^{-1}$ heating rate of the surrounding heater. The onset temperatures for TiAP-8M HNO_3 system was found to be lower than that of TiAP-4M HNO_3

system and this substantiates the fact that the decomposition of TiAP is accelerated by nitric acid and the onset temperature has a strong dependence on the concentration and amount of nitric acid present in the system. Pressure rise behaviour (Fig.6.1 curve 3a) was also found to follow a similar trend as in the case of TiAP-4M HNO_3 system.

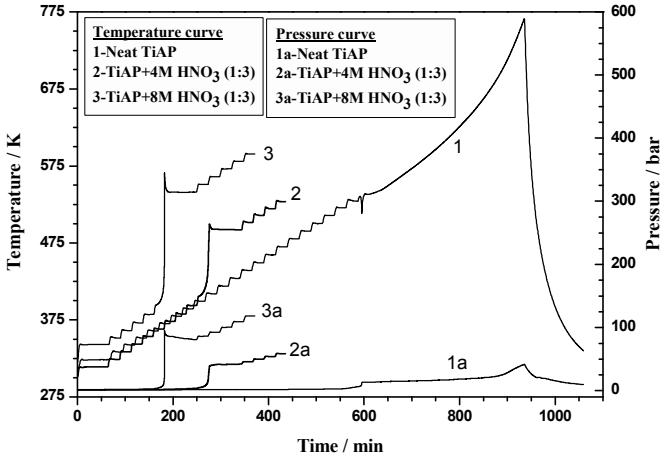

Fig.6.1: Plot of temperature and pressure vs time for the decomposition of (1) Neat TiAP, (2) TiAP-4M HNO_3 (1:3) and (3) TiAP-8M HNO_3 (1:3)

Thermal decomposition behaviour of unirradiated TBP in the presence of 4 and 8M HNO_3 is shown in Fig. 6.2. Curves 2 and 3 of Fig. 6.2 are the temperature profiles for the systems TBP-4M HNO_3 (1:3) and TBP-8M HNO_3 (1:3) respectively. Pressure profiles for the corresponding systems are shown in curves 2a and 3a. The decomposition of TBP commences at 410 K in the presence of 4M HNO_3 while it starts decomposing at lower temperature (395 K) in the presence of 8M HNO_3 (Table 6.2). The temperature and pressure rise was found to be 70 K, 168 K and 29 and 92 bar, respectively with 4 and 8M nitric acid.

6.2.3 Effect of organic to acid volume ratio

The effect of volume ratio of organic to acid on the decomposition behaviour of 1.1M TiAP/n-DD with 8M HNO_3, is presented in Fig. 6.3, in the form of temperature and pressure profiles versus time. Biphasic systems of 1.1M TiAP/n-DD and 8M HNO_3 with volume ratios 1:3 and 3:1 exhibit decomposition at 401 ± 2 K, whereas the sample with volume ratio 1:1 decomposes at 384 K (Table 6.1). However, the temperature rise showed a systematic

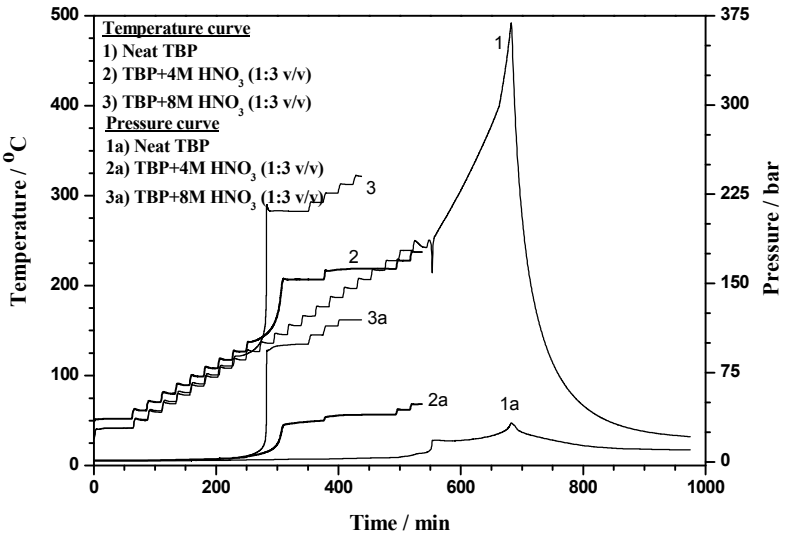

Fig.6.2: Plot of temperature and pressure vs time for the decomposition of 1) Neat TBP, 2) TBP-4M HNO_3 (1:3) and 3) TBP-8M HNO_3 (1:3)

decrease with increase in organic to nitric acid phase ratio. It was also observed that temperature and pressure rise is lower in the presence of a diluent compared to neat TiAP-HNO_3 systems, except with 8M HNO_3 (1:3). In this case, possibly n-DD might have decomposed along with TiAP due to the presence of higher concentration and volume of nitric acid, resulting in higher rise in temperature and pressure compared to neat TiAP-8M HNO_3 (1:3). The temperature rise for the decomposition of 1.1M TiAP/n-DD-8M HNO_3 with different volume ratios 1:3, 1:1 and 3:1 were found to be 175, 82 and 51 K respectively and corresponding pressure rise was found to be 97, 24 and 11 bar respectively. The temperature and pressure rise were found to be higher in the case of 1:3 (TiAP/HNO_3) and found to be negligible in the case of 3:1, revealing that the magnitude of decomposition of TiAP is higher with higher nitric acid content.

Similarly, the effect of volume ratio (organic/acid) on thermal decomposition of 1.1M TBP/n-DD) has been investigated under identical conditions (Fig.6.4). The corresponding mole fraction of nitric acid for 4M and 8M is represented in Table 6.2. The onset temperature increases with decrease of nitric acid mole fraction (χ_{HNO3}) indicating that the decomposition gets initiated at lower temperature when the mole fraction of nitric acid is higher. For e.g. for

TBP-4M HNO_3 system, onset of decomposition temperatures are 410 and 421K when the mole fractions of nitric acid (χ_{HNO3}) are 0.76 and 0.27 respectively (Table 6.2).

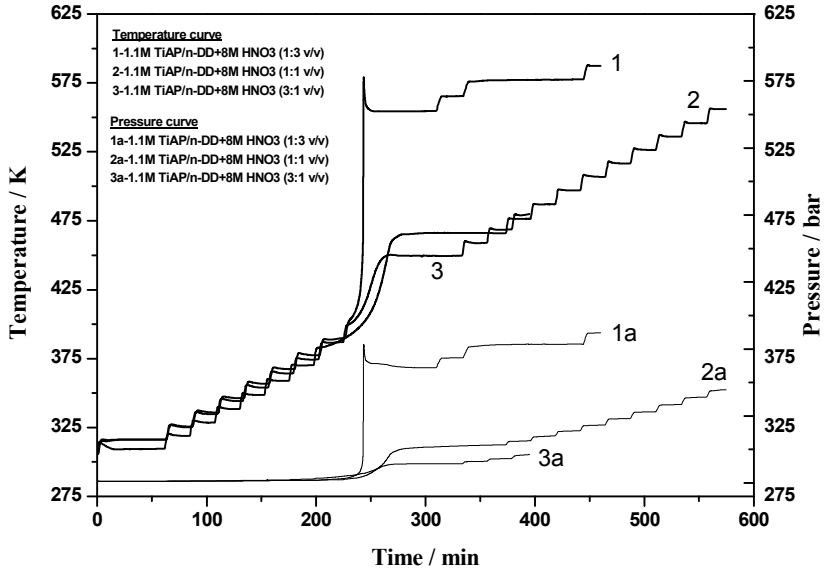

Fig.6.3: Effect of phase ratio (HNO_3/TiAP) on temperature and pressure vs time for the decomposition of unirradiated TiAP-HNO_3 system. 1)1.1M TiAP/n-DD-8M HNO_3 (1:3v/v), 2) 1.1M TiAP/n-DD-8M HNO_3 (1:1 v/v), 3)1.1M TiAP/n-DD-8M HNO_3 (3:1 v/v)

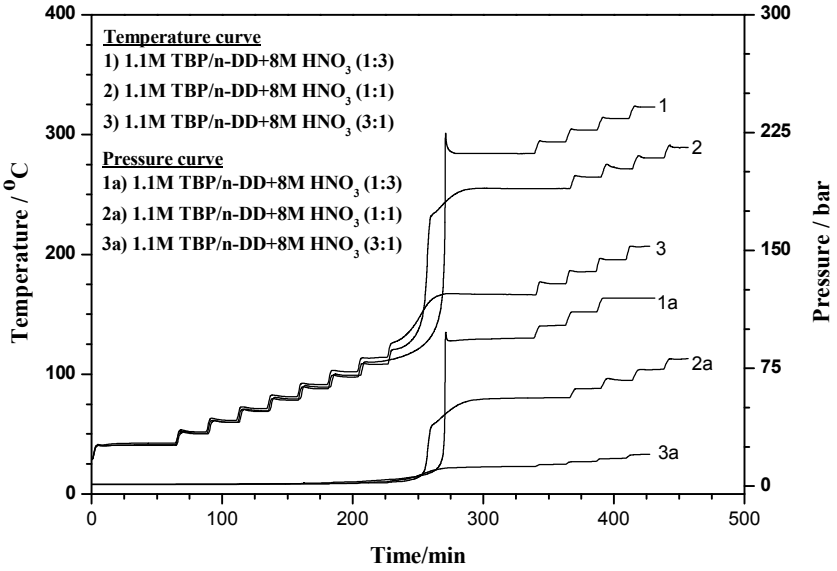

Fig.6.4: Effect of phase ratio (organic/acid) on temperature and pressure vs time for the decomposition of un-irradiated 1.1M solution of TBP in n-DD-HNO_3 system

6.2.4 Effect of diluent (n-DD)

The effect of diluent on thermal decomposition of TiAP and TBP was studied using n-DD. A solution of 1.1M TiAP in n-DD is thermally stable up to 525 K and subsequently exhibits an exothermic decomposition in the absence of nitric acid and the temperature rise

exceeded 773 K (limit of the calorimeter). The presence of nitric acid decreases the thermal stability of 1.1M TiAP/n-DD leading to decomposition at lower temperatures from 384 to 412 K. Similarly, the onset of decomposition for 1.1M TBP/n-DD is found to be 509 K and is significantly lower compared to that of neat TBP (527K). The thermal decomposition of 1.1M TBP/n-DD system was studied in the presence of nitric acid with different volume ratios. In most of the cases for 1.1M TBP/n-DD-HNO_3 system, the decomposition commences at lower temperature than that of neat TBP-HNO_3 system under identical conditions. However in the case of 1.1M TBP/n-DD-4M HNO_3 (3:1), the onset temperature is found to be significantly higher compared to neat TBP system and this may be due to insufficient nitric acid for oxidation of 1.1M TBP/n-DD. The temperature rise and pressure rise for 1.1M TBP/n-DD-HNO_3 system is significantly lower compared to that of TBP-HNO_3 system, except in the case of 8M HNO_3(1:3). In this case, the temperature rise was found to be significantly higher (191K) compared to that of TBP-8M HNO_3 (168K). This may be due to complete decomposition of TBP and n-DD in the presence of high nitric acid (15mmoles).

6.2.5 Effect of irradiation

Fig.6.5 depicts thermal decomposition behavior of irradiated samples of neat TiAP, TiAP-8M HNO_3 (1:1) and 1.1M TiAP/n-DD-8M HNO_3 (1:1) systems. Results obtained indicate that the onset temperature for irradiated TiAP is lower (493 K) than that of unirradiated TiAP (538 K). Similarly, thermal decomposition behavior of irradiated neat TBP, TBP-8M HNO_3 (1:1 v/v) and 1.1M TBP/n-DD-8M HNO_3 (1:1 v/v) are shown in Fig. 6.6. Irradiated neat TBP is found to be stable up to 513 K. Decomposition of irradiated TiAP-4M HNO_3 mixtures with volume ratios 1:3, 1:1 and 3:1 begins at temperature 404 ± 2 K (Table 6.3) indicating that these systems are almost comparable to unirradiated TiAP-4M HNO_3 system. The rise in temperature and pressure were found to be 59, 31, 7 K and 11, 10, 3 bar respectively, for the decomposition of irradiated TiAP-4M HNO_3 (3:1, 1:1 and 3:1) systems (Table 6.3). The corresponding values for the decomposition of unirradiated TiAP-

4M HNO_3 systems were found to be 96, 54, 6 K and 38, 17, 3 bar respectively. The rise in temperature and pressure for the decomposition of irradiated TiAP-HNO_3 systems are significantly lower compared to unirradiated TiAP-HNO_3 systems.

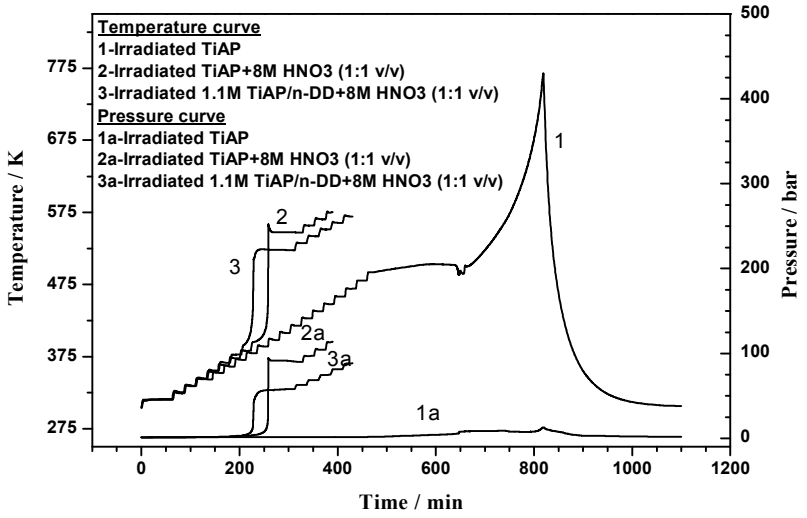

Fig.6.5: Plot of temperature and pressure vs time for the decomposition of irradiated 1) TiAP, 2) TiAP-8M HNO_3 (1:1) and 3) 1.1M TiAP/n-DD-8M HNO_3 (1:1)

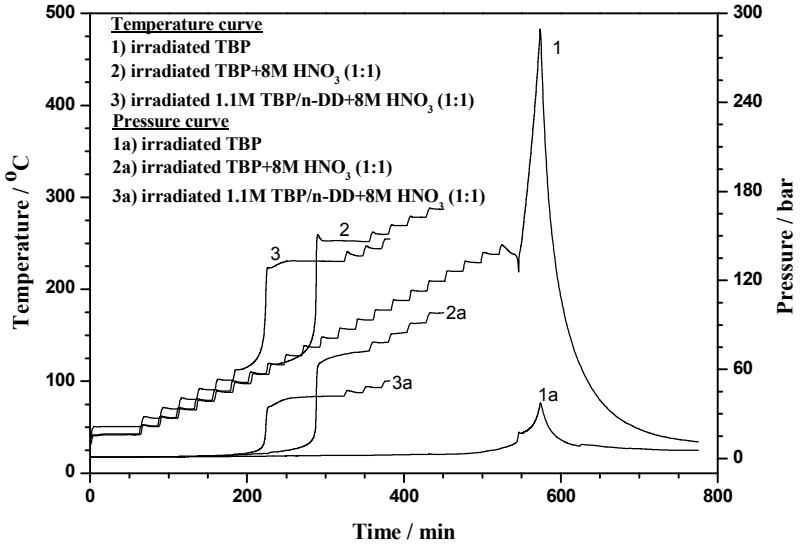

Fig.6.6: Plot of temperature and pressure vs time for the decomposition of irradiated 1) TBP, 2) TBP-8M HNO_3 (1:1) and 3) 1.1M TBP/n-DD-8M HNO_3 (1:1)

6.2.6 Thermal decomposition of DBP+MBP-HNO_3

Thermal decomposition of DBP and MBP has been investigated in the presence of nitric acid. The decomposition behaviors of neat DBP+MBP, DBP+MBP-4M HNO_3 and DBP+MBP-8M HNO_3 are presented in Fig. 6.7. The neat DBP+MBP (30-50%) mixture is

found to be stable up to 487 K. The decomposition of DBP+MBP in the presence of 4M and 8M HNO_3 (1:1) commences at 394 and 388 K, respectively (Table 6.2); the resulting increase in temperature was about 55 and 131 K, indicating an enhancement of decomposition reaction and lowering of onset temperature due to oxidation of DBP+MBP in the presence of HNO_3 compared to that of neat DBP+MBP. The corresponding pressure rise in the presence of 4M and 8M HNO_3 is about 15 and 54 respectively (Table 6.2).

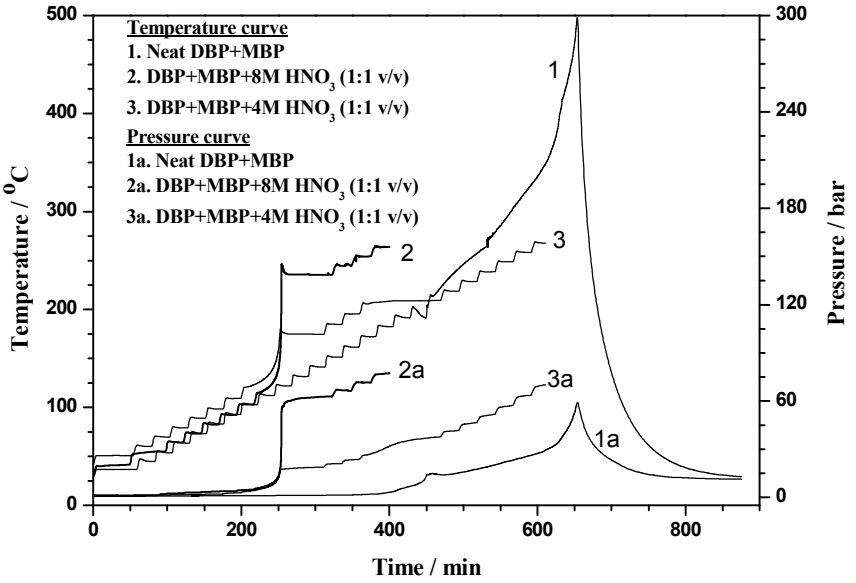

Fig.6.7: Plot of temperature and pressure vs time for the decomposition of 1) Neat DBP+MBP, 2) DBP+MBP-8M HNO_3(1:1) and 3) DBP+MBP-4M HNO_3(1:1)

6.3 Adiabatic temperature rise

The true adiabatic temperature (T_{ad}) and pressure rise (P_{ad}) per unit mass of TiAP and TBP decomposition are plotted against mole fraction of nitric acid and are shown in Fig. 6.8 and Fig.6.9, respectively. T_{ad} and P_{ad} increases exponentially with increase in mole fraction of nitric acid (χ_{HNO3}) for TiAP-HNO_3 and TBP-HNO_3 systems. The temperature and pressure rise per gram of TiAP decomposition are about 16 K and 1.8 bar, respectively when χ_{HNO3} is 0.31 and are about are 1195 K and 189 bar when χ_{HNO3} is 0.88. These values are about 75 and 105 times higher when χ_{HNO3} increased from 0.31 to 0.88 respectively (Table 6.1). The exponential rise of T_{ad} and P_{ad} reveals that the system under evaporation with higher HNO_3 to TiAP or TBP ratios may result in runaway reactions, if heated beyond ~ 390 K and it could

reach high temperature (~ 1,195 K) and pressure (190 bar) per gram of TiAP or TBP decomposition and. Hence, to ensure safety of the plant and personnel, efforts must be taken to avoid presence of solubilised or entrained TiAP or TBP in the aqueous streams during evaporation.

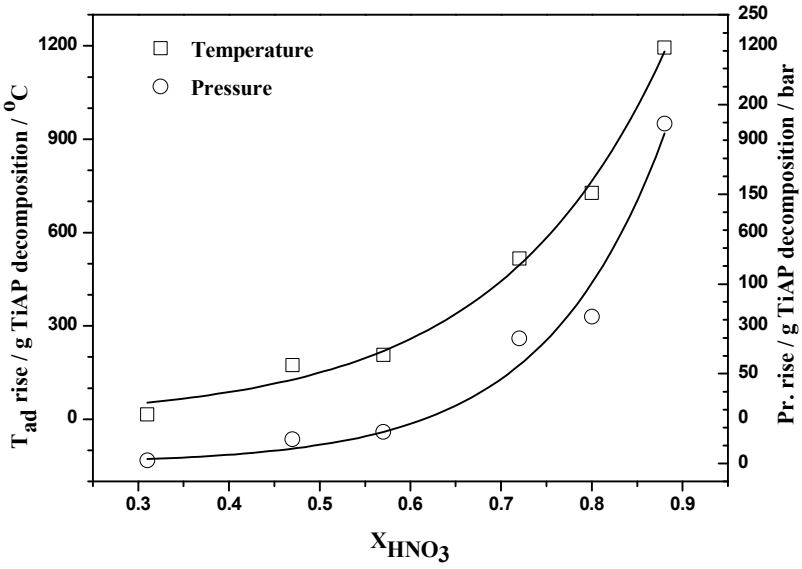

Fig.6.8: Plot of rise in true temperature and pressure per gram of TiAP decomposition for unirradiated TiAP-HNO_3 system

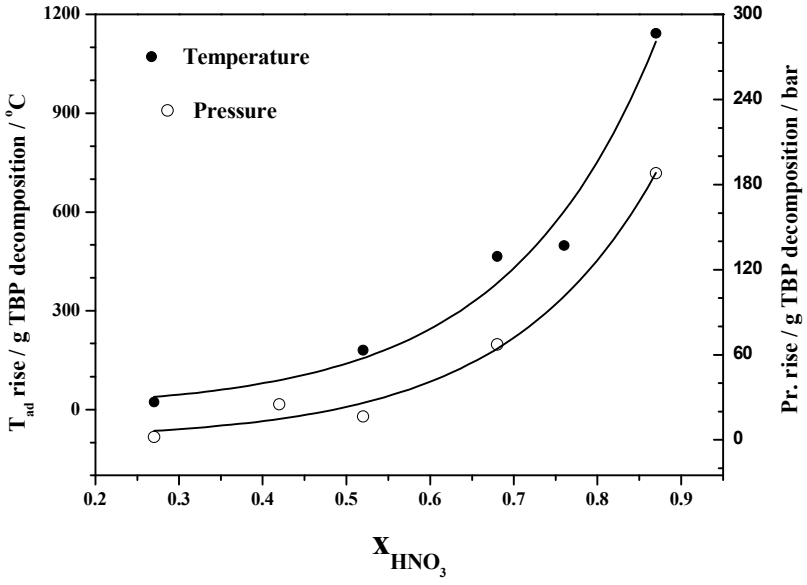

Fig.6.9: Plot of rise in true temperature and pressure per gram of TBP decomposition for unirradiated TBP-HNO_3 system

Table 6.1: List of experiments carried out with unirradiated TiAP-HNO_3 system

System/(TiAP:HNO_3 v/v ratio) (M = mol dm^{-3})	T_i/K	ΔT_{exp} (K)	ΔP_{exp} (bar)	Φ factor	ΔT_{ad} (K)	χ_{HNO3}	$-\Delta H$ / kJ kg^{-1} (Error ±1%)	E_a / kJ mol^{-1} (Error ±1%)[#]	A (Error ±1%) [#]	n (Error ±5%)
Neat TiAP[a]	540									
TiAP-4M HNO_3 (1:3)	404	96	38	3.53	338	0.80	677	134	$1.1x10^{14}$	1.40
TiAP-4M HNO_3 (1:1)	404	54	17	3.63	195	0.58	390	167	$3.5x10^{18}$	1.89
TiAP-4M HNO_3 (3:1)	413	6	3	3.80	22	0.31	46	329	$1.1x10^{40}$	0.76
TiAP-8M HNO_3 (1:3)	393	173	91	3.33	575	0.89	1149	139	$1.1x10^{16}$	1.86
TiAP-8M HNO_3 (1:1)	393	139	62	3.52	491	0.73	981	128	$4.3x10^{14}$	1.79
TiAP-8M HNO_3 (3:1)	399	66	19	3.71	245	0.47	490	187	$8.3x10^{21}$	1.91
1.1M TiAP/nDD[a]	525	-	-	-	-	-	-	-	-	
1.1M TiAP/n-DD-4M HNO_3 (1:3)	408	61	21	3.64	223		447	124	$4.2x10^{13}$	1.24
1.1M TiAP/n-DD-4M HNO_3 (1:1)	409	24	7	3.87	93		186	116	$7.3x10^{9}$	1.06
1.1M TiAP/n-DD-4M HNO_3 (3:1)[b]	412	2	2	-	-		-	-	-	
1.1M TiAP/n-DD-8M HNO_3 (1:3)	403	175	97	3.42	601		1202	84	$6.7x10^{6}$	0.93
1.1M TiAP/n-DD-8M HNO_3 (1:1)	384	82	24	3.67	302		606	119	$1.1x10^{11}$	1.17
1.1M TiAP/n-DD-8M HNO_3 (3:1)	399	51	11	3.96	204		408	147	$2.3x10^{15}$	1.97

[a]Temperature rise exceeded 773 K calorimeter limit and hence, thermo-kinetic parameters not calculated.

[b]Temperature rise too small and hence, thermo-kinetic parameters not calculated

[#]The errors obtained for the experiments conducted in duplicates / triplicates

Table 6.2: List of experiments carried out with unirradiated TBP-HNO_3 system

System	χ_{HNO3}	T_i/K	ΔT_{exp}/ K	ΔP_{exp}/bar	Φ factor	ΔT_{ad}/ K	-Δ H/ kJ kg^{-1} (Error ±1%)[#]	E_a/ kJ mol^{-1} (Error ±1%)[#]	A (Error ±1%)[#]	n (Error ±5%)[#]
Neat TBP[a]		527	-	-	-	-	-	-	-	-
TBP-4M HNO_3 (1:3)	0.76	410	70	29	3.53	247	495	136	$6.7x10^{14}$	0.87
TBP-4M HNO_3(1:1)	0.52	414	48	16	3.63	174	349	135	$1.09x10^{16}$	0.99
TBP-4M HNO_3(3:1)	0.27	421	9	3	3.80	34	68	259	$2.77x10^{30}$	0.77
TBP-8M HNO_3(1:3)	0.87	395	168	92	3.33	559	1122	132	$4.65x10^{14}$	1.05
TBP-8M HNO_3(1:1)	0.68	403	129	66	3.52	454	897	134	$2.2x10^{14}$	0.99
TBP-8M HNO_3(v/v ratio) (3:1)	0.42	405	103	36	3.71	382	747	166	$1.15x10^{16}$	0.94
Neat 1.1M TBP/n-DD[a]	-	509	-	-	-	-	-	-	-	-
1.1M TBP/n-DD-4M HNO_3(1:3)		400	51	17	3.58	182	362	75	$2.97x10^{7}$	0.73
1.1M TBP/n-DD-4M HNO_3 (1:1)		408	28	7	3.84	107	213	63	$1.52x10^{6}$	0.89
1.1M TBP/n-DD-4M HNO_3 (3:1)[b]		499	-	-	-	-	-	-	-	-
1.1M TBP/n-DD-8M HNO_3 (1:3)		383	191	93	3.39	647	1295	103	$1.62x10^{11}$	1.08
1.1M TBP/n-DD-8M HNO_3 (1:1)		394	135	53	3.65	493	981	55	$1.86x10^{5}$	1.32
1.1M TBP/n-DD-8M HNO_3 (3:1)		394	34	9	3.94	134	267	116	$1.30x10^{13}$	0.87
Neat DBP+MBP[a]		487	-	-	-	-	-	-	-	-
(DBP+MBP)-4M HNO_3 (1:1)		394	55	15	3.51	194	409	165	$2.04x10^{19}$	0.87
(DBP+MBP)-8M HNO_3 (1:1)		388	131	54	3.37	441	887	140	$1.66x10^{16}$	1.44

[a]Temperature rise exceeded 773 K calorimeter limit and hence, thermo-kinetic parameters not calculated.

[b]Temperature rise too small and hence, thermo-kinetic parameters not calculated

[#]The errors obtained for the experiments conducted in triplicates

6.4 Enthalpies of decomposition

The enthalpy of decomposition for unirradiated TiAP-4M HNO_3 with v/v ratios 1:3, 1:1 and 3:1 was derived and found to be −677, −390 and −46 kJ kg^{-1} of mixture, respectively, while the enthalpies obtained for the decomposition of TiAP-8M HNO_3 systems were found to be, −1149, −981, −490 kJ kg^{-1} of mixture, respectively. The enthalpy change increases with increase in concentration of nitric acid from 4 to 8M HNO_3 under identical conditions. Thus, in addition to the lower onset temperatures, the decomposition of TiAP exhibits higher temperature rise, pressure rise and enthalpy change in the presence of nitric acid.

The irradiated TiAP-HNO_3 system exhibits lower enthalpy change for the decomposition compared to their unirradiated counterparts. The enthalpies of decomposition of irradiated TiAP-4M HNO_3 mixtures with volume ratios of 1:3, 1:1 and 3:1 were found to be −418, −230 and −55 kJ kg^{-1}, respectively, whereas the enthalpies obtained for the decomposition of TiAP-8M HNO_3 systems were found to be −1088, −835, −284 kJ kg^{-1}, respectively. Thus, the decomposition of irradiated TiAP-HNO_3 exhibits lower temperature rise, pressure rise and enthalpy change compared to their unirradiated counterparts.

The enthalpy change for the decomposition of 1.1M TiAP/n-DD-8M HNO_3 (1:1 and 3:1) was also found to be less negative in the presence of diluent in most of the cases except in the case of 1.1M TiAP/n-DD-8M HNO_3 (1:3) system. The enthalpy change for the decomposition of 1:3 v/V ratio for 1.1M TiAP/n-DD-8M HNO_3 was found to be marginally more negative (- 1202 kJ kg^{-1}) when compared to TiAP-8M HNO_3 (- 1149 kJ kg^{-1}); the possible reason could be partial decomposition of n-DD in addition to decomposition of TiAP. The pressure and temperature rise were found to be negligible for 1.1M TiAP/n-DD-4M HNO_3 (3:1) system since the amount of nitric acid was relatively lower (~2 mmoles). Hence, in addition to the lower rise in temperature and pressure, 1.1M TiAP/n-DD systems also exhibit a lower enthalpy change. The enthalpy values of decomposition of TBP (both irradiated and un-irradiated) in the presence of nitric acid showed a strong dependency on

concentration and volume of nitric acid present in the mixture (Tables 6.2 and 6.4). TBP-HNO_3 systems also exhibit similar enthalpies of decomposition similar to TiAP-HNO_3 systems under the present experimental conditions.

6.5 Kinetic parameters

The kinetic parameters (E_a, *A and n)* for the decomposition of TiAP-HNO_3 systems were obtained from the calorimetric data by employing multiple linear regression method. A typical plot of ln k vs 1000/T is presented in Fig.6.10 for the decomposition of TiAP-4M HNO_3 (1:3). The order of the reaction is found to be 1.40. Activation energy and pre-exponential factor obtained from the multiple linear regression method are found to be 134 kJ mol^{-1} and $1.1x10^{14}$ respectively for TiAP-4M HNO_3 (1:3). Similar procedure was followed for other systems and the results are presented in Table 6.1. The activation energy versus the mole fraction of nitric acid for the decomposition of unirradiated TiAP-HNO_3 and TBP-HNO_3 systems are depicted in Fig. 6.11 and Fig. 6.12, respectively. These further confirm that the thermal stability of TiAP and TBP are lower for mixtures with higher nitric acid content and are amenable to undergo thermal excursions.

The kinetic parameters for the decomposition of irradiated TiAP-HNO_3 systems were also obtained by employing similar method and the data is given in Table 6.3. The activation energy for irradiated TiAP-HNO_3 system also decreases exponentially with mole fraction of nitric acid as in the case of unirradiated systems. These studies indicate a lower thermal stability of irradiated TiAP in higher nitric acid concentration..

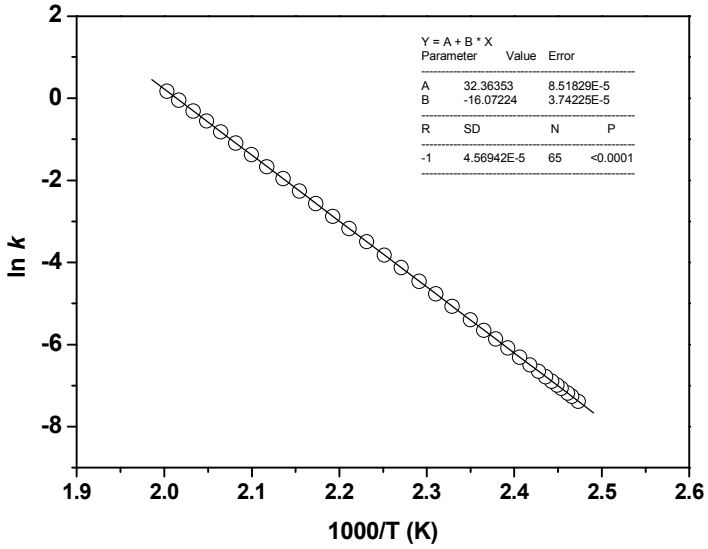

Fig.6.10: Arrhenius plot for the decomposition of TiAP-4M HNO_3 (1:3)

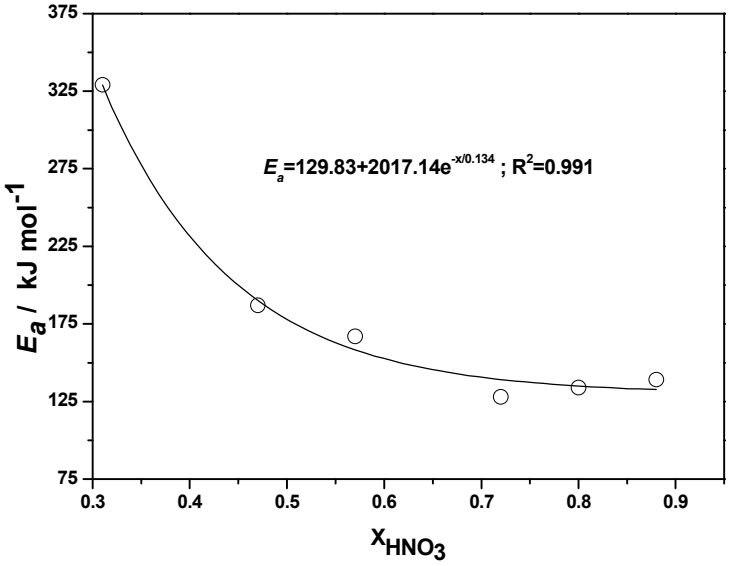

Fig.6.11: Activation energy versus mole fraction of nitric acid for the decomposition of TiAP-HNO_3

Table 6.3: List of experiments carried out with irradiated TiAP-HNO_3 system

System/(TiAP:HNO_3 v/v ratio) (M = mol dm^{-3})	T_i/K	ΔT_{exp}/K	ΔP_{exp}/bar	Φ factor	ΔT_{ad}/K	χ_{HNO3}	-ΔH / kJ kg^{-1} (Error ±1%)	E_a / kJ mol^{-1} (Error ±1%)[#]	A (Error ±1%)[#]	n (Error ±5%)[#]
Neat TiAP[a]	493									
TiAP-4M HNO_3 (1:3)	406	59	11	3.57	209	0.80	418	130	$3.3x10^{14}$	0.69
TiAP-4M HNO_3 (1:1)	403	31	10	3.70	115	0.57	230	175	$2.0x10^{14}$	1.23
TiAP-4M HNO_3 (3:1)	405	7	3	3.77	28	0.30	55	-	-	
TiAP-8M HNO_3 (1:3)	395	163	89	3.33	544	0.79	1088	96	$2.1x10^{10}$	1.82
TiAP-8M HNO_3 (1:1)	390	118	17	3.53	417	0.57	835	121	$9.1x10^{13}$	1.87
TiAP-8M HNO_3 (3:1)	389	38	16	3.68	142	0.30	284	124	$3.2x10^{14}$	0.86
1.1M TiAP/n-DD[a]	536	-	-	-	-	-	-	-	-	
1.1M TiAP/n-DD-4MHNO_3 (1:1)	396	34	9	3.81	128	-	225	94	$3.8x10^{9}$	0.64
1.1M TiAP/n-DD-8M HNO_3 (1:1)	392	132	53	3.63	479	-	959	113	$3.2x10^{11}$	1.06

[a]Temperature rise exceeded 773 K of calorimeter limit and hence, thermo-kinetic parameters not calculated.

[#] The error obtained for the experiments conducted in duplicates / triplicates

Table 6.4: List of experiments carried out with irradiated TBP-HNO_3 system

System	χ_{HNO3}	T_i/K	ΔT_{exp} /K	ΔP_{exp} /bar	Φ factor	ΔT_{ad}/K	-Δ H/ kJ kg^{-1} (Error ±1%)[#]	*Ea*/kJ mol^{-1} (Error ±1%)[#]	*A* (Error±1%)[#]	*n* (Error ±1%)[#]
Neat TBP[a]		513	-	-	-	-	-	-	-	-
TBP-4MHNO_3 (1:3)	0.77	410	67	26	3.54	237	473	123	$1.89x10^{13}$	0.75
TBP-4MHNO_3 (1:1)	0.52	406	31	11	3.64	113	224	134	$1.28x10^{15}$	0.79
TBP-4MHNO_3 (3:1)	0.27	407	8	3	3.81	30	64	260	$2.77x10^{28}$	0.82
TBP-8MHNO_3 (1:3)	0.87	396	178	81	3.33	593	1187	131	$2.66x10^{14}$	1.42
TBP-8MHNO_3 (1:1)	0.69	393	139	67	3.46	481	969	134	$1.46x10^{15}$	1.86
TBP-8MHNO_3 (3:1)	0.42	404	50	15	3.65	182	368	163	$3.09x10^{17}$	1.89
1.1M TBP/n-DD[a]		503	-	-	-	-	-	-	-	-
1.1M TBP/n-DD-4MHNO_3 (1:1)		406	28	8	3.83	107	216	98	$3.67x10^{10}$	0.73
1.1M TBP/n-DD-8MHNO_3 (1:1)		385	119	38	3.68	438	873	99	$1.03x10^{10}$	0.74

[a]Temperature rise exceeded 773 K calorimeter limit and hence, thermo-kinetic parameters not calculated.

[#]The errors obtained for the experiments conducted in triplicates

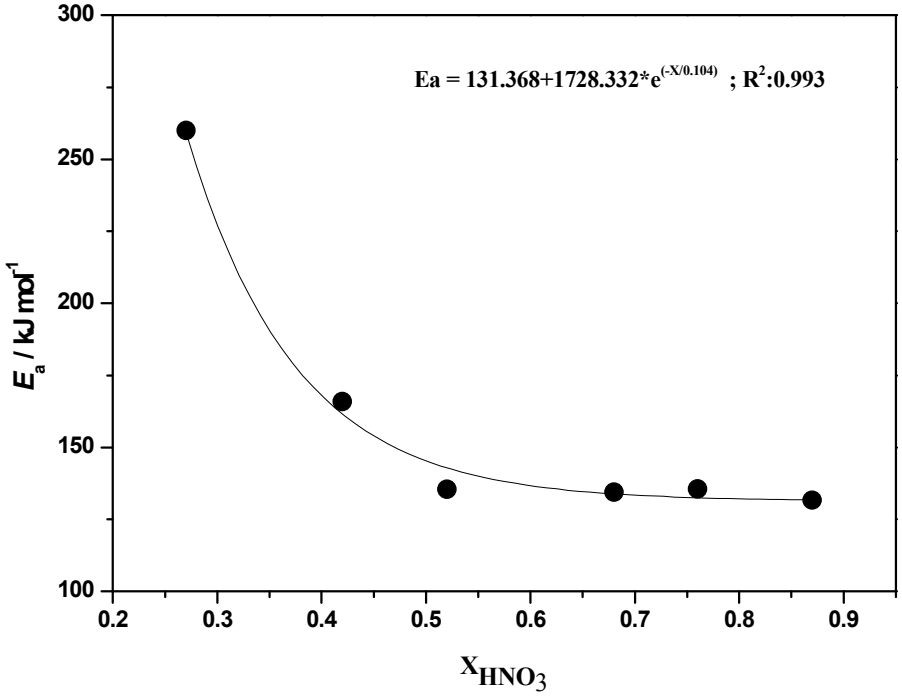

Fig.6.12: Activation energy versus mole fraction of nitric acid for the decomposition of TBP-HNO_3

A typical plot of ln k vs 1000/T is presented in Fig.6.13 for the decomposition of DBP+MBP in the presence of 4M and 8M HNO_3(1:1). The order of the reaction was found to be about 0.87 for 4M and 1.44 for 8M HNO_3. Activation energy obtained from the multiple linear regression method are found to be 165 and 140 kJ mol^{-1} for DBP+MBP in presence of 4M and 8M HNO_3 (1:1), respectively.

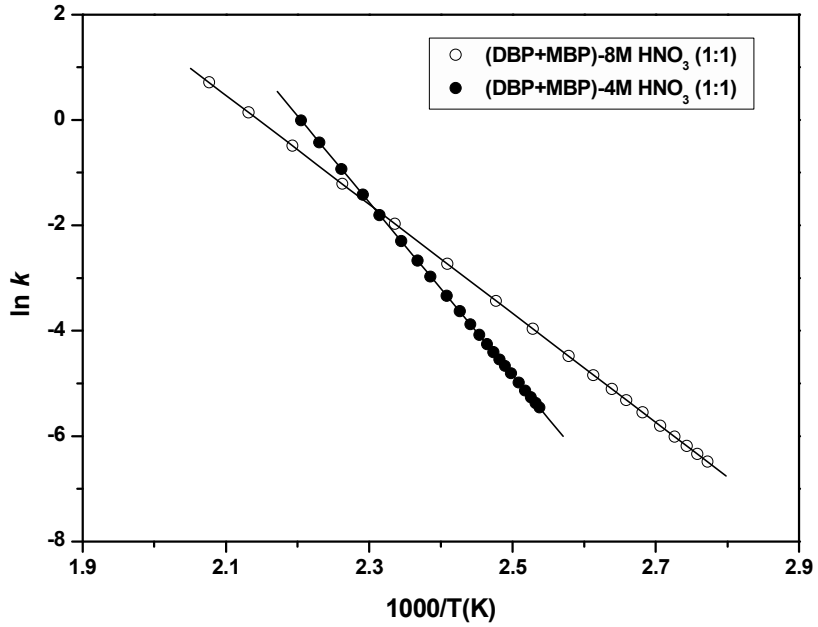

Fig.6.13: Arrhenius plot for the decomposition of 1) DBP+MBP-8M HNO_3 (1:1) and 2) DBP+MBP-4M HNO_3 (1:1)

6.6 Characterisation of decomposition products

6.6.1 IR analysis

Fig. 6.14a, Fig. 6.15a and 6.15b are the typical IR spectrum recorded for the gaseous products formed during the decomposition of irradiated TiAP-4M HNO_3 (1:3), TBP-8M HNO_3 (1:1) and 1.1M TBP/n-DD-8M HNO_3 (1:3) systems. Examination of the infrared spectra revealed that the major products are CO_2, CO, NO_x and hydrocarbons such as CH_4, C_2H_2, C_2H_4, C_3H_8 and C_4H_8 etc. The peaks at 1290 and 1270 cm^{-1} correspond to the P=O stretch, which are possibly due to the evaporation of unreacted TiAP. The typical IR spectrum recorded for the solid residue collected after the decomposition of irradiated TiAP-4M HNO_3 (1:3) system is shown in Fig. 6.14b. The noticeable feature of the IR spectrum is broad band in the region 3000-3500 cm^{-1}, which could be due to the presence of –OH group of mono and di-iso-amyl phosphoric acids. The expected C-H stretch observed at 2960 cm^{-1} could be attributed to the alkyl groups. IR spectra were also recorded for the irradiated systems; analysis of the spectra revealed that spectral features are identical for both irradiated and unirradiated TiAP-HNO_3 and TBP-HNO_3 systems.

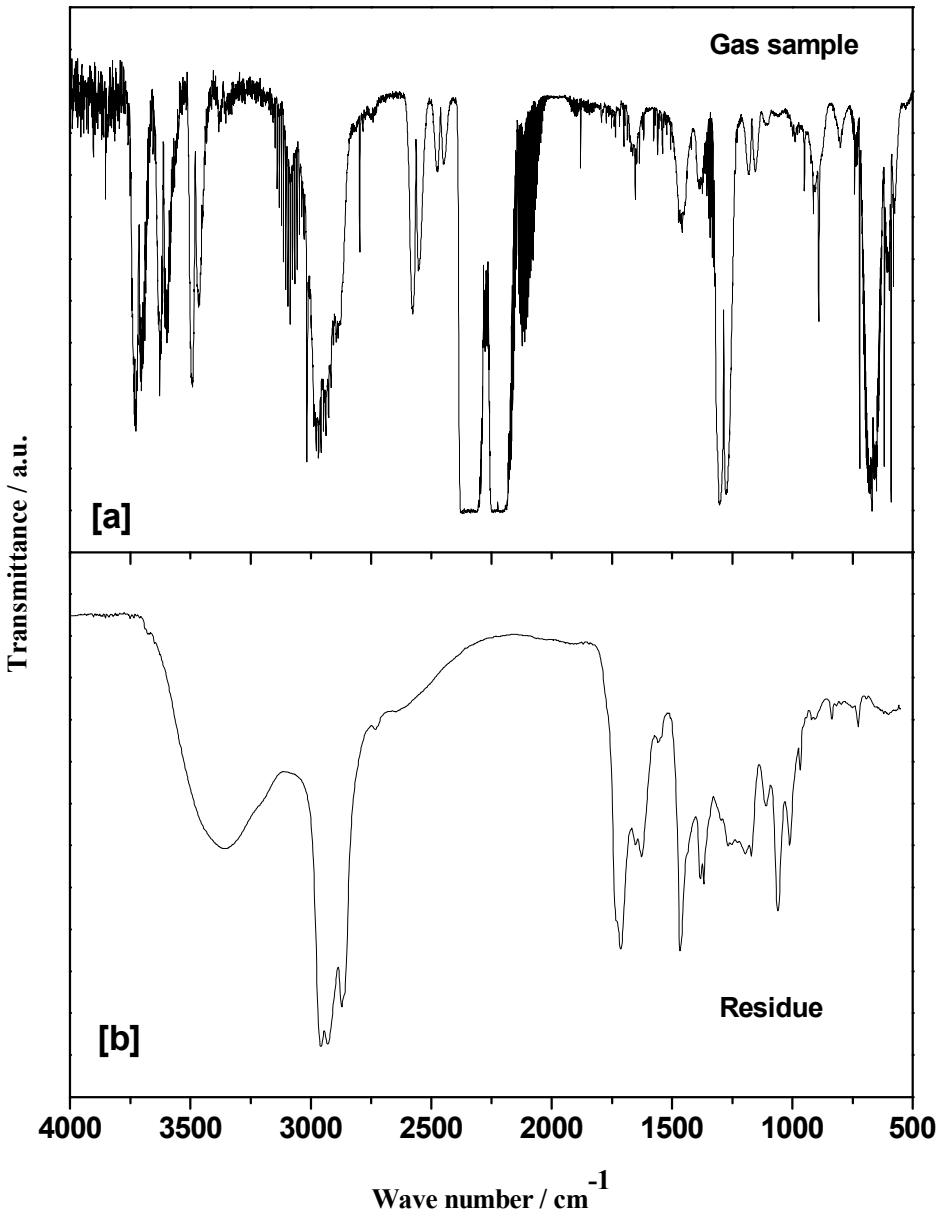

Fig.6.14: IR spectra of [a] gaseous products and [b] solid residue collected for the decomposition of Irradiated TiAP-4M HNO_3 (1:3)

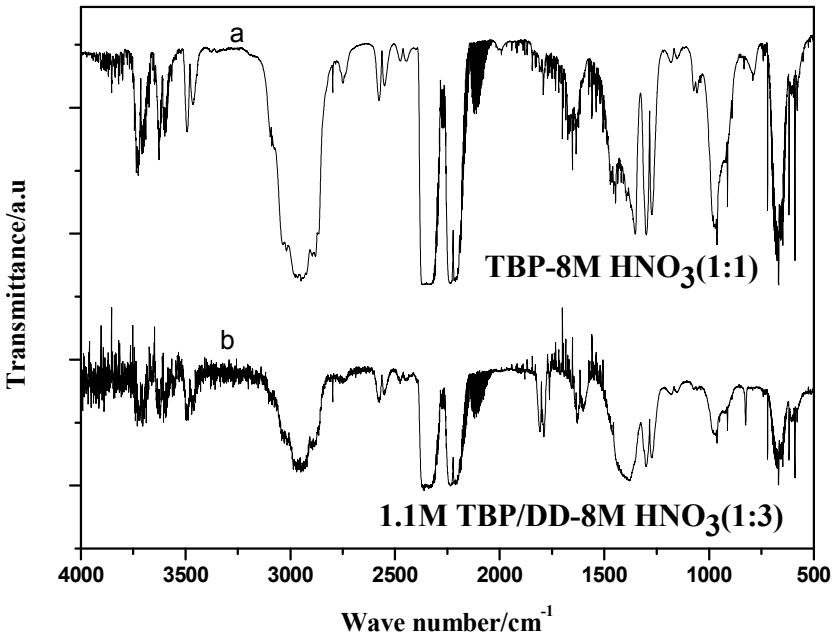

Fig.6.15: IR spectra of [a] TB-8M HNO_3 (1:1) and [b] 1.1M TBP/n-DD-8M HNO_3 (1:1)

6.6.2 QMS studies analysis

Mass spectra were obtained for gaseous products evolved under various experimental conditions during the decomposition of TiAP-HNO_3 systems. Fig. 6.16 shows mass spectrum of gaseous products evolved during the decomposition of neat TiAP. The spectrum show prominent peaks at *m/z* 28, 32 and 55. These peaks could be assigned as 28 (CO+ or $C_2H_4^+$), 32 (O_2^+) and 55 ($C_4H_7^+$).

Fig.6.17a shows the mass spectrum of gases evolved during the decomposition of 1.1M TiAP/n-DD and it shows cluster of peaks. The peaks can be assigned as 2 (H_2^+), 16 (CH_4^+), 27 ($C_2H_3^+$), 28 (CO^+ or $C_2H_4^+$), 29 ($C_2H_5^+$), 32 (O_2^+), 41 ($C_3H_5^+$), 43 ($C_3H_7^+$) and 55 ($C_4H_7^+$). A peak at 70 (low intensity) can be assigned to $C_5H_{10}^+$. The mass spectra of gases evolved during the decomposition of 1.1M TiAP/n-DD and neat TiAP are different and this may be due to the presence of the diluent (n-DD). Fig.6.17b shows the mass spectrum of the gases evolved from the decomposition of TiAP-8M HNO_3 (1:1) and it shows two major peaks at 28 (CO^+/ N_2^+ / $C_2H_4^+$) and 44 (N_2O^+ / CO_2^+ / $C_2H_4^+$). In addition to these peaks, it also shows low intensity peaks at 2 (H_2^+), 16 (CH_4^+), 32 (O_2^+), 55 ($C_4H_7^+$), 70 ($C_5H_{10}^+$). Similarly

the mass spectra of the gases evolved from the decomposition of 1.1M TiAP/n-DD-8M HNO_3 (1:1) shows only two major peaks at 28 and 44 as seen in curve "c" of Fig.6.17, indicating that in the presence of nitric acid, decomposed gaseous products from nitric acid are prominent compared to the decomposed products of organic compounds (neat TiAP or 1.1M TiAP/n-DD). The organic compounds also produce gaseous decomposition products; however intensities of the decomposed products from organic compounds are lower compared to intensities of nitric acid decomposed products. Therefore, only two major peaks at 28 and 44 could be seen. This may be possible reason for large pressure rise in the presence of nitric acid.

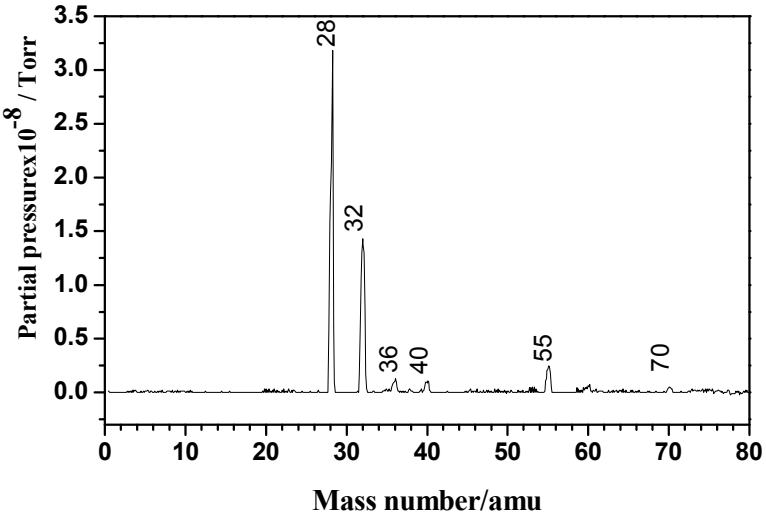

Fig.6.16: Mass spectrum of gaseous products collected after the decomposition of neat TiAP

The mass spectra of gaseous products evolved during the decomposition of irradiated neat TiAP and 1.1M TiAP/n-DD (Fig.6.18a) are identical to their unirradiated counterparts. Analysis of the mass spectrum indicate that gamma irradiation of organic compounds does not produce any additional gaseous decomposition products, which are flammable or hazardous in nature. In the presence of nitric acid, mass spectra (neat TiAP, 1.1M TiAP/n-DD and n-DD) also show only two major peaks at 28 and 44 (Fig.6.18b and c) as in the case of unirradiated solvents. The mass spectrum of neat n-DD was recorded and it shows cluster of peaks as shown in curve (a) of Fig.6.19. The gaseous products of irradiated n-DD (Fig.6.19b)

in the presence of nitric acid show only two prominent peaks at 28 and 44 like other TiAP systems.

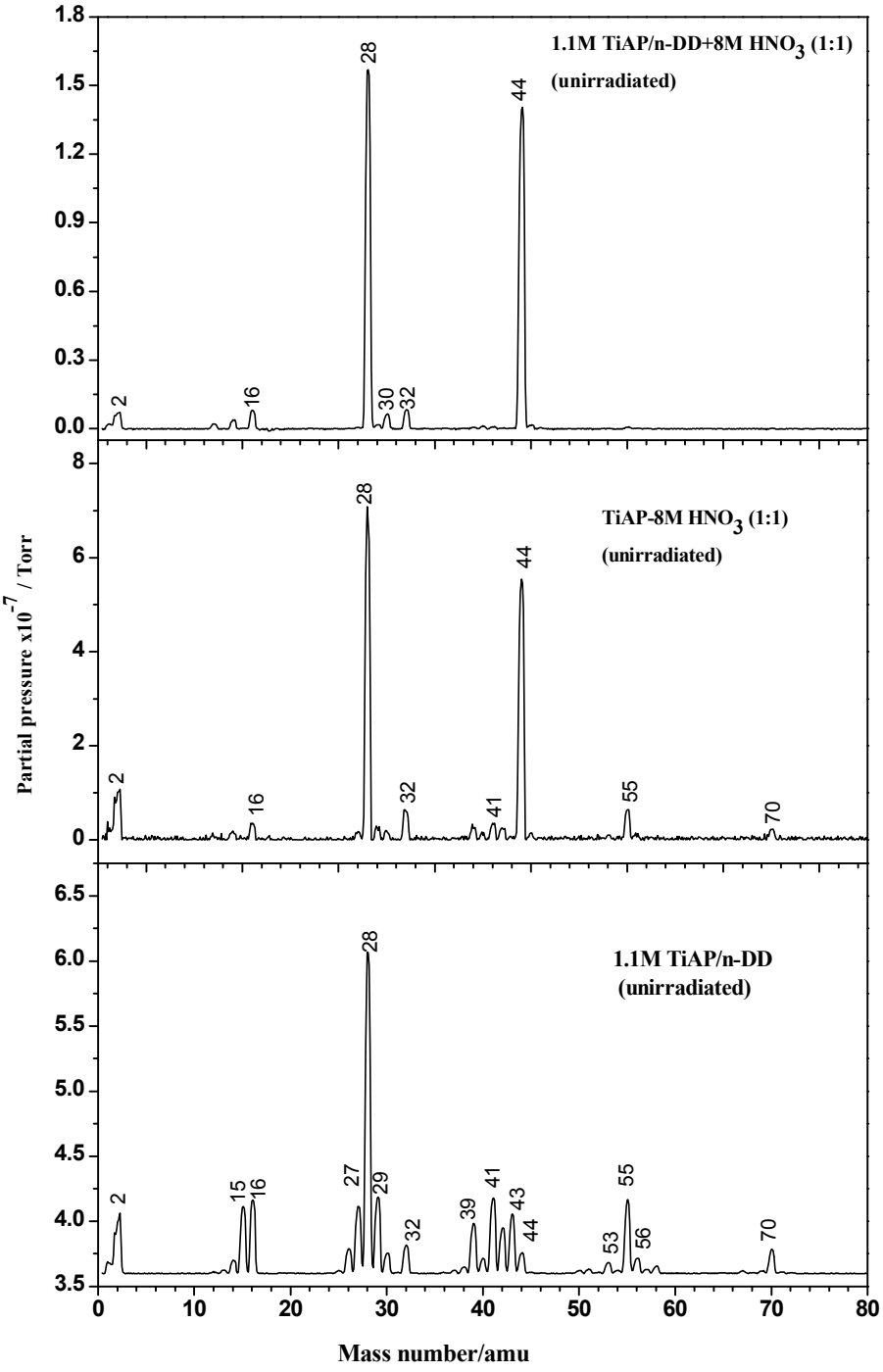

Fig.6.17: Mass spectra of gaseous products collected after the decomposition of [a]1.1M TiAP/n-DD, [b] TiAP-8M HNO_3(1:1) and [c] 1.1M TiAP/n-DD-8M HNO_3(1:1).

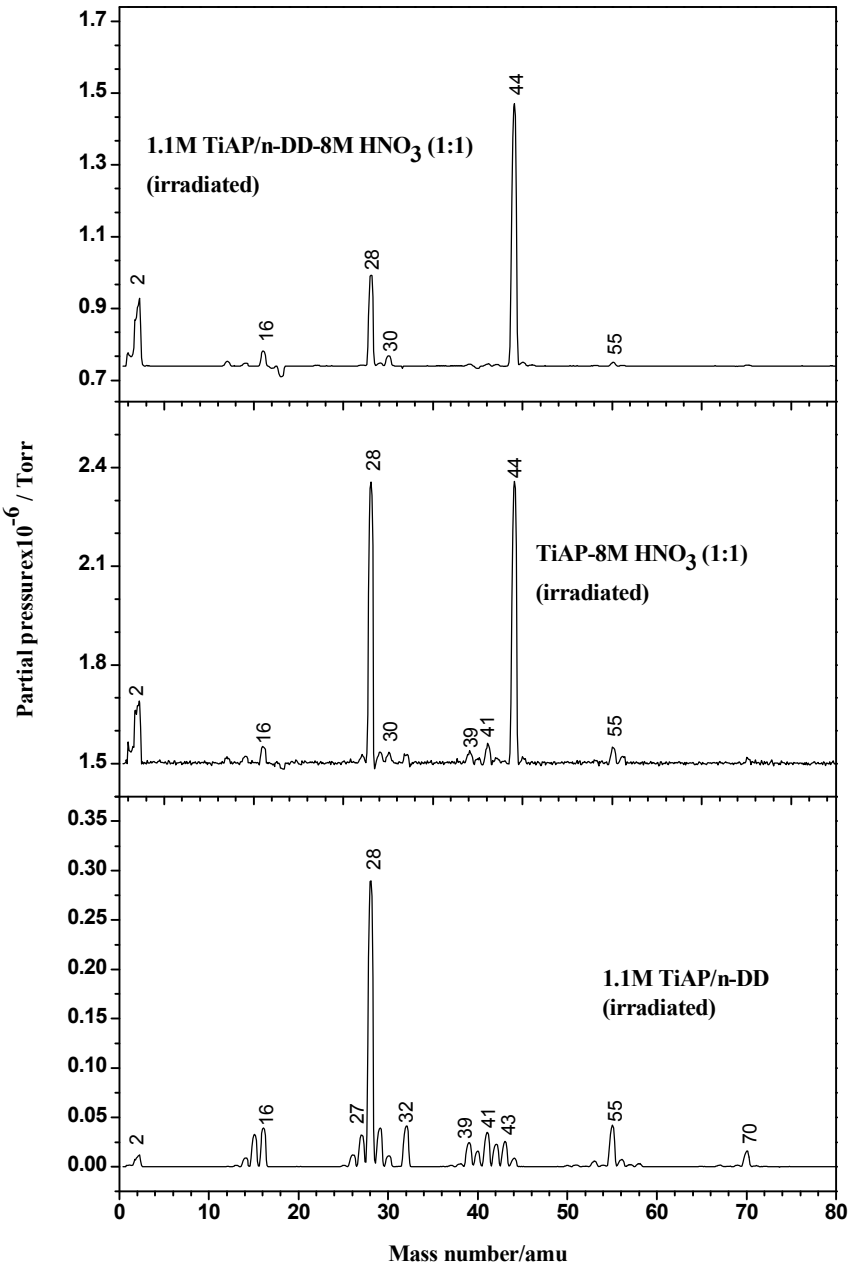

Fig.6.18: Mass spectra of gaseous products collected for the decomposition of irradiated [a] 1.1M TiAP/n-DD, [b] TiAP-8M HNO_3(1:1) and [c] 1.1M TiAP/n-DD-8M HNO_3(1:1)

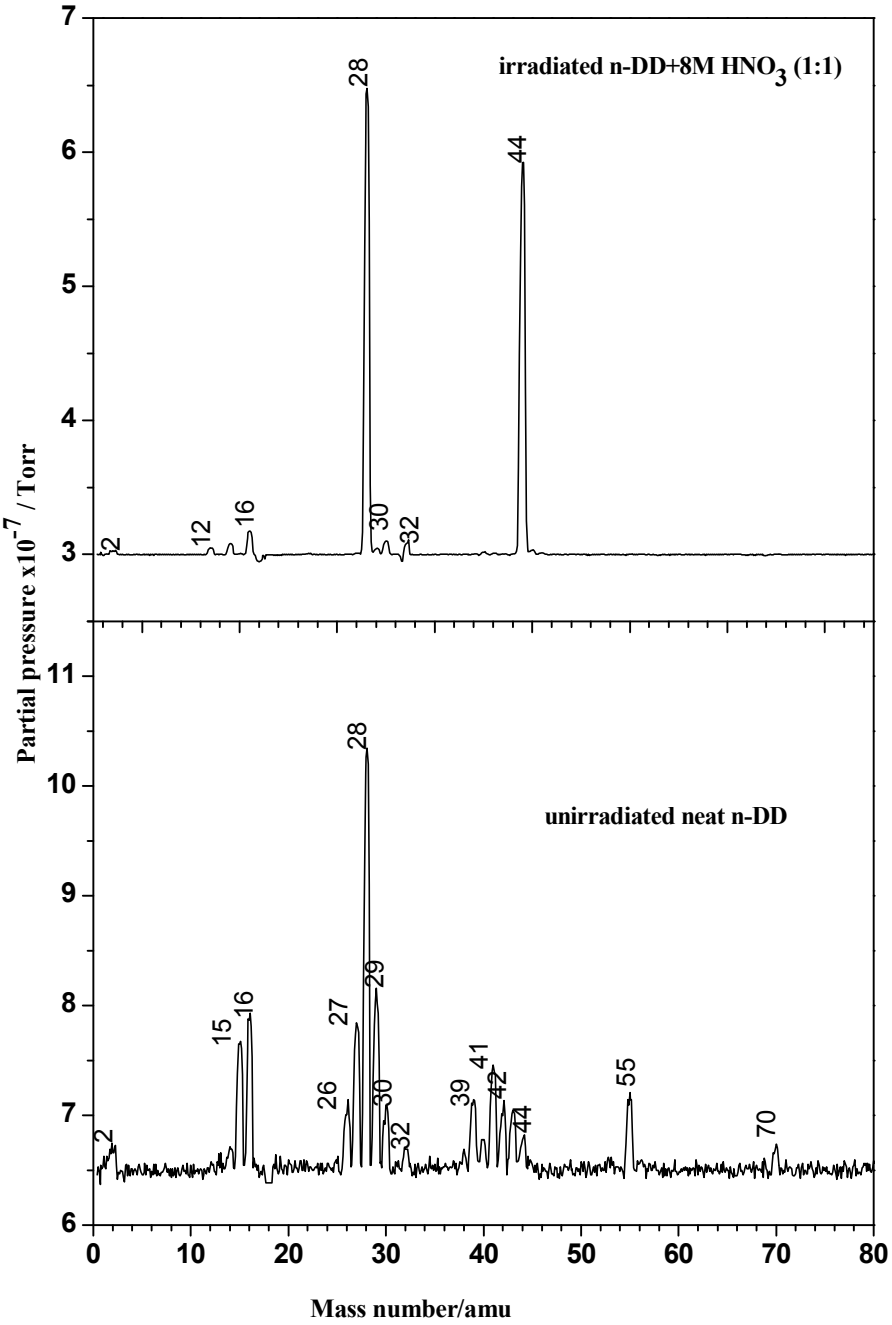

Fig.6.19: Mass spectra of gaseous products collected for the decomposition of [a] unirradiated n-DD and [b] irradiated n-DD-8M HNO_3 (1:1)

Mass spectra were obtained for gaseous products evolved under various experimental conditions during the decomposition of TBP-HNO_3 systems. Fig. 6.20a shows the mass spectrum of gaseous products evolved during the decomposition of neat TBP; it show prominent peaks at *m/z* 27, 28, 32. 39, 41 and 56. These can be assigned as 28 (CO^+ / $C_2H_4^+$), 32 (O_2^+) and 56 (C_4H8^+). The peaks at 39 and 41 ($C_3H_5^+$) can be assigned as fragments of

butene. Fig.6.20b shows mass spectrum of gases evolved during the decomposition of neat TBP-4M HNO_3(1:1) and the spectrum shows cluster of peaks at regular intervals of about 14(CH_2) units. The peaks can be assigned as 2 (H_2^+), 16 (CH_4^+), 27 ($C_2H_3^+$), 28 (CO^+, $C_2H_4^+$), 29 ($C_2H_5^+$), 32 (O_2^+), 41 ($C_3H_5^+$), 44(N_2O^+, CO_2^+) and 56 (C_4H8^+).

Mass spectra were obtained for gaseous products evolved during the decomposition of DBP-HNO_3 systems (Fig.6.21). Mass spectrum show prominent peaks for neat DBP system without nitric acid at m/z 2, 28, 32 41 and 56. These peaks are assigned as 28 (CO+, $C_2H_4^+$), 32 (O_2^+) and 56 ($C_4H_8^+$). In the presence of 4M HNO_3 (1:1), peaks can be assigned as 2 (H_2^+), 18 (H_2O^+), 28 (CO^+, $C_2H_4^+$), 44 (N_2O^+, CO_2^+, $C_2H_4^+$). Mass spectrum of the gases evolved from the decomposition of DBP+MBP-8M HNO_3 (1:1) was obtained and the spectra shows the major peaks at 2 (H_2^+), 28 (CO^+,N_2^+,$C_2H_4^+$), 44 (N_2O^+,CO_2^+,$C_2H_4^+$) and 56 ($C_4H_8^+$).

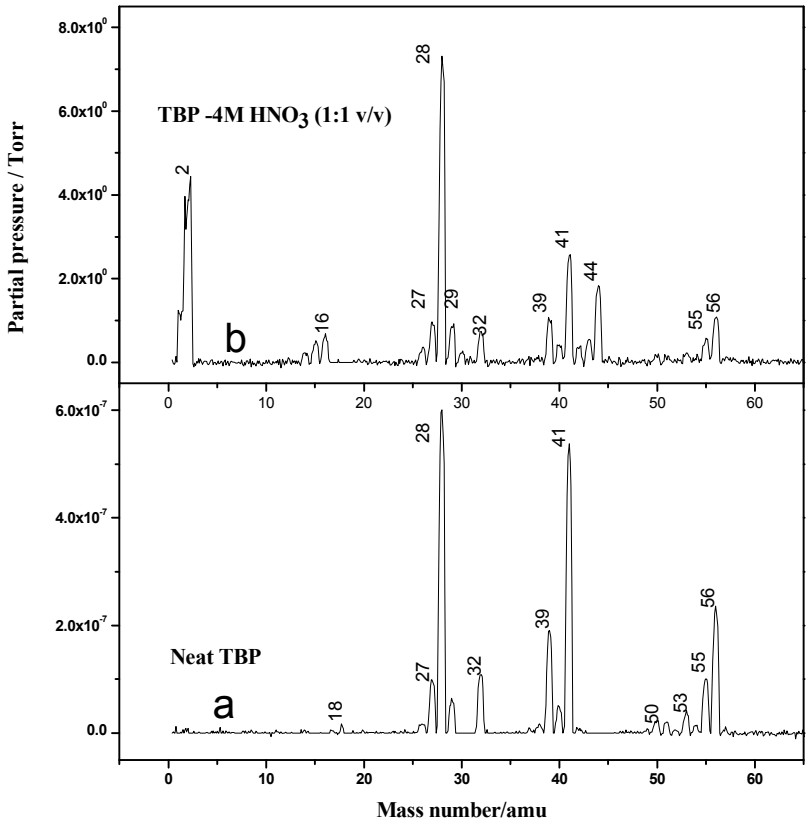

Fig.6.20: Mass spectra of gaseous products collected after the decomposition of [a] TBP [b] TBP-4M HNO_3(1:1)

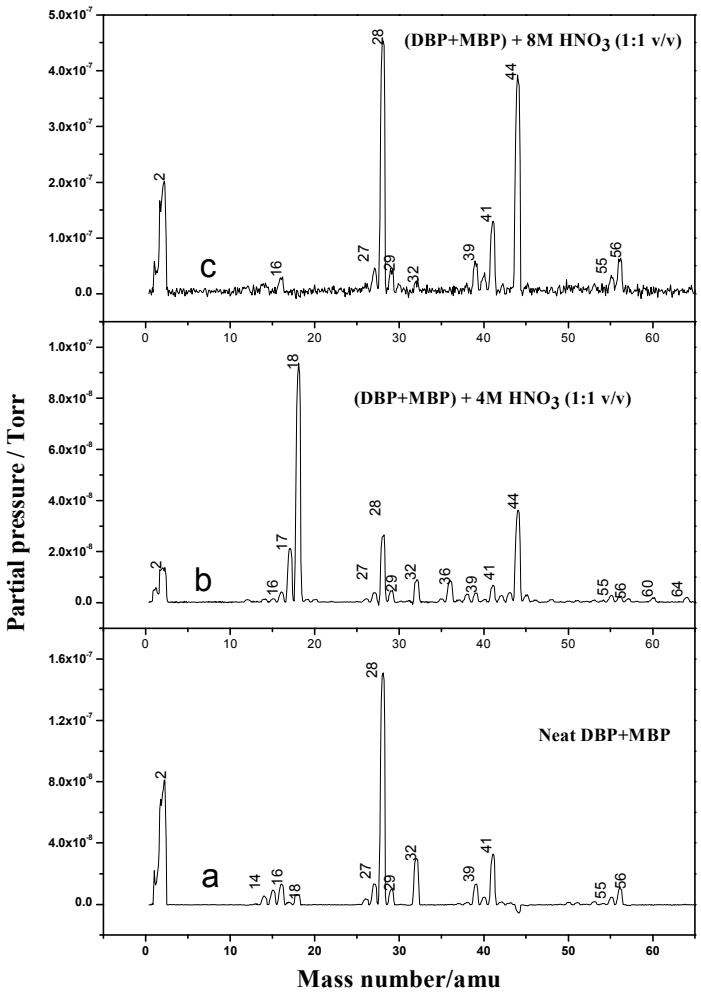

Fig.6.21: Mass spectra of gaseous products collected for the decomposition of [a] Neat DBP+MBP, [b] DBP+MBP-4M HNO_3(1:1) and [c] DBP+MBP-8M HNO_3(1:1)

6.7 Conclusions

The thermal stability of irradiated and unirradiated TiAP and TBP in the presence and absence of nitric acid have been investigated in detail using an adiabatic calorimeter. Neat TiAP and TBP were found to be thermally stable up to 540 and 527 K respectively whereas it decomposes at a lower temperature in the presence of nitric acid. The exothermic nature of TiAP and TBP decomposition has strong dependency on concentration of nitric acid and volume. The presence of diluent (n-DD) along with nitric acid does not alter the onset temperature of decomposition of TiAP and TBP and exhibits lower enthalpy change. The temperature rise, pressure rise and enthalpy change for irradiated TiAP and TBP systems are

significantly lower compared to their unirradiated counterparts. Radiolytic degradation products have no measurable effect on the thermal decomposition of TiAP and TBP. Thermal decomposition of TiAP and TBP on decomposition produces gaseous products containing mostly CO, CO_2, NOx, hydrocarbons and a highly viscous black liquid. Thus in comparison to TBP, neat TiAP performs better with respect to onset temperature. Considering the lower aqueous phase solubility of TiAP, these studies indicate that the performance of TiAP is equivalent to TBP if not better under thermal decomposition conditions.

Chapter 7

7 RADIOLYTIC DEGRADATION STUDIES WITH TiAP

7.1 Introduction

As described in Chapter 1, a mixture of 30% TBP and n-paraffins or kerosene is employed as a solvent in PUREX process for the extraction of uranium and plutonium from nitric acid medium in reprocessing plants. During the extraction of metal ions, nitric acid also gets extracted into the organic phase. The solvent is expected to undergo degradation by various mechanisms such as hydrolysis, radiolysis, nitrolysis and oxidation at various stages of processing. Degradation products alter the fission product decontamination factors, physicochemical properties (density, viscosity, phase separation time and interfacial tension) and also changes the extraction and stripping behavior of U, Pu and fission products [112, 134].

DBP, MBP, H_3PO_4 and butanol are the main degradation products of TBP, whereas the degradation of diluent (n-DD) leads to the formation of hydrocarbons, nitroalkanes, which were produced by the nitration of n-paraffin hydrocarbon diluents and derivatives of the nitro alkanes such as carboxylic acids and hydroxamic acids [146]. The extent of degradation of TBP and n-DD depends on several factors such as concentration of nitric acid, absorbed dose and temperature.

Prior to the deployment of a solvent in a reprocessing plant, it is important to investigate its radiolytic stability. The objective of the present study is to measure the physicochemical properties such as density, viscosity and IFT for neat and 1.1M TiAP/n-DD (unirradiated and irradiated). Additionally the extraction and stripping behaviour and metal retention studies with uranium and plutonium by 1.1M TiAP/n-DD (unirradiated and irradiated) have been carried out. Effect of alpha degradation on stripping of plutonium by 1.1M TiAP/n-DD has been investigated. An attempt has been made to identify the radiolytic

degradation products of TiAP using a mass spectrometric method. Similar experiments were also performed with TBP system under identical experimental conditions.

7.2 Physicochemical properties of TiAP based solvent system

Density, viscosity and IFT of neat (100%) and 1.1M solutions of TiAP as well as TBP in n-dodecane (unirradiated and irradiated) were measured at 298 K. The densities of either neat or 1.1M TiAP/n-DD which was equilibrated with 4M HNO_3 are higher compared to the densities of organic phases, which were not equilibrated with nitric acid (Table 7.1). For example, the density of neat TiAP is 0.944 g/mL and when it was equilibrated with 4M HNO_3, it increased to 0.989 g/mL. However, the change in density of TiAP based solvent system was not observed during gamma irradiation studies of the solvent. The densities of neat TiAP (unirradiated) and irradiated solvent were found to be 0.944 and 0.949 g/mL, respectively. Like TiAP, TBP based solvents also exhibits similar results. In the case of 1.1M TiAP/n-DD, density does not change by gamma irradiation and it increases only with nitric acid equilibration. The increase in density with nitric acid equilibration is due to the extraction of nitric acid (Table 7.2). Venkatesan et al. [127] have also obtained similar results for chemically and radiolytically degraded TBP/n-DD-HNO_3 system.

Table 7.1: Density, in g/mL at 298 K for 100% TiAP and 100% TBP

Solvent	Density (g/mL)			
	Neat	Irradiated (100M Rad)	Pre-equilibrated with 4M HNO_3	Pre-equilibrated with 4M HNO_3 (100M Rad)
100% TBP	0.979	0.978	1.020	1.018
100% TiAP	0.944	0.949	0.989	0.989

Table 7.2: Density, in g/mL at 298 K for 1.1M TiAP/n-DD and 1.1M TBP/n-DD

Solvent/n-DD	Density(g/mL)					
	Neat	Irradiated (100M Rad)	Pre-equilibrated with 4M HNO_3	Pre-equilibrated with 4M HNO_3 and Irradiated		
				10M Rad	50M Rad	100M Rad
1.1M TBP	0.811	0.816	0.833	0.833	0.833	0.832
1.1M TiAP	0.813	0.820	0.837	0.837	0.837	0.837

Viscosity of neat TiAP is found to be 4.66 cP and it increases with gamma irradiation as well as with chemical degradation induced by nitric acid (Table 7.3). Similar trend is also observed in the case of 1.1M TiAP/n-DD system. The viscosities of 1.1M TiAP/n-DD and 1.1M TBP/n-DD (equilibrated with 4M HNO_3 and irradiated) increases with increase in absorbed dose (Fig.7.1). The viscosity of 1.1M TiAP/n-DD (1.80 cP) is marginally higher compared to that of 1.1M TBP/n-DD (1.62 cP) (Table 7.4). However, it is sufficiently low enough (<2 cP) for the steady flow of solutions and for the efficient phase dispersion and phase separation.

The increase in viscosity with increase in absorbed dose is due to the formation of species which are highly viscous compared to TiAP / TBP molecules. In addition, diluent degradation products (nitro and nitrite compounds of alkanes, alcohols, unsaturated alcohols, nitro alcohols, nitro alkenes, ketones and carboxylic acids) produced having higher viscosity also will contribute and hence viscosity of degraded solvent is higher than that of unirradiated diluent (n-DD).

Table 7.3: Viscosity (cP) at 298 K for 100% TiAP and 100% TBP

Solvent	Viscosity (cP)			
	Neat	Irradiated (100M Rad)	Pre-equilibrated with 4M HNO_3	Pre-equilibrated with 4M HNO_3 (100M Rad)
100% TiAP	4.66	6.72	6.76	9.61
100% TBP	3.12	4.19	5.38	6.59

Table 7.4: Viscosity in cP at 298 K for 1.1M TiAP/n-DD and 1.1M TBP/n-DD

Solvent/n-DD	Viscosity(cP)					
	Neat	Irradiated (100M Rad)	Pre-equilibrated with 4M HNO_3	Pre-equilibrated with 4M HNO_3 and Irradiated		
				10M Rad	50M Rad	100M Rad
1.1M TBP/n-DD	1.62	1.87	1.73	1.77	1.90	2.05
1.1M TiAP/n-DD	1.80	2.19	1.95	2.03	2.19	2.36

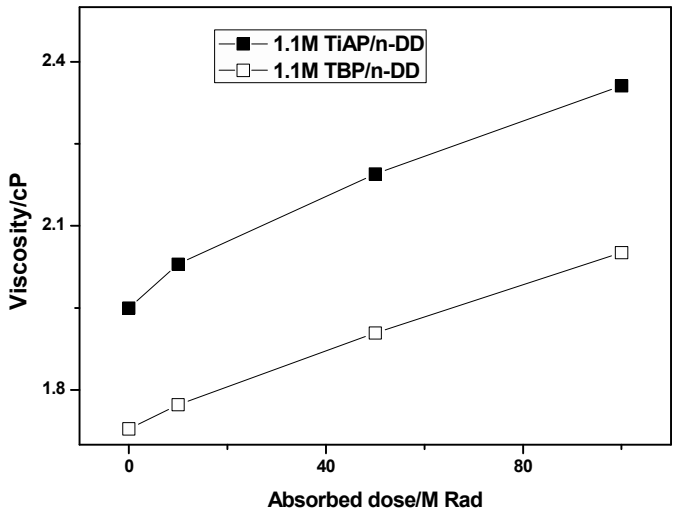

Fig.7.1 Viscosity as a function of absorbed dose for 1.1M solutions of TiAP and TBP in n-DD (equilibrated with 4M HNO_3)

Viscosities of neat and 1.1M solutions of TiAP and TBP in n-DD were measured as a function of temperature. The variation of viscosity with temperature is shown in Fig.7.2. The viscosity decreases with increase in temperature for all the systems. The slope (*m*) of the linear fit is found to be lower for TBP systems compared to that of TiAP, indicating decrease in viscosity with temperature is higher for TiAP systems. For example, the slope for neat TiAP system is - 0.0786 and the corresponding slope for TBP system is -0.0489. Further, the decrease in viscosity with temperature for neat TiAP and TBP is higher compared to that of 1.1M solutions of TiAP and TBP in n-DD, which is indicated by the slope of the linear fit. The effect of temperature on the viscosity is fitted with the Arrhenius type of relation as

shown in equation 7.1. Activation energy was calculated from the slope of the straight lines. The activation energy for neat TiAP system (16.2kJ/mol) is found to be marginally higher than that of TBP system (14.4 kJ/mol). The activation energy for 1.1M solutions of TiAP and TBP in n-dodecane is marginally lower than that of neat TiAP and TBP systems. The activation energies were found to be nearly similar for both 1.1M TiAP/n-DD (11.3 kJ/mol) and 1.1M TBP/n-DD (11.1 kJ/mol) systems.

$$\eta = \eta_o e^{Ea/RT} \quad \text{.....(7.1)}$$

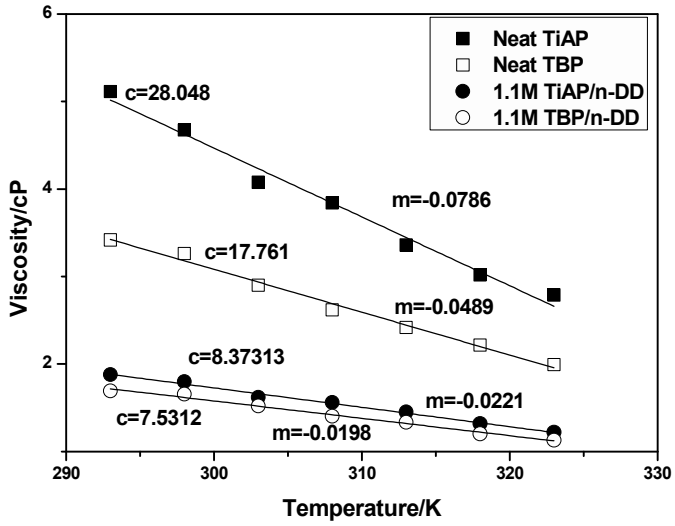

Fig.7.2 Viscosity as a function of temperature for neat and 1.1M solutions of TiAP and TBP in n-DD

IFT values were measured for neat and 1.1M solutions of TiAP and TBP in n-DD (unirradiated and irradiated) at 298K against 4M HNO_3. Results indicate that IFT of neat TiAP-HNO_3 system (11.2 mN/m) is marginally lower than that of 1.1M TiAP/n-DD-HNO_3 system (15.9 mN/m). The presence of non-polar diluent enhances the hydrophobicity of 1.1M TiAP/n-DD system and hence an increase in the IFT. Also, IFT values for unirradiated TiAP-HNO_3 system (11.2 mN/m) is higher than that of irradiated TiAP-HNO_3 system (10.6 mN/m), indicating that the irradiated solvents take longer time for phase separation. Similar experiments were performed with TBP-HNO_3 system and the results are presented in

Table 7.5. In all the cases, IFT values for TiAP-HNO_3 systems are marginally higher than that of TBP-HNO_3 system, indicating that the phase separation time will be lower for TiAP systems compared to TBP systems. The higher IFT of TiAP systems may be due to the presence of additional "three -CH_2- groups" in TiAP molecule, which increases its hydrophobicity compared to TBP-HNO_3 systems.

Table 7.5: Interfacial tension of TiAP and TBP systems measured by drop-weight method at 298K

System	Density		IFT (mN/m)	System	Density		IFT (mN/m)
	Org	Aq			Org	Aq	
100% TiAP	0.981	1.079	11.2	100% TBP	1.012	1.073	7.80
1.1M TiAP/n-DD	0.833	1.104	15.9	1.1M TBP/n-DD	0.830	1.103	12.9
Irr 100% TiAP	0.987	1.081	10.6	Irr 100% TBP	1.019	1.076	7.40
Irr 1.1MTiAP/n-DD	0.838	1.107	14.1	Irr1.1MTBP/n-DD	0.839	1.107	11.8

7.3 Extraction and stripping studies of U and Pu with 1.1M TiAP/n-DD and 1.1M TBP/n-DD (unirradiated and irradiated)

The extraction behaviour of U(VI) and Pu(IV) from 4M HNO_3 was studied with irradiated samples of 1.1 M solutions of TiAP and TBP in n-dodecane at 303K. Results indicate that *D* values for U(VI) and Pu(IV) increase with increase in absorbed dose due to increase in the concentration of their degradation products (Table 7.6). These degradation products such as dialkyl phosphates (DalP) and monoalkyl phosphates (MalP) have higher affinity towards U(VI) and Pu(IV). TiAP, a higher homologue of TBP is also expected to undergo degradation similar to TBP and generate similar degradation products such as di-iso-amyl phosphate (DiAP) and mono-iso-amyl phosphate (MiAP). Apart from the degradation products of the extractant, diluent degradation products are also responsible for the retention of metal ions and increase in the *D* values. Tripathi et al. [191] have identified the radiolytic degradation products of 30% TBP/n-DD-HNO_3 by gas chromatographic technique and their role in the retention behavior of Pu(IV). They also reported that increase in the concentration

of degradation products with absorbed dose parallels increase in the retention of Ru, Zr and Pu. The species were identified as nitro alkanes, alcohols and long chain hydrocarbons by gas chromatography.

Table 7.6: Extraction behaviour of U(VI) and Pu(IV) with 1.1M solutions of TiAP and TBP in n-DD from 4M HNO_3 at 303 K

Dose, M Rad	$D_{U(VI)}$		$D_{Pu(IV)}$	
	TiAP	TBP	TiAP	TBP
0	35.20	30.90	29.33	24.12
10	44.96	41.38	30.80	26.10
50	52.61	59.13	49.83	55.50
100	63.48	60.13	89.08	82.96

Stripping behaviour of U(VI) and Pu(IV) were studied with 1.1M solutions of TiAP and TBP in n-DD at 0.01M and 0.1M HNO_3, respectively. The *D* values for U and Pu were measured at 0.01M and 0.1M HNO_3 at 303K for unirradiated and irradiated (100M Rad) solvents (Table 7.7). The *D* values for U and Pu were found to be higher for irradiated solvents compared to that of unirradiated solvents. This may be due to the formation of acidic degradation products such as DBP and MBP in the case of 1.1M TBP/n-DD-HNO_3 system. These acidic degradation products have higher affinity for metal ions at lower acidities, thereby increasing the *D* values. In the case of irradiated solvents, the *D* values for TiAP system are marginally higher compared to that of TBP system. The extraction mechanism of U(VI) with HDBP is shown in the following equation.

$$UO_2^{2+}{}_{(aq)} + 4\ HDBP \leftrightarrow UO_2(DBP)_2 \cdot 2HDBP_{(org)} + 2H^+ \text{……..(7.2)}$$

Two TBP molecules are replaced with two molecules of HDBP (referred to DBP) when HDBP is present along with TBP (Eq.7.3) [192]. HDBP forms complex with UO_2^{2+} metal cation by liberating a hydrogen ion at lower acid concentrations or by solvation mechanism through P=O group at higher acid concentrations.

$$UO_2(DBP)_2 \cdot 2HDBP_{(org)} + 2\ TBP \leftrightarrow UO_2(DBP)_2 \cdot 2TBP_{(org)} + 2HDBP \text{……..(7.3)}$$

Table 7.7: Stripping behaviour of U(VI) and Pu(IV) with 1.1M solutions of TiAP and TBP in n-DD with 0.01M HNO_3 and 0.1M HNO_3 respectively

Solvent	$D_{U(VI)}$		$D_{Pu(IV)}$	
	Unirradiated	Irradiated (100M Rad)	Unirradiated	Irradiated (100M Rad)
TiAP	0.01	91.45	0.09	46.52
TBP	0.01	85.53	0.07	40.37

Retention studies were carried out with U(VI) and Pu(IV) using 1.1M solutions of TiAP and TBP in n-DD at 303K. The Pu(IV) was stripped with 0.5M HNO_3 to avoid the hydrolysis/polymerisation. These studies indicate that the metal ions retained in the organic phase increase with increase in absorbed dose (Table 7.8). The amounts of U(VI) and Pu(IV) retained in the organic phase for unirradiated TiAP were found to be 0.35 and 1.08 mg/L, respectively and the amount of metal ion retained in the solvent increase with increase in absorbed dose. Significant amounts of U(~180.5 mg/L) and Pu(~14.67 mg/L) were retained in the organic phase after three successive contacts with 0.01M and 0.5M HNO_3, respectively in the case of 1.1M TiAP/n-DD(irradiated to 10M Rad) solvent. The results for TBP system is presented in Table 7.8. The retention of U and Pu by TiAP is comparable to that of TBP system indicating that radiolytic degradation of TiAP is on par with TBP.

Parikh et al. [128] reported radiolytic degradation of N, N-Dihexyl Octanamide (DHOA) and TBP under process conditions. Retention behaviour of U, Pu and fission products was studied with 1.1M DHOA/n-DD and 1.1M TBP/n-DD. In the case of 1.1M TBP/n-DD system, it is reported that ~24 mg/L of Pu(IV) was retained in the organic phase after three successive contacts with 0.5M HNO_3 (pre-equilibrated with 3M HNO_3 and irradiated to 60M Rad) and in the present study it was found to be ~18 mg/L (pre-equilibrated with 4M HNO_3 and irradiated to 50M Rad). The amount of Pu retained in the organic phase (irradiated to 10M Rad) was found to be negligible (0.02 mg/L) after three successive contacts with 1M Na_2CO_3. In the case of samples irradiated to 50 and 100M Rad, emulsification of the

organic phase was observed, which resulted in the accumulation of deposits at the aqueous-organic interface during organic solvent treatment with 1M Na_2CO_3. The amount of U(VI) retained in the organic phase was found to be ~26 mg/L after three successive contacts with 0.01M HNO_3.

Table 7.8: Retention studies with U(VI) and Pu(IV) with 1.1M solutions of TiAP and TBP in n-dodecane; strippant: 0.01M and 0.5M HNO_3 for U(VI) and Pu(IV), respectively (after three successive contacts) (1 Wh/L=360000 Rad)

Dose		$[U(VI)]_{org}$, mg/L		$[Pu(IV)]_{org}$, mg/L	
M Rad	Wh/L	TiAP	TBP	TiAP	TBP
0	0	2.67	2.63	1.08	1.03
10	27.7	180.5	147.7	14.67	15.55
50	138.8	205.7	200.9	15.46	18.02
100	277.7	207.0	209.4	19.79	22.27

7.4 Effect of α-degradation on stripping of plutonium from 1.1M TiAP/n-DD and 1.1M TBP/n-DD

The effect of α-degradation on TiAP and TBP was studied by loading Pu(IV) into the organic phase and measuring the amount of Pu retained in the organic phase after stripping with nitric acid. The amount of Pu loaded in the organic phase was ~10.3 and 10.8 g/L for 1.1M TiAP/n-DD and 1.1M TBP/n-DD systems, respectively. The absorbed dose increases with increase in contact time of Pu in the organic phase (Table 7.9). The Pu retained in the organic phase was stripped as a function of time; the loaded organic phase was found to contain ~12 mg/L Pu at zero hours of contact time and it was ~600 mg/L when Pu loaded organic phase was kept for 424 h followed by stripping. The retention of Pu in the organic phase increases with increase of absorbed dose. In the case of TBP system, the Pu retained in the organic phase (after stripping) was found to be ~4 and ~534 mg/L at zero and 403 hr, respectively. The Pu retention by 1.1M TiAP/n-DD and 1.1M TBP/n-DD is nearly

comparable under identical conditions, indicating that the degradation behaviour could also be similar. The Pu retained in the organic phase was also measured after treating with 1M oxalic acid. The amount of Pu retained in the organic phase was found to be 0.01 mg/L after treating with 1M oxalic acid for the TiAP system; it increases with increase in absorbed dose and similar trend was also observed for TBP system.

Degradation of TBP in plutonium nitrate solution was studied by Kuno et al. [193]; degradation follows first-order kinetics and depends upon concentration of Pu. Lloyd et al. [194] also studied the alpha radiolysis and hydrolysis of TBP and identified that DBP and MBP are the most important degradation products responsible for retention of Pu. The degradation rate of TBP either by alpha radiolysis or chemical hydrolysis depends on temperature. Pearson et al. [131] studied the degradation of 1M solution of TBP in n-dodecane in a mix of low and high linear energy transfer (LET) radiation by irradiating samples in the reactor and utilizing the $^{10}B(n,\alpha)^{7}Li$ reaction. Their results indicate that the degradation of TBP (G^{-}_{TBP}) was found to be 0.36 and 0.14 μmol/J for low and high LET radiation, respectively. The formation of dibutyl phosphoric acid, DBP, (G^{+}_{DBP}) in this solution was found to be 0.18 and 0.047 μmol/J for low and high LET radiation, respectively.

Table 7.9: Retention studies with Pu by α-degradation using 1.1M TiAP/n-DD and 1.1M TBP/n-DD. strippant: 0.5M (after three successive contacts) (1 Wh/L=360000 Rad)

1.1M TiAP/n-DD				1.1M TBP/n-DD			
Loaded Amount of Pu:10.25 g/L				Loaded Amount of Pu:10.78 g/L			
Contact period with Pu/hr	Dose (M Rad)	$[Pu]_{org}$, mg/L	$[Pu]_{org}$, mg/L (treated with 1M oxalic acid)	Contact period with Pu/hr	Dose (M Rad)	$[Pu]_{org}$, mg/L	$[Pu]_{org}$, mg/L (treated with 1M oxalic acid)
0	-	12	0.01	0	-	4	-
70	0.61	95	0.03	70	0.64	92	0.0074
164	1.44	212	0.13	164	1.51	211	0.0209
236	2.07	350	0.20	236	2.17	304	0.0373
350	3.07	430	0.30	332	3.06	426	0.1638
424	3.72	600	0.39	403	3.72	534	0.5437

7.5 Mass spectrometric studies

It is important to investigate the degradation products that are formed by gamma irradiation of TiAP. Preliminary results on identification of radiolytic degradation products of TiAP are presented. The mass spectrum obtained for neat TiAP (unirradiated) is shown in Fig. 7.3. The major species are the sodium salt of molecular ion and protonated phosphoric acid (HPA). However, the mass spectrum obtained for TBP under similar experimental conditions displays only the sodium salt of the molecular ion and non-protonated phosphoric acid peak (Fig. 7.4). The mass spectrum obtained for the irradiated TiAP sample is shown in Fig.7.5. In this case, no molecular ion feature could be detected. In addition to protonated phosphoric acid, a peak corresponding to mono iso-amyl phosphate (169 amu) and an intense peak with 202 amu were observed. No definite molecular species has been assigned for the ion of mass of 202 amu. One possible assignment could be $[H_3P.O=P\text{-}OC_5H_{11}(OH)_2]^+$ or $[P(C_5H_{11})_2 C_2H_5]^+$. Similarly, the mass spectrum was obtained for irradiated TBP samples (Fig.7.6). A protonated phosphoric acid (*m/z* 99), dimer of TBP (*m/z* 553) along with other intense peaks at *m/z* of 202, 242 etc. were observed. These peaks could not be assigned to any molecular ion species. Similar experiments with isotopically substituted samples may provide identity of the species. Other than ^{31}P, all the isotopes of P are radioactive and are relatively short lived. Hence, one needs to use isotopic substitution by ^{13}C or ^{2}H. The less intense peaks also could not be assigned properly.

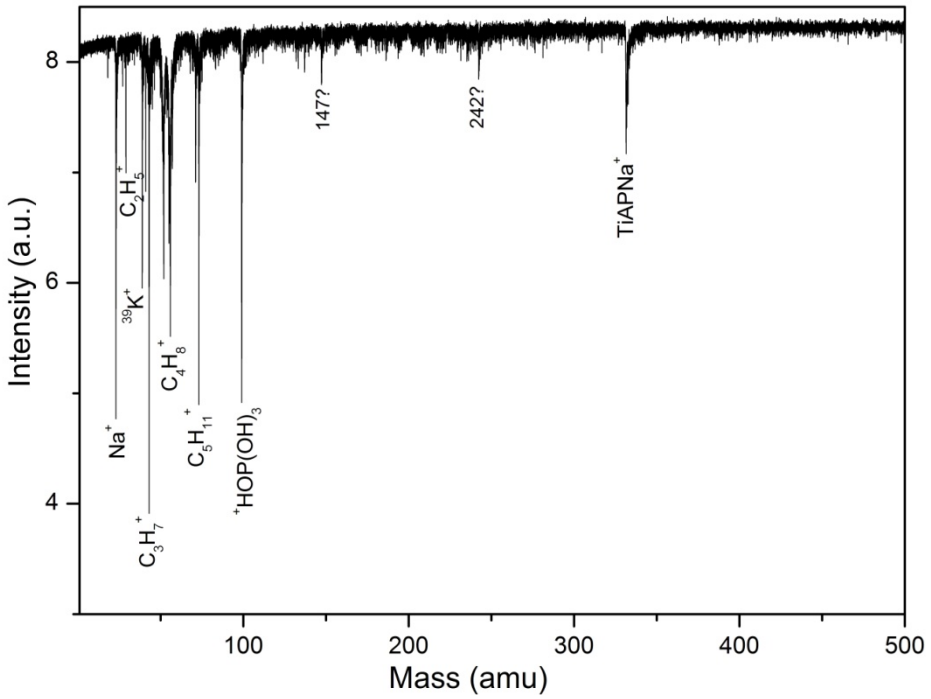

Fig.7.3 Mass Spectrum of unirradiated TiAP

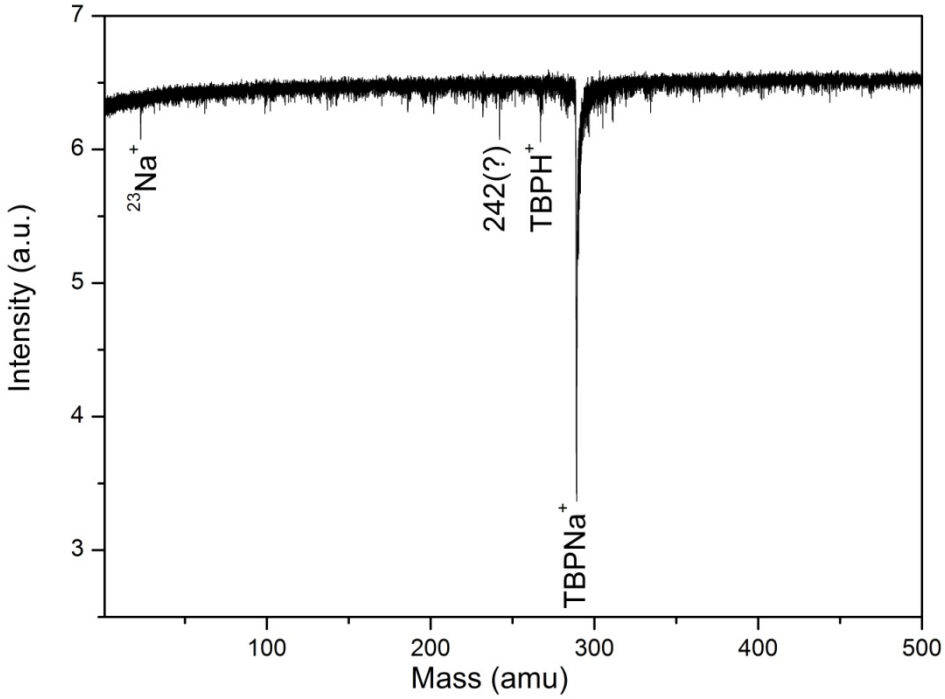

Fig.7.4 Mass Spectrum of unirradiated TBP

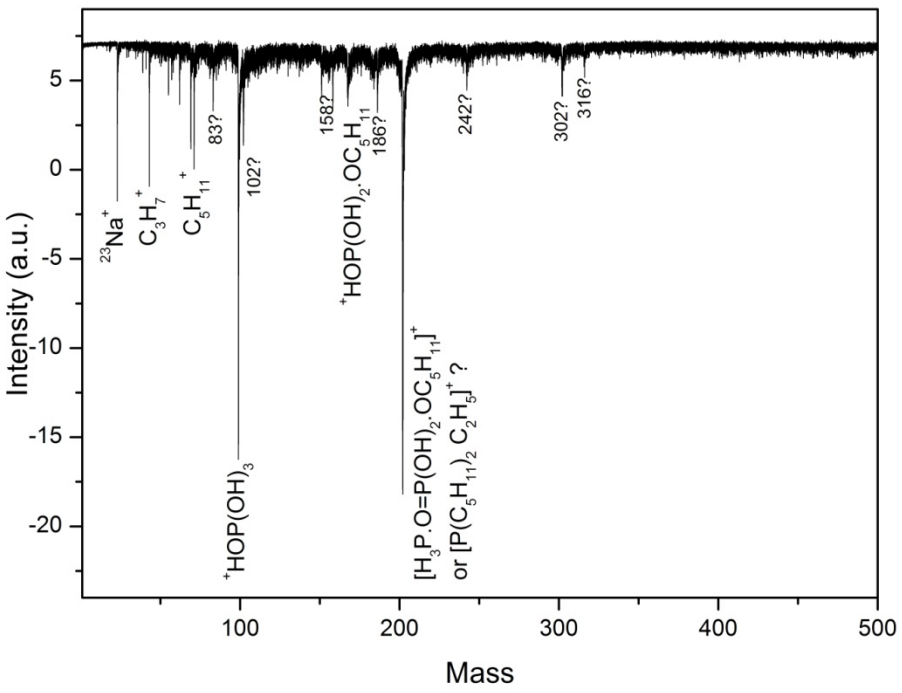

Fig.7.5 Mass Spectrum of irradiated TiAP

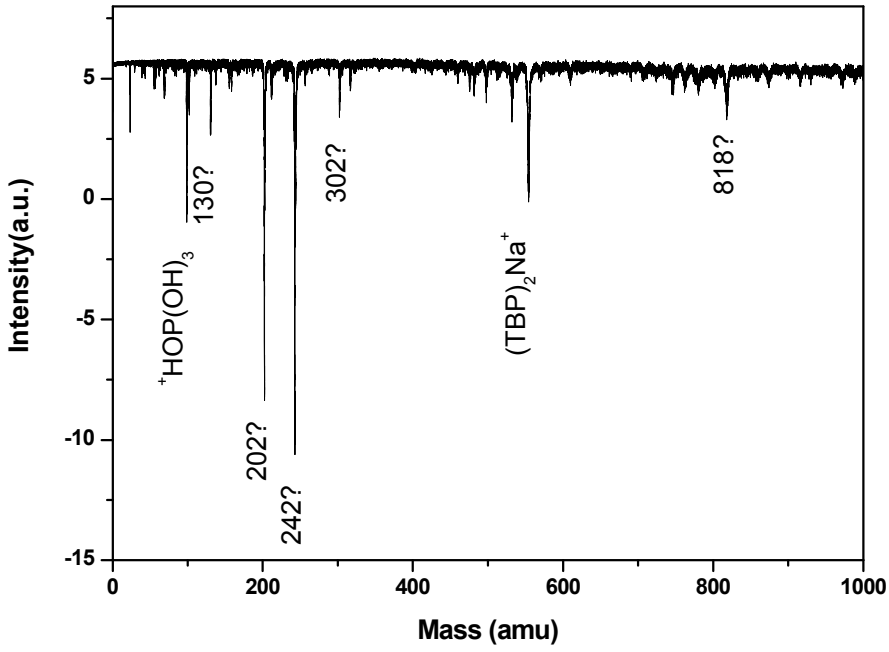

Fig.7.6 Mass Spectrum of irradiated TBP

7.6 IR studies

The IR spectra of radiolytically degraded TiAP and TBP samples are shown in Figs. 7.7 and 7.8 respectively. In the case of neat TiAP, the stretching frequency of P=O is assigned at 1276 cm^{-1} and upon gamma irradiation (100M Rad), no changes in the stretching frequencies of TiAP were observed. Like TiAP, the IR spectrum of unirradiated TBP was found to be similar to that of irradiated TBP. When neat TiAP was pre-equilibrated with 4M HNO_3, it was observed that the band responsible for P=O stretching (1272 cm^{-1}) was significantly broadened and shifted to 1207 cm^{-1}; and the stretching frequency for P-O-C did not change. The broadening of band for P=O stretch may also happen due to nitric acid extraction by TiAP. The band observed at 1643 cm^{-1} can be assigned to asymmetrical stretching of the NO_2 group. When the above sample was irradiated to 100M Rad, additional two bands were observed at 1728 (carbonyl group) and 1554 cm^{-1} (nitro group). Under identical conditions, IR spectra were recorded for TBP system and similar absorption frequencies were observed. Absorption bands assigned in the IR spectra at 1554 and 1643 cm^{-1} can be attributed to the presence of nitro (C-NO_2) and nitrite (C-O-N=O) compounds. It is reported that upon gamma irradiation, dialkyl and monoalkyl phosphates were formed. The IR spectra of DiAP and DBP+MBP (~30-50%) mixtures are shown in Fig.7.9. The spectral features of DBP+MBP (30-50%) are similar to DiAP. However the spectral features of dialkyl phosphates are completely different form trialkyl phosphates. In the case of DiAP, it is observed that the band responsible for P=O stretching is significantly broadened and is shifted to 1235 cm^{-1} and the broadening is more in the case of DBP+MBP; the P=O stretching shifted to 1225 cm^{-1}. Broad bands responsible for P-O-C and P-O-H stretch are observed at ~1030 and ~2320 cm^{-1} in both the compounds. The broad bands at ~2878, 2314 and 1683 cm^{-1} are also responsible for O=P-OH (single OH) stretch.

The IR spectrum was recorded for 1.1M TiAP/n-DD and 1.1M TBP/n-DD (pre-eqilibrated with 4M HNO_3; irradiated to 100M Rad) (Fig.7.10). The spectral features of these

solutions are different from neat TiAP and TBP systems. Several bands were observed at ~2970-2950 cm^{-1}(C-H stretch), ~1736 cm^{-1}(C=O stretch), ~1645-1375 cm^{-1} (symmetric and asymmetric N-O stretch) for both the TiAP and TBP systems. Tripathi et al. [126] reported IR spectrum of gamma radiolyzed 30% TBP/n-DD–HNO_3 system as a function of absorbed dose. It is reported that absorbance at 1556 cm^{-1} (nitroparaffins) are greater than those at 1720 cm^{-1} (carbonyl group), indicating that nitroparaffins are the primary radiolytic degradation products and carbonyl species are generated subsequently through their derivatization. Venkatesan et al. [127] reported the IR spectrum of chemically degraded TBP samples. Tallent et al. [143] also recorded the IR spectra of degraded 30%TBP/Normal Paraffin Hydrocarbon (NPH); nitro, nitrite and carboxylic acids were identified in the degraded samples.

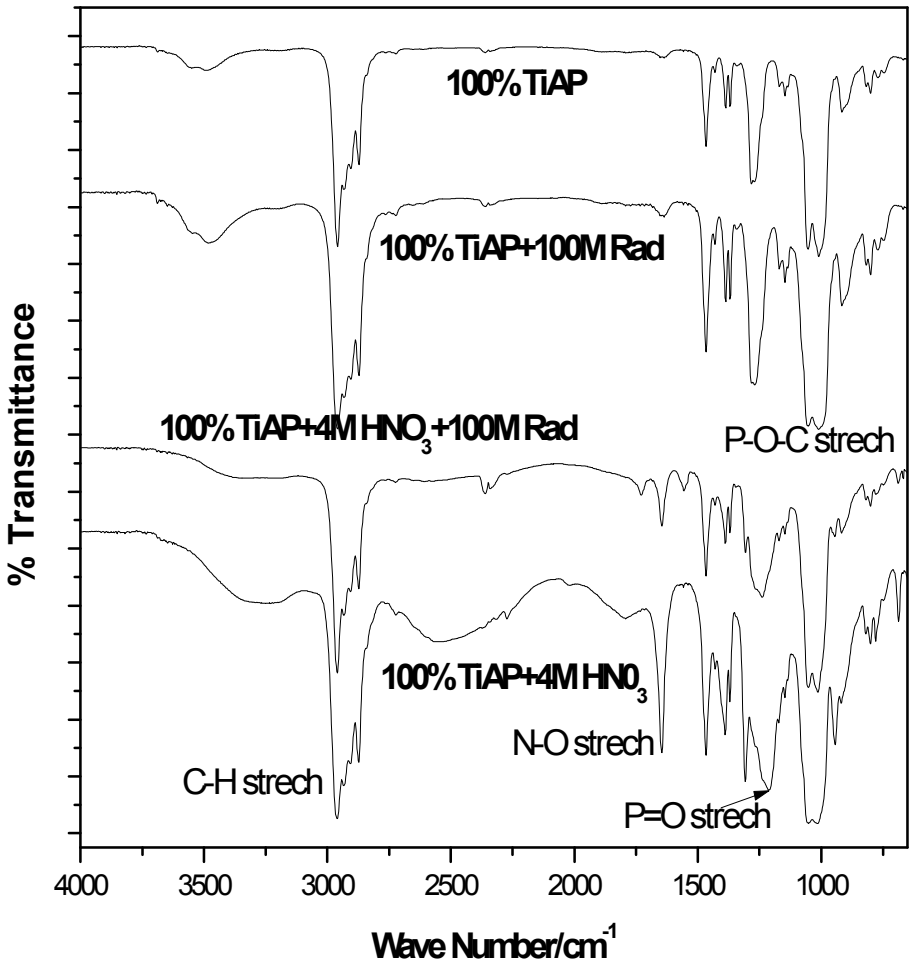

Fig.7.7: IR spectra of neat TAP samples under different conditions

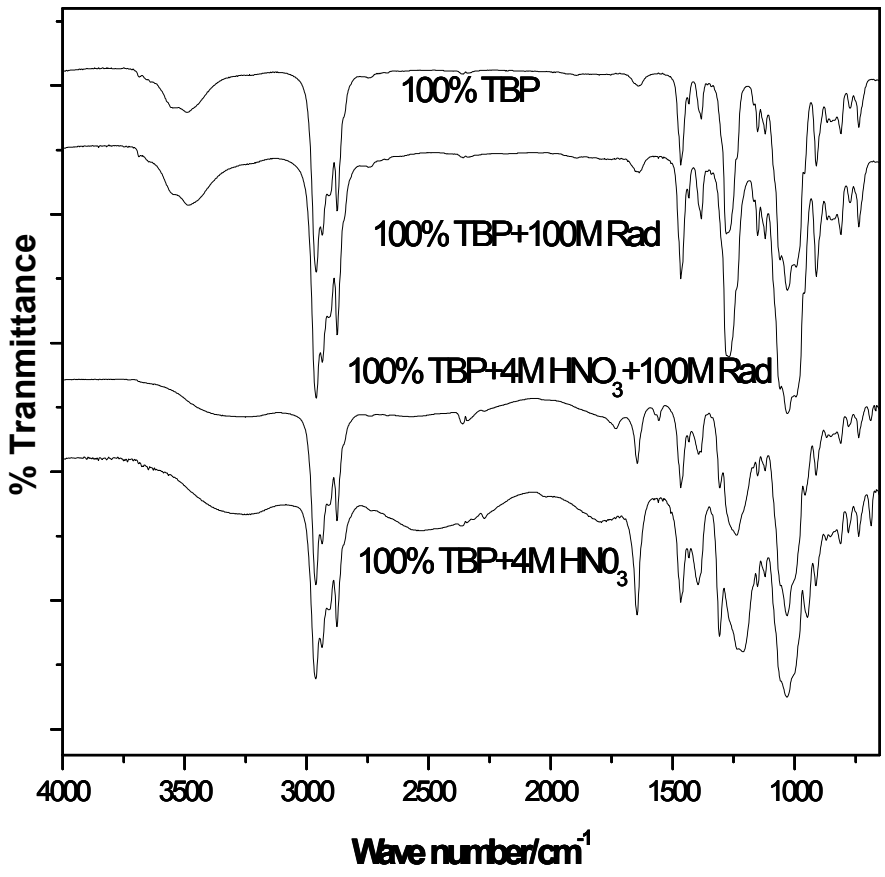

Fig.7.8: IR spectra of neat TBP samples under different conditions

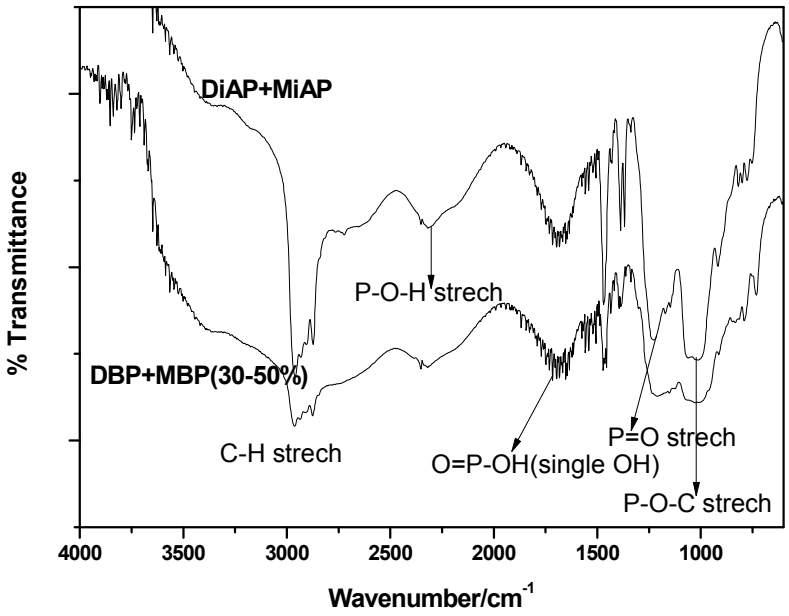

Fig.7.9: IR spectra of DiAP+MiAP and DBP (30-50% MBP) samples

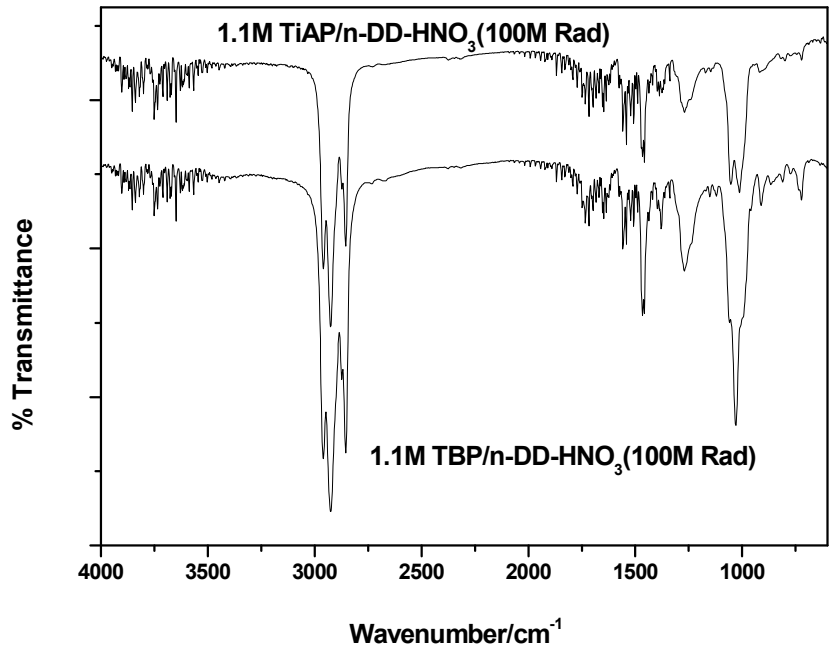

Fig.7.10: IR spectra of 1.1M solutions of TiAP and TBP in n-DD (pre-equilibrated with 4M HNO_3 and irradiated to 100M Rad)

7.7 Physico-chemical properties of TiAP and comparison with TBP

Physico-chemical properties of TiAP were compiled and compared with TBP (Table 7.10). The densities of 1.1M TiAP/n-DD and 1.1 TBP/n-DD are found to be similar; viscosity and IFT of TiAP system are higher than that of TBP system; aqueous solubility of TiAP system is lower than that of TBP system. When it comes to third phase formation with tetravalent metal ions, TiAP has significant advantage over TBP. Third phase formation was not observed with Pu(IV) under various experimental conditions; Limiting Organic Concentrations (LOC) for Th(IV) and Zr(IV) for TiAP system are higher compared to TBP system. The amount of Pu(IV) retained in the organic phase is nearly similar under identical conditions for TiAP and TBP samples irradiated to identical dose levels indicating that the radiolytic degradation of TiAP system is on par with TBP system. The onset of decomposition for TiAP system is marginally higher than that of TBP system, indicating that TiAP is relatively more stable than TBP system.

Table 7.10: Physico-chemical properties for TiAP and comparison with TBP

Property	Undiluted TalP		1.1 M TalP/n-DD	
	TBP	TiAP	TBP	TiAP
Density (g/cc)	0.979	0.944	0.811	0.813
Viscosity (cP) at 298K	3.12	4.66	1.616	1.802
IFT against 4M HNO_3(mN/m) at 303 K	7.80	11.2	12.9	15.9
Aqueous solubility (mg TalP/L water) at 303K [112]	400	<80	225	-
Solubility of water in TalP based organic phase (g water/L solution) at 303K [150]	67	41.1	9.1	7.1
Third Phase limits with Pu (g/L) at 4M HNO_3	-	-	~55[74]	No third phase formation
Third Phase limits with Th (g/L) at 4M HNO_3[152]	-	-	~35	~73
Third Phase limits with Zr (g/L) at 6M HNO_3 [160]	-	-	~8.17	~19.4
Alpha radiation degradation [Pu(IV) Retention test (mg/L)]	-	-	92	95
Onset of Decomposition/K [156]	527	540	508	525

7.8 Conclusions

In the present study, physicochemical properties such as density, viscosity and IFT were measured for unirradiated and irradiated solutions of TalP systems. There was no significant change in the density of the irradiated TiAP samples; there was an increase in the viscosity and decrease in the IFT of the irradiated TiAP samples. Significant retention of U and Pu was observed with the irradiated TiAP and TBP samples after three successive contacts with the stripping solutions. Alpha radiolysis of TiAP system was found to be comparable to that of TBP system. The present study indicated that the radiolytic degradation behaviour of TiAP system is on par with TBP.

Chapter 8

CONCLUSIONS

8

This chapter summarizes the results of the work explained in the thesis. The principal objective of this study is to explore the possible use of TiAP for spent fuel reprocessing, especially for fast reactor fuel reprocessing. The conclusions drawn based on several investigations that are centralized about this objective are elaborated in this chapter.

8.1 Extraction behaviour of U(VI), Pu(IV) and fission products with TiAP-Batch studies

The extraction behaviour of Pu(IV) and HNO_3 was investigated as a function of equilibrium aqueous phase acidity and Pu(IV) concentration using 1.1M TiAP/DD from nitric acid medium. TiAP based solvent does not form third phase during the extraction of Pu(IV) with high feed concentrations (75-285 g/L) from aqueous solutions; however, TBP has been reported to form third phase under similar conditions. It is also established that Pu(IV) can be extracted into the organic phase up to theoretical loading. Co-extraction studies of U(VI) and Pu(IV) in cross-current mode by TiAP indicate that the loss of U and Pu into the raffinate streams is negligible. The extraction behaviour of fission products (lanthanides, ruthenium, technetium and zirconium) as well as that of americium was investigated using TiAP; the results revealed that the *D* values with TiAP and TBP are more or less similar. The effect of radiolytic degradation on the extraction of fission products has been investigated; the *D* values for Zr increase, whereas for Ru, Tc, Lns, the *D* values doesn't increase with absorbed dose. The possible conditions for interfacial crud formation during the alkali wash of solvent were also examined in the present work. These studies will be useful in designing flowsheet for the processing of spent nuclear fuels.

8.2 Mixer-settler runs with TiAP based solvent

The extraction behaviour of U(VI) with high concentration of aqueous feed solution (~ 240 g U(VI)/L) was carried out using an ejector mixer-settler in counter-current mode.

Results indicate that the performance of the solvent as well as the equipment was found to be satisfactory under high solvent loading conditions. Mixer-settler runs were also demonstrated for the separation of U and Pu from Lns and Am with TiAP based solvent. Flowsheet for the above mixer-settler runs consists of one extraction run for the loading and two strip runs for the recovery of metal ions. Results obtained revealed that the loss of U and Pu into the raffinate and lean organic streams has been negligible. The flowsheet developed in the present study will be useful for the deployment of TiAP for actual reprocessing applications.

8.3 Dissolution, characterization and solvent extraction studies with U-Zr and U-Pu-Zr alloy fuels

Dissolution of U-Zr and U-Pu-Zr metallic alloys in nitric acid media established complete dissolution of uranium/plutonium and partial dissolution of Zr under nitric acid reflux method as well as using EODT. A modified spectrophotometric method has been developed for the determination of zirconium in a large excess of uranium and plutonium (U: Pu: Zr = 1000:400:1). Both TiAP and TBP based systems were examined to study the extraction and stripping behaviour with U-Zr and U-Pu-Zr feed solutions in stage-wise mode. Batch studies for the co-processing of U-Zr and U-Pu-Zr feed solutions with TiAP and TBP extractant systems indicate that zirconium was partially extracted into the organic phase along with uranium and plutonium and scrubbing of organic phase was required to recover pure fractions of U and Pu. The extraction and stripping (%) of metal ions were computed in each stage and quantitative loading and recovery of metal ions were observed with TiAP and TBP based solvents in stage-wise mode.

8.4 Thermal decomposition studies with TiAP and TBP

Thermal decomposition of TiAP and TBP has been investigated using an adiabatic calorimeter. Effect of various parameters on thermal decomposition of TiAP as well as TBP were examined viz. concentration of nitric acid, diluent, irradiation, aqueous to organic phase

ratio. Neat TiAP performs better with respect to onset temperature, while the acid-solvates of TiAP seem to perform better with respect to the enthalpy of decomposition, activation energy and frequency factor but poorer with respect to the onset temperature of decomposition. Present study reveals that the evaporation of aqueous streams with higher proportions of HNO_3 to TiAP can lead to generation of high temperature and pressure. This may result in runaway reactions with low activation energies. The studies highlight the significance in the removal of dissolved or entrained TiAP from aqueous streams prior to evaporation to ensure safety to the plant and personnel. The lower aqueous phase solubility of TiAP (~ 80 μg/mL) has a greater advantage in minimising runway reactions compared to TBP (400 μg/mL).

8.5 Radiolytic degradation studies with TiAP

Physicochemical properties such as density, viscosity, IFT and extraction behaviour of U and Pu with gamma irradiated solvents were examined with TiAP and TBP based solvents. Results obtained show that TiAP has a marginal advantage over TBP with respect to IFT. The *D* values for U and Pu increase with increase of absorbed dose (gamma irradiation) for both TiAP and TBP solvents. Alpha radiolysis of TalPs by Pu was measured by the amount of its retention in the organic phase and the results indicate that concentration of Pu in the organic phase increases with dose (WhL^{-1}). An attempt has been made to identify the possible radiolytic degradation products of TalPs using mass spectrometry. The present study indicates that variations in density, viscosity and also the extraction behaviour of U and Pu with the degraded TiAP are not very different from that observed for the degraded TBP. Thus any hydrodynamic issues observed during a solvent extraction process with the employment of TiAP as solvent would be nearly similar to those encountered in the analogous TBP/DD system, indicating that the radiolytic degradation behaviour of TiAP system is on par with TBP.

8.6 Future perspectives

Further studies can be carried out as a continuation in order to deploy TiAP as a solvent for the reprocessing of various spent nuclear fuels such as metallic fuels and thorium based fuels for actual reprocessing applications. The following studies are recommended:

- Dissolution aspects of un-irradiated metallic fuels under various experimental conditions
- Batch solvent extraction studies with simulated feed solutions of U-Pu-Zr under various conditions (as a function aqueous phase acidity, feed composition e.g. in the absence and presence of HF) in cross-current mode
- Mixer-settler runs with dissolver solutions of metallic fuels (simulated dissolver solution)
- Mixer-settler runs with actual dissolver solutions of metallic as wells as oxide fuels
- Development of flowsheets for AHWR spent fuels (U-Pu-Th)O_2 using TiAP based solvents and comparison with TBP system; batch studies followed by mixer-settler runs
- Complete characterisation of degradation products of TiAP based system and regeneration of the solvent for its subsequent usage.

REFERENCES

1. Grover R, Chandra S (2006) Scenario for growth of electricity in India. *Energy Policy*. 34(17):2834-2847
2. Ramachandran A, Gururaja J (1977) Perspectives on Energy in India. *Annual Review of Energy*. 2:365-386
3. Ramanna R (1997) Inevitability of nuclear energy. *Curr. Sci*. 73 (4):319-326
4. Grover R (2013) Green growth and role of nuclear power: A perspective from India. *Energy Strategy Rev*. 1(4):255-260
5. Bajaj S, Gore A (2006) The Indian PHWR. *Nucl. Eng. Des.* 236:701-722
6. Balakrishnan K, Kakodkar A (1994) Optimization of the initial fuel loading of the Indian PHWR with thorium bundles for achieving full power. Annals of Nuclear Energy. 21(1):1-9
7. Waltar AE, Reynolds AB (1981) Fast breeder reactors. Pergamon Press. ISBN: 9780080259833
8. Cochran TB, Feiveson HA, Patterson W, Pshakin G, Ramana MV, Schneider M, Suzuki T, von Hippel F (2010) Fast breeder reactor programs: history and status. International Panel on Fissile Materials
9. Chidambaram R, Ganguly C (1996) Plutonium and thorium in the Indian nuclear programme. *Curr. Sci.* 70(1):21-35
10. Ganguly C, Hegde PV, Jain GC, Basak U, Mehrotra RS, Majumdar S, Roy PR (1986) Development and Fabrication of 70% PuC—30% UC Fuel for the Fast Breeder Test Reactor in India. *Nucl. Technol.* 72(1):59-69
11. Chetal SC, Balasubramaniyan V, Chellapandi P, Mohanakrishnan P, Puthiyavinayagam P, Pillai CP, Raghupathy S, Shanmugham TK, Pillai CS (2006) The design of the prototype fast breeder reactor. *Nucl. Eng. Des.* 236(7):852-860
12. Sinha R, Kakodkar A (2006) Design and development of the AHWR—the Indian thorium fuelled innovative nuclear reactor. *Nucl. Eng. Des*. 236(7):683-700
13. Anantharaman K, Shivakumar V, Saha D (2008) Utilisation of thorium in reactors. *J. Nucl. Mater.* 383(1):119-121
14. Srinivasan G, Kumar KVS, Rajendran B, Ramalingam PV (2006) The fast breeder test reactor—design and operating experiences. *Nucl. Eng. Des*. 236(7):796-811

15. Chetal SC, Chellapandi P, Puthiyavinayagam P, Raghupathy S, Balasubramaniyan V, Selvaraj P, Mohanakrishnan P, Raj B (2011) Current status of fast reactors and future plans in India. *Energy Procedia.* 7:64-73
16. Raj B, Kamath HS, Natarajan R, Rao PRV (2005) A perspective on fast reactor fuel cycle in India. *Progress in Nuclear Energy.* 47(1):369-379
17. Sinha R, Kakodkar A (2003) The road map for a future Indian nuclear energy system. No. IAEA-CN-108.
18. Kumar KVS, Babu A, Anandapadmanaban B, Srinivasan G (2011) Twenty five years of operating experience with the fast breeder test reactor. *Energy Procedia*. 7:323-332
19. Chellapandi P, Puthiyavinayagam P, Balasubramaniyan V, Ragupathy S, Rajanbabu V, Chetal SC, Raj B (2010) Design concepts for reactor assembly components of 500MWe future SFRs. *Nucl. Eng. Des.* 240(10):2948-2956
20. Rodriguez P, Bhoje S (1998) The FBR program in India. *Energy*. 23(7):629-636
21. Taebi B, Kloosterman JL (2008) To recycle or not to recycle? An intergenerational approach to nuclear fuel cycles. *Science and Engineering Ethics.* 14(2):177-200
22. Ewing RC (2006) The nuclear fuel cycle: A role for mineralogy and geochemistry. *Elements*. 2(6):331-334
23. Bunn M, Holdren JP, Fetter S, Van Der Zwaan B (2005) The economics of reprocessing versus direct disposal of spent nuclear fuel. *Nucl. Technol.* 150(3):209-230
24. Carter LJ, Pigford TH (1999) The world's growing inventory of civil spent fuel. Arms Control Today 29(1):8
25. Natarajan R, Raj B (2007) Fast reactor fuel reprocessing technology in India. *J. Nucl. Sci. Technol.* 44(3):393-397
26. Sood DD, Patil SK (1996) Chemistry of nuclear fuel reprocessing: Current status. *J. Radioanal. Nucl. Chem. Art.* 203:547-573
27. Natarajan R (1998) Challenges in fast reactor fuel reprocessing. IANCAS. 14:27-32
28. Takata T, Koma Y, Sato K, Kamiya M, Shibata A, Nomura K, Ogino H, Koyama T, Aose SI (2004) Conceptual design study on advanced aqueous reprocessing system for fast reactor fuel cycle. *J. Nucl. Sci. Technol.* 41(3):307-314
29. Ananthasivan K, Anthonysamy S, Chandramouli V, Kaliappan I, Rao PRV (1996) Reprocessing of carbide fuels: Conversion of carbide to nitride as a head end step. *J. Nucl. Mater.* 228(1):18-23

30. Chandramouli V, Sreenivasan N, Yadav RB (1990) Chemical head-end steps for aqueous reprocessing of carbide fuels. *Radiochim. Acta.* 51:23-26
31. Natarajan R, Vijayakumar V, Rao RS, Pandey NK (2015) Experiences of reprocessing of plutonium-rich mixed carbide fuels. *J. Radioanal. Nucl. Chem.* 304:401-407
32. Status of Developments in the Back End of the Fast Reactor Fuel Cycle. IAEA Nuclear Energy Series. 2011(NF-T-4.2) International atomic energy agency, Vienna
33. Gindler JE (1962) Radiochemistry of uranium. Argonne National Lab., IL (USA)
34. Pocev S, Johansson G (1973) Hydrolysis of the Uranium (IV) Ion in Aqueous Perchlorate. *Acta Chem. Scand.* 27:2146-2160
35. Laue C, Gates-Anderson D, Fitch T (2004) Dissolution of metallic uranium and its alloys. *J. Radioanal. Nucl. Chem.* 261:709-717
36. Sato T (1958) The extraction of uranyl nitrate from nitric acid solutions by tributyl phosphate. *J. Inorg. Nucl. Chem.*6:334-337
37. Cleveland JM (1970) The chemistry of plutonium. (No. TID-25526)
38. Coleman GH (1965) The radiochemistry of plutonium. Lawrence Radiation Lab., Univ. of California, Livermore
39. Ryan JL, Bray LA (1980) Dissolution of plutonium dioxide: A critical review. In actinide separations.
40. Lee MH, Park YJ, Kim WH (2007) Absorption spectroscopic properties for Pu (III, IV and VI) in nitric and hydrochloric acid media. *J. Radioanal. Nucl. Chem.* 273(2):375-382
41. Choppin G, Bond A, Hromadka P (1997) Redox speciation of plutonium. *J. Radioanal. Nucl. Chem.* 219:203-210
42. Connick RE (1949) Mechanism of the disproportionation of Plutonium (V). *J. Am. Chem. Soc.* 71(5):1528-1533
43. Madic C, Begun GM, Hobart DE, Hahn RL (1984) Raman spectroscopy of neptunyl and plutonyl ions in aqueous solution: Hydrolysis of neptunium (VI) and plutonium (VI) and disproportionation of plutonium (V). *Inorg. Chem.* 23(13):1914-1921
44. Costanzo DA, Biggers RE, Bell JT (1973) Plutonium polymerization—IA spectrophotometric study of the polymerization of plutonium (IV). *J. Inorg. Nucl. Chem.*35(2):609-622
45. Brunstad A (1959) Polymerization and precipitation of plutonium (IV) in nitric acid. *Ind. Eng. Chem.* 51:38-40

46. Toth LM, Friedman HA, Osborne MM (1981) Polymerization of Pu (IV) in aqueous nitric acid solutions. *J. Inorg. Nucl. Chem.*43:2929-2934
47. Best GF, Mckay HA, Woodgate PR (1957) Tri-n-butyl phosphate as an extracting solvent for inorganic nitrates—III The plutonium nitrates. *J. Inorg. Nucl. Chem.*4:315-320
48. Healy T, Mckay H (1956) The extraction of nitrates by tri-n-butyl phosphate (TBP). Part 2.—The nature of the TBP phase. *Transactions of the Faraday Society* 52:633-642
49. Ramanujam A, Ramakrishna VV, Patil SK (1978) The effect of temperature on the extraction of plutonium (IV) by tri-n-butyl phosphate. *J. Inorg. Nucl. Chem.*40:1167-1171
50. Holder JV (1978) A review of the solvent extraction process chemistry of fission products. *Radiochim. Acta.* 25:171-180
51. Connick RE, McVey WH (1949) The aqueous chemistry of zirconium. *J. Am. Chem. Soc.* 71:3182-3191
52. Lister BAJ, McDonald LA (1952) 827. Some aspects of the solution chemistry of zirconium. *J. Chem. Soc.*(resumed):4315-4330
53. McKibben J (1984) Chemistty of the Purex Process. *Radiochim. Acta.* 36:3-16
54. Ekberg C, Källvenius G, Albinsson Y, Brown PL (2004) Studies on the hydrolytic behavior of zirconium (IV). *J. Solution Chem.* 33:47-79
55. Solovkin AS (1974) Thermodynamics of extraction of tetravalent plutonium, uranium, thorium and zirconium. *J. Radioanal. Nucl. Chem.* 21:15-29
56. Hardy CJ, Scargill D (1961) Studies on mono-and di-n-butylphosphoric acids-III The extraction of zirconium from nitrate solution by di-n-butylphosphoric acid. *J. Inorg. Nucl. Chem.*17:337-349
57. Pai SA, Shukla JP, Subramanian MS (1982) Extraction behavior of uranium, zirconium and ruthenium with gamma-irradiated sulfoxides and tri-normal-butyl phosphate. *J. Radioanal. Nucl. Chem.* 74:31-38
58. Siczek AA, Steindler MJ (1978) The chemistry of ruthenium and zirconium in the PUREX solvent extraction process. *Atomic Energy Review* 16:575-618
59. Maya L (1981) Chemistry of extractable nitrosyl ruthenium species in the system nitric acid-tributyl phosphate-dodecane. *J. Inorg. Nucl. Chem.*43:385-390

60. Boswell GG, Soentono S (1981) Ruthenium nitrosyl complexes in nitric acid solutions. *J. Inorg. Nucl. Chem.*43:1625-1632

61. Natarajan R, Dhamodharan K, Sharma PK, Pugazhendi S, Vijayakumar V, Pandey NK, Rao RVS (2013) Optimization of Flowsheet for Scrubbing of Ruthenium during the Reprocessing of Fast Reactor Spent Fuels. *Sep. Sci. Technol.* 48:2494-2498

62. EI-Kot AM (1992) Solvent-extraction of heptavalent technetium. *J. Radioanal. Nucl. Chem. Art.* 163:363-373

63. Rulfs CL, Pacer RA, Hirsch RF (1967) Technetium chemistry oxidation states and species. *J. Inorg. Nucl. Chem.* 29:681

64. Pruett DJ (1981) The solvent-extraction of heptavalent technetium by tributyl-phosphate. *Sep. Sci. Technol.* 16:1157-1179

65. Garraway J, Wilson PD (1985) Coextraction of pertechnetate and zirconium by tri-normal-butyl phosphate. *J. Less-Common Met.* 106:183-192

66. Lisman FL, Abernathey RM, Maeck WJ, Rein JE (1970) Fission Yields of Over 40 Stable and Long-Lived Fission Products for Thermal Neutron Fissioned ^{233} U, ^{235}U, ^{239}Pu, and ^{241}Pu and Fast Reactor Fissioned ^{235}U and ^{239}Pu. *Nucl. Sci. Eng.* 42:191-214

67. Fidelis I (1970) Temperature effect on the extraction of lanthanides in the TBP-HNO_3 system. *J. Inorg. Nucl. Chem.*32:997-1003

68. Rao PRV, Kolarik Z (1996) A review of third phase formation in extraction of actinides by neutral organophosphorus extractants. *Solvent Extr. Ion Exch.* 14:955-993

69. Horner DE (1971) Formation of third phases and the effect of temperature on the distribution of plutonium and uranium in extractions by tri-n-butyl phosphate. ORNL- 4724

70. Srinivasan TG, Rao PRV (2014) Red Oil Excursions: A Review. *Sep. Sci. Technol.* 49:2315-2329

71. Singh RK (1998) Experience on PHWR spent fuel reprocessing in india. In: Nuclear fuel reprocessing. IANCAS, 21-26

72. Srinivasan TG, Dhamodaran R, Rao PRV, Mathews CK (1988) Effect of uranium on third-phase formation in the Pu(IV)-HNO_3 -TBP-dodecane system. *Sep. Sci. Technol.* 23:1401-1408

73. Nakashima T, Kolarik Z (1983) The formation of a third phase in the simultaneous extraction of actinide (IV) and uranyl nitrates by tributyl phosphate in dodecane. *Solvent Extr. Ion Exch.* 1:497-513
74. Srinivasan TG, Ahmed MK, Shakila AM, Dhamodaran R, Rao PV, Mathews CK (1986) Third phase formation in the extraction of plutonium by tri-normal-butyl phosphate. *Radiochim. Acta.* 40:151-154
75. Rydberg J, Musikas C, Choppin GR (1992) Principles and practices of solvent extraction. M. Dekker; New York
76. Pratt HRC (1983) Computation of stagewise and differential contactors: Plug flow, In: Handbook of Solvent Extraction. TC Lo, MHI Baird, C. Hanson (eds).
77. Hartland S, Mecklenburgh JC (1966) A comparison of differential and stagewise counter current extraction with backmixing. Chemical Engineering Science 21:1209-1229
78. Lewis WK (1916) Laboratory and plant: The principles of counter-current extraction. *Ind. Eng. Chem.* 8:825-833
79. Pratt HRC (1983) Interphase mass transfer, In: Handbook of Solvent Extraction. TC Lo, MHI Baird, C. Hanson (eds). USA
80. Koganti SB (1998) Equipment for spent fuel aqueous reprocessing: The scope and the challenges, In: Nuclear Fuel Reprocessing. Pillai MRA (ed) IANCAS, BARC, Mumbai, 33-39.
81. Srinivasan N, Nadkarni MN, Balasubramanian GR, Ramanujam A, Venkatesan M, Gopalakrishnan V (1973) Development of Air Pulsed Mixer Settler Equipments for Solvent Extraction Studies. BARC-672; BARC Report. Mumbai
82. Koganti SB, Rajagopalan CV, Periasamy K, Sreedharan V, Balasubramanian GR (1993) Development of high efficiency air pulsed ejector mixersettler. In: Solvent Extraction in the Process Industries, . In: Proc. Int. Sol. Extr. Conf.,(ISEC-93), p 103-110
83. Walter CM, Golden GH, Olson NJ (1975) U-Pu-Zr Metal Alloy: A Potential Fuel for LMFBRs. Argonne National Laboratory.
84. Carmack WJ, Porter DL, Chang YI, Hayes SL, Meyer MK, Burkes DE, Lee CB, Mizuno T, Delage F, Somers J (2009) Metallic fuels for advanced reactors. *J. Nucl. Mater.* 392:139-150

85. Walters LC, Seidel BR, Kittel JH (1984) Performance of metallic fuels and blankets in liquid-metal fast breeder reactors. *Nucl. Technol.* 65:179-231
86. Crawford DC, Porter DL, Hayes SL (2007) Fuels for sodium-cooled fast reactors: US perspective. *J. Nucl. Mater.* 371:202-231
87. Seidel BR, Tracy DB, Griffiths V, (1991) Apparatus for injection casting metallic nuclear energy fuel rods. United States patent US 5,044,911. 1991 Sep 3. DOE, USA.
88. Ackerman JP (1991) Chemical basis for pyrochemical reprocessing of nuclear fuel. *Ind. Eng. Chem. Res.*30:141-145
89. Nawada HP, Fukuda K (2005) Role of pyro-chemical processes in advanced fuel cycles. *J. Phys. Chem. Solids.* 66:647-651
90. Larsen RP (1959) Dissolution of uranium metal and its alloys. *Anal. Chem.* 31:545-549
91. Rodrigues L, Falleiros N, De O. Forbicini CA (2002) Kinetics of the electrodissolution of metallic uranium. *J. Radioanal. Nucl. Chem.* 253:511-515
92. Nikitin SA, Maslennikov AG (2014) Electrochemical properties and dissolution of U-5 wt% Zr Alloy in HNO3 solutions. *Radiochemistry.* 56:241-246
93. Harmon HD (1975) Evaluation of fluoride, cerium (IV) and cerium (IV)-fluoride mixtures as dissolution promoters for PuO_2 scrap recovery Processes. US-ERDA Report DP-1382. EI du Pont de Nemours & Co., Savannah River Laboratory Aiken, South Carolina
94. Palamalai A, Rajan SK, Chinnusamy A, Sampath M, Varghese PK, Ravi TN, Raman VR, Balasubramanian GR (1991) Development of an electro-oxidative dissolution technique for fast reactor carbide fuels. *Radiochim. Acta.* 55:29-36
95. Christian JD Aqueous reprocessing of U-Pu-Zr metal fuels–dissolution considerations. In, 3122 Homestead Lane, Idaho Falls
96. Larsen RP, Shor RS, Feder HM (1954) A study of the explosive properties of uranium-zirconium alloys. Argonne National Lab.
97. Martin F, Field B (1958) The reactions of zirconium and zirconium based alloys with nitric and nitric-hydrofluoric acids. part i. hazardous aspects. part ii. dissolution rates. United Kingdom Atomic Energy Authority. Research Group. Atomic Energy Research Establishment, Harwell, Berks, England

98. Roth H (1952) Explosions Occurring During Chemical Etching or Pickling of Uranium-zirconium Alloys. Massachusetts Inst. of Tech., Cambridge. Metallurgical Project
99. Hurford W (1953) Explosions Involving Pickling of Zirconium and Uranium Alloys. Westinghouse Electric Corp. Atomic Power Div., Pittsburgh
100. Gens T (1961) Zircex and Modified Zirflex Processes for Dissolution of 8% U-91% Zr-1% H TRIGA Reactor Fuel. Oak Ridge National Lab., Tenn.
101. Gens T (1963) Continuous dissolution of zirconium reactor fuels in titanium equipment: Laboratory demonstration. Oak Ridge National Lab., Tenn.
102. Flagg JF, Liebhafsky HA, Winslow EH (1949) A Spectrophotometric Study of Three Zirconium Lakes. *J. Am. Chem. Soc.* 71:3630-3632
103. Oesper RE, Klingenberg JJ (1949) Use of glycolic acid derivatives in determination of zirconium. *Anal. Chem.* 21:1509-1511
104. Larsen RP, Ross LE, Kesser G (1960) Spectrophotometric determination of zirconium in uranium alloys of the fission elements. *Talanta*. 4:108-114
105. Rafiq M, Rules CL, Elving PJ (1963) Determination of small amounts of zirconium-I: gravimetric procedures using mandelic acid and its derivatives. *Talanta* 10:696-701
106. Evans HB, Hrobar AM, Patterson JH (1960) Determination of Zirconium in Uranium Fissium Alloys. *Anal. Chem.* 32:481-483
107. Buchanan RF, Hughes JP, Bloomquist CAA (1960) The colorimetric determination of zirconium in plutonium-uranium-'fissium'alloys. *Talanta*. 6:100-104
108. Cheng K (1959) Analytical applications of xylenol orange-I: Determination of traces of zirconium. *Talanta*. 2:61-66
109. Cheng K (1959) Analytical applications of xylenol orange-II: Spectrophotometric study on the zirconium-xylenol orange complex. *Talanta* 2:266-269
110. Gercke RHJ, McVey WH (1953) The Dissolution of Zirconium-Clad Uranium Target Elements.
111. Kyser E (2001) Extraction of plutonium into 30% tributyl phosphate from nitric acid solutions containing fluoride, aluminum, and boron. *Sep. Sci. Technol.* 36:729-741
112. Wright A, Paviet-Hartmann P (2010) Review of physical and chemical properties of tributyl phosphate/diluent/nitric acid systems. *Sep. Sci. Technol.* 45:1753-1762

113. Tripathi SC, Sumathi S, Ramanujam A (1999) Effects of solvent recycling on radiolytic degradation of 30% tributyl phosphate-n-dodecane-HNO_3 system. *Sep. Sci. Technol.* 34:2887-2903

114. Gordon PL, O'dell C, Watkin JG (1994) Synthesis and energetic content of red oil. *J. Hazard. Mater.* 39:87-105

115. Gordon PL, O'dell C, Watkin JG (1994) Investigation of red oil decomposition by simulated Hanford tank wastes. *J. Hazard. Mater.* 39:69-86

116. Colven TJ, Nichols GM, Siddall TH (1953) TNX Evaporator Incident. January 12, 1953. USAEC Report DP-25, EI du Pont de Nemours & Co., Savannah River Laboratory, Aiken, SC.

117. Sege G (1953) Overconcentration in Initial Operation of Uranium Evaporator -231 Building. USAEC Report. HW-28690, General Electric Co., Richland, Washington

118. Davis Jr W, Baldwin WH, Meservey AB (1959). Chemistry of the Intercycle Evaporator Incident of November 20, 1959. Oak Ridge National Lab., Tenn.;

119. Durant WS (1983) Red oil explosion at the savannah river plant. DPMS-83-142.

120. Paddleford DF, Fauske HK (1994) Safe Venting of Red Oil Runaway Reactions. WSRC-MS-94-0649. Westinghouse Savannah Ricer Company, Savannah River Site, South Carolina.

121. Paddleford DF, Hou Y, Barefield EK, Tedder DW, Abdel-Khalik SI (1995) Thermal Decomposition of Nitrated Tributyl Phosphate, WSRC-RP-95-259.

122. Hyder ML (1994) Safe Conditions for Contacting Nitric acid or Nitrates with Tributyl Phosphate, . WSRC-TR-94-059, Westinghouse Savannah River Company, Savannah River Site, South Carolina.

123. Higgins CE, Baldwin WH (1961) The thermal decomposition of tributyl phosphate-1. *J. Org. Chem.* 26:846-850

124. Usachev VN, Markov GS (2003) Incidents caused by red oil phenomena at semi-scale and industrial radiochemical units. *Radiochemistry.* 45:1-8

125. Mishra S, Ganesh S, Velavendan P, Pandey NK, Mallika C, Mudali UK, Natarajan R (2013) Thermodynamics of solubility of tri-n-butyl phosphate in nitric acid solutions. *Advan. Chem. Eng. Res.*2 (3):55-60

126. Tripathi SC, Ramanujam A (2003) Effect of radiation-induced physicochemical transformations on density and viscosity of 30% TBP-n-dodecane-HNO_3 system. *Sep. Sci. Technol.* 38:2307-2326

127. Venkatesan KA, Robertselvan B, Antony MP, Srinivasan TG, Vasudeva Rao PR (2006) Physiochemical and plutonium retention properties of hydrolytic and radiolytically degraded tri-n-amylphosphate. *Solvent Extr. Ion Exch.* 24:747-763

128. Parikh KJ, Pathak PN, Misra SK, Tripathi SC, Dakshinamoorthy A, Manchanda VK (2009) Radiolytic Degradation Studies on N, N-dihexyloctanamide (DHOA) under PUREX Process Conditions. *Solvent Extr. Ion Exch.* 27:244-257

129. Kuno Y, Hina T (1993) Degradation of Tributylphosphate in Highly Radioactive Liquid Waste of Nuclear Fuel Reprocessing. *Radiochim. Acta* 60:193-198

130. Bellido AV, Rubenich MN (1984) Influence of the diluent on the radiolytic degradation of TBP in TBP, 30%-diluent-HNO_3 systems. *Radiochim. Acta.* 36:61-64

131. Pearson J, Nilsson M (2014) Radiolysis of tributyl phosphate by particles of high linear energy transfer. *Solvent Extr. Ion Exch.* 32:584-600

132. Pearson J, Jan O, Miller GE, Nilsson M (2012) Studies of high linear energy transfer dosimetry by $^{10}B0(n,\alpha)^{7}Li$ reactions in aqueous and organic solvents. *J. Radioanal. Nucl. Chem.* 292:719-727

133. Neace JC (1983) Diluent degradation products in the purex solvent. *Sep. Sci. Technol.* 18:1581-1594

134. Mincher BJ, Modolo G, Mezyk SP (2009) Review Article: The Effects of Radiation Chemistry on Solvent Extraction: 1. Conditions in Acidic Solution and a Review of TBP Radiolysis. *Solvent Extr. Ion Exch.* 27:1-25

135. Tsujino T, Ishihara T (1966) Radiation Damage to TBP/Kerosene Solvent,(II) Effect on Extraction Behavior of Uranium and Thorium and on their Loading Effect. *J. Nucl. Sci. Technol.* 3:144-149

136. Blake Jr CA Davis Jr W, Schmitt JM (1963) Properties of degraded TBP-Amsco solutions and alternative extractant-diluent systems. *Nucl. Sci. Eng.* 17:626-637

137. Zimmer E, Borchardt J (1986) Crud formation in the purex and thorex processes. *Nucl. Technol.* 75:332-337

138. Ritcey G (1980) Crud in solvent extraction processing-a review of causes and treatment. *Hydrometallurgy.* 5:97-107

139. Meisenhelder JH, Siczek AA (1980) An infrared study of zirconium retention in 30% tributyl phosphate. *Radiochim. Acta.* 27:223-228

140. Kolarik Z, Pipkin N (1982) Interfacial tension in systems involving TBP in dodecane, nitric acid, uranyl nitrate and water. Kernforschungszentrum Karlsruhe GmbH (Germany)
141. Lane ES (1963) Performance and degradation of diluents for TBP and the cleanup of degraded Solvents. *Nucl. Sci. Eng.* 17:620-625
142. Smith DN, Edwards HG, Hughes MA, Courtney B (1997) Odorless kerosene degradation and the formation of interfacial deposits during the alkaline solvent wash in the PUREX process. *Sep. Sci. Technol.* 32:2821-2849
143. Tallent OK, Mailen JC, Dodson KE (1985) Purex diluent chemical degradation. *Nucl. Technol.* 71:417-425
144. Sze Y, McDougall TE, Martin CG (1987) Chemical degradation of tri-n-butyl phosphate/diluent solvents tm used in candu thorium fuels reprocessing development. *Solvent Extr. Ion Exch.* 5:129-150
145. Lesage D, Virelizier H, Jankowski CK, Tabet JC (1998) Identification of isomeric tributylphosphate dimers formed by radiolysis using tandem mass spectrometry and stable isotopic labelling. *Eur. Mass Spectrom.* 4:47-54
146. Lesage D, Virelizier H, Jankowski CK, Tabet JC (1997) Identification of minor products obtained during radiolysis of tributylphosphate (TBP). Spectroscopy. 13:275-290
147. Lanham WB, Runion TC (1949) PUREX process for plutonium and uranium recovery. Oak Ridge National Lab., Tenn.
148. Balasubramaniam GR, Chitnis RT, Ramanujam A, Venkatesan M (1977) Laboratory studies on the recovery of uranium-233 from irradiated thorium by solvent extraction using 5% TBP Shell Sol-T as Solvent. Bhabha Atomic Research Centre
149. Herbst RS, Baron P, Nilsson M (2011) Standard and advanced separation: PUREX processes for nuclear fuel reprocessing. Woodhead Publishing, Cambridge, MA
150. Suresh A, Srinivasan TG, Rao PRV (2009) The Effect of the Structure of Trialkyl Phosphates on their Physicochemical Properties and Extraction Behavior. *Solvent Extr. Ion Exch.* 27:258-294
151. Suresh A, Srinivasan TG, Rao PRV (1994) Extraction of U(VI), Pu(IV) and Th(IV) by some trialkyl phosphates. *Solvent Extr. Ion Exch.* 12:727-744

152. Suresh A, Srinivasan T, Rao PRV (2009) Parameters Influencing third-phase formation in the extraction of $Th(NO_3)_4$ by some trialkyl Phosphates. *Solvent Extr. Ion Exch.* 27:132-158

153. Shukla JP, Gautam MM, Kedari CS, Hasan S, Rupainwar D (1997) Extraction of uranium(VI), plutonium(IV) and some fission products by tri-iso-amyl phosphate. *J. Radioanal. Nucl. Chem.* 219:61-67

154. Hasan SH, Shukla JP (2003) Tri-iso-amyl phosphate (TAP): An alternative extractant to tri-butyl phosphate (TBP) for reactor fuel reprocessing. *J. Radioanal. Nucl. Chem.* 258:563-573

155. Srinivasan TG, Vasudeva Rao PR, Sood DD (1998) Diluent and extractant effects on the enthalpy of extraction of uranium (VI) and americium (III) nitrates by trialkyl phosphates. *Solvent Extr. Ion Exch.* 16:1369-1387

156. Sahoo TK, Chandran K, Muralidaran P, Ganesan V, Srinivasan TG (2012) Calorimetric studies on thermal decomposition of tri isoamyl phosphate–nitric acid systems. *Thermochim Acta.* 534:9-16

157. Sahoo TK, Srinivasan TG, Vasudeva Rao PR (2009) Effect of temperature on the extraction of uranium by TiAP/n-dodecane. *Desalin. Water. Treat.* 12:40-44

158. Sahoo TK, Srinivasan T, Vasudeva Rao PR (2011) Effect of temperature in the extraction of uranium and plutonium by triisoamyl phosphate. *Solvent Extr. Ion Exch.* 29:260-269

159. Benadict Rakesh K, Suresh A, Vasudeva Rao PR (2014) Extraction and stripping behaviour of tri-iso-amyl phosphate and tri-n-butyl phosphate in n-dodecane with U (VI) in nitric acid media. *Radiochim. Acta.* 102:619-628

160. Benadict Rakesh K, Suresh A, Sivaraman N, Aswal K, Vasudeva Rao PR (2016) Extraction and third phase formation behaviour of tri-iso-amyl phosphate and tri-n-butyl phosphate with Zr(IV) and Hf(IV): A comparative study. *J. Radioanal. Nucl. Chem.*:1-12

161. Suresh A, Rao CVSB, Srinivasulu B, Sreenivasan NL, Subramaniam S, Sabharwal KN, Sivaraman N, Srinivasan TG, Natarajan R, Vasudeva Rao PR (2013) Development of alternate extractants for separation of actinides. *Energy Procedia.* 39:120-126

162. Joseph M, Manoravi P, Sivakumar N, Balasubramanian R (2006) Laser mass spectrometric studies on rare earth doped UO_2. *Int. J. Mass spectrom*. 253:98-103

163. Mayankutty PC, Ravi S, Nadkarni M (1982) Determination of free acidity in uranyl-nitrate solutions. *J. Radioanal. Nucl. Chem.* 68:145-150

164. Chiarizia R, Jensen MP, Rickert PG, Kolarik Z, Borkowski M, Thiyagarajan P (2004) Extraction of zirconium nitrate by TBP in n-octane: Influence of cation type on third phase formation according to the "sticky spheres" model. *Langmuir.* 20:10798-10808

165. Crouch E (1977) Fission-product yields from neutron-induced fission. Atomic Data and Nuclear Data Tables 19:417-532

166. Harkins WD, Brown FE (1919) The determination of surface tension (free surface energy), and the weight of falling drops: The surface tension of water and benzene by the capillary height method. *J. Am. Chem. Soc.* 41:499-524

167. Wawrzyńczak WS, Paleska I, Figaszewski Z (1991) Study of supporting electrolyte adsorption in the water/nitrobenzene partition system: I. A new drop weight technique for interfacial tension measurements. *J. Electroanal. Chem. Interfacial Electrochem.* 319:291-301

168. Prochaska K (2002) Interfacial activity of metal ion extractant. *Adv. Colloid Interface Sci.* 95:51-72

169. Gopinath N (2008) Chemical characterization of nuclear fuels. Tomar BS (ed) IANCAS, 156-168

170. Suresh A, Patre DK, Srinivasan TG, Rao PRV (2002) A new procedure for the spectrophotometric determination of uranium(VI) in the presence of a large excess of thorium(IV). *Spectrochim. Acta Mol. Biomol. Spectrosc*. 58:341-347

171. Rao R, Damodaran K, Kumar G Ravi T (2000) Determination of uranium and plutonium in high active solutions by extractive spectrophotometry. *J. Radioanal. Nucl. Chem.* 246:433-435

172. Celon E, Degetto S, Marangoni G (1979) Rapid-determination of milligram amounts of uranium in organic complexes with pyridine-2,6-dicarboxylic acid as titrant and arsenazo-i as indicator after oxygen-flask combustion. *Talanta.* 26:160-162

173. Datta A, Sivaraman N, Srinivasan TG, Vasudeva Rao PR (2011) Liquid chromatographic behavior of lanthanides and actinides on monolith supports. *Radiochim. Acta* 99:275-283

174. Townsend DI, Tou JC (1980) Thermal hazard evaluation by an accelerating rate calorimeter. *Thermochim Acta.* 37:1-30

175. Chandran K, Sahoo TK, Muralidaran P, Ganesan V, Srinivasan TG (2012) Calorimetric studies on the thermal decomposition of tri n-butyl phosphate-nitric acid systems. *J. Therm. Anal. Calorim.* 110:879-890

176. Rao CVSB, Chandran K, Krishnan RV, Ramanathan N, Muralidaran P, Ganesan V, Srinivasan TG (2012) Thermodynamics and kinetics of thermal decomposition of diamylamyl phosphonate-nitric acid systems. *Thermochim Acta.* 545:116-124

177. Venkatesan KA, Chandran K, Ramanathan N, Anthonysamy S, Ganesan V, Srinivasan TG (2014) Thermal decomposition characteristics of octyl(phenyl)-N,N-diisobutylcarbamoylmethylphosphine oxide-tri n-butyl phosphate-nitric acid systems. *J. Therm. Anal. Calorim.* 115:1979-1988

178. Iwata Y, Momota M, Koseki H (2006) Thermal risk evaluation of organic peroxide by automatic pressure tracking adiabatic calorimeter. *J. Therm. Anal. Calorim.* 85:617-622

179. Chu YC, Chen JR, Tseng JM, Tsai LC, Shu CM (2011) Evaluation of runaway thermal reactions of di-tert-butyl peroxide employing calorimetric approaches. *J. Therm. Anal. Calorim.* 106:227-234

180. Iizuka Y, Surianarayanan M (2003) Comprehensive kinetic model for adiabatic decomposition of di-tert-butyl peroxide using Batch CAD. *Ind. Eng. Chem. Res.* 42:2987-2995

181. Shaw DH, Pritchard HO (1968) Thermal decomposition of di-tert-butyl peroxide at high pressure. *Can. J. Chem.* 46:2721-2724

182. Borkowski M, Chiarizia R, Jensen MP, Ferraro JR, Thiyagarajan P, Littrell KC (2003) SANS study of third phase formation in the Th(IV)-HNO_3/TBP-n-octane system. *Sep. Sci. Technol.* 38:3333-3351

183. Kulkarni PG, Gupta KK, Gurba PB, Janardan P, Changrani RD, Dey PK, Manchanda VK (2006) Solvent extraction behaviour of some fission product elements with N, N-dihexyl octanamide and tri-n-butyl phosphate under simulated PUREX process conditions. *Radiochim. Acta* 94:325-329

184. Li C, Zuo C, Yan T, Zheng W (2014) Study on the technology of U-Pu Co-stripping process for reprocessing spent fuel of fast reactor. *Radiochim. Acta* 102:1075-1081

185. Nakahara M, Koma Y, Nakajima Y (2013) Co-processing of uranium and plutonium for sodium-cooled fast reactor fuel reprocessing by acid split method for plutonium partitioning without reductant. *J. Nucl. Sci. Technol.* 50:1062-1070

186. Gonda K, Oka K (1984) Accumulation process of plutonium 3rd phase in mixer-settlers. *Nucl. Technol.* 64:14-18

187. Tachimori S, Morita Y (2009) Overview of solvent extraction chemistry for reprocessing. Moyer BA (ed) Ion Exchange and Solvent Extraction: A Series of Advances. 1-64

188. Agarwal RP, Moreno EC (1971) Stability constants of aluminium fluoride complexes. *Talanta*. 18:873-880

189. Alcock K, Bedford FC, Hardwick WH, McKay HA (1957) Tri-n-butyl phosphate as an extracting solvent for inorganic nitrates-I: Zirconium nitrate. *J. Inorg. Nucl. Chem.*4:100-105

190. Pruett DJ, Schulz WW, Navratil JD (1987) Application of TBP in nuclear fuel reprocessing.

191. Tripathi SC, Ramanujam A, Gupta KK, Bindu P (2001) Studies on the identification of harmful radiolytic products of 30% TBP-n-dodecane-HNO_3 by gas liquid chromatography. i. formation of diluent degradation products and their role in Pu retention behavior. *Sep. Sci. Technol.* 36:1463-1478

192. Healy TV, Kennedy J (1959) The extraction of nitrates by phosphorylated reagents .1. the relative extraction rates and solvating mechanisms for uranyl nitrate. *J. Inorg. Nucl. Chem.* 10:128-136

193. Kuno Y, Hina T (1992) Degradation of tributylphosphate in plutonium nitrate solution. *J. Nucl. Sci. Technol.* 29:762-767

194. Lloyd MH, Fellows RL (1985) Alpha radiolysis and other factors affecting hydrolysis of tributyl phosphate. Report ORNL TM-9565; Order No. DE85015071, Oak Ridge National Laboratory